A STUDY OF THE ANTIWEAR BEHAVIOR AND OXIDATION STABILITY OF FLUORINATED ZINC DIALKYL DITHIO PHOSPHATE IN THE PRESENCE OF ANTIOXIDANTS

by

ANURADHA SOMAYAJI

Presented to the Faculty of the Graduate School of

The University of Texas at Arlington in Partial Fulfillment

of the Requirements

for the Degree of

DOCTOR OF PHILOSOPHY

THE UNIVERSITY OF TEXAS AT ARLINGTON

May 2008

ACKNOWLEDGEMENTS

It was only through the support of several people that this doctoral program came to fruition. This tribute is but a small measure of my immense gratitude to them.

Exceptional advisors are indeed hard to come by. In that respect, I consider myself fortunate to have found Dr. Pranesh Aswath. His infectious enthusiasm, wise guidance and tutelage of a caring mentor have undeniably been the foundations of my success in this endeavor. Without his direction, this dissertation wouldn't have seen the light of day. I thank my committee members Dr. Roger Goolsby, Dr. Choong-Un Kim, Dr. Wen Chan, Dr. Efstathios Meletis and Dr. Harold Shaub for being a constant source of input, encouragement and support. Many thanks also go to Dr. Ronald Elsenbaumer for his care and counsel throughout this research.

Ramoun Mourhatch and Dr. Xin Chen have helped me through countless experiments and painstaking data analyses, and for this I owe them a great deal of appreciation. I also wish to credit Krupal Patel, Aparna Prasad, Solmaz Torabi, Sara Kiani, BoHoon Kim and Hande Demirkiran for their valuable assistance during this program. In fact, the entire tribology group including Mihir Patel, Eray Erkan, Hansika Parekh, Arunya Suresh and Beibei Wang, has been a great team. Many thanks go to Dr. Nancy Michael who was not only instrumental in seeing me through my AES work, but also a source of reassurance and encouragement. Thanks also go to Dr. Jiechao Jiang's, through whose efforts it was possible to obtain TEM images for my samples. Prudence Brett, Donna Woodhead, Jennifer Standlee and Libia Cuauhtli were extremely helpful in guiding me through the inescapable administrative hoops of a research project. A special note of thanks goes to Platinum Research Organization whose backing and patronage made this research effort possible. Cork Jaeger, Matt Hawkins and David Owen have been exceptionally supportive in driving this work forward all the way through this

dissertation. Several external sources have been crucial in providing timely impetus to this project: Dr. Yongfeng Hu and Dr. Lucia Zuin of Canadian Light Source Center, Dr. Arup K. Gangopadhyay and Kelly Keller of Ford Motor Co., and Jim Reinhart of Denver Instruments have all contributed considerably to this project.

My parents, Badavide Nagesh Rao and Bharathi Nagesh Rao have been my lifelong inspiration, the pillars of my strength and the bedrock of my achievements. I am immensely proud to dedicate this dissertation to them. My husband Manjunath Somayaji has been my rock during turbulent times and the force that propelled me onwards when things seemed impossible. He has been my staunchest ally during my darkest moments and my guiding light every step of the way. Never once did he lose faith in me. Without him, I never would have achieved this dream today. Manjunath's parents, Dr. B.V. Somayaji and Varalakshmi Somayaji have also been very supportive during this process. My brothers, Venkatakrishna and Rammohan, sisters Annapoorna and Anupama, and brothers-in-law Sudarshan Holla, Srinivasa Upadhyaya and Ganesh Somayaji have been a significant source of encouragement as well. My grandparents Dr. A. Rammohan Rao and Lola Rao were unwavering in their confidence in me, and never ceased to provide comfort and motivation from half a world away. I cannot thank them enough for their part in bringing me to where I am today. My dear friends Hunter and Jill Johnson, his parents Charles and Agnes, and Troy and Rhonda Hutchison were all sources of encouragement during this journey and therefore deserve special recognition as well.

These acknowledgements would remain incomplete without mention of Prof. E.S. Dwarakadasa, who to this day remains one of my most cherished role models. If it wasn't for him, this journey would not even have begun, let alone come to completion. I owe him a huge debt of gratitude.

April 24, 2008

ABSTRACT

A STUDY OF THE ANTIWEAR BEHAVIOR AND OXIDATION STABILITY
OF FLUORINATED ZINC DIALKYL DITHIO PHOSPHATE
IN THE PRESENCE OF ANTIOXIDANTS

Anuradha Somayaji, Ph.D.

The University of Texas at Arlington, 2008

Supervising Professor: Dr. Pranesh B. Aswath

The antiwear additive Zinc dialkyl dithio phosphate (ZDDP) is one of the most important components of engine-oil additives and a major source of phosphorus. Phosphorus plays a crucial part in mitigating engine wear, yet has been proven harmful to modern catalytic converters. Progressive regulatory caps on phosphorus content in automotive lubricants have led to widespread efforts to reduce its levels. A new fluorinated ZDDP (F-ZDDP) complex developed at the University of Texas at Arlington has found to breakdown at lower temperatures compared to ZDDP and has showed better wear performance than ZDDP alone. This would allow the possibility of further reduction of phosphorus in engine oils than current levels.

This work begins with a study of the interaction of ZDDP and fluorinated ZDDP with the antioxidant alkylated diphenyl amine. The impact of antioxidant on wear performance was examined using a custom-built ball-on-cylinder tribometer. Interactions between ZDDP and fluorinated ZDDP with antioxidant were studied using Fourier transform infrared spectroscopy and

nuclear magnetic resonance, and the surface of the tribofilm was examined using scanning electron microscopy, transmission electron microscopy and Auger electron spectroscopy.

Nanoscale mechanical properties of *in-situ* tribofilms generated from ZDDP and F-ZDDP in the presence of alkylated diphenyl amine are compared to films obtained from ZDDP and F-ZDDP without antioxidant. Tribofilms in the thickness regime of 100nm to 200nm are developed *in-situ* during wear tests using ZDDP and F-ZDDP. The influence of alkylated diphenyl amine on the creation and characteristics of these tribofilms is studied. Nanomechanical properties such as hardness, modulus, scratch resistance and nano-wear resistance of the films thus formed are explored to understand the effect of various variables on the nature of these tribofilms. A focused ion beam is used to image the substrate-tribofilm interface and measure tribofilm thickness. Oxidative stability of oil formulations containing ZDDP and F-ZDDP with various antioxidants is examined through measurements of viscosity and total acid number. Oxidation products formed are identified through Fourier transform infrared spectroscopy. Several of these formulations are subjected to tribological conditions and the nature of the chemical composition of these films is studied using X-Ray near-edge absorption spectroscopy.

TABLE OF CONTENTS

LIST OF ILLUSTRATIONS

LIST OF TABLES

CHAPTER 1

INTRODUCTION

1.1 Historical Background

Throughout the course of human history, economic activity has been inextricably linked with the ability to transport people and commodities from one place to another. For millennia, transportation was largely achieved either through the use of animal or human locomotion such as stagecoaches, chariots and rowboats; or by harnessing the elements of nature in the form of sailing ships. Over the last century however, the primary means of transportation has been overwhelmingly dominated by automotive technologies; one of the most prominent among them being the internal combustion engine.

Internal combustion engines in general and reciprocating engines in particular have evolved a great deal from its early simple designs with compression-less combustion and simple overhead valves, to today's state-of-the-art microprocessor-controlled high-precision machines. Modern power plants employ sophisticated optimization techniques intended to maximize efficiency and performance while minimizing environmental footprint. Power output has dramatically improved over the years, as have reliability, fuel economy and emission control systems. Today's engines that are comparable in weight and displacement to early twentieth-century models generate much more power but only a fraction of environmental pollutants, while doing so at a much lower fuel consumption rate. To illustrate, a subcompact vehicle built in the late 1980s typically boasts four times the horsepower and nearly twice the fuel economy, but with hydrocarbon emissions only about a thirtieth of a 1921 Ford Model T [1].

1.1.1 Evolution of Lubricants

In spite of such tremendous advances, the one requirement that has remained unchanged over the years is the need for effective lubrication to ensure and maintain smooth

operation of these engines. The concept of lubrication in various forms has existed for centuries, but only recently in 1966 the area of study dealing with this discipline came to be formally recognized as a scientific research field. This field was termed 'tribology', which was defined as the "science and technology of interacting surfaces in relative motion and the practices related thereto" [2].

Improvements in engine performance over the decades have generally been accompanied by progress in the development of lubricant technology. In the early stages of engine development, automotive lubricants mainly consisted of petroleum-based crude oil which manufacturers subsequently learnt to refine into narrow distillation classes with varying grades of viscosities. The next step on the evolutionary ladder was the addition of specific compounds to this base oil to enhance its lubricating properties, thus giving rise to the age of formulated automotive lubricants.

1.1.2 Additives in Automotive Lubricants

Additives to base lubricating oils began to be widely used in 1947 when the American Petroleum Institute (API) started categorizing engine oils by severity of service [3]. Today, these additives are intended to serve in various roles such as antiwear and anti-corrosive agents, antioxidants, extreme pressure (EP) additives, dispersants and detergents, rust and corrosion inhibitors, friction modifiers, foam depressants, pour point depressants and viscosity index improvers, to name a few [4]. Antiwear agents serve to prevent contact between moving metal surfaces thereby improving the service life of machines, whereas the anti-corrosive behavior involves the inhibition of corrosion in metals and alloys. Antioxidants operate to retard the oxidation of the lubricating oil thereby helping to prolong the life of the lubricant and extend the service interval of engines. Extreme pressure additives find use in heavy-load machinery that tend to exhibit boundary lubrication conditions – a situation in which a complete fluid film does not form between rubbing surfaces. Dispersants helps prevent unwanted engine deposits such as sludge and varnish by suspending particles in a colloidal state. Detergents play a

similar role whereby they are used to control varnish, piston ring-zone deposits and rust by keeping particles in a colloidal state. However, dispersants are mainly distinguished from detergents in that the former is non-metallic while the latter is usually metallic, thereby tending to leave a slight ash when the oil is burned. For the same reason, dispersants are sometimes referred to as ashless. Dispersants and detergents are often used in combination with each other.

1.1.3 Role of Zinc Dialkyl-Dithio-Phosphate as a Lubricant Additive

One of the most prominent additives to dominate the lubrication landscape over the past several decades is the compound Zinc Dialkyl-Dithio-Phosphate (ZDDP), which first appeared with the filing of four patents in 1941 [5]. The antiwear properties of this additive remained un-noticed throughout the 1940s, but in 1955 it was discovered that oils containing ZDDP generally resulted in superior wear performance when compared to oils that didn't contain this additive, particularly in the then newly introduced V8 engines. This result led to the widespread adoption and acceptance of ZDDP as the principal choice of automotive lubricant antiwear additive in the automobile industry within a few short years. To this day, ZDDPs have arguably remained the most successful automotive lubricant additives ever invented [5]. The appeal of ZDDP as a preferred additive stems from the multifaceted nature of its performance as a lubricant additive. ZDDP exhibits antiwear and anti-oxidant properties [6-9], while also demonstrating its effectiveness as an extreme pressure (EP) additive [7] and a detergent [8-10]. It has been noted that no single additive provides the same benefit of wear prevention, corrosion protection and oxidation control as cost effectively as ZDDP [11].

1.2 Motivation for Research

In spite of its remarkable success as a lubricant additive, the use of ZDDP comes with its share of drawbacks. It is the main source of phosphorus in conventional engine oils and therefore a contributor to environmental pollution through automotive emissions. During the course of normal engine operation, traces of phosphorus mix with exhaust gases and

contaminate the catalytic converter. Over time, this accumulation of phosphorus causes the poisoning of the catalytic converter, thus reducing its effectiveness and shortening its service life. Poisoning by lubricant-based pollutants such as ZDDP is of particular concern because of the irreversible nature of catalyst degradation [12]. As a result, recent regulations by the Environmental Protection Agency (EPA) and similar agencies around the world have called for better emission controls and extended life of catalytic converters, which in turn have resulted in a push for the reduction of phosphorus levels in engine oils [5, 12-15].

One goal of this research effort is to find ways to reduce phosphorus levels in engine oils through the use of a more promising alternative to ZDDP while still remaining cost effective and retaining many of its important properties such as antiwear and antioxidancy. The EPA and the lubrication industry expect such research to lead to improved fuel economy, better emission controls, increased lifespan of catalytic converters and extended drain and service intervals in automobiles.

The antiwear mechanism of ZDDP involves its thermal and tribological degradation leading to the formation of a protective antiwear film that consists of polyphosphates & sulphates. The structure of the antiwear film is almost similar in both types of degradations. In general, ZDDP's antiwear performance is influenced by its interactions with other additives such as some friction modifiers, EP agents, antioxidants, detergents and dispersants that are present in engine oils [16], wherein the breakdown efficiency and therefore the antiwear effectiveness of ZDDP could be diminished by its parallel reaction as well as the antagonistic effects of these additives.

In an effort to lower phosphorus levels in lubricants, the tribology research group at the University of Texas at Arlington (UTA) has synthesized a new compound namely Fluorinated Zinc Dialkyl-Dithio-Phosphate (F-ZDDP), which has been shown to exhibit improved antiwear properties over ZDDP [17]. The enhanced antiwear performance of this new compound is attributed to the presence of P-F bonds which forms when ZDDP is fluorinated. This new

compound would allow the possibility of further reduction of phosphorus in engine oils than current levels. However, this reduction could potentially affect the antioxidant capabilities in the formulated lubricant. Antioxidants play an important role in retaining the properties of base oils in harsh environments in the presence of active radicals by serving as radical scavengers. Due to the importance of this additive in lubricating oils, this research effort concentrates on understanding its influence on the antiwear performance of F-ZDDP. F-ZDDP being new, its interactions with other additives in the lubricant are still unknown and therefore this study attempts to develop a better understanding of the influence of antioxidants on the antiwear performance of F-ZDDP. Another central part of this investigation is the study of the oxidation stability of the base oil to which F-ZDDP has been added. This examination is necessary since poor oxidation stability could lead to the formation of deposits, sludge and corrosive acids in the oil which in turn increases wear in the mechanical system [18]. The oxidation stability of a lubricant is also an important indicator of its service life.

1.3 Outline of Proposed Research

The presence of P-F bonds in F-ZDDP was first detected as a result of the unique fluorination process at UTA. This new discovery opens up fresh avenues of investigation into the antiwear performance of F-ZDDP in the presence of various lubricant additives, chief among them being antioxidants. This research presents findings on the antiwear performance of F-ZDDP in the presence of various antioxidants. These formulations have never been previously attempted nor have their performance been evaluated. This work aims to establish the superiority of the antiwear properties of F-ZDDP over that of ZDDP in the presence of antioxidants, and does so through novel approaches to chemical and mechanical characterization of tribofilms. The antiwear performance of ZDDP through thermal or tribological breakdown in the presence of other additives is a very complex process and much effort has been previously dedicated to understanding the mechanism of its degradation and interaction with these additives [16, 19]. The behavior of ZDDP is therefore a good reference to

which the properties of the newly synthesized compound F-ZDDP may be compared. In this study, the interaction of antioxidants with ZDDP and F-ZDDP and the resulting effects on the antiwear performance of these respective formulations are investigated by using the antioxidant alkylated diphenyl amine (ADPA). Test apparatus such as ball-on-cylinder lubricity evaluator (BOCLE) were custom-built at UTA to serve the unique test conditions of this research. These equipments allow evaluation of oil performance in nominal amounts (< 100 ml) and in a closed system. These conditions help understand the changes that the oil undergoes throughout its operational lifecycle. Initial results of wear tests at UTA showed that F-ZDDP exhibits better wear performance over ZDDP in the presence of this antioxidant in the base lubricating oil. This encouraging outcome paved the way for a detailed exploration and analysis of the antiwear performance of F-ZDDP in the presence of alkylated diphenyl amine.

In the first part of this research, the interaction of ZDDP and Fluorinated ZDDP with alkylated diphenyl amines are investigated chemically using nuclear magnetic resonance (NMR) spectroscopy techniques. The antiwear performance under boundary conditions is evaluated using a custom-built ball-on-cylinder lubricity evaluator developed at UTA. The tribofilm formed under boundary lubrication was studied using Auger electron spectroscopy (AES), scanning electron microscopy (SEM) and transmission electron microscopy (TEM).

In the second part of the work, nanoscale mechanical properties of *in-situ* tribofilms generated from ZDDP and F-ZDDP with antioxidants are examined and the results are compared with tribofilms generated from ZDDP and F-ZDDP in the absence of the same antioxidant. Most research efforts by various groups in this field have mainly focused on nanoindentation as a means of finding the mechanical properties of the film. This research introduces new mechanical characterization techniques such as nanoscratch and nanowear tests which are necessary to understand the abrasion resistance of the tribofilm, its adhesion to the substrate and its uniformity. Tribofilms with thickness ranging from 100nm to 200nm are developed *in-situ* during wear tests using ZDDP and F-ZDDP and the influence of alkylated

diphenyl amine on the formation and properties of these tribofilms is examined. To develop an understanding of the effect of various variables on the nature of the tribofilms, the nanomechanical properties including the hardness, modulus, scratch resistance and nano-wear resistance of the films formed from ZDDP and F-ZDDP in the presence of the antioxidant alkylated diphenyl amine are examined with the goal of comparing the results to films obtained from ZDDP and F-ZDDP without antioxidant under similar conditions. In addition to the nanomechanical properties of the tribofilms, morphology and chemical composition of the tribofilms play a role in determining their properties. Therefore, focused ion beam (FIB) is also used to image the substrate-tribofilm interface and thus measure the thickness of the tribofilms. The elemental distribution depth profile of the film is analyzed using Auger electron spectroscopy and the nature of the wear debris is analyzed using transmission electron microscopy.

In the third part of this study, the oxidation stability of F-ZDDP in the presence of antioxidant is investigated and compared against that of ZDDP with antioxidant. Oxidative degradation reduces the effectiveness of lubricants, increases acidity and viscosity, and contributes to the formation of sludge and deposits. All these oil insoluble compounds lead to increased wear in mechanical systems. Analysis of a lubricant's oxidation stability therefore contributes to a better understanding of its effectiveness under normal operating conditions. Oxidation studies are generally performed through accelerated aging of oil samples under high temperatures in the presence of controlled amounts of air. These samples are then measured for changes in viscosity, total acid number (TAN) and wear volume, which in turn may be used to assess the stability of the oil and its suitability for formulating automotive lubricants. The types of oxidation products formed are identified using Fourier transform infrared spectroscopy (FT-IR) and the nature of the tribofilms is studied using X-Ray near-edge absorption spectroscopy (XANES).

CHAPTER 2

OVERVIEW OF TRIBOLOGY CONCEPTS

The genesis of the term 'Tribology' is attributed to the Greek word 'tribos', meaning to rub or slide [20]. This comparatively new branch of science dealing with the study of interacting surfaces in relative motion is instrumental in understanding and explaining the role of lubrication in automotive technologies. This chapter therefore provides a brief introduction to the fundamental concepts of tribology, with particular emphasis on topics relating to automotive lubrication. The basic principles of friction and wear are first reviewed, followed by an overview of tribofilms and the different regimes of lubrication. A description of the important properties of ZDDP, its molecular structure, and its role as a key antiwear agent in formulated lubricants are then provided. A similar outline of the properties of F-ZDDP is given, and its antiwear properties are visited. The theory of oxidation stability and the importance of its study to the performance of automotive lubricants are then described.

The latter part of this chapter presents a concise explanation of some of the instrumental analysis methods employed in this research. Additionally, novel nano-mechanical characterization techniques that are employed to evaluate the nano-scratch behavior and nano-wear resistance of tribofilms are explained.

2.1 Friction and Wear in Tribosystems

Automotive technologies for transportation inevitably involve mechanical motion, which in turn entails varying degrees of contact and interaction between different types of surfaces, often under environments of extreme pressure and high load-bearing stresses. The rubbing components and their constituent contacting surfaces together with any lubricants and other materials (such as debris) present in the interacting environment is often collectively referred to as a tribosystem. An unavoidable consequence of contact between moving surfaces is a force

resisting this relative motion. This force is called friction. Internal combustion engines – which are thermally and mechanically quite inefficient to begin with – are particularly susceptible to significant energy losses due to friction. In addition to energy losses, friction has the undesirable effect of causing wear in various mechanical components of engines. Mechanical losses due to friction in valve trains, piston assemblies and bearings account for nearly 12% of the total power dissipated in such engines and 80% of its mechanical losses [21]. Given the global scale of internal combustion engine usage, this level of energy wastage easily translates to billions of dollars in worldwide economic overhead, not to mention the environmental costs involved. It is therefore evident that even incremental improvements in engine efficiency could go a long way in reducing overall fuel consumption and emissions while enhancing the average lifespan of automobile powertrains. Figure 2.1 illustrates this distribution of typical energy losses in these engines.

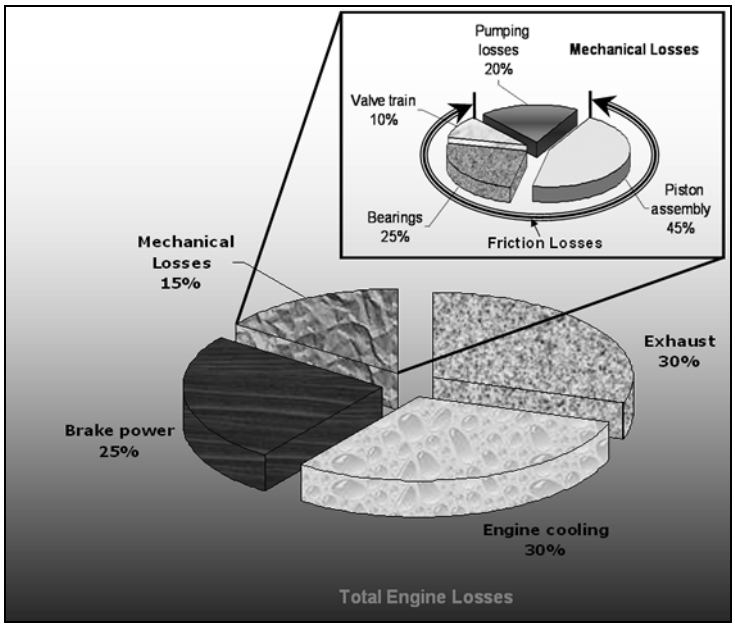

Figure 2.1: Distribution of typical energy losses in an internal combustion engine.

For example, one analysis reveals that increasing mechanical efficiency by 5% through improved lubrication in worm gear drives in the United States alone would result in savings of

about US$600 million per year [20]. In another study conducted by the United States Department of Energy, it was estimated that the US economy could see savings to the tune of US$120 billion as a result of lowering friction and wear in engines and drive train components [22].

2.1.1 Wear Modes and Mechanisms

Wear has been defined as “the phenomenon of material removal from a surface due to interaction with a mating surface” [23]. Wear mechanisms may be explained by taking complex changes during friction into account. In practice, wear hardly occurs as a result of a single mechanism. Moreover, when multiple modes and mechanisms are in effect, the dominant mode may change over time as a result of alterations in surface material properties and dynamic system responses. It therefore is quite important to understand the various wear modes and mechanisms that could occur under such diverse operating conditions. *In all cases, it is very important to note that wear is not a material property; instead, it is a system response* [24].

One of the ways in which wear occurs involves microfracture-induced physical separation which causes removal of material from contacting surfaces. Physical separation could be due to ductile, brittle or fatigue fracture. Chemical dissolution also causes wear, as does melting due to various causes, one of which is friction-induced heat at the interface between interacting entities. The former process could occur due to oxidation and diffusion, while the latter may be observed in conditions where lubrication is lacking or absent, or in sustained high-temperature operating environments.

Wear is often studied from the perspective of different contact configurations such as unidirectional and reciprocal sliding and rolling, compression and separation along the normal or inclined directions and rolling with slip. Contact configurations may also include free solid particles that attack interacting surfaces. Wear encountered in such configurations may be expressed as sliding, rolling, impact, fretting or slurry wear. These expressions are not accurate

scientific representations of wear mechanisms; rather they are mere descriptions based on the appearance of the contact configurations. In order to examine wear mechanisms from the standpoint of a generalized nature of contact configurations, it is useful to classify actual and apparent contact conditions at the interacting interfaces. One simple condition deals with the severity of contact and the resulting deformation state, and may be classified into two broad types, namely elastic and plastic contact conditions. Such a condition is a tribological system response as a function of dynamic, material and environmental parameters.

Four fundamental and major wear modes have been generally recognized and broadly accepted. These are [25], adhesive, abrasive, fatigue and corrosive wear. Figure 2.2 presents a schematic representation of the four wear modes that may be encountered in a system.

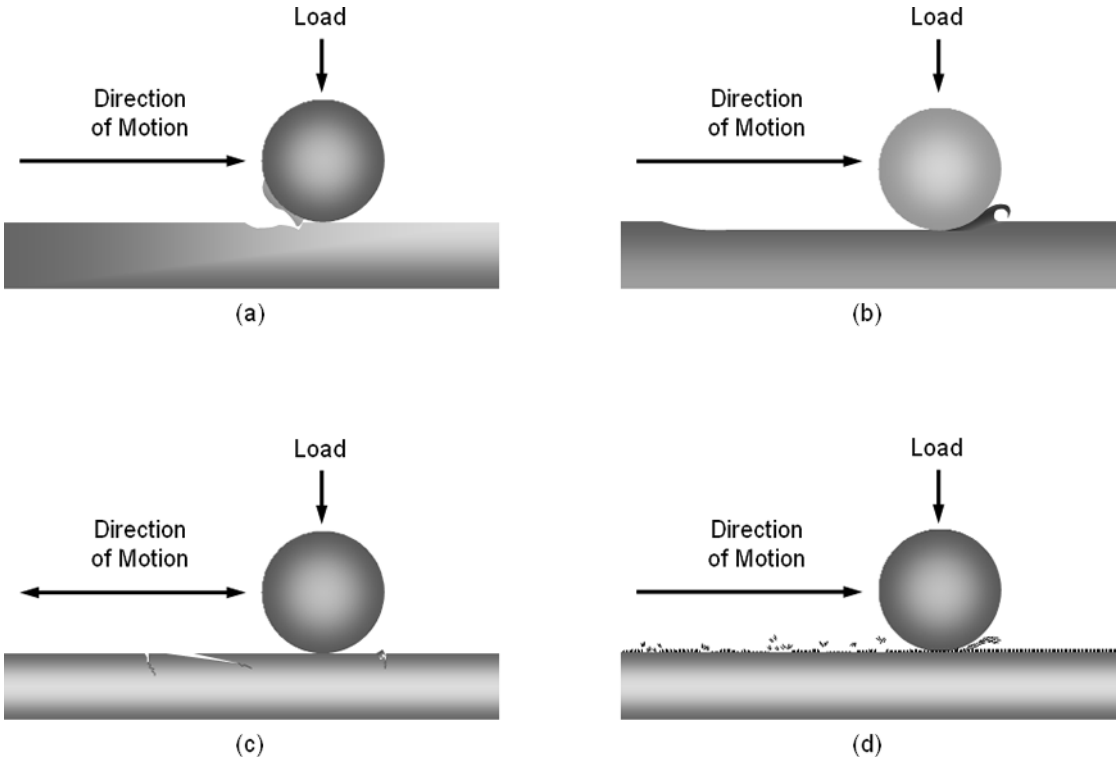

Figure 2.2: Wear modes in tribosystems: (a) adhesive wear; (b) abrasive wear; (c) fatigue wear and (d) corrosive wear.

Adhesive wear is a mode that is generated under plastic contact [23]. This type of contact between similar materials gives rise to adhesive bonding at the contact interface. For

example, breakdown of lubricating films hampers smooth relative movement between solid objects, thereby serving to greatly increase the adhesive force between their interacting surfaces. Wear due to film failure is typically quite severe in nature. When this scenario results in fracture at one or both of the interacting surfaces, the ensuing wear is known as adhesive wear, regardless of the nature of the fracture.

When a hard material comes into plastic contact with a relatively softer material, the relative motion between these two surfaces causes the former to penetrate or plough into the latter. The outcome of fracture due to such forces is known as *abrasive wear*, irrespective of the fracture mode encountered. The byproducts of such abrasive forces are asperities and wear debris, which in the case of relatively ductile metallic surfaces are much harder than the surfaces they originated from. This is because these asperities are generally work-hardened and turn brittle quickly due to oxidation. In the case of lubricating films, such wear can therefore occur when hard particles are present in significant quantities and flows only against one of the interacting bodies without supporting the other. Related forms of abrasive wear are erosive wear, which is caused by impacting particles and cavitation wear, which is brought about by fast-flowing liquids.

The operational effectiveness of a lubricating film may sometimes be below desired levels, resulting in greater-than-normal frictional forces between interacting surfaces. In such a scenario, repeated stresses and recurring friction cycles often cause fatigue and surface failure, thereby generating *fatigue wear*. This form of wear is milder than the others and can be observed in both elastic as well as plastic contacts.

In some cases, interacting surfaces may undergo undesired chemical reactions, the results of which may initially serve to provide some lubrication, but eventually bring about substantial wear in the long term. The ensuing loss of material is said to be due to *corrosive wear*. Both plastic and elastic contacts can give rise to corrosive wear. Sometimes, these chemical reactions are accelerated or highly activated by friction-induced deformation and

heating, microscopic fractures or consecutive depletion of reaction products. In air, the leading corrosive agent is oxygen and hence when this phenomenon occurs in an atmospheric environment, it is known as oxidative wear.

Wear may be further classified on a macroscopic level into mechanical, chemical, and thermal wear. Since adhesive, abrasive, fatigue wear occur due to fracture, these modes therefore fall under the classification of mechanical wear. On the other hand, corrosive wear is usually considered to be chemical wear or tribochemical wear. Alternately, when wear is induced by thermal stresses or elevated temperatures due to friction, it is categorized as thermal wear.

2.1.2 Evaluation of Wear

Wear is typically quantified by the amount of material lost during surface interaction. The quantity of material removed from the original surface is measured in terms of wear volume. Together with the nature of wear surface roughness and wear particle shape, wear volume provides important data that is instrumental in the characterization of wear. Wear volume may be analyzed as a function of sliding distance or contact cycles, and such a plot of the former versus the latter is known as a wear curve. The slope of a wear curve gives information about the rate at which material is lost, or in formal terms, wear rate. Wear rate is therefore the wear volume per unit distance traveled across the surfaces of the interacting components. When this wear rate is measured per unit load, it is termed as specific wear rate. Wear coefficient is then defined as the product of the specific wear rate and the hardness of the wearing material [23].

2.1.3 Wear Stages in Tribology

During the lifecycle of tribosystems, at least three distinct stages of the wear process may be identified. The break-in or run-in stage occurs at the beginning of the operational lifecycle and involves high rates of wear. At this stage, asperities on interacting surfaces induce significant abrasion in the course of creating conformal surfaces wherein the load is more

favorably distributed across these surfaces. In lubricated tribosystems, this period is marked by the formation of hitherto absent low-friction protective films known as tribofilms. During this phase, conditions are being set up for the next steady-state wear stage. The duration of this stage in most tribosystems is typically very short when compared to the overall lifecycle of the wear process. Yet, this short period plays an important role in fostering the necessary conditions to initiate and sustain tribochemical reactions imperative to the formation of lubricating anti-wear tribofilms. These tribofilms are crucial components that serve to protect surfaces and prolong the service life of these tribosystems during later stages of the wear process.

After the brief break-in period, the steady-state stage comprises the longest period of the tribological lifecycle in most systems. Here, the wear rate nearly levels off and friction values are relatively low. In lubricated tribosystems, this stage is sustained by the presence a tribofilm between interacting surfaces. One way in which these tribofilms work is by providing a durable low-friction sliding interface between the otherwise contacting surfaces, thereby considerably lowering the wear rate. Another way they operate is by acting as a sacrificial layer that wears out in place of the adjacent metallic surfaces, but is constantly replenished at the same rate as the wear process.

To the extent that conditions favor continued efficient operation of tribofilms or support an environment amenable to sustained tribofilm replenishment, the steady-state wear stage will continue. On the other hand, when steady-state wear eventually alters the mechanical clearances and surface properties to the point that continued lubrication is no longer possible, the protective tribofilm fails, resulting in a short-lived catastrophic stage in which extreme wear rates cause severe and irreversible surface damage. This stage then marks the end of the useful service life of the tribosystem and usually the larger machinery of which it is a part. Figure 2.3 describes the nature of wear rates during each of these three stages in a tribosystem.

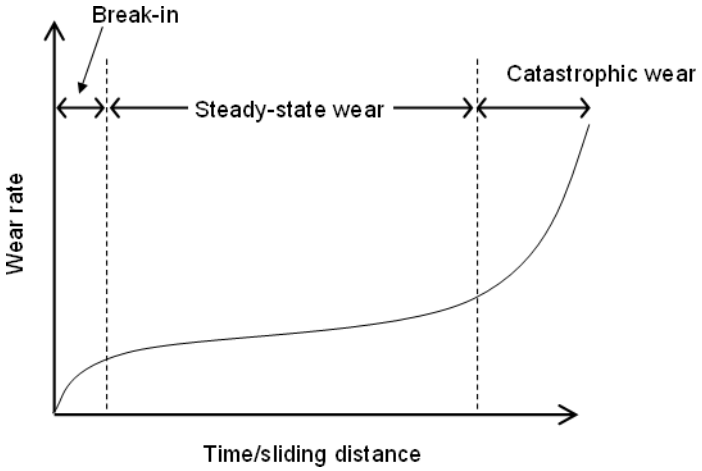

Figure 2.3: Wear rate as a function of time during various wear stages in a tribosystem.

Of the three wear stages, characterization of long-term tribological properties is best served by studying wear rates and friction forces during the longer and more stable steady-state conditions [23]. In automotive systems, this period encompasses the useful lifetime of engines and associated machinery.

2.2 Automotive Lubrication

Lubrication involves the practice of reducing friction coefficients between interacting surfaces under load to such a low degree that wear rates are diminished significantly, thereby sustaining efficient operation of the tribosystem. Lubrication is achieved by introducing a material known as a lubricant between the sliding surfaces. This material may be either in solid or liquid form and sometimes may comprise of a combination of both forms. In some environments, gases may also be used as lubricants.

Automotive machinery such as engines and bearings employ liquid lubricants for their lubrication needs. In addition to reducing friction and wear, these lubricants work to redistribute loads in the tribosystem, carry away or dissolve contaminants such as wear debris and dissipate the heat generated during normal operation. The most common base material for these lubricants comes from mineral oils. However, recent advances have seen the

introduction of synthetic base oils that exhibit superior performance compared to their mineral oil based counterparts.

The choice of lubricant for a particular application is determined by factors such as the environment in which the lubricant is expected to function, including the temperature and pressure ranges demanded by the application and the type of lubricant - whether solid or liquid - that best serves the needs of the system. Some important properties of lubricants that play a critical role in determining the lubricating material for an application are therefore discussed in this chapter.

2.2.1 Viscosity of Lubricants

Viscosity is arguably the most important parameter that defines the lubricating capability of engine oils. It is measured in terms of the resistance of a fluid to deformation under the influence of external stresses, most notably shear stress. Fluids that exhibit high viscosity are said to be "thick" whereas those with low viscosity are considered "thin" fluids. For engine oils, it is important that the viscosity must be high enough to maintain a satisfactory lubricating film, but low enough that the oil can flow around the engine parts satisfactorily to keep them well coated under all conditions. In addition, the accurate determination of viscosity of many petroleum fuels is important for the estimation of optimum storage, handling and operational conditions.

Oil viscosity is susceptible to changes with temperature, pressure and shear rate. In tribosystems, the thickness of the lubricating film is usually proportional to these parameters. In this section, a simplified model of viscosity for Newtonian fluids - one in which the rate of shear and flow are always directly proportional to the applied stress - is discussed. This model is valid for most automotive tribological applications. Consequently, two types of viscosity measures are briefly described herein.

2.2.1.1 Dynamic Viscosity

Dynamic viscosity is defined as the ratio of the shear stress acting on the fluid to the shear rate. To illustrate, consider the tribosystem shown in Figure 2.4, where two flat interacting surfaces with wetted contact area A are separated by a lubricating fluid film of thickness d. The force F required to move one of the surfaces is directly proportional to the relative velocity v and the wetted area, and may be expressed as

$$F \quad \alpha \quad A \times \frac{v}{d} \tag{2.1}$$

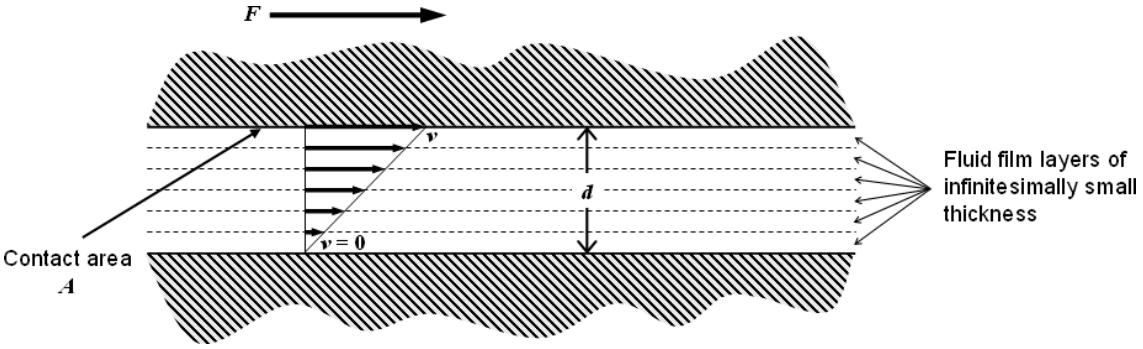

Figure 2.4: Schematic representation of fluid film between two interacting surfaces.

Most fluids exhibit this relationship, the key distinction between different fluids manifesting in the form of a proportionality constant 'η'. This constant is the defining parameter of the fluid's viscous properties and is known as dynamic viscosity. The force F is then given by

$$F \quad = \quad \eta \times A \times \frac{v}{d} \tag{2.2}$$

The shear stress τ acting on the fluid is given by $\tau = F/A$. Rearranging terms and using this relationship for shear stress, the dynamic viscosity may be expressed as

$$\eta \quad = \quad \tau \times \frac{v}{d} \tag{2.3}$$

The dynamic viscosity η of a Newtonian fluid is thus seen to be the ratio of the shear stress τ to the shear rate (v/d). Prior to the advent of the SI system, the unit for dynamic viscosity was the

Poise (P) [20]. A smaller unit, the centiPoise (cP) was more commonly used to better represent viscosity values found in most practical applications. Today, the SI unit for dynamic viscosity is Pascal-second (Pas).

2.2.1.2 Kinematic Viscosity

In quantifying viscosity, one can also take into account the density of the fluid. In this case, the resulting parameter is known as kinematic viscosity, and is defined as the ratio of the dynamic viscosity to fluid density. The unit for kinematic viscosity that has found the most widespread use is the Stoke (S). Since the Stoke is a large unit when it comes to representing the dynamic viscosity in most situations, a smaller unit called the centiStoke (cS) is often employed. The SI unit for kinematic viscosity is m^2/s [20].

It may ostensibly seem that the thicker the tribofilm and therefore greater the viscosity, the better the lubrication properties achieved in a tribosystem. However, thicker fluids have greater shear resistance, thereby requiring more energy to provide sliding action between contacting surfaces. One byproduct of such power consumption is greater heat generation resulting in elevated temperatures, thereby potentially harming the machinery. On the other end of the spectrum, too thin a lubricant would hardly generate adequate film thickness needed to support the contact loads, thereby resulting in increased wear. It is therefore important to choose lubricants with the right viscosities for a particular application, a decision that is made all the more difficult due to the acute dependence of an oil's viscosity on operating temperatures.

2.2.2 Viscosity-Temperature Dependence

The viscosity of lubricating oils is extremely sensitive to the operating temperature and has an inverse relationship to it. In some instances, an oil's viscosity can drop by nearly 80% with just a short temperature increase of 25°C [20]. Determination of the lubricant viscosity at any given temperature may either be computed with the help of viscosity-temperature equation, or through viscosity-temperature charts published by the American Society for Testing and Materials (ASTM). Among the several available viscosity-temperature equations, some are

derived from theoretical models, while others are purely empirical. The earliest among them is the Reynolds equation, which presently finds only limited use due to it's applicability for only a narrow temperature range. Today, the Vogel equation finds the greatest use in engineering applications as it is the most accurate among all the different equations available.

2.2.3 Viscosity Index

The viscosity index (VI) is an entirely empirical, yet widely accepted approach to describing the temperature response of the viscosity of an oil. A higher value of viscosity index indicates lower viscosity variation across a range of temperatures, and vice versa. Therefore, oils with higher VI values are preferred, as it means that its lubricating properties are more consistent for a given temperature range, or alternately, these oils could potentially be utilized over a larger range of temperatures.

Viscosity index is obtained by comparing the kinematic viscosity of the oil under test to that of two reference oils. These reference oils are such that the temperature sensitivity of their viscosity is significantly different from each other. The reference oils are chosen in such a way that the VI of one of them equals zero, while the VI of the other equals 100 at 100°F (37.8°C), but both have the same viscosity at 210°F (98.89°C) as the oil under test [20]. The viscosity index is then obtained by the relation

$$\mathrm{VI} = \frac{(\mathrm{L}-\mathrm{U})}{(\mathrm{L}-\mathrm{H})} \times 100 \tag{2.4}$$

where U is the measured kinematic viscosity of the test oil at either 40°C or at 100°C, and L and H are the corresponding values of the reference oils at 100°C, obtained from ASTM D2270 tables. In formulated oils, additives are often introduced to improve the VI of the lubricant.

A related property of oil is its pour point. This is the minimum temperature that enables a liquid lubricant to flow, or be pumped. It is an important indicator of the minimum achievable operating temperature of the lubricant.

2.2.4 Hertzian Model of Contact Stresses

A large volume of engineering applications involve non-conformal contact between interacting surfaces, examples of which may be found in gears, cams and rolling contact bearings, among others. The tiny contact areas involved inevitably give rise to very high operating pressures in such systems. Given that any two contacting surfaces under load will undergo elastic or plastic deformation, it becomes critical from a design perspective to accurately model the stresses encountered in these tribosystems for such applications. Analytical formulae based on the theory of elasticity were derived by Hertz in 1880 [26] to model these stresses. The Hertzian model of contact stresses makes the following simplifying assumptions [27].

- Contact stresses are primarily due to normal loads (tangential forces are absent),
- The interacting surfaces are made of homogeneous materials,
- The stresses involved are below the yield stresses of the materials,
- The contact area is much smaller than the contacting entities,
- Surface roughness has negligible effect,
- The contacting entities are at rest and in equilibrium.

This model has subsequently been refined by other researchers, but the basic principles continue to form the foundation of stress modeling in machine design to this day.

2.2.5 Lubrication Regimes

The nature and magnitude of the load between contacting surfaces give rise to different lubrication conditions, which may be broadly classified into different lubrication regimes. These are described herein.

2.2.5.1 Fluid-Film Lubrication

In this regime, the contact loads between the sliding surfaces is fully supported by a thin liquid film between them. Under this condition, direct contact between the metallic surfaces is avoided. This is therefore the preferred mode of operation since the lack of direct metal-to-

metal contact results in minimal wear in the system. Fluid-film lubrication may be further categorized into hydrodynamic and hydrostatic lubrication regimes.

Hydrodynamic lubrication is the scenario where no external pressure is required to maintain an operational, load-bearing fluid film between sliding contacts. The relative velocity between the metallic surfaces causes fluid flow to be directed into the convergent gap between the sliding components. In order to sustain hydrodynamic lubrication, sufficient relative velocity is therefore necessary between the sliding surfaces to enable continuous film formation. As long as sufficient relative velocity, proper lubricant viscosity, adequate film thickness and lubricating properties are maintained, this form of lubrication can theoretically prolong the service life of machinery for indefinite periods of time.

A special case of hydrodynamic lubrication called elastohydrodynamic lubrication occurs when elastic deformation of the contacting surfaces together with notable changes in lubricant viscosity under pressure play an important role in the tribosystem. Under such conditions, a fluid film is present and provides relatively effective lubrication, albeit with greatly reduced film thickness. This phenomenon was first observed in cases where the wear rates were very low, yet the calculated film thickness was much less than what was then theoretically accepted as required for effective wear mitigation. The lubricating film in this case is normally very thin (less than 1μm thick) compared to the film thickness encountered in hydrodynamic lubrication [20].

A lubrication regime in which external pressure is required to keep the lubricant in the conjunction between the metallic surfaces is known as hydrostatic lubrication. The amount of load that can be borne is independent of film thickness and therefore this type of lubrication is capable of supporting very large loads. The main drawback is that ancillary equipment is generally needed to maintain the pressure so that an effective film may form between the sliding contacts.

2.2.5.2 Boundary Lubrication

Sometimes, tribosystems may encounter a scenario where a complete fluid film does not or hasn't yet formed between the contact surfaces. This regime is known as boundary lubrication, and is encountered when the depth of the composite surface coarseness is greater than the average lubricating fluid film thickness [28]. Such scenarios witness direct physical contact between the surface asperities when these surfaces slide against each other. Even though fluid-film lubrication is preferred, boundary lubrication conditions are sometimes unavoidable. For example, during starting and stopping of engines, boundary lubrication conditions are observed when relative sliding velocities required for successful hydrodynamic lubrication are not yet or no longer in effect. Boundary lubrication regimes may often be found in extreme-pressure environments involving bearings, piston rings and cylinder-wall interfaces, transmissions and cams, to name a few.

In most practical tribosystems, multiple regimes are often simultaneously in effect - in other words, some asperities are in the hydrodynamic mode, some others in elastohydrodynamic mode and yet others in boundary lubrication mode. This situation is referred to as a mixed lubrication regime.

Lubrication regimes are characterized using a controlling parameter known as the Stribeck number, which is quantified as [20],

$$\text{Stribeck number} = \eta\frac{U_S}{W} \tag{2.5}$$

where η is the dynamic viscosity of the lubricant, U_s is the sliding speed of the interacting surfaces and W is the pressure or load in the tribosystem. A plot of friction coefficient versus Stribeck number is called the Stribeck curve and is a useful representation illustrating the domains of the various lubrication regimes.

2.3 Lubricant Additives

Contemporary lubrication technology has witnessed performance enhancement of automotive lubricants through the use of various additives. Some of the main goals that these formulated lubricants are intended to address may be listed as follows:

- Reduction of friction and wear, and prevention of equipment failure,
- Enhancement of oxidation stability, thus prolonging the service life of the oil,
- Corrosion inhibition,
- Improvement of the viscosity index of the lubricant,
- Lowering of the pour point of the oil and,
- Restriction of contamination by wear particles and reaction products.

Additives which improve wear and friction properties are probably the most important of all the additives used in oil formulations [20]. They control the lubricating performance of the oil. The presence of these additives in optimum amounts is very important for safe operation of engines, as oil without these additives could lack proper lubricating ability, resulting in excessive wear and friction almost as soon as the oil is introduced into the machine.

There are three different types of boundary lubricant additives available, whose use in tribosystems depends on the severity of the condition in which they are employed. The types of wear and friction additives commonly used include:

- Adsorption or boundary additives,
- Extreme pressure additives
- Anti-wear additives

2.3.1 Adsorption or Boundary Additives

Adsorption or boundary additives are added to the lubricant to control the adsorption type of lubrication. These additives are sometimes referred to as ‘friction modifiers’. Their main use in the lubricated system is to prevent the occurrence of slip-stick phenomenon. The most common of these types of additives are fatty acids and the esters and amines of the same fatty

acids, e.g., stearic acid derivatives such as methyl and ethyl stearates. They usually have a polar group (–OH) at one end of the molecule and react with the contacting surfaces through the mechanism of adsorption [20]. The important characteristic of these additives is an unbranched chain of carbon atoms with sufficient length to ensure a stable and durable film. Adsorption additives are very sensitive to the effects of temperature and find use only at relatively low temperature and loads. Usually, they lose their effectiveness at temperatures between 80°C and 150°C depending on the type of additive used. The critical temperature at which these additives become ineffective can be altered by changing the concentration of additives, i.e. a higher concentration results in a higher critical temperature, but the cost is also increased.

2.3.2 Extreme Pressure Additives

Extreme pressure (EP) additives are designed to react with metal surfaces under extreme conditions of load and velocity, i.e. slowly moving, heavily loaded gears. EP additives usually contain non-metals such as sulphur, antimony, iodine or chlorine [20, 23]. As extreme conditions of load and velocity increase, the operating temperature rises and the metal surfaces in contact become very hot; this makes the EP additives to react with exposed metal surfaces resulting in a protective film of low shear strength on the surface. As the reaction between the extreme pressure additive and metal surfaces is a mild form of corrosion, balanced concentration of the additive is necessary. If the concentration of EP additive is too high, then excessive corrosion may occur. However, with low concentrations of the additive, the surfaces may not be fully protected and failure could result. EP additives, if they contain sulphur or phosphorus, may suppress oil oxidation but decomposition of these additives may occur at even moderate temperatures. There are several different types of EP additives currently used in oils. The most commonly used are dibenzyldisulphide, phosphosulphurized isobutene, trichlorocetane and chlorinated paraffin, sulphurchlorinated sperm oil, sulphurized derivatives of fatty acids and sulphurized sperm oil, cetyl chloride, mercaptobenzothiazole, chlorinated wax,

lead naphthenates, chlorinated paraffinic oils and molybdenum disulphide [29]. Molybdenum disulphide is one of the most commonly used extreme pressure lubricant additive which provides lubrication at high contact stresses. It functions by depositing a solid lubricant layer on the contacting surfaces. It is non-corrosive but very sensitive to water contamination, as water causes the additive to decompose.

2.3.3 Anti-Wear Additives

In order to protect contacting surfaces at higher temperatures, several different types of anti-wear additives are currently used in oil formulations. The most commonly used anti-wear additive in engine oil is zinc dialkyldithiophosphate (ZDDP) [20, 23]. In gas turbine oils, tricresylphosphate or other phosphate esters are used. Additives containing phosphorous find use in lubricants when antiwear protection in relatively low load (mild wear) conditions is required. These additives react with the surfaces through the mechanism of chemisorption and form a protective sur6face layer which is much more durable than that generated by adsorption or boundary agents. Examples of these additives include zinc dialkyldithiophosphate, tricresylphosphate, dilauryl phosphate, diethylphosphate, dibutylphosphate, tributylphosphate and triparacresylphosphate. These additives are used in concentrations of 1% to 3% by weight. Tricresylphosphate (TCP) has been used as an anti-wear additive for more than 50 years. It functions by chemisorption to the operating surfaces and is very effective in reducing wear and friction at temperatures up to about 200°C [20].

2.3.4 Antiwear Additives and Boundary Lubrication

Technical studies have shown that a significant portion of wear (nearly 70%) in engines occurs during the brief start up and acceleration periods [30]. This is because there is not enough oil present in bearing and on surfaces of the cylinder to provide effective fluid film lubrication during these times. This situation results in asperity–asperity contact at these locations i.e., boundary lubrication regime. Control of wear in this regime requires the addition of antiwear additives which can form a protective film under these conditions [30]. The general

antiwear action has been identified to be of two types by Martin et al., depending on the chemical nature of antiwear additives [30, 31]:

1. Formation of tribofilms by a tribochemical reaction processes involving an active participation of both the contact surface material(s), environmental factors (atmosphere, water etc) and their chemical interaction with the anti-wear additive. Depending on the type of the additives and nature of their reactions with surfaces, this results in two types of mechanisms as explained below:
    i. Additives that chemically react with the surface directly e.g. sulphur and chlorine chemical compounds, fatty acids, fluorinated compounds.
    ii. Anti-wear action by the additives through thermal and/or oxidative degradation process of the additive e.g. Metal Dithiophosphates (ZDDP) and phosphorus containing organic compounds.
2. In the case of polymeric and non-sacrificial films, contact surfaces do not chemically participate in the formation of the anti-wear film, although they may catalyze the process. This process also involves formation of high molecular weight compounds through polymerization process, e.g., complex esters, solid lubricant additive like oil soluble molybdenum compounds, borate additives, double bond containing molecules, etc.

Of all the antiwear agents discussed so far, ZDDP has been the most cost effective and is extensively used in the engine oil for both its excellent antiwear and antioxidant properties. The following section introduces the structure of ZDDP and some of its important film formation mechanisms.

2.4 Zinc Dialkyl Dithio Phosphate

2.4.1 Chemical structure and properties of ZDDP

The general chemical structure of ZDDP [4] is shown Figure 2.5.

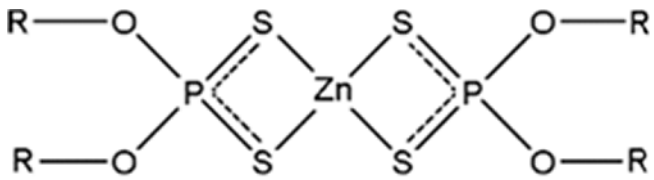

Figure 2.5: Structural formula of (neutral) ZDDP. R = 1°,2°,3° alkyl or aryl group.

In this figure, R represents alkyl or aryl groups. In the case of alkyl ZDDPs, these alkyl groups can be primary, secondary or tertiary alkyl groups. The presence of these R groups (as well as the chain length) in the structure of ZDDP [5, 32] depends on types of the alcohols used in the manufacturing of ZDDP [4]. ZDDP is usually manufactured by a reaction of phosphorus pentasulfide with suitable alcohols, with dialkyldithiophosphates as intermediates. It has been observed that the antiwear activity of ZDDP (inversely proportional to thermal stability) is dependent on the alkyl group of the structure [5]. Shown below is the ranking order of their antiwear effectiveness.

secondary alkyl > primary alkyl > aryl.

The above order ranking also holds good for their hydrolytic stability with secondary alkyl ZDDP representing better hydrolytic stability than others. Besides the classification based on the presence of alkyl groups of ZDDP, commercially available ZDDP belongs to two types, namely neutral ZDDP with formula – $[(RO)_2PS_2]_2Zn$ and basic ZDDP – $[(RO)_2PS_2]_6Zn_4O$ [4]. Both NMR [33, 34] and vibrational spectroscopy have shown that neutral ZDDP exists as an equilibrium between monomer and dimer in relatively polar solutions, as illustrated in Figure 2.6.

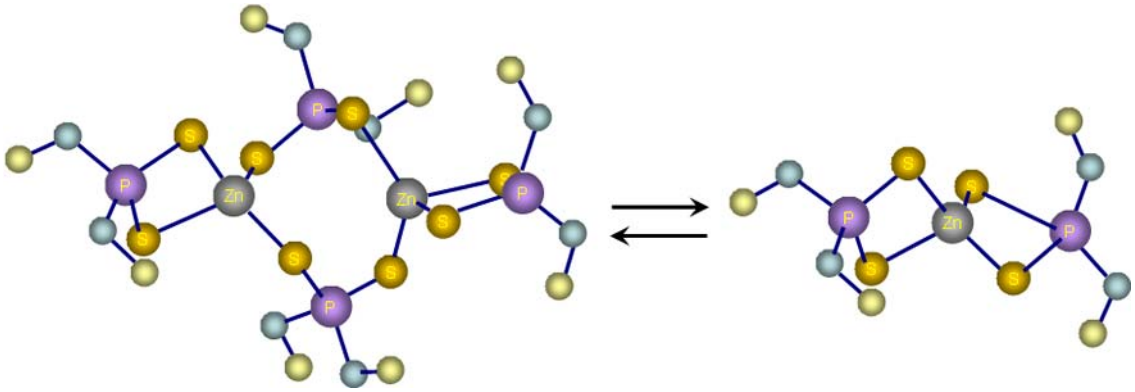

Figure 2.6: Monomer–dimer structure equilibrium of neutral ZDDP

This equilibrium moves to favor the monomer as the temperature is increased and in both structures, four sulphur atoms are arranged equivalently in a tetrahedron around the zinc atom. Figure 2.6 shows the structure of ZDDP in polar solutions; recent studies using dynamic light scattering method has suggested that there may be tetrameric or even higher ZDDP structures present in low polarity mineral oil solutions [35].

Basic ZDDP has the linear formula $[(RO)_2PS_2]_6Zn_4O$. A Zn_4O core with four Zinc atoms in an almost prefect tetrahedral arrangement about a central oxygen atom constitutes the structure of basic ZDDP. Figure 2.7 shows the structure of basic ZDDP in solution [5].

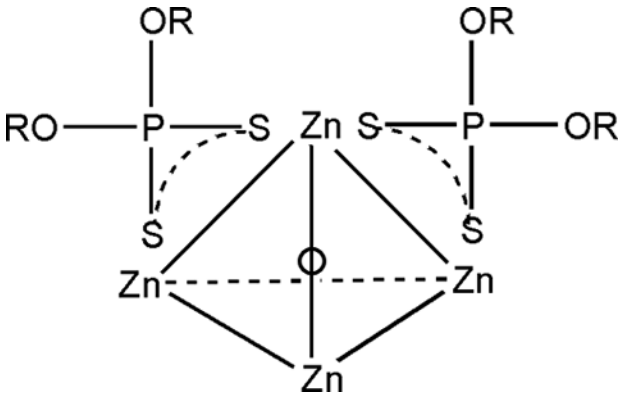

Figure 2.7: Structure of basic ZDDP: basic-ZnDTP, $(DTP)_6Zn_4O$. (2 of 4 DDP ligands shown.)

At elevated temperatures, basic ZDDP has been found to convert to neutral ZDDP and ZnO [36]. A number of studies have examined the antioxidant, film forming [37] and antiwear

properties [38] of basic and neutral forms of ZDDP. NMR studies have shown that equilibrium exists between basic and neutral ZDDP in solution. Studies have shown that basic and neutral forms of ZDDP differs slightly in terms of their levels of reactivity but in terms of antioxidant and antiwear properties they are essentially the same [37-39].

2.4.2 Antiwear mechanism of ZDDP

In general it is agreed that the antiwear activity of ZDDP is to form a wear resistance film on the rubbing surfaces [5, 40]. These films are of two types: (i) extreme pressure (EP) films formed at high local temperatures under extreme contact conditions whose function is to inhibit the onset of scuffing and (ii) antiwear films formed under moderate contact conditions. It is found that ZDDP is a mild EP additive and a strong antiwear agent.

In spite of 60 years of research on ZDDP, the composition and the mechanism controlling the film formation of ZDDP is not very clear. This is in large part due to the fact that decomposition of ZDDP is a complex chemistry which may involve thermal [41], catalytic (by chemisorption on metal) [42-45], hydrolytic [46, 47] or oxidative (by reaction with hydroperoxides or peroxy radical) [46, 48, 49] processes.

2.4.2.1 Thermal Degradation

In the absence of significant level of hydroperoxides or peroxy radicals, ZDDPs is found to react in solution at high temperatures by thermal or thermo-oxidative degradation – where the mechanism involves the exchange between O and S in ZDDP molecules with the alkyl groups which are initially bonded to oxygen atoms in ZDDP, being transferred to the sulphur atoms – leading to the formation of solid zinc phosphate deposits, alkyl sulphides, mercaptans, hydrogen sulphides and olefins [5, 50]. It was found that the temperature of thermal degradation was dependent on the alkyl groups present (and metal cation) but usually occurred between 130°C and 230°C. ZDDP's antiwear activity (and thermal instability) is dependent on the alkyl group structure with the ranking of antiwear effectiveness [5] as follows:

Secondary alkyl > primary alkyl > aryl.

In the 1960s, there was a considerable amount of debate regarding the above mentioned thermal degradation mechanism. However, this mechanism was confirmed by Coy and Jones [51, 52] by the use of ^{1}H and ^{31}P NMR and showed that O/S exchange represents a well-known property of organic thiophosphates.

2.4.2.2 Hydrolysis

Thermal decomposition experiments (in an N_2 atmosphere) carried out by Spedding and Watkins [47, 53] with ZDDP solutions showed that addition of water would accelerate the decomposition of ZDDP. They proposed a hydrolytic mechanism of phosphate formation. Their work showed that ZDDP is not substantially chemically adsorbed on the metal surface but its hydrolytic decomposition products are. Watkins later showed that these decomposition products serve as precursors of antiwear action of ZDDP by interacting with metal surface forming fusible glassy compounds, phosphates and iron sulfide as ternary eutectic with iron oxide. While there is a general agreement that hydrolysis probably plays an important role in film formation, a substantial amount of work shows that ZDDP decomposition by hydroperoxides and free radicals proceeds rapidly at lower temperatures than those required for hydrolysis to proceed at a reasonable rate.

2.4.2.3 Oxidative Decomposition

It has been proposed by Willermet et al [48, 54] that under moderate wear conditions the formation of an antiwear film by ZDDP proceeds by a thermo-oxidative mechanism. In order to prove this they conducted four-ball wear experiments in air and inert atmosphere, and studied the nature of the film formed, by AES. The film formed under air was rich in zinc and oxygen and Auger elemental analysis of the data showed that it is consistent with long-chain polyphosphates. The films formed were depleted in sulphur and rich in oxygen when compared to the original ZDDP, indicating that ZDDP or its decomposition products reacted with hydroperoxides, resulting in the replacement of sulphur bonded to phosphorus by oxygen. The films formed under inert atmosphere were low in Zn, O, and P but rich in S when compared to

the film formed under air. These films were also high in carbon and iron. Wear produced under an inert atmosphere was greater with the generation of soluble iron. All the results from the inert atmosphere were equivalent to the thermal decomposition of ZDDP by producing iron sulphides and organosulphides. By adding hydroperoxide [55] to ZDDP solutions run under an inert atmosphere, the wear performance became equivalent to ZDDP that was run under air, indicating the correlation between antiwear and antioxidant mechanism of ZDDP. Further experiments by Willermet et al confirmed that products from oxidation decomposition were similar to phosphate composition as observed in wear experiments. However, thermal decomposition produced a structure similar to that observed at occasional scuff marks concluding that principal mode of film formation involved the oxidative decomposition of ZDDP.

2.4.2.4 Surface Adsorption

Absorption studies of ZDDP on metal surfaces [44, 45, 56, 57] indicated that the first stage in film formation mechanism ZDDP must be diffusion and adsorption of ZDDP molecules or other moieties on the metal surface. Studies done by Yamaguchi et al showed that the adsorption of ZDDP on iron surface was through sulphur from the P=S bond [57]. Dacre and Bovington studied the adsorption of ZDDP and its decomposition products on ferrous metal over a temperature range of 19–81°C. As the temperature was raised over 60°C, large loss of Zn ions occurred and adsorption became irreversible. In studies by Dacre and Bovington, the coupons used in the experiments were solvent-rinsed before analysis, leaving only species adsorbed on the surface, but removing any potentially ZDDP enriched but weakly bonded near the surface layer. The possibility of existence of such a layer on the metal surface was further investigated by Plaza who examined the adsorption of ZDDP on the iron powder and iron oxide. Plaza by using ^{31}P NMR as an analytical technique found basic ZDDP to be the major P–containing species from ZDDP solution exposed to iron powder at 80°C and 100°C. Willermet supposed that the basic ZDDP found by Plaza resulted from the reaction with basic (hydrated sites) on the iron powder, resulting in a lowered zinc level and increased sulphide at the

surface. Formation of this basic ZDDP in this way suggested the formation of a surface bonded film precursor [40]. Willermet suggested that formation of basic ZDDP would account for the surface Zn depletion reported by Dacre and Bovington. Willermet further proposed the following steps under moderate wear conditions for the mechanism of ZDDP film formation by reviewing his and others' work:

- Adsorption of ZDDP on the metal surface and formation of zinc rich near the surface region.
- Reaction of ZDDP with the metal surface to form phosphate/phosphothionic moieties chemical bonded to the metal.
- Formation of phosphate film precursors from the antioxidant reactions of ZDDP.
- Condensation of phosphates/phosphothionates and their esters, the growing phosphate chains being terminated by reaction with zinc-containing compounds and in the presence of overbased detergents, by reaction with the metal surface.

Apart from the above mentioned theories of ZDDP antiwear film formation, a new theory based on computer simulations of zinc phosphates under extreme conditions suggests that pressure-induced cross-linking is a key mechanism in the formation and functionality of anti-wear tribofilms [58-60].

Despite the enormous amounts of research work to understand the film formation mechanism, to date there no single complete reaction mechanism that has been agreed upon so far. According to Spedding and Watkins [47, 53], this complexity of mechanism is due to two main reasons. First, the antiwear process itself is multidisciplinary and requires knowledge of metallurgy, chemistry, metrology and mechanical design. Second, the ZDDP itself undergoes complex reactions which require the knowledge of the surface adsorption, organic and inorganic chemistry. All these fields are vast in themselves and require a combined expertise before drawing conclusions about entire antiwear mechanisms of ZDDP in tribological conditions.

2.4.3 Antiwear Properties

Thermal degradation studies of ZDDP showed that antiwear effectiveness of ZDDP was inversely proportional to its thermal stability, indicating that thermal degradation was necessary for the generation of antiwear films [5]. Studies have suggested that antiwear behavior of ZDDP results from its ability to form a phosphate film. From current literature, three main ways that ZDDP acts as an antiwear agent have been proposed: (1) by forming a mechanically protective film, (2) by removing corrosive peroxides or peroxy radicals and (3) by digesting hard and thus abrasive iron oxide particles. It is believed that the antiwear action of ZDDP stems from the fact that the tribofilm produced acts as mechanical barrier, thus preventing direct contact between interacting surfaces. With this type of antiwear action, once a ZDDP film forms, it is assumed that practically all subsequent wear that occurs is of the ZDDP film itself.

According to the second proposed mechanism, ZDDP reacts with peroxides in the lubricant and prevents these peroxides from corrosively wearing the metal surfaces. According to the third mechanism, ZDDP tribofilms embed the iron oxide particles (which can cause abrasive wear) and digest them to form relatively soft iron phosphate, thus reducing their harmful wear effect. Depending on the mechanism of their formation on metal surfaces, ZDDP films are classified into two types, namely thermal film and tribofilm.

2.4.4 Thermal Film Formation

A transparent, solid reaction film is found to form on the metal surfaces (copper, steel) immersed in ZDDP solution heated above ~100°C. These films are referred to as thermal films in contrast to tribofilms which form under rubbing conditions. X-Ray absorption studies by Bancroft et al showed that the composition of thermal films were similar to that of tribofilms [61], except that the main cation in the polyphosphate glass of thermal films formed on the iron surface was zinc [5]. The thermal films appear to grow as separate islands (pad like structures) to form mound-like features which coalesce to then create a smooth structure at higher temperatures [62]. Fuller et al [63] showed that the rate of formation of thermal films increased

with temperature and reached about 200 nm thick on steel surfaces. This is confirmed by the observation of thermal films of about 400 nm thick on gold surfaces in a solution heated to 200°C by Aktary et al [64]. Rubbing experiments on thermal films has shown that these films also have wear resistant properties [61]. However it has been shown that these thermal films can also form below the decomposition of ZDDP without any significant degradation in the liquid phase and metal surface preferred by this mechanism over others. Since most of thermal film formation occurs well above the decomposition temperature, it is difficult to distinguish any surface-specific thermal reactions from the bulk degradation reactions described for tribofilm formation. Based on high temperature work, it has been suggested that the mechanism of thermal films involve deposition of thermal degradation materials from the liquid phase onto the metal surface [64, 65]. Iron and iron oxides are Lewis acids and are found to catalyze the thermal degradation reaction. Secondly, the zinc in ZDDP is known to exchange with other available metal ions including iron, to form dithiophosphates which are significantly less stable than ZDDP itself. The fact that the thermal films form on metal surfaces by S/O exchange was confirmed to some extent by Fuller et al [65], where they observed the exchange isomer of the type dithionyl phosphate formed on steel surfaces immersed in heated ZDDP solutions.

2.4.5 Tribofilm Properties

In recent years, extensive research has been carried out to understand the nature of the tribofilms formed on the steel surfaces. As a result, there is now a considerable amount of information available on their composition and structure due to the advent of various surface analytical techniques. Some of the definite knowledge about the nature of the ZDDP tribofilms as listed by Spikes is shown below:

1. ZDDP tribofilms form at lower temperatures than thermal films; they can also form at room temperatures but at a very slow rate. The rate of film formation increases with increasing temperature [66].

2. These tribofilms form only on the rubbing surfaces i.e., they form only in actual sliding conditions and do not form in rolling contact or if the hydrodynamic film thickness is significantly greater than the surface roughness [21, 66].
3. They have similar chemical composition to thermal films, but are mechanically stronger [37, 61, 65].
4. They tend grow to a thickness of about 50-150nm on steel surfaces and then stabilize at these levels [63, 66].
5. They initially form as separate patches on steel and these gradually develop to form an almost continuous, but still pad-like, structure [62].
6. These pads consist mainly of glassy phosphates, with a thin, outer layer of zinc polyphosphate, grading to pyro– or ortho– phosphate in the bulk [67, 68]. The outer parts of the pad have mainly Zn cations, but there is an increasingly large proportion of Fe towards the metal surface [68].
7. Within the pads, there is negligible thiophosphate [37, 69] but sulphur is present as zinc sulphide [5].
8. On the metal surface below these pads, there may be a sulphur-rich layer of zinc or iron sulphide [70], although this has been disputed by Martin et al [68].
9. Basic ZDDPs form very similar tribofilms to neutral salts but with shorter polyphosphate chains in the tribofilm [39].

2.4.6 Additive Interactions of ZDDP

Modern engine oils incorporate many additives in order to enhance the specific physical and chemical properties of the base oil employed. These additives in formulations cover a wide range of functions; additives such as antiwear additives make a direct contribution to the lubricating effectiveness whereas other additives such as antioxidants, detergents and corrosion inhibitors protect the lubricant or the lubricated system against deleterious chemical changes during use [5, 71]. When employed in formulations, reactive and surface active additives are

likely to interact or compete with each other so that the resultant behavior of the mixtures is not necessarily the sum of the individual constituent components. Many of these interactions affect friction and wear behavior and thus present both problems and opportunities for the tribologist [72]. Some combinations of additives may work synergistically to enhance the net lubricant performance, while others may work against one another to produce a cumulative antagonistic effect. Comprehending the complex nature of these additive interactions and their influence on the overall performance would hence go a long way in diagnosing and solving tribological problems, aiding the development of newer and better oil formulations and advancing technological progress in lubricating systems [72].

In this section, additive interaction is used to describe the performance interaction i.e., the phenomenon where the additive combinations give a significantly different performance than that is expected from the sum of individual components [5]. Numerous efforts have been done by many authors to study these additive interactions [16, 67, 73-78]. Such studies are made complicated by the fact that a large number of additive combinations, several types of constituent materials, and diverse blends, concentrations, formulating procedures and environments are theoretically possible. Moreover, no two groups of researchers maintain identical conditions with respect to the above likely permutations. Additionally, in spite of extensive research, even the mechanisms interactions between individual additives such as antiwear agents and extreme pressure additives are not clearly understood to this day. All these factors make it very difficult to draw a coherent picture on the additives interaction despite the availability of a large amount of information on additives interactions.

When the combined effect of two or more additives is greater than that expected from simple addition the phenomenon is called synergism. On the other hand, when one additive suppresses the activity of another, the effect is called antagonism. Interactions can occur between the additives of the same class and additives with different functions. In general, some level of interaction exists between all pairs of additives and whether the effect is recognized or

not depends on the sensitivity of the performance test methods employed. Spikes reviewing his work and others, has categorized the additive interactions into following broad groups: (1) direct interactions in the liquid phase, (2) direct interactions on surfaces, (3) complementary/exclusory effects and (4) graded response. Table 2.1 summarizes some of the additive interactions' responses for different additives pair observed in lubricated systems [19].

Table 2.1: Nature of additive interactions

Additive pair	Major type of interaction	Nature of interaction
Antioxidant–antioxidant	Complementary response	Synergistic
AW/EP–AW/EP	Exclusory effects at the surface (EP/EP) Complementary or graded response (AW/AW, EP/AW)	Antagonistic Synergistic
EP–Friction modifier	Exclusory effect at the surface	Antagonistic
EP–Rust inhibitor	Exclusory effect at the surface	Antagonistic
ZDDP–Dispersant	Complex formation in liquid Complex formation at surface	Antagonistic Synergistic
ZDDP–Detergent	Direct reaction in liquid phase	Antagonistic

The most widely studied interaction of ZDDP with other additives includes ZDDP-detergent and ZDDP-dispersant pairs. In general, the interactions between ZDDP and detergents such as calcium alkyl sulphonates and phenates are strongly antagonistic to the wear reducing properties of ZDDP [16, 80]. Four-ball wear studied conducted by Rounds [16] demonstrated that the antiwear effect of ZDDP can be adversely affected by the presence of some friction modifiers, EP agents, oxidation inhibitors, detergents and dispersants. By conducting ZDDP decomposition experiments, they showed that the rate of ZDDP

decomposition can be retarded in the presence of overbased sulphonates. Complex-formation in the bulk oil and competition for surface appears to be the phenomena involved. Huq et al [80] report a similar effect of increase in decomposition temperatures of ZDDP, along with observations of increased wear in formulations containing detergents with ZDDP, thereby indicating the antagonistic behavior of these additives on the antiwear properties of ZDDP. Yin et al [67] employed XANES spectroscopy to understand the chemical nature of the antiwear formed from secondary ZDDP in the presence of detergent and dispersants. They found that different detergents interacted with ZDDP at different rates (strong or mild interaction) and have different effects on the chemistry of the antiwear tribofilms formed. From their study, they inferred that calcium sulphonate detergents interacted with ZDDP only when treated at higher concentrations, i.e., greater than 2wt%. The main effect of this detergent was the depletion of sulphur in the antiwear film, but the presence of this detergent had little bearing on the polyphate formation. However, in the calcium phenates detergent with ZDDP, interaction was observed when the detergent was present in low concentrations. The presence of the detergent in small concentrations had an effect on the length of polyphate formed, wherein the length of poly phosphate decreased with increasing amounts of detergent. Strong interaction was also observed for ZDDP and polyisobutylene succinic anhydride polyamide dispersant, even with low concentrations of dispersant. In this case, the tribofilms formed were free from any unchanged ZDDP, and the films were composed of short-chain polyphate. Additionally, these films were very thin and almost free of sulphur. In general, strong interaction was found to occur between succinimides dispersants and ZDDP, with the effect being antagonistic on the wear-reducing property of ZDDP. It has also been suggested that the antagonistic effect of succinimides on the antiwear property of ZDDP may stem from the dispersant solubilizing the protective antiwear film off the rubbed surfaces, thereby negating the antiwear effects of ZDDP [19].

2.5 Fluorinated Zinc Dialkyl Dithiophosphate (F-ZDDP)

As phosphorus present in the engine oil is found to decrease the (poison) efficiency of catalytic converter in reducing the release of harmful gases to the environment, there is a race to reduce phosphorus in engine oil. However this phosphorus is necessary for antiwear action in the engine and is tied up with main antiwear agent found in the engine oil. This has put direct constraints on the concentration of this additive that can be employed. Phosphorus levels have been decreased from 0.12 wt.% in 1994 to 0.08 wt.% in 2004 [5]. It is still not sure whether further limitations will be imposed on the amount of P in engine oils leading perhaps to the eventual disappearance of ZDDP. Therefore, all the aforementioned factors have lead to research and development efforts concerning the reduction of phosphorus in engine oils, development of new environmentally friendly agents that exhibit similar or superior performance as ZDDP and possible avenues of using non phosphorus material as an additive. In this regard, Platinum Research Organization (PRO), Dallas TX along with UTA was looking for an approach to obtain metal surfaces chemically modified by polytetrafluoroethyelene (PTFE) to significantly improve wear protection on metals, keeping in mind the limits of phosphorus level regulations. However, the general chemisorption process is significant only at high temperatures. It was later found by PRO that the above reaction can catalyze by the presence of FeF_3, so that the reaction can proceed at much lower temperatures (at normal operating temperatures of engines – 100°C). This technology has been patented (Patent #5, 877,128) by PRO and involves fluorinating metal surfaces from dilute PTFE dispersions in engine oils at normal engine operating temperatures [81].

2.5.1 Synergy between FeF_3 and ZDDP

DSC studies by Huq et al showed that the FeF_3 used for catalyzing the metal surface with PTFE was found to work in synergy with ZDDP where FeF_3 was found to lower the decomposition of ZDDP [80]. This implied that the protective antiwear films could be formed at lower temperatures and earlier in the wear process resulting in better protection of the surfaces

against wear. Extensive research in this area by Patel et al indicated that the presence of dispersed FeF_3 has found to significantly improve the wear performance of ZDDP even at very low levels of phosphorus [81].

2.5.2 Iron (III) Fluoride and ZDDP Interactions

There is enough work that has been done to understand the interaction of FeF_3 with ZDDP. Here the possibility of interactions of FeF_3 with ZDDP was explored using techniques such as NMR and wear test by Parekh et al [17, 31, 82]. In this work an attempt has been made to study the intermediate and final products of decomposition of ZDDP with time and temperatures as variables, in order to understand the underlying mechanism of interactions. ^{31}P NMR studies decoupled with proton together with ^{19}F NMR showed that fluorinated phosphorus compounds are the products formed during the early stages of the reaction with the end products of these reactions being protective fluorocarbon compounds. According to Parekh et al, this fluorination of ZDDP was found to be a two-step process with complex formation of FeF_3, with ZDDP being a first step followed by formation of ZDDP-containing fluorinated phosphorus compounds as the second step. It was found that time and temperature played an important role in the observation of these products i.e., higher the temperature (temperature used in the study was 80°C and 150°C), the lower the time, and vise versa. It was found that these compounds could also form at room temperature but time required for this to occur was very long (1–6 months). The fact that the fluorination of ZDDP was occurring at temperatures well below the thermal degradation temperature of ZDDP was beneficial in optimizing the fluorination process of ZDDP. From the study, the optimum time and temperature for this process was found to be 6 hours and 80°C respectively, in a nitrogen atmosphere [31, 82-84]. The proposed structure of fluorinated ZDDP by Parekh et al is shown in Figure 2.8.

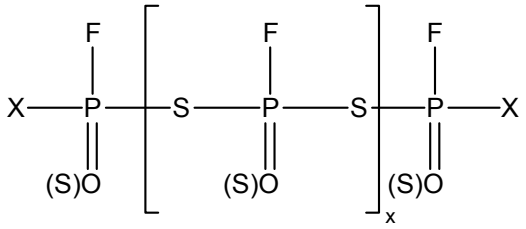

Figure 2.8: Structure of F-ZDDP. X = R, OR, SR; R may be same or different; x ≥ 1.

Wear performance of the decanted part of the formulations containing FeF_3 with ZDDP baked at 150°C in the nitrogen atmosphere were significantly better than that of formulations containing only baked ZDDP without FeF_3 and formulations containing just unbaked ZDDP. It was found that the presence of P–F bonds which exist in the structure of fluorinated ZDDP was responsible for the observed superior wear performance of F-ZDDP over that of ZDDP.

2.6 Oxidation Stability of Automotive Lubricants

Engine oils are composed of base stocks and various chemical additives. These additives are necessary to enhance the performance of these oils and to restore constituent compounds which may have been lost during the refinement process [71]. While the final application determines the exact nature of the formulation, these oils typically contain around 10% w/w of additives. These formulated lubricants tend to serve different functions in an engine. Some of the important functions include controlling friction and wear, cooling the surfaces, removing debris and contaminants, and redistributing stresses over various operating surfaces. The two major classes of basestocks used in formulating engine oils are (a) petroleum or mineral-oil derived; and (b) specially synthesized oils known as synthetic basestock. The latter exhibit greater thermal and oxidative stability than the former, but are much more expensive. On the other hand, since most liquid lubricants derived from inexpensive mineral oil basestocks are hydrocarbons, they tend to oxidize, thermally decompose, and polymerize relatively quickly [20, 23].

2.6.1 General Oxidation Mechanisms

Oxidation of lubricants occurs by free radical mechanisms [85, 86] and involves the following four steps: initiation, propagation, branching and termination. The process is initiated by the formation of alkyl free radicals as a result of exposure of the lubricant to high temperatures, light and/or metal catalysts. This reaction is generally a very slow process.

The next step is the propagation step which involves faster reaction of alkyl free radicals with oxygen to form a peroxy radical. The peroxy radical then reacts with a molecule of base stock to abstract a hydrogen atom, thereby producing an alkyl free radical and hydroperoxide. The alkyl free radical thus produced reacts with another molecule of oxygen, resulting in the repetition of the propagation step. This process occurs repeatedly until it is stopped by the termination process leading to the self oxidation of basestock.

At higher temperatures (>120°C), decomposition of hydroperoxide into alkoxy and hydroxyl free radical occurs. This is called the branching step. The free radicals thus produced further react with the molecules of the basestock and regenerate the alkyl free radicals that feed the propagation step of the mechanism.

In the termination step, the mechanism stops with the formation of oxidation products such as acids and sludge. The combination of two radicals ends the chain reaction. The following sequences of reactions illustrate the oxidation process explained above:

Initiation:	R—H	→	R • (alkyl radical)
Propagation:	R • + O2	→	RO2 • (peroxy radical)
	RO2 • + RH	→	R • + RO2H (hydroperoxide)
Branching:	ROOH	→	RO • + • OH (alkoxy and hydroxyl radicals)
	RO • + RH	→	ROH + R •
	• OH + RH	→	H2O + R •
Termination:	R • + R •	→	Alcohols
	R • + RO2 •	→	Aldehydes

	RO2 • + RO2 •	→	Ketones
	RO • + R •	→	Acids

Metals such as iron, chromium, copper and nickel have known catalytic activities with hydrocarbons [23, 87]. Metals may be introduced into the lubricants as a result of wear or acidic corrosion of the equipment [20, 23, 85]. Carboxylic acids formed due to the reaction of hydrocarbon with oxygen adsorb into the metal surface and react with the metal, forming metal-forming complexes (soaps). The general reaction scheme corresponding to metal-catalyzed oxidation mechanism is shown below:

Initiation:	$R_nM + RH$	→	$R\bullet + RH + R_{n-1}M$
Propagation:	$R\bullet + O_2$	→	$ROO\bullet$
	$ROO\bullet + RH$	→	$ROOH + R\bullet$
	$R_{n-1}M + ROOH$	→	$ROO\bullet + R_{n-1}MH$
	$R_{n-1}MH + ROOH$	→	$RO\bullet + R_{n-1}M + H_2O$
	$R_{n-1}MH + ROH$	→	$R\bullet + R_{n-1}M + H_2O$
Termination:	$R\bullet + R_{n-1}MH$	→	$ROH + R_{n-1}M$
	$R\bullet + R_{n-1}M$	→	$R—R + R_{n-2}M$
	$ROO\bullet + R_{n-1}M$	→	$R_{n-1}M—ROO$

Antioxidants play an important role in protecting the lubricant against injurious chemical transformations during the life of its operation. There are many different types of antioxidants available for use in engine oils. The suitability of antioxidants in engine oils depends on its oil solubility [23]. Antioxidants act in two different ways: (1) by radical scavenging and (2) By decomposition of hydroperoxides. Radical scavengers react with peroxy radicals (ROO •), preventing further propagation of the free radical chain [71] and are referred to as primary antioxidants, as they operate by breaking the propagation chain [85]. Peroxide decomposers react with the hydroperoxide (ROOH) molecule, preventing the formation of peroxy radicals.

These decomposers are referred to as secondary antioxidants since they function by inhibiting the branching step.

The important classes of antioxidants used in engine oils include hindered phenols, amines, and sulphur and phosphorus compounds [23]. The two types of primary antioxidants are hindered phenol and aromatic amines. Both function by donating a hydrogen atom to a peroxy radical. Examples of hindered phenols include 2, 6-di-tert-butyl-4-methylphenol phenols, in which the hydroxyl group is sterically blocked or hindered. Aromatic amines act as peroxide-radical traps to interrupt the oxidation chain reaction. Examples of aromatic amines include N-phenyl–naphthylamine and alkylated diphenyl amine. The general oxidation mechanism in the presence of primary antioxidants is given below.

$$ROO\bullet + AH \rightarrow ROOH + A\bullet$$

$$ROO\bullet + A\bullet \rightarrow AO_2R$$

$$2A\bullet \rightarrow A—A$$

$$A\bullet + RH \rightarrow AH + R\bullet \text{ (undesirable)}$$

where $R\bullet$ is the alkyl radical, $RO_2\bullet$ is the peroxy radical, AH is an antioxidant (hindered phenol or aromatic amine) and $A\bullet$ is the free radical derived from the antioxidant.

Sulphur and phosphorus-containing antioxidants include hydroorganosulphur and organophosphorus compounds which act as hydroperoxide decomposers. These are secondary antioxidants and function by inhibiting the branching step by decomposing hydroperoxides. Sulphur and phosphorus compounds find use in high-temperature situations where metals are present to help offset the catalytic behavior of these metals during hydrocarbon oxidation [20, 23]. Examples of secondary antioxidants include thioethers, phosphates, zinc dithiocarbamates and zinc dialkyldithiophosphates.

2.6.2 ZDDP as an Antioxidant

Oxidation of hydrocarbon lubricants leads to the formation of oxygen-containing species such as peroxy radicals, hydroperoxides, acids, alcohols and water by free radical steps. ZDDP

has been found to react with any one the above, and most readily with peroxy radicals and hydroperoxides. Reaction of ZDDP with peroxy radical and hydroperoxides contribute to the antioxidant activity of ZDDP.

The process of ROOH decomposition and ROO • termination by ZDDP has been studied by many researchers [46, 49, 88-91]. Antioxidant mechanisms of ZDDP proposed by different authors appear to differ significantly. There is no single explanation available to comprehensively describe the antioxidant mechanism of ZDDP and there is no general consensus among researchers on the various existing models. This may be largely attributed to the differences in the reaction conditions employed, which may highlight one or another of various possible reaction paths. Below are some of the possible antioxidant mechanism paths of ZDDP depending on reaction conditions.

Ohkatsu et al [92] suggested that in ZDDP and ROOH solutions, strong sulphur–oxygen acids were the main ROOH decomposing species. This conclusion was based on observation of $ZnSO_4$ or H_2SO_4 in solutions containing ZDDP and ROOH. From their work containing ZDDP–$[(RO)_2P(S)S]_2$ mixtures, they concluded that $[(RO)_2P(S)S]_2$ reacted with ROOH to give H_2SO_4 which then reacted with ZDDP to yield $ZnSO_4$. Willermet et al [40] observed the formation of $ZnSO_4$ in 80% yield, together with some side reactions yielding SO_2 in solutions containing ZDDP and H_2SO_4, thereby confirming the hypothesis that ZDDP–H_2SO_4 reactions may be critical in the overall ZDDP decomposition process.

Bridgewater et al. [46] studied the kinetics of decomposition of cumene hydroperoxide by ZDDP and related compounds. They considered the case where ROOH was in excess compared to ZDDP and suggested that the thiolic acid formed by the decomposition of ZDDP was responsible for the decomposition of hydroperoxide. They proposed the following reaction scheme

$$2(RO)_2P(S)SH + ROOH \rightarrow [(RO)_2PS_2]_2 + ROH + H_2O$$

$$[(RO)_2P(S)S]_6Zn_4O \rightarrow 3[(RO)_2P(S)S]_2Zn + ZnO$$

$$[(RO)_2P(S)S]_2 \rightarrow 2(RO)_2P(S)S\bullet$$

$$(RO)_2P(S)S\bullet + ROOH \rightarrow (RO)_2P(S)SH + ROO\bullet$$

$$[(RO)_2P(S)S]_2Zn + H_2O \rightarrow [(RO)_2P(S)S]ZnOH + (RO)_2P(S)SH$$

However, the above reaction scheme did not account for the sulphate observed in the solution of ZDDP–ROOH mixtures by other researchers. As this study was aimed at obtaining the rate-determining steps under a given set of conditions where ROOH was in excess over ZDDP, it is believed that this may not be a realistic representation of a typical lubricant oxidation process, at least in the beginning stages of the oxidation process.

Colclough [49] considered the resultant mixture of strong sulphur–oxy acids to be responsible for the catalytic decomposition of ROOH and stated that the following unbalanced reaction path ways are the key in ZDDP antioxidant chemistry.

$$(RO)_2P(S)S^- + ROO\bullet \rightarrow [(RO)_2P(S)S\bullet]^+ + [ROO:]^-$$

$$(RO)_2P(S)S^- + ROOH \rightarrow [(RO)_2P(S)SO_xH + H_2SO_4]$$

$$(RO)_2P(S)SO_xH \rightarrow (RO)_2P(S)SO_{x-2}H + SO_2$$

Furthermore, Willermet et al. have experimentally confirmed that hydroperoxides are decomposed by H_2SO_4 and SO_2, but were unable to determine which of these two compounds served as the key catalyst for decomposition [40].

Oxidation of ZDDP by cumene hydroperoxide in cyclohexane through Raman and ^{31}P NMR spectroscopy was studied by Paddy et al [91], where ROOH was present in excess over ZDDP in the ratio of 3:1. They found the decomposition products to be disulphide, trisulphide, tetrasulphide and Zn monothiophosphate. Based on this result, they proposed the following key steps:

$$4[(RO)_2P(S)S]_2Zn + ROOH \rightarrow [(RO)_2P(S)S]_6Zn_4O + ROH + [(RO)_2PS_2]_2$$

They also made the following observations:

ZDDP → BZDDP (rapid)

BZDDP → Disulphide (slower)

BZDDP $\rightarrow$ Trisulphide, tetrasulphide, Zinc monothiophosphate, etc.

It has been suggested that in the antioxidant process of ZDDP, sulphur from ZDDP is oxidized to SO_4^{-2} and/or SO_2 under some conditions, and the phosphorus–sulphur bonds in the original additive are gradually replaced by phosphorus–oxygen bonds [49, 88-90, 92].

Willermet et al. reasoned that the above reactions might occur in a multi-step process with overall expressions such as the reactions shown below, with the possibility that an intermediate species of the type $(RO)_2P(S)SO_3H$ might be the highly efficient hydroperoxide decomposer [46, 88, 93].

$$(RO)_2P(S)SH + 4R'OOH \rightarrow (RO)_2P(S)OH + H_2SO_4 + R'OH + R''CHO$$

$$[(RO)_2P(S)S]_2Zn + 4R'OOH \rightarrow (RO)_2P(S)OH + (RO)_2P(S)SZn^+OH + H_2SO_4 + 3R'OH + R''CHO$$

ZDDP's reactions with peroxy radicals as radical scavengers are not well understood. It has been suggested [40] that each ZDDP molecule consumes about two radicals in the termination reaction, and that the most likely locus for reaction is at a sulphur atom. This is presumed to produce an intermediate S–O radical along with an alkoxy anion that takes the place of a DTP anion at the central zinc atom. This intermediate radical is believed to react with dissolved oxygen and yield sulphur dioxide as shown below:

$$ZDDP + R'OO\bullet + O_2 \rightarrow (RO)_2P(S)SZnOR' + (RO)_2P(S)OH + SO_2$$

Secondary antioxidants are not as effective as primary when employed as the sole oxidative stabilizer in the formulation as they do not prevent the propagation step of the oxidation mechanism [85].

2.6.3 Synergy of Antioxidants

When the stabilization obtained from a formulation containing a mixture of antioxidants is larger than that expected from the sum of the individual constituent antioxidants, the effect is called synergism [85, 86, 94, 95]. Synergism can be achieved by various means. It is usually done by using a mixture of different types of antioxidants, i.e., primary and secondary. This is

because different types of antioxidants influence different reaction steps or different species in the oxidation process. Synergism has been found to occur in various types of primary antioxidants, example of which include mixtures of hindered phenols and aromatic amines. When used in this fashion (in a mixture of hindered phenol and aromatic amine), one antioxidant acts to regenerate the other [85, 86]. Synergism is beneficial in a formulation, as different antioxidants used in a mixture target different temperature ranges of operation and operate at different rates so that effective inhibition is obtained usually with lower amounts of mixtures of antioxidants. The reaction steps shown in Figure 2.9 explain the synergism between the hindered phenol and substituted aromatic amine:

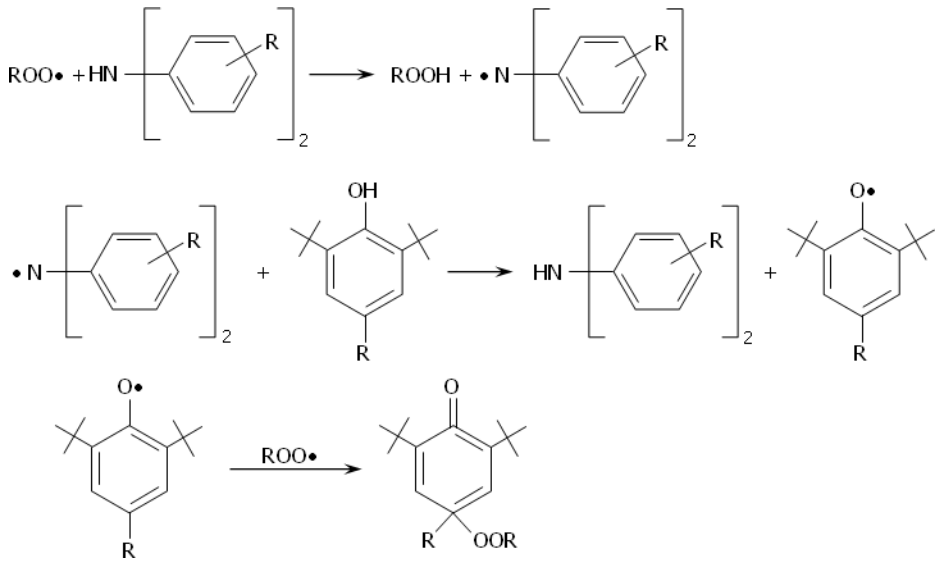

Figure 2.9: Oxidation Synergism.

In the above process, the substituted diphenyl amine reacts at a much faster rate with the peroxy radical than the hindered phenol. The reaction between the aminyl radical and second peroxyl radical therefore occurs at a slower pace compared to the reaction between the aminyl radical and hindered phenol to yield the original amine.

2.6.4 Oxidation Stability

Oxidation stability of a lubricant is its resistance to molecular decomposition or alteration at raised temperatures in an ordinary air environment [20]. A lubricant can oxidize in the presence of air, and its oxidation stability has a very strong correlation to the life of the oil. The rate of oxidation depends on several factors such as operating conditions, presence of metal catalysts and degree of refinement; and it generally increases with temperature. Some of the effects of oxidation include changes in viscosity and acidity of the lubricating oil; qualities that can influence its overall performance, life expectancy and operating costs. As effects of oxidation include changes in viscosity and acidity of lubricating oil monitoring these would be very important for safe operation of the machine.

2.6.5 Acid Number

Acidic constituents that may be present in new and used lubricants may include additives, degradation products of oxidation which may be produced during service. As these products of oxidation tend to be acidic in nature, they tend to increase the total acidity of the lubricating oil. Increased acidity causes the oil to be more corrosive and viscous, and works to restrict oil flow by depositing insoluble products on operating surfaces [20]. The measure of this amount of acidic substance in the oil is called the acid number which is always under the conditions of the test and the relative amount these acidic substances can be found by titrating them with bases. A measure of the total acid number is therefore used as a guide in the quality control of lubricating oil formulations.

According to ASTM D-664, acid number is the quantity of base expressed in milligrams of potassium hydroxide per gram of sample required to titrate a sample in a titration solvent from its initial meter reading to a meter reading corresponding to a freshly prepared aqueous basic buffer solution or a well defined inflection point. In new and used oils the constituents which may be considered to have acidic nature include organic and inorganic acids, esters, phenolic compounds, lactones, resins, salts of heavy metals, salts of ammonia, and other weak

bases, acid salts of polybasic acids and additional agents such as inhibitors and detergents. The test can be used find out the relative changes in acidity that occur in an oil during use under oxidizing condition regardless of the color or other properties of the resulting oil.

2.7 Auger Electron Spectroscopy

Auger electron spectroscopy is one of the most commonly employed surface analysis techniques to determine the composition of the surface layer of a sample [23, 96, 97]. In this technique, electrons with energy ranging from 3 to 30 keV are incident upon the surface of a specimen [96]. This in turn results in the ejection of resident electrons from the surface of the sample. These emitted electrons are named Auger electrons after Pierre Auger, the physicist who first observed this effect. Energy analysis of Auger electrons provides important information about the surface composition of the specimen under study.

2.7.1 Principles of Auger Electron Spectroscopy

In the Auger process, an incident electron removes an electron from the K shell (core electron) as seen in Figure 2.10 (a). The resulting vacancy in the core level is filled by an outer level electron (L_2) and the energy released is used to eject another electron from the atom (L_3) leaving vacancies in two shells i.e., L_2 and L_3.

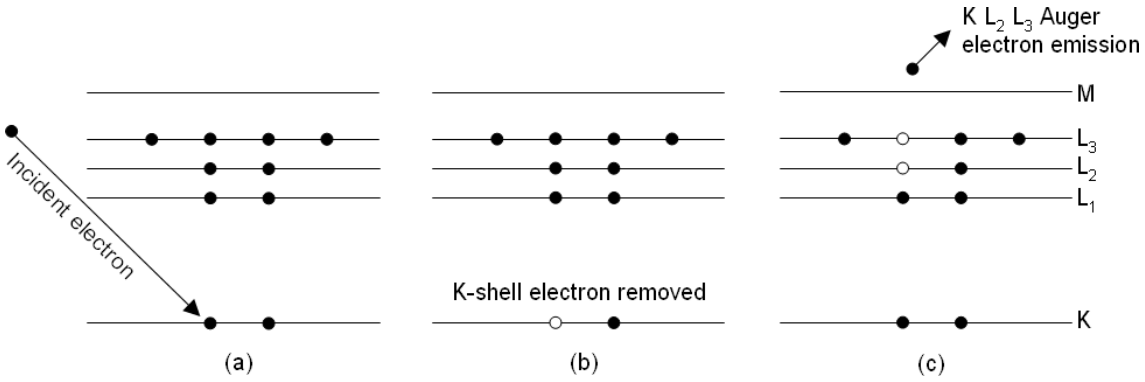

Figure 2.10: Illustration of Auger process: (a) atom showing electrons present in filled K and L levels before an electron is removed from the K level, (b) after removal of an electron from the K level and (c) following the Auger process where a KL2L3 Auger electron is emitted.

The Auger electron is denoted by the three levels involved in the process and in this case is called KL_2L_3 Auger electron. Hydrogen and helium cannot be detected with AES as these atoms do not have enough electrons. The energy of emitted electrons depends only on the difference on the energy levels involved. The relationship for the above transition is given by

$$E_{Auger} = E(KL_2L_3) = E(K) - E(L_2) - E(L_3) \tag{2.6}$$

Auger electron kinetic energies are the characteristics of the emitting atoms. Therefore, measurement of these energies is useful in identifying the element that is responsible for the emission of these Auger electrons. Such an analysis can yield information about the chemical composition of a surface and help identify the elements present in the specimen. A plot of the number of electron detected as function of kinetic energy constitutes an Auger spectrum. Concentration of the elements present can be determined by the intensities of the Auger spectrum. Traditionally, the first derivative spectra would be considered, since the actual Auger peaks are generally quite small compared to the slowly varying background of secondary and backscattered electrons. This treatment of the data enhanced the visibility of Auger electrons and reduced signal-to-noise problems. However, this approach made the quantification process harder due to the fact that a simple relationship does not readily exist between the area under the original peak and the magnitude of the peak-to-peak distance in the corresponding derivative curve [23]. Today, the introduction of digital computer processing techniques has greatly enhanced the ability to perform highly sophisticated analyses of experimental data. Figure 2.11 depicts a schematic representation of the AES apparatus.

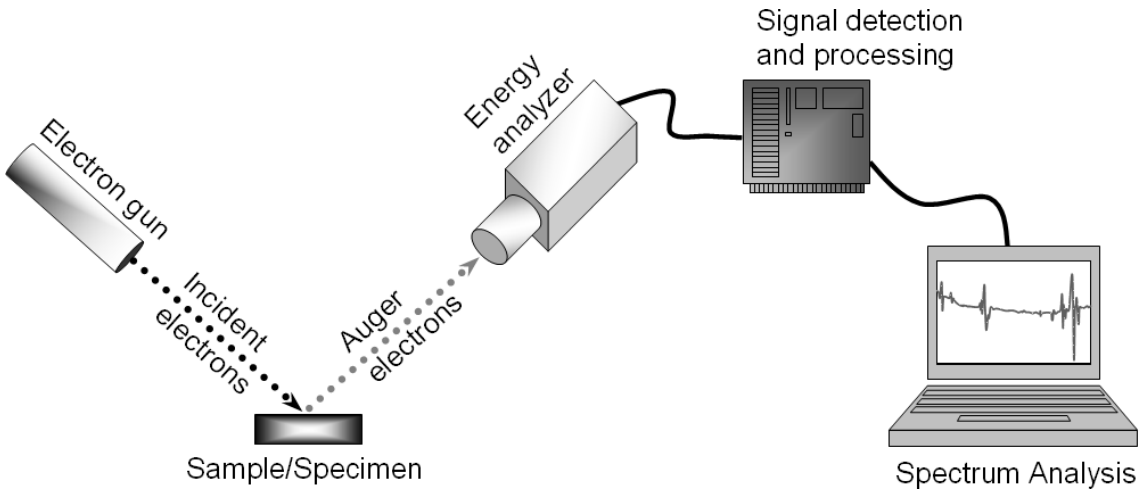

Figure 2.11: Schematic layout of the Auger electron spectroscopy apparatus.

2.7.2 Modes of Detection

Since an electron beam can be focused to a very small area, composition analysis of small regions (less than 500Å) on the surface becomes possible. This is referred to as point analysis. Auger line-scan can also be performed by scanning the electron beam across the sample in a straight line and the data can be obtained as a function of beam position. Similar two-dimensional analysis may also be performed by scanning over a given area of the surface. This is known as scanning Auger microscopy (SAM). Often, SAM is used in conjunction with scanning electron microscopy (SEM) to locate the region of interest while performing surface analysis. Another widely used offshoot of the basic AES technique is Auger depth profiling, which is used to determine the variation of sample composition as a function of depth. In this process, inert gas ions are used to sputter the surface layers, thereby exposing the underlying layers [96]. Meanwhile, the Auger signals from the newly revealed surfaces are measured and the composition at this depth determined. Such techniques are particularly useful in tribology because of the wealth of information that can be obtained on the composition of tribofilms generated during the wear process, the nature of which is largely rough and inhomogeneous.

2.8 Mechanical Properties and Nano-mechanical Testing of Tribofilms

The dynamic properties of ZDDP tribofilms have a signature influence on its antiwear performance. These properties are a result of the tribofilm's combined chemical and mechanical characteristics. In order to understand the antiwear properties of ZDDP, it therefore becomes imperative that these chemical and mechanical traits are studied at the appropriate length scales. However, only static measurements are currently possible due to present-day limitations in experimental capabilities. In practice, mechanical characterization of tribofilms involves the evaluation of such properties as Young's modulus and hardness.

Most research work reflected in current available literature focus primarily on nano-indentation to characterize mechanical properties of tribofilms [32, 62, 98-103]. This dissertation presents results of nano-mechanical characterization obtained through novel techniques such as nano-scratch and scanning wear tests. While nano-indenters are known to have been extensively employed for their primary purpose, i.e., nano-indentation, there appears to be little if any literature presenting nano-mechanical characterization studies utilizing these new techniques. The nano-scratch and scanning wear tests and analyses introduced in this study are therefore original works of this research.

It is known that the breakdown of a tribofilm during prolonged periods of its operation results in the generation of hard debris. Entrapment of this debris in the contact area results in the scratching of the film and eventually its failure. Scratch resistance of the tribofilms can hence be used as a measure of the resistance of a tribofilm to abrasion. In this work, nano-indentation, nano-scratch and nano-scale scanning wear tests were conducted on tribofilm samples generated from ZDDP and Fluorinated ZDDP with alkylated diphenylamine in base oil. Hysitron® nano-mechanical test equipment at Hysitron Corporation's nano-mechanics research laboratory in Minneapolis, MN was used for this purpose. The nano-indentation tests at the Hysitron® nano-mechanics research laboratory employed a NorthStar® cube-corner probe with tip radius of less than 40nm.

2.8.1 Principles of Operation

Nano-indentation is a technique established in recent years to investigate the hardness of a small volume of material. In traditional indentation tests such as macro or micro indentation, test samples are probed with a calibrated tip with much greater hardness than the test sample and whose mechanical properties are known. The load placed on the indenter tip is increased up to a pre-defined value as the tip penetrates further into the specimen. As the load applied reaches a maximum or pre-defined value, it may be held constant or removed. The area of the residual indentation (or penetration) in the sample is measured and the hardness (H) is calculated from the maximum load (P_{max}) divided by the residual indentation area (A_r)

$$H = \frac{P_{max}}{A_r} \tag{2.7}$$

For most macro or micro-indentation techniques, the projected area may be measured directly using optical microscopy. However, indenter rigs at the macro or micro scales tend to lack very high spatial resolutions. Additionally, indenter tips can come in a vastly diverse permutation of tip shapes. These limitations make it very difficult and often pointless to compare results of experiments conducted in different laboratory environments.

The principles behind nano-indentation are essentially similar to its macroscopic counterparts, the primary difference being that the former is conducted at the nanometer scale. Indenter tips in this realm have been fabricated with very precise tip shapes. Furthermore, placement of these tips can be accomplished with very high accuracy in terms of spatial resolution. Extraction of real-time load-displacement information is also achievable while the indentation is still underway.

Since the tip size and loads are very small, it can be rather challenging to find and identify the indentation and the contact area made by the tip. While a number of microscopy techniques with sub-optical resolution – such as scanning electron microscopy or atomic force microscopy – may in theory be exploited to find the contact area, such approaches are

generally unwieldy and tedious. A more efficient approach involves the use of a standardized indenter tip such as a Berkovich tip. The geometry and dimensions of this tip are known to a high degree of precision. The magnitude of applied load and depth of penetration into the test sample are recorded, and the area of contact is then calculated through knowledge of the indenter geometry. A plot of applied load versus resulting indenter displacement may be obtained and utilized to characterize the mechanical properties of the tribofilm. Modulus is calculated from the initial slope unloading of load – displacement cure as shown below . A typical load-displacement curve is shown in Figure 2.12.

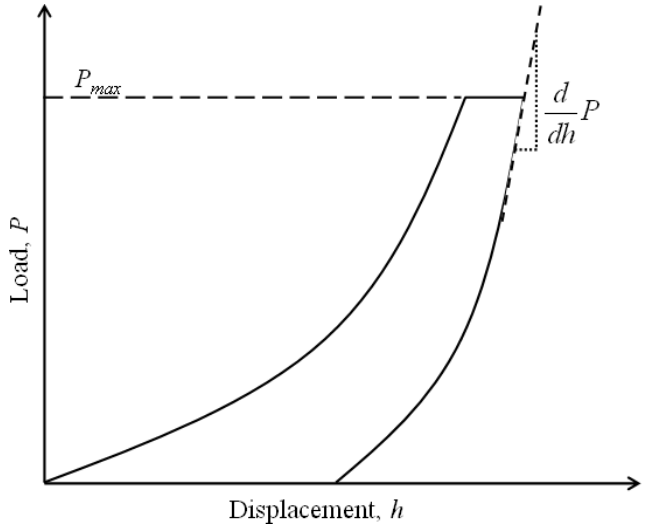

Figure 2.12: Load-displacement curve obtained during nano-indentation of a test sample.

Since the magnitudes of load and displacement are extremely small, the test equipment must be very sensitive to collect accurate readings of these data parameters. While conducting these experiments, it is therefore critical to ensure that the nano-indenter equipment is environmentally isolated to eliminate or considerably minimize the impact of vibrations, atmospheric temperature and pressure variations, as well as thermal fluctuations within the components and test samples themselves.

2.9 Fourier Transform Infrared Spectroscopy

Fourier transform infrared spectroscopy is a non-destructive instrumental analysis technique that is useful in the determination of molecular structures and the identification of compounds [104]. While infrared frequencies span the electromagnetic spectrum from 780 nanometers up to a millimeter, most applications that call for FT-IR spectroscopy employ wavelengths that fall between 2.5μm and 15μm, which translates to a wavenumber ranging from 4000cm^{-1} to 670cm^{-1}. Figure 2.13 shows the band of wavelengths in the infrared region that is utilized by most FT-IR applications.

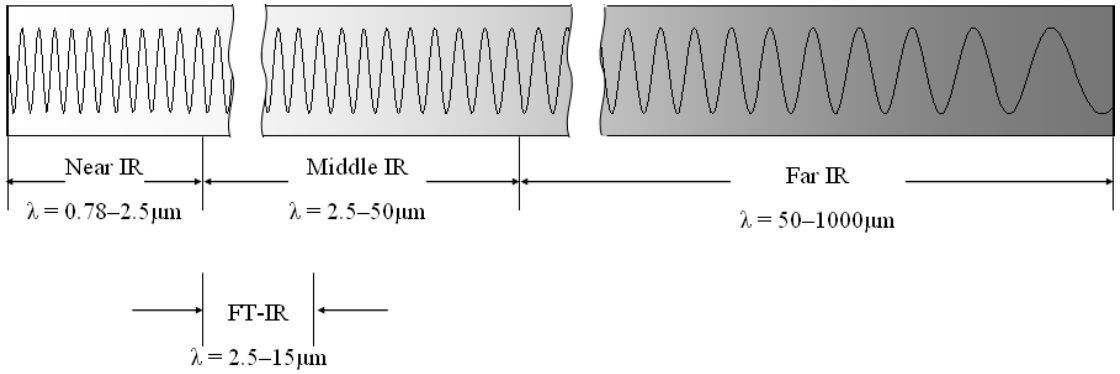

Figure 2.13: Operating wavelength region for Fourier transform infrared spectroscopy.

Infrared spectroscopy works only for samples whose compounds exhibit a dipole moment, or in other words, are said to be polar. When the sample is irradiated with a coherent light source of well-defined energy (known wavelength), absorption of the incident energy occurs if the frequency of the radiation exactly matches the inherent vibrational frequency of the molecules [97]. The spectral signature of the absorption process is then used to identify the types and nature of the compounds present in the sample.

An improved version of infrared spectroscopy that yields better sensitivity and resolution involves spectral analysis through the use of Fourier transform techniques. The FT-IR spectrometer consists of a modified Michelson interferometer in which one of the two fully-

reflecting mirrors is movable as shown in Figure 2.14: Operating principle of a Fourier-transform infrared spectrometer.

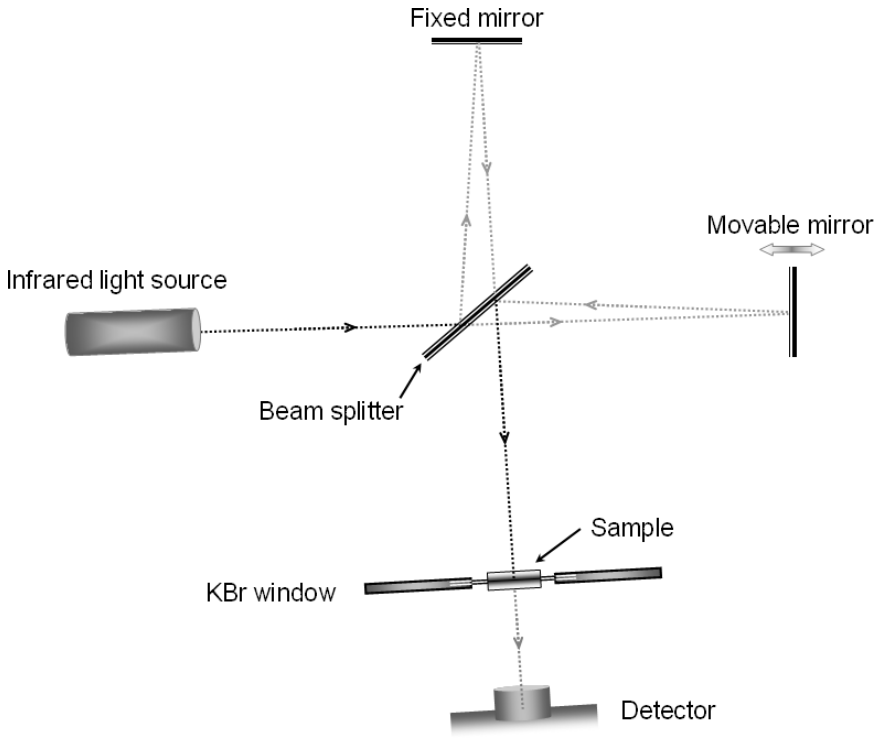

Figure 2.14: Operating principle of a Fourier-transform infrared spectrometer

The sample is irradiated with a coherent light source of well-defined energy, and the optical path of one of the split beams is varied by moving the mirror [23]. When the light source is made up of polychromatic radiation, the Fourier transform of the spatially modulated beam passed through the sample yields a spectrum that is representative of the constituent compounds of that sample. Table 2.2 lists some of the important IR absorptions observed in various compounds [105].

Table 2.2: FT-IR absorption spectral regions for various groups of compounds.

Functional Group	Characteristic Absorption (s) (cm^{-1})
Alkyl C–H Stretch	2950 – 2850 (m or s)
Alkenyl C–H Stretch Alkenyl C=C Stretch	3100 – 3010 (m) 1680 – 1620 (v)
Alkynyl C–H Stretch Alkynyl C=C Stretch	~3300 (s) 2260 – 2100 (v)
Aromatic C–H Stretch Aromatic C–H Bending Aromatic C=C Bending	~3030 (v) 860 – 680 (s) 1700 – 1500 (m, m)
Alcohol/Phenol O–H Stretch	3550 – 3200 (broad, s)
Carboxylic Acid O–H Stretch	3000 – 2500 (broad, v)
Amine N–H Stretch	3500 – 3300 (m)
Nitrile C=N Stretch	2260 – 2220 (m)
Aldehyde C=O Stretch	1740 – 1690 (s)
Ketone C=O Stretch Ester C=O Stretch Carboxylic Acid C=O Stretch Amide C=O Stretch	1750 – 1680 (s) 1750 – 1735 (s) 1780 – 1710 (s) 1690 – 1630 (s)
Amide N–H Stretch	3700 – 3500 (m)

2.10 X-Ray Absorption Near-edge Spectroscopy

X-ray absorption near edge spectroscopy is a nondestructive analysis technique that today finds increased utility due to its capability of probing the local structural environment around selected atoms [106]. The present-day availability of synchrotron radiation beams has enabled the use of XANES to extensively study surface films. These synchrotron radiation beams permit the X-ray energies to be tuned to probe the atomic species in which excitation occurs [67, 107].

2.10.1 Principles of XANES

When the photon energy of an incident synchrotron X-ray beam reaches a sufficient level to excite a core shell electron from its bound inner shell into material's conduction band, a well defined and discontinuous break in the absorption spectrum of the material occurs. This discontinuity in the absorption is called an edge because it is usually sharp i.e., absorbance falls off rapidly with decreasing energy.

This even occurs when an X-ray beam has sufficient energy to excite a core electron to an unoccupied orbital within the material. Usually, small oscillations can be seen superimposed on the edge step and these oscillations gradually die away as the X-ray energy increases. The oscillations, which appear relatively close to the edge (within about 40 eV), are known as near-edge X-ray absorption fine structure (NEXAFS) or X-ray absorption near-edge structure (XANES). The oscillations are due to the multiple scattering of photoelectrons by the atoms in a local cluster around the absorbing atom. The structure observed from 30–40 eV beyond the edge is called extended X-ray absorption fine structure (EXAFS), and is due to the interference between the outgoing photoelectron wave and the same wave following the backscattering from neighboring atoms. Figure 2.15 illustrates the edge, XANES and EXAFS regions observed in an example absorption spectrum.

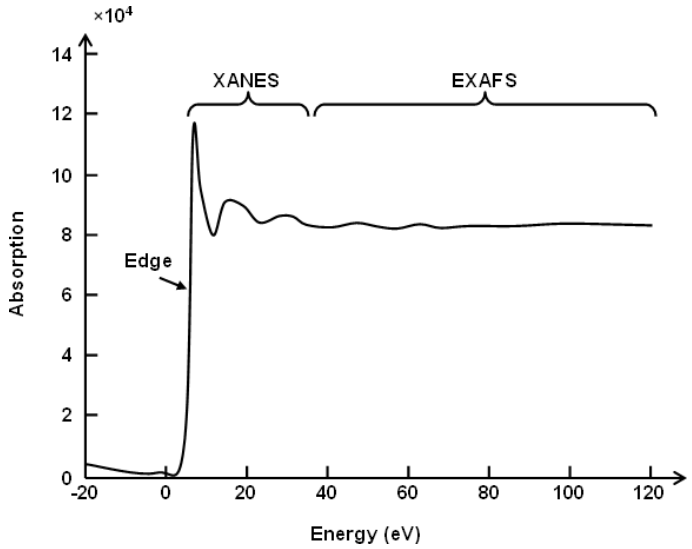

Figure 2.15: Example of a typical XANES absorption spectrum

Analysis of an EXAFS structure provides the information on the local atomic structure around the absorbing atom. Analysis of these XANES oscillations in the spectrum of a particular sample can provide information about vacant orbitals, electronic configurations and the site symmetry of the absorbing atom. Theoretical multiple scattering calculations can be compared with the experimental spectrum to determine the geometrical arrangement of atoms surrounding the absorbing atom. The absolute position of the edge position is related to the oxidation state of the absorbing atom with main edge shifting to higher energy with increased oxidation state [108, 109].

There are two types of detection modes which can be used to analyze the surface as well the bulk of the tribofilm. Total electron yield (TEY) mode is useful to analyze the surface layer, while fluorescent yield (FY) is used to analyze the bulk of the tribofilm. The depth of the layer which can be probed by TEY mode can be approximately 50Å for the phosphorus and sulphur L- edge and that by FLY mode is 500Å for phosphorus and sulphur L- edge. For TEY phosphorus and sulphur K- edge it is 500A^{o} and 3000A^{o} for FLY. By changing the detection mode, different thicknesses can be probed without any degradation of the specimen. XANES can be used to explain the nature of polyphosphates, chain lengths and variation in composition

by probing through the thickness of the tribofilm. However, XANES can neither provide information about the exact chemical compositions of the different polyphosphate glasses which exist in ZDDP tribofilms nor an accurate determination of the thickness of the tribofilm probed [68].

Assignment of the fine structure can be obtained using the spectra of model compounds and comparison of published data. The proportion of the different compounds detected in the material can be evaluated by simulating the spectrum by a linear combination of reference spectra. XANES at the P L-edge, P K-edge, S K-edge, Mo M-edge and Mo L-edge can be recorded to fully characterize the phosphates and sulfides in the tribofilms. Collimated plane grating monochromator (PGM) beam line may be used to characterize P L-edge, S-L edge, while double crystal monochromator beam line may be utilized to characterize P K-edge and S K-edge.

2.11 Summary

The scientific principles of tribology form the foundations upon which the technological development of automotive lubricants is established. It is seen that friction and wear are fundamental phenomena that need to be carefully controlled in order to efficiently operate the vast array of machines that are vital to modern society.

- Wear occurs when two surfaces come into contact and interact with each other, leading to the removal of native material from one or both surfaces. Wear may be classified into adhesive, abrasive, fatigue and corrosive modes, and may be further categorized on a macroscopic level into mechanical, chemical and thermal wear. One of the most important traits of wear is that it is not a function of material properties, but instead an integrated response of the overall tribosystem.
- The science of automotive lubrication deals with the mitigation of wear to manageable levels so as to ensure optimal operation of mechanical machinery. This alleviation of wear is realized by introducing a lubricant that acts as an interface between two interacting

surfaces. While lubricants may generally be either in solid, liquid or gaseous form, the vast majority of automotive lubricants are liquids in the form of oils. The choice of lubricants for a given application is dictated by the operating conditions and certain oil properties, the most important among them being viscosity. Various additives are commonly employed in lubricating oils to enhance these properties and increase their usefulness.

- Zinc dialkyl dithiophosphate is the most dominant antiwear additive seen in automotive lubricants today. It is one of the most cost-effective antiwear agents in engine oils and is known to exhibit antioxidant properties, in addition to being an effective extreme pressure agent and a detergent. However, it contains phosphorus, which is known to contribute to environmental pollution and catalytic converter poisoning.
- Research at the University of Texas at Arlington has yielded a new compound, namely fluorinated zinc dialkyl dithiophosphate, which has shown to exhibit superior wear properties over ZDDP while containing lower levels of phosphorus. This research aims to investigate the effects that various antioxidant additives have on the wear performance and oxidation stability of lubricant formulations containing F-ZDDP.
- Oxidation stability of a lubricant is the measure of its resistance to deterioration and an important indicator of its service life. Oxidation stability can be evaluated by measurements of viscosity and total acid number of a formulation. In addition, chemical characterization through techniques such as Fourier transform infrared spectroscopy, Auger electron spectroscopy and X-ray absorption near-edge spectroscopy may be performed on formulations to examine their behavior and usefulness as automotive lubricants.

CHAPTER 3

ANTIWEAR PERFORMANCE OF F-ZDDP IN THE PRESENCE OF ANTIOXIDANTS

The natural process of oxidative degradation is frequently accompanied by the accumulation of oil insoluble materials such as sludges and deposits. These undesirable byproducts usually tend to increase wear in mechanical systems [32]. Antioxidants are added to engine oils in order to fight against the ravages of oxidation. These additives react by various free radical mechanisms to either consume the harmful products of degradation or limit their production. Inhibition of oxidation occurs through the use of radical scavengers or hydroperoxide decomposers. Radical scavengers react with peroxy radicals and prevent the formation of free radicals. Peroxide inhibitors react with hydroperoxide molecules and prevent further formation of peroxy radicals [71, 85, 86].

In lubricating oils, antioxidant behavior mainly comes from hindered phenols, aromatic amines and to a certain extent from the decomposition products of ZDDP – the main anti-wear agent in engine oils. Both hindered phenols and aromatic amines function by donating a hydrogen atom to the peroxy radical and form a stable free radical [85]. The anti-oxidation behavior of ZDDP has been extensively studied [40], whereby ZDDP was found to act as a radical scavenger as well as a peroxide decomposer. The anti-wear or anti-oxidant behavior of ZDDP requires its thermal or tribological breakdown. However, the presence of other additives in engine oils causes ZDDP to react with them in a complex manner resulting in a reduction of its breakdown efficiency [40]. Degradation of ZDDP is a very complex process and much effort has been dedicated to understand the mechanism of its degradation and interaction with other additives. A detailed review of the antioxidant behavior or degradation mechanism of ZDDP is beyond the scope of this work.

The fluorinated ZDDP complex developed at the University of Texas at Arlington (UTA) has shown better wear performance compared to ZDDP in bench tests [82, 84]. In the present study, the interaction of antioxidants with ZDDP and Fluorinated ZDDP are studied by using the antioxidant, alkylated diphenylamine. Interactions of ZDDP and Fluorinated ZDDP with alkylated diphenylamine are investigated chemically using nuclear magnetic resonance spectroscopy technique. The wear performance under tribological conditions is evaluated under boundary conditions using ball-on-cylinder lubricity evaluator. The tribofilms formed under boundary lubrication was studied using Auger electron spectroscopy.

3.1 Experimental Procedure

3.1.1 Materials for Nuclear Magnetic Resonance Studies

A solution containing 68% by weight ZDDP – a mixture of Basic and Neutral forms of secondary ZDDP in 100 N base oil was used to prepare all the solutions in this study. The antioxidant alkylated diphenylamine (ADPA) was obtained from R. T. Vanderbilt, CT, USA. Fluorinated ZDDP (F-ZDDP) was synthesized by reacting ZDDP and FeF_3 (Advance Research Chemicals, Tulsa, OK). This FeF_3 acts as a fluorinating agent, yielding Fluorinated ZDDP. For NMR studies, the mixtures studied were:

a) A solution containing ZDDP (50 wt.%) in mineral oil baked for one hour at 80°C in the presence of N_2 to show decomposition products.
b) A solution containing ZDDP in mineral oil (68 wt.% ZDDP) is baked at 80°C for 1 hour. This mixture is blended with ADPA to yield a mixture that contains 50 wt.% ZDDP, 25 wt.% mineral oil and 25 wt.% ADPA and is baked again at 80°C for one additional hour in nitrogen.
c) A solution containing 50 wt.% F-ZDDP in mineral oil.
d) A solution that contains 50 wt.% of F-ZDDP and 25 wt.% mineral oil baked with 25 wt.% ADPA for 1hr at 80°C in the N_2 atmosphere.

The ^{31}P NMR spectra of ZDDP and fluorinated ZDDP with antioxidants in $CDCl_3$ were obtained by using JEOL Eclipse 300 MHz spectrometer. ^{31}P NMR decoupled with proton were obtained at operating frequency of 121.66 MHz, relaxation delay of 6[s], sweep of 30.488 [KHz] and 2000 scans. 85 % Phosphoric acid was used as an external reference. All chemical shifts in the low field direction are defined positive. Approximately 0.3 grams of sample in 1.5 ml of $CDCl_3$ (lock solvent) was found to give good shimming and good intensity signals, using 5mm OD tubes.

3.1.2 Wear Studies

Wear performance was evaluated using ball-on-cylinder lubricity evaluator developed at UTA. All the tests were done under boundary lubrication conditions. Details of BOCLE and testing protocols are reviewed in reference [110]. The different formulations used in the study correspond to

a) ZDDP (0.1 wt.% P, 0.21 wt.% S, 0.11 wt.% Zn) + base oil
b) F-ZDDP (0.1 wt.% P, 0.21 wt.% S, 0.11 wt.% Zn, 0.01 wt.% F) + base oil
c) ZDDP (0.1 wt.% P, 0.21 wt.% S, 0.11 wt.% Zn) + 2 wt.% alkylated DPA + base oil
d) F-ZDDP (0.1 wt.% P, 0.21 wt.% S, 0.11 wt.% Zn, 0.01 wt.% F) + 2 wt.% alkylated DPA + base oil

In all cases, the base oil was 100 Neutral. 50 micro liters of oil mixture was used in each case. Oil was applied at the contact point between the ball and the ring using a surgical syringe capable of dispensing oil in amounts smaller that 5 µl increments. Tests were run for 15000 cycles at 24 Kg load and 50,000 cycles at 20 Kg load at 700 rpm using 0.25" Tungsten carbide (WC) ball (78 HRc) on Timken 50 mm diameter hardened steel rings (62 HRc hardness). Both balls and rings were ultrasonicated and cleaned with hexane and acetone. Surface roughness of the ring was measured using a profilometer to make sure that only the rings with surface roughness, R_a values ranging from 0.25 to 0.4 µm were chosen for the test. After the wear test, the rings were cleaned using hexane and acetone. The wear width and depth was then

measured using a profilometer (Mahr M1 Perthometer) at six locations on each ring at intervals of 60°. Volumetric wear was calculated by multiplying the average area under the wear track by the circumference of the ring.

3.1.3 Auger Electron Spectroscopy Studies

After the wear test, the rings were cut to examine the elemental distribution of the tribofilm under an Auger electron spectrometer. Care was taken to preserve the film on the surface of the ring. Samples were mounted on a specimen holder and placed in the spectrometer. The elemental analysis of the solid film formed on the surface of the ring was examined using Perkin – Elmer PHI 560 ESCA/SAM system with a spot size of 2 μm. The operational pressure was maintained at 1.2×10^{-7} torr during acquisition. The depth profile in terms of counts per second versus sputtering time was carried out using AES with ion gun excitation voltage at 2 KV. Samples studied were tribological surfaces of rings that were tested for 50,000 cycles at a load of 20 Kg for the following two chemistries:

a) ZDDP (0.1 wt.% P) + 2 wt.% alkylated DPA + base oil

b) F-ZDDP (0.1 wt.% P) +2 wt.% alkylated DPA + base oil

3.2 Results and Discussion

3.2.1 Nuclear Magnetic Resonance Studies

The use of ^{31}P NMR to identify the decomposition and degradation products containing P has been used by many authors [47, 51, 90]. Figure 3.1 is the baseline spectra of ZDDP (50 wt.%) in base oil. ^{31}P NMR spectra of ZDDP indicate the presence of 6-7 phosphorus environments. The peak at 99.9 ppm corresponds to secondary basic ZDDP and the peak at 93.8 ppm corresponds to secondary neutral ZDDP. These assignments are in agreement with values mentioned in literature by many others [83, 90, 111-113]. The majority of the minor peaks appearing in the range of 40-110 ppm, including the one at 77 ppm, are thiophosphorus compounds, and the possible products corresponding to these peaks are identified in detail in the literature [83].

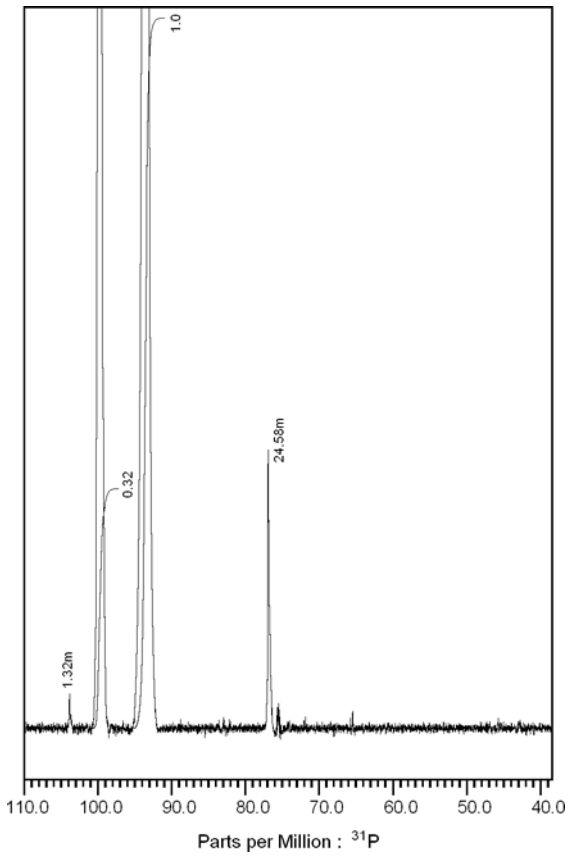

Figure 3.1: Proton decoupled ^{31}P NMR spectra of unbaked ZDDP. The formulation consisted of 50 wt.% ZDDP in mineral oil.

Figure 3.2 shows the proton decoupled ^{31}P NMR spectra of ZDDP (50 wt.%) in mineral oil baked at 80°C for one hour. The second spectrum is the proton decoupled ^{31}P NMR spectra of a solution containing ZDDP in mineral oil (68 wt.% ZDDP) baked at 80°C for 1 hour and blended with alkylated DPA to yield a mixture that contains 50 wt.% ZDDP, 25 wt.% mineral oil and 25 wt.% alkylated DPA and is further baked at 80°C for one additional hour in nitrogen. The peaks between 40-50 ppm are degradation products of the basic ZDDP and some of the impurities in the original ZDDP, and are of the kind $(RO)_2P(S)O^-$, $R_3P(O)$ with R > CH_3 [90, 111]. In comparison with spectra of baked ZDDP by itself, ^{31}P NMR spectra of 50 wt.% ZDDP (baked for 1 hour at 80°C) mixed with 25 wt.% alkylated DPA and baked for an additional 1 hour

at 80°C in nitrogen shows no change in the intensity of basic ZDDP. There are no new peaks formed due to the interaction of ZDDP with alkylated DPA.

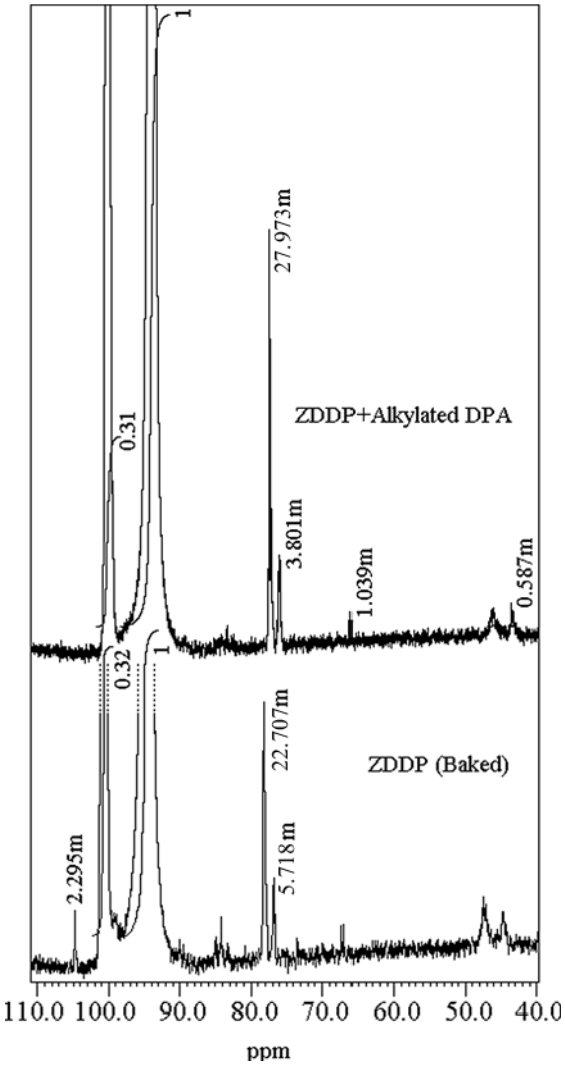

Figure 3.2: Proton decoupled ^{31}P NMR spectra of baked ZDDP with and without ADPA. The formulation consisted of 50 wt.% ZDDP in mineral oil baked at 80°C for one hour in nitrogen (Bottom); Proton decoupled ^{31}P NMR spectra of ZDDP baked for one hour at 80°C in nitrogen mixed (at 68 wt.% ZDDP) with 25 wt.% ADPA to yield a mixture that contains 50 wt.% ZDDP, 25 wt.% mineral oil and 25 wt.% ADPA, and baked for another hour at 80°C (Top).

It evident from comparison of spectra of baked ZDDP (Figure 3.2) alone with F-ZDDP (Figure 3.3), the peak at 77 ppm is decreased in intensity in F-ZDDP (0.029 in ZDDP vs. 0.0017 in F-ZDDP). In addition, the intensity of basic ZDDP peak in the F-ZDDP is also decreased to

almost half of the intensity seen in baked ZDDP (0.18 in F-ZDDP Vs. 0.32 in ZDDP) indicating the faster reaction of basic ZDDP to form the F-ZDDP [83]. The doublets at 66 ppm and 57 ppm with a coupling constant of 1.80k are the set of peaks formed mainly in the F-ZDDP as these peaks are absent in ZDDP alone. These peaks have been attributed to the formation of P-F bonds [83].

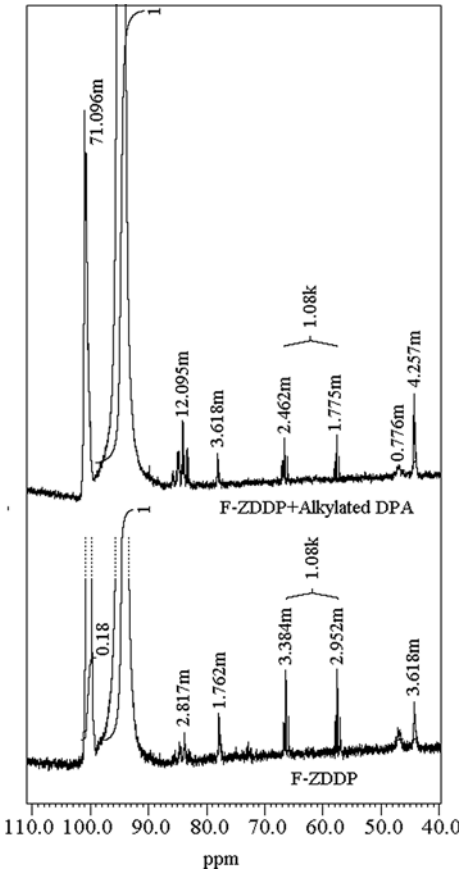

Figure 3.3: Proton decoupled ^{31}P NMR spectra of baked F-ZDDP with and without ADPA. The formulation consisted of 50 wt.% F-ZDDP in mineral oil (Bottom), and 50wt.% F-ZDDP with 25 wt.% ADPA in mineral oil baked for one hour at 80°C (Top).

The ^{31}P NMR spectra of F-ZDDP in mineral oil and the ^{31}P NMR spectra of 50 wt.% F-ZDDP and 25 wt.% alkylated DPA in mineral oil are compared in Figure 3.3. When compared with the spectra of F-ZDDP alone, intensity of basic ZDDP in the mixture with alkylated DPA is decreased drastically (0.18 in F-ZDDP Vs. 0.071 in F-ZDDP + alkylated DPA), indicating

decomposition of the basic ZDDP. The intensity of peaks at 83 ppm is increased in the mixture containing alkylated DPA (0.0028 in F-ZDDP Vs. 0. 012) indicating the formation of degradation products of the type $(RO)_2P(S)(SR)$ and $RP(S)(SR)_2$ [90, 111]. The intensity of the doublets at 65 and 57 ppm in the F-ZDDP decreased in the presence of alkylated DPA indicating that the antioxidant diphenyl amine being basic in nature scavenges some of the fluorine present in the F-ZDDP. However, a significant fraction of the fluorine is still associated with the phosphorus in the form of a P-F bond.

3.2.2 Friction and Wear Performance Studies

The coefficient of friction versus number of cycles and temperature versus number of cycles for the test carried out on BOCLE with a ¼" tungsten carbide ball at an applied load of 24Kg to 15000 cycles for different formulations detailed in section 2.3 of experimental section are plotted in Figure 3.4. All the formulations show the same trend in the coefficient of friction i.e., increase in coefficient of friction in the beginning of the test (5000 cycles) followed by a plateau region. The appearance of this plateau region is associated with the formation of a protective film (tribofilm). In the early stages of the test, prior to the formation of a stable tribofilm, substantial wear occurs as reflected by the sharp jump in friction coefficient and local rise in temperature. However, once a stable tribofilm is formed, it is reflected by the stable and flat coefficient, a gradual rise in temperature and minimal wear. In both ZDDP and F-ZDDP with addition of 2 wt.% alkylated DPA, there is a marginal increase in coefficient of friction that appears to lie within the range of experimental uncertainty.

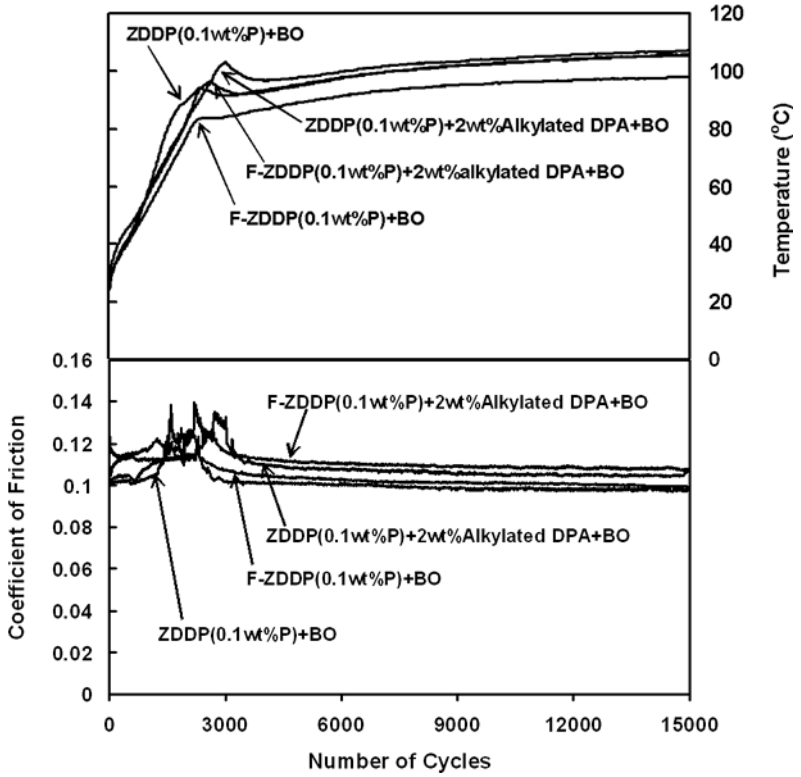

Figure 3.4: Temperature and friction data for short-term wear tests. Plots show temperature vs. number of cycles and coefficient of friction vs. number of cycles for the wear test run at 24 Kg load, with ¼" tungsten carbide ball on 50 mm Timken ring for 15000 Cycles. The different formulations used in the test are ZDDP (0.1 wt.% P) + base oil, ZDDP (0.1 wt.% P) + 2 wt.% ADPA + base oil, F-ZDDP (0.1 wt.% P) + base oil, F-ZDDP (0.1 wt.% P) + 2 wt.% ADPA + base oil.

Description of ball-on-cylinder lubricity evaluator and testing procedure are detailed by Mourhatch and Aswath [110] and hence is not repeated here. Figure 3.5 and Figure 3.6 show the wear performance of four different formulations at different loads in terms of wear volume. Each value of wear volume in each case is an average of 18 measurements. In both cases (i.e., higher load-lower number of cycles and lower load-higher number of cycles), wear volume of ZDDP alone in mineral oil is found to be worse than all other formulations while the wear performance of F-ZDDP is found to be the best. This may be due to the fact that the P-F bond formed in F-ZDDP is responsible for binding the phosphorus and yielding an improved tribofilm on the surface, thereby minimizing wear.

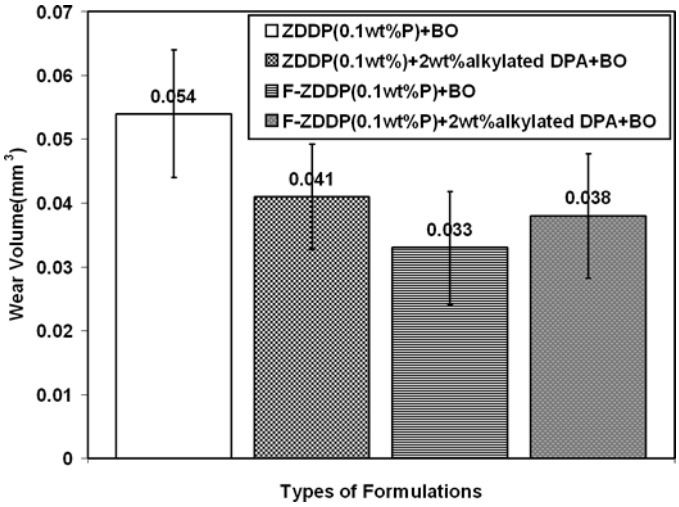

Figure 3.5: Wear volume vs. type of formulation for short-term tests. The different formulations used are: ZDDP (0.1 wt.% P) + base oil, ZDDP (0.1 wt.% P) + 2 wt.% alkylated DPA + base oil, F- ZDDP (0.1 wt.% P) + base oil and F-ZDDP (0.1 wt.% P) + 2 wt.% alkylated DPA + base oil. The tests were run at 24 Kg loads with ¼" tungsten carbide ball on 50 mm Timken ring for 15000 cycles at a speed of 700 rpm.

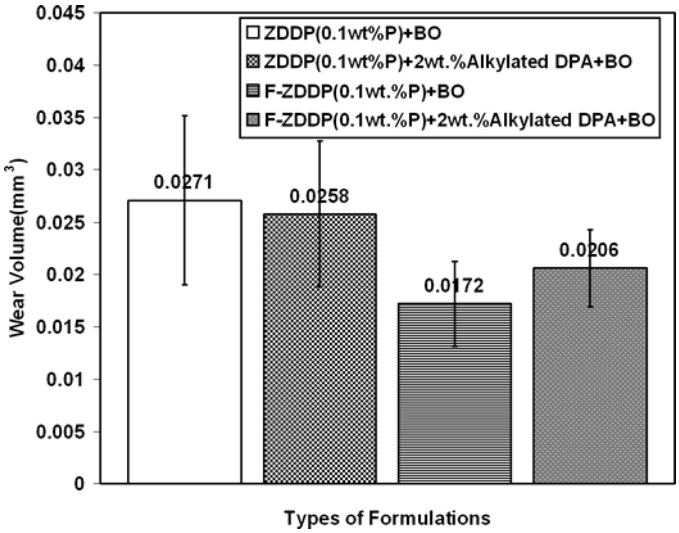

Figure 3.6: Wear volume vs. type of formulation for long-term tests. The different formulations used are: ZDDP (0.1 wt.% P) + base oil, ZDDP (0.1 wt.% P) + 2 wt.% alkylated DPA + base oil, F- ZDDP (0.1 wt.% P) + base oil and F-ZDDP (0.1 wt.% P) + 2 wt.% alkylated DPA + base oil. The tests were run at 20 Kg loads with ¼" tungsten carbide ball on 50 mm Timken ring for 50,000 cycles at a speed of 700 rpm.

From the comparisons of wear volumes at short term tests (15000 cycles), it has been found that addition of antioxidant to ZDDP has shown some improvement over ZDDP, while the

addition of antioxidant to F-ZDDP has shown a weak antagonistic effect when compared to the wear volume of F-ZDDP alone. With the addition of antioxidants to ZDDP, the oxidation of ZDDP could be minimized and its antiwear characteristics enhanced, leading to improved antiwear performance. However, on addition of antioxidants to F-ZDDP, there is an increase in the extent of wear. This may be because the antioxidant being aminic in nature naturally binds to the fluorine in the F-ZDDP as reflected in the decreased intensity of the doublets at 57 and 66 ppm in the NMR spectra of Figure 3.3. However, the binding is not sufficient to completely suppress the presence of the P-F bond and the beneficial effects of the fluorinated chemistry.

Another reason for the observed weak antagonistic effect of F-ZDDP with ADPA when compared to F-ZDDP alone could be due to the fact that ADPA being basic, it complexes with some of the fluorine (which is electronegative) present in F-ZDDP to form a weak hydrogen-like bonding. This proposed complex formation mechanism is illustrated below.

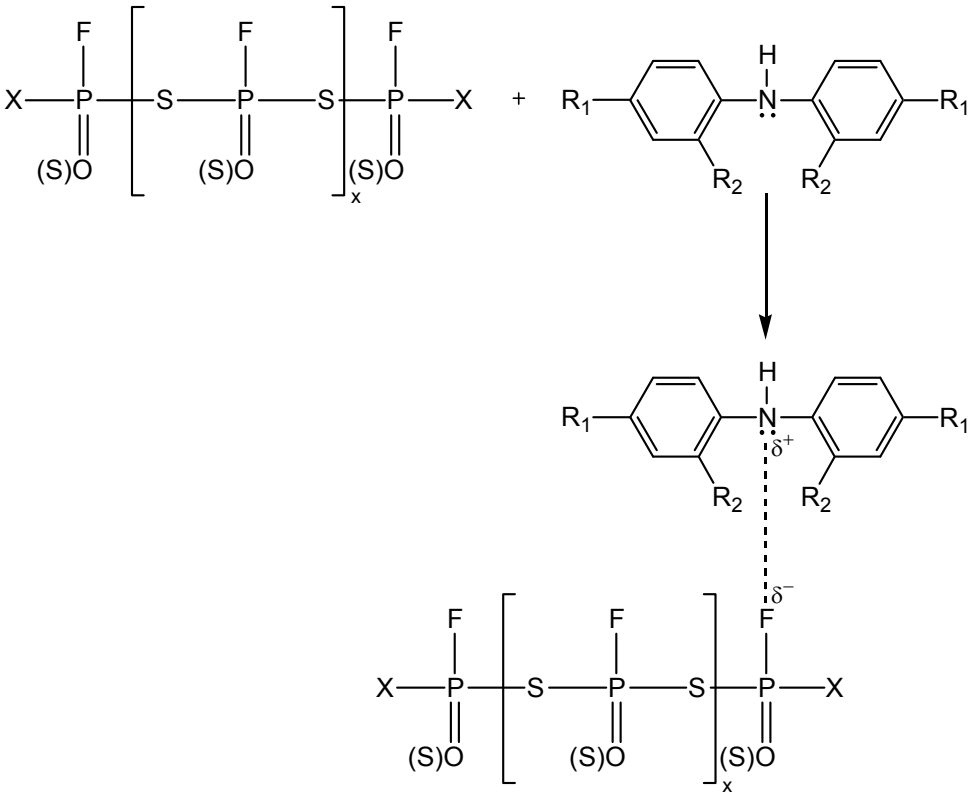

(3.1)

This complex formation inhibits the ability of F-ZDDP to quickly reach the surface and form a protective film. Since this complex formation is weak, significant quantities of F-ZDDP could remain free of complex formation and be available for wear protection.

From the observation of wear volumes at long term tests (50,000 cycles) and lower loads (20Kg), it's seen that there is little improvement over ZDDP by adding antioxidant to ZDDP. However, from the comparison of wear performance of ZDDP plus antioxidant with F-ZDDP, plus antioxidant, addition of antioxidant to F-ZDDP shows some improvement over ZDDP with antioxidant. Long term tests reveal that the durability of the proactive film is much better in the case of F-ZDDP compared to ZDDP, both in the presence and absence of antioxidant.

3.2.3 Surface Analysis by Auger Electron Spectroscopy

After the wear test, the rings were cut to examine the elemental distribution of the film in an Auger electron spectrometer. Steel rings from two different tests having two different formulations were chosen for the analysis. Samples were mounted on a specimen holder and placed in the spectrometer. Initially, samples were surveyed by (rough scan) AES at low spatial resolution to determine an image acquisition strategy. As antiwear film is believed to be composed of phosphorus, sulphur, zinc, iron, oxygen and carbon, these elements were selected for analysis [68, 114].

Figure 3.7 shows the SEM micrographs of the wear tracks of the rings tested for 50,000 cycles at a load of 20Kg for (a) ZDDP (0.1wt.%P) + 2wt.% alkylated diphenylamine in mineral oil and (b) F-ZDDP(0.1wt.%P) + 2wt.% alkylated diphenylamine in mineral oil. Figure 3.8 (a), (b) and (c) show the plots of relative concentration versus sputtering time of P, S, Fe, O, and C for ZDDP(0.1 wt.%P) + 2wt.% alkylated diphenylamine in mineral oil at different locations. Figure 3.9 (a), (b), (c) similarly shows the corresponding plots for F-ZDDP (0.1 wt.%P) + 2wt.% alkylated diphenylamine in mineral oil.

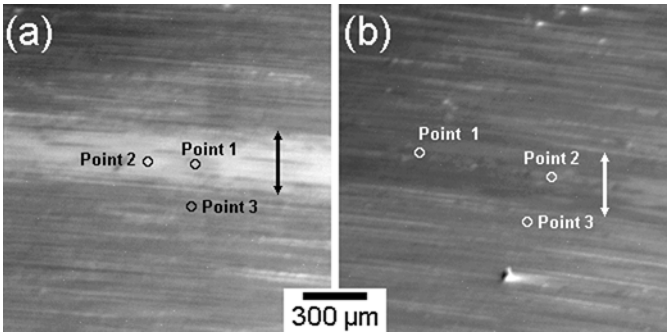

Figure 3.7: SEM of wear tracks of ZDDP and F-ZDDP, with ADPA. The wear tracks shown are of the ring tested for 50,000 cycles at a load of 20Kg for (a) ZDDP(0.1 wt.%P)+2wt.%Alkylated DPA in mineral oil and (b) F-ZDDP(0.1 wt.%P)+2wt.%Alkylated DPA in mineral oil.

A 2mm × 2mm area was sputtered using an argon ion beam with energy 2kV, and Auger electron spectra were acquired from 3 spots; 2 within the wear track and one outside. Peaks for Fe, O, P, S and C were the only major peaks observed. The area under the peaks were measured and added. The (relative) concentration of each element was calculated by scaling with the total measured area of all peaks.

Comparison of the AES depth profile from spots within the tribofilm in both ZDDP and F-ZDDP with antioxidant indicates that the film is significantly thicker in the case of F-ZDDP plus antioxidant, compared to ZDDP plus antioxidant. In addition, the film formed from F-ZDDP plus antioxidant incorporates a larger amount of P and S in it, while the film in the case of ZDDP plus antioxidant has more oxygen. The presence of more oxygen in the tribofilm is usually associated with the onset of oxidation of the film that eventually results in its breakdown. The presence of oxide particles in the tribofilm has been shown to be detrimental to the tribological process, resulting in poorer wear properties [115]. When the AES spectra within the wear track are compared to the region just outside the wear track, the thickness of the protective film is very small in the latter region. It is covered by the oil during the test and reaches temperatures of around 100°C–120°C, resulting in some thermal decomposition of ZDDP and F-ZDDP, and the formation of a thermal film.

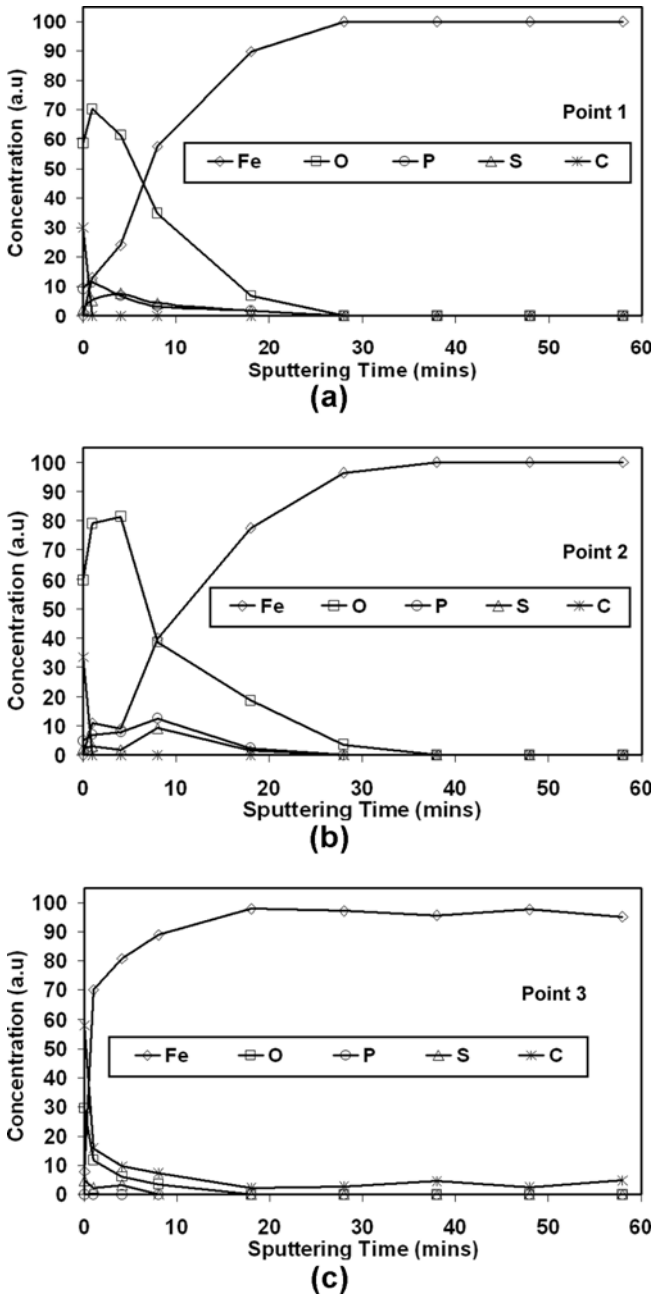

Figure 3.8: Elemental composition of tribofilms of ZDDP with ADPA. Plots show concentration (a.u) vs. sputtering time (min) of phosphorus, sulphur, iron, oxygen and carbon for ZDDP (0.1 wt.% P) +2 wt.% ADPA in mineral oil at different locations. Point 1 in (a) and point 2 in (b) represent data from within the wear track, while point 3 in (c) is from outside the wear track.

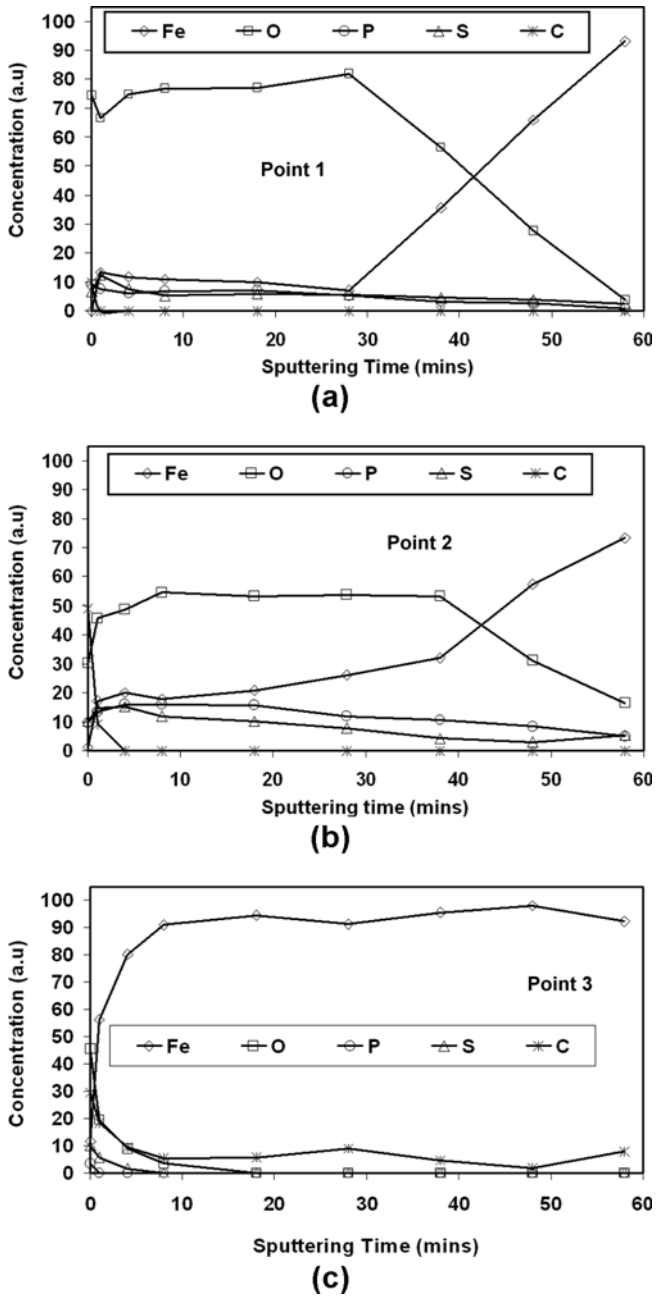

Figure 3.9: Elemental composition of tribofilms of F-ZDDP with ADPA. Plots show concentration (a.u) vs. sputtering time (min) of phosphorus, sulphur, iron, oxygen and carbon for F-ZDDP (0.1 wt.% P) +2 wt.% ADPA in mineral oil at different locations. Point 1 in (a) and point 2 in (b) represent data from within the wear track, while point 3 in (c) is from outside the wear track.

However, these thermal films are substantially thinner than the tribofilm formed as shown in Auger spectra in Figure 3.8 (c) and Figure 3.9 (c), both in the case of ZDDP and F-ZDDP. Comparing the Auger depth profiles of the thermal films shown in Figure 3.8 (c) and Figure 3.9 (c) with the Auger depth profiles of the tribofilms seen in Figure 3.8 (a), (b) and Figure 3.9 (a), (b), it is apparent that the thermal films are much thinner than the tribofilms as reflected by the time it takes to sputter down to the underlying Fe substrates.

3.3 Summary

The interactions between fluorinated ZDDP and ZDDP with alkylated diphenylamine were studied using NMR, and its impact on wear performance was examined using ball-on-cylinder tribometer. The surface of the tribofilm was examined using Auger spectroscopy. The ^{31}P NMR spectra of ZDDP and F-ZDDP with alkylated diphenylamine were compared with the ^{31}P NMR spectra of 50 wt.% ZDDP at room temperature, 50 wt.% baked ZDDP and F-ZDDP.

There were no new peaks formed due to the interaction of ZDDP with alkylated diphenylamine. However, when compared to the spectra of F-ZDDP, F-ZDDP with alkylated diphenylamine showed drastic changes in the intensity of basic ZDDP and the intensity of doublets at 65 and 57 ppm decreased considerably, indicating the interaction of antioxidants with fluorinated ZDDP.

Ball-on-cylinder wear tests were carried out with ZDDP and F-ZDDP with alkylated diphenylamine and these were compared with wear performance of ZDDP and F-ZDDP in mineral oil alone. The wear performance of F-ZDDP alone in mineral oil was found to be the best among all cases and wear performance of ZDDP in mineral oil alone being the worst. Addition of antioxidants showed improved wear performance in the case of ZDDP, whereas addition of antioxidants to F-ZDDP showed a marginal increase in wear.

The Auger electron spectroscopy of ZDDP and F-ZDDP with alkylated diphenylamines indicated that film from F-ZDDP with alkylated diphenylamine was thicker compared to that of ZDDP with alkylated diphenylamine. The film from F-ZDDP with alkylated diphenylamine

incorporated more P and S in the tribofilm, whereas the tribofilm from ZDDP with alkylated diphenylamine contained more oxygen.

CHAPTER 4

NANOSCALE MECHANICAL PROPERTIES OF IN-SITU TRIBOFILMS

Under thermal and tribological condition ZDDP breaks down to form abrasion resistant glassy films consisting of polyphosphates and metal sulfides which protect the sliding surfaces against wear [5, 47, 65, 68]. Degradation of ZDDP is a very complex process and much effort has been dedicated to understand the mechanism of its degradation and interaction with other additives. Computer simulation of zinc phosphate structure under extreme loading conditions indicates that pressure induced cross linking is a key mechanism in the formation and functionality of antiwear films [116].

The presence of other additives in engine oils results in ZDDP interacting with them in a complex fashion resulting in a reduction of its breakdown and film forming efficiency [19, 40, 76, 77, 117]. These effects as well as the limitations observed in the anti wear performance of ZDDP [118] pose challenges to efforts made to reduce the amount of ZDDP in engine oils. In a tribological study it has been shown that fluorinated ZDDP exhibits significant improvements in wear behavior in comparison to ZDDP [82, 84]. This would allow the possibility of further reduction of phosphorus in engine oils than current levels.

Antioxidants play an important role in retaining the properties of base oils in harsh environments in the presence of active radicals by serving as radical scavengers. An excellent and most extensively used group of antioxidants are alkylated diphenyl amines. However, the influence of this group of antioxidants on the nature of the tribofilms as well as the antiwear performance of oils is still a matter of study and forms the basis of this study.

Under many different lubrication regimes, where ZDDP or F-ZDDP are present as antiwear agents in lubricants, the in-situ breakdown of these antiwear agent during early stages, is responsible for the formation of antiwear tribofilm. However, over longer periods of time and

harsher lubrication conditions (e.g. boundary lubrication), these films can potentially breakdown or be removed, resulting in the formation of hard debris. Entrapment of the debris in the contact area results in the scratching of the film and its eventual failure. Scratch resistance of the tribofilms can be use as a measure for the resistance of a tribofilm to abrasion. In a study of tribofilms formed with fully formulated oils, the hardness near the surface layer of the tribofilm is less than the hardness of the deeper layers of the tribofilm thus causing the surface layer to shear off easily and reform on the surface just as easily [101, 110]. This has been indicated as the reason for the superior wear performance of tribofilms. In this study, the nanomechanical properties including the hardness, modulus, scratch resistance and nano-wear resistance of the films, formed from ZDDP and F-ZDDP in presence as well as absence of antioxidants have been examined to develop an understanding of the effect of various variables on the nature of the tribofilms.

In addition to nanomechanical properties of the tribofilms, morphology and chemical composition of the tribofilms play a role in determining their properties. In this study, scanning electron microscopy and focused ion beam were used to image the substrate-tribofilm interface and thus measure the thickness of the tribofilms. The elemental distribution depth profile of the film was analyzed using Auger electron spectroscopy. The nature of the wear debris was analyzed using transmission electron microscopy.

4.1 Experimental Procedure

4.1.1 Tribofilm Analysis

Wear tests were conducted on the formulations described in section 3.1.2 and the tribofilms formed were subjected to various analyses as described in the following sections. The tribofilm generated on the wear track was isolated by cutting small portions from tested rings. In order to keep the tribofilm intact, and to avoid the effects of over heating and contamination during cutting of the samples, the rings were cut with a low speed diamond blade immersed in mineral oil.

4.1.2 Scanning Electron Microscopy Studies of Tribofilms

Samples used for the scanning electron microscopy (SEM) study consisted of a small section of the ring containing the wear track after the wear test. Samples were cleaned with hexane and acetone thoroughly and mounted on the sample holder and examined using a JEOL, JSM-IC845A scanning microscope with acceleration voltage of 20KV.

4.1.3 Focused Ion Beam Analysis

In order to study the tribofilm/ substrate interface and measure thickness of these films a small section of the ring was mounted in a Zeiss Leo FIB 1540XB microscope. An area of uniform tribofilm on the wear track was located and then an area of 8 µm by 10 µm was milled using a gallium ion beam. The depth of the sputtered area in each case was around 4 µm. This process exposes the side profile of the tribofilm and the underlying substrate (steel). A secondary electron micrograph of the cross section of the film was generated using the secondary electron detector located at an angle of 54° from the direction vertical to the surface of the sample.

4.1.4 Surface Analysis of Tribofilms by Auger Electron Spectroscopy

The elemental distribution depth profile of the tribofilm was examined using a Perkin–Elmer PHI 560 ESCA/SAM system. The operational pressure was maintained at 1.2 x 10-7 torr. during acquisition. A 2mm by 2 mm area that included the tribofilm and its surrounding area was selected. In order to obtain Auger electron spectra from different depths of the tribofilm, the selected area was sputtered with argon ion beam with an excitation voltage of 2 KV for one minute before every scan. Each scan was run in spot mode with a spot size of 2 µm for 5 minutes right at the center of the sputtered area to obtain an overall spectrum as well as the spectra for oxygen, sulphur, iron, phosphorus and carbon peaks.

4.1.5 Transmission Electron Microscopy of Wear Debris

Wear debris generated in boundary lubrication conditions were obtained by collecting the oil from the wear track after the test with a thin sheet of plastic, since this debris represents

a very small portion of the additive induced tribofilm formed during the tribological process. The oil containing the wear debris was transferred to a copper grid covered with a carbon film and the grid was repeatedly cleaned with hexane to remove oil from the carbon film. Bright-field image and selective area electron diffraction pattern of the wear debris adhered to the carbon film were obtained using JEOL TEM-ASID (1200EX), 120 KV.

4.1.6 Nano Indentation of Tribofilms

The nano indentation, nano scratch and scanning nano wear tests were run on tribofilms generated from wear tests using the four different formulations mentioned above using a Hysitron TriboIndenter® and data from nano indentation was used to calculate the reduced modulus and hardness of the tribofilm. Nanoscale indentation tests were performed by applying a force to an indenter tip and measuring the tip displacement into the sample. During indentation, the applied load and tip displacement are continually measured, creating a load-displacement curve for each indent. The quasi-static nano indentation tests were performed with a NorthStar® cube corner probe with a tip radius of <40 nm. Each indent consisted of a trapezoidal load function comprised of a 5-second loading segment, a 2-second holding segment, and a 5-second unloading segment.

4.1.7 Nano Scratch Tests

Scratch tests were performed using a Hysitron TriboIndenter® in scratch mode. The TriboIndenter® is load-controlled and displacement sensing in the normal direction to the sample surface, while simultaneously displacement-controlled in the lateral direction parallel to the sample surface. Scratch tests were performed under 30-second 5000 μN ramping load with a 90° conical probe with 2μm tip radius on each tribofilm sample. During a scratch test, a normal force is applied to the indenter tip as a function of time in accordance with the scratch load function, while the tip is also driven towards the predetermined lateral position within a specified amount of time. Normal force, normal displacement, lateral force, and lateral

displacement are measured and recorded as a function of time. From these four parameters, material properties and film adhesion characteristics can be deduced.

4.1.8 Scanning Wear Tests

Scanning wear tests were performed using the instrument's in-situ Scanning Probe Microscopy (SPM) mode. In this mode, wear regions were created by raster scanning the indenter tip across the sample surface while maintaining a specified normal force. Scanning wear tests were performed using 90° conical probe with 2μm tip radius. An area of 4μm square was selected for scanning and four passes were carried out in each case subsequent to the scanning wear tests the tip was used in Scanning Probe Mode (SPM) to acquire topographical information of the worn region of the tribofilm.

4.2 Results and Discussion

4.2.1 Scanning Electron Microscopy of Tribofilms

SEM micrographs in secondary electron mode of the wear tracks generated from four different tests are shown in Figure 4.1. To generate the SEM samples, wear tests were run under 3.56 GPa contact load for 15000 cycles on four oils samples containing 0.10 wt% phosphorus. It can be seen in Figure 4.1, that, the observed image of the wear track is very smooth in the case of F-ZDDP (0.1 wt % P) and F-ZDDP with alkylated DPA in mineral oil indicating the presence of stable tribofilm which is associated with the best wear performance in the case of F-ZDDP. When compared to the wear track of F-ZDDP or F-ZDDP with alkylated DPA, the wear track of ZDDP and ZDDP with alkylated DPA shows more abrasion and removal of the film from a larger region of the wear track which is reflected in the observed poor wear of ZDDP (0.1 wt.% P) in mineral oil. It must be noted that the onset of tribofilm breakdown and the beginning of abrasive wear correspond to the initial formation of deep scratches on the tribofilm caused by the abrasive action of the wear debris. Tribofilm formed with greater abrasion resistance offer better wear behavior as evidenced by film formed with F-ZDDP both in the presence and absence of antioxidant.

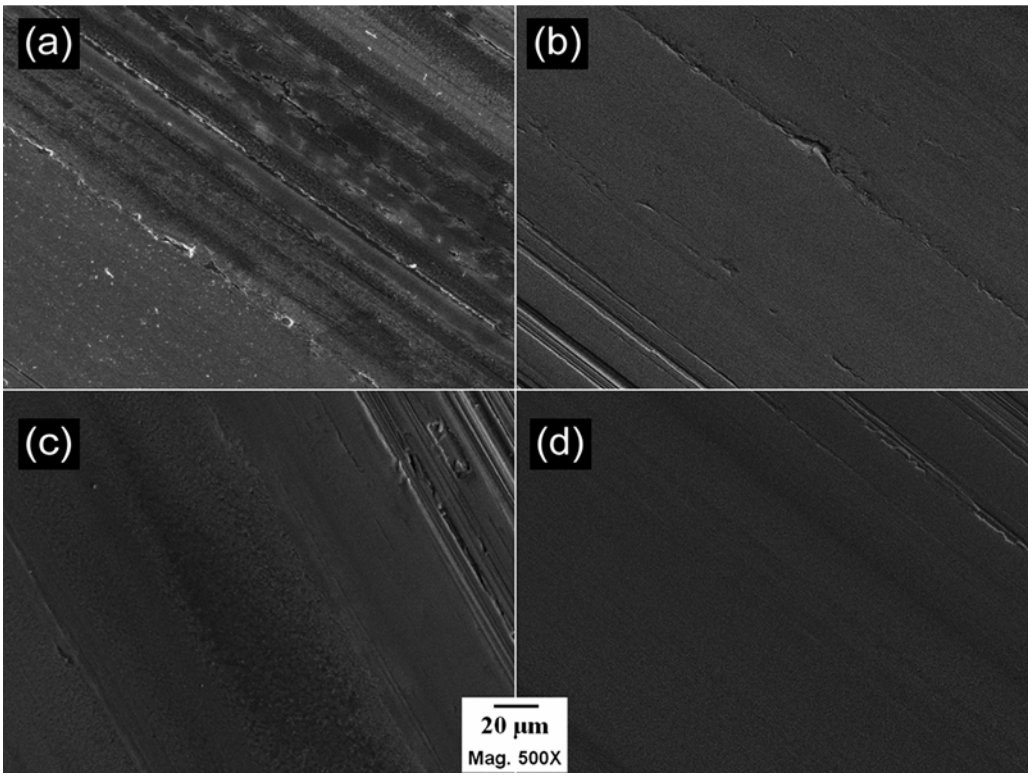

Figure 4.1: SEM of wear tracks of ZDDP and F-ZDDP, with and without ADPA. SEM micrographs show the wear tracks of the rings tested for 15000 Cycles at a load of 24 Kg for (a) ZDDP(0.1 wt.% P) in mineral oil, (b) ZDDP(0.1 wt.% P)+2 wt.% ADPA in mineral oil, (c) F-ZDDP(0.1wt.% P) in mineral oil, (d) F-ZDDP(0.1 wt.% P)+2 wt.% ADPA in mineral oil.

4.2.2 Focused Ion Beam Sectioning of Tribofilms

A focused ion beam was used to generate trenches within the wear track of the tribofilms for four samples described above. The gallium ion beam was used to mill an 8 µm by 10 µm area inside the wear track. Care was taken to choose a region with a visually uniform and continuous tribofilm. The trench was sputtered to an approximate depth of 4µm to expose the cross section of the tribofilm.

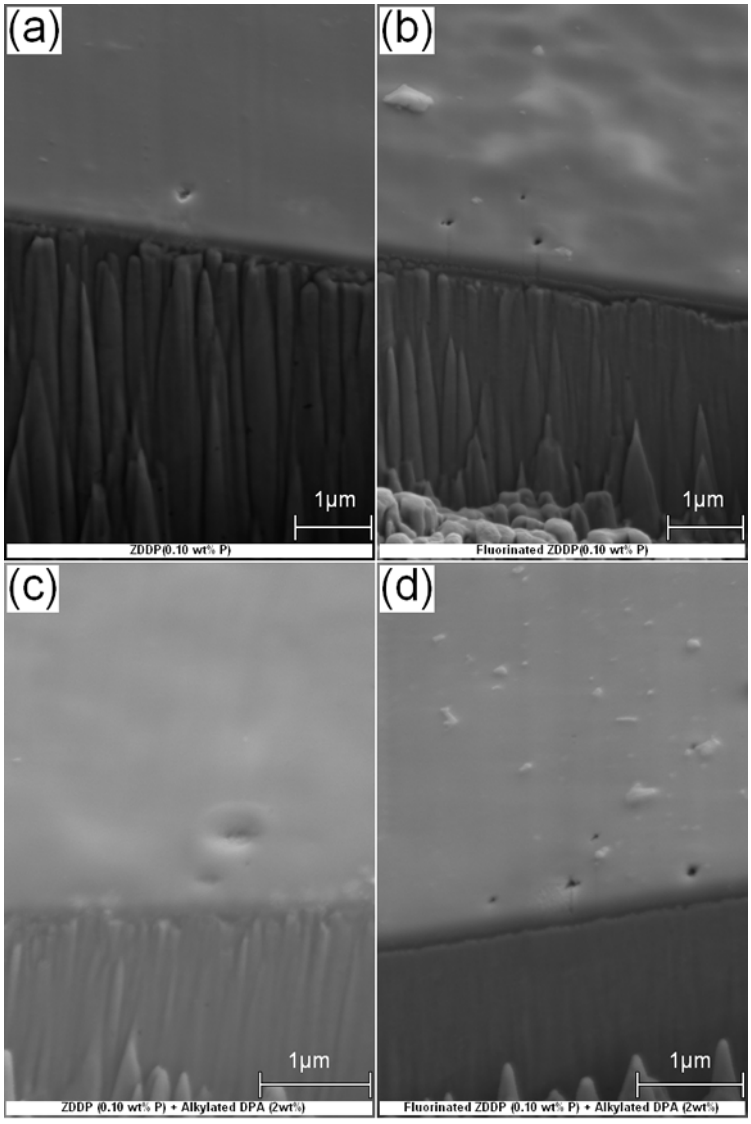

Figure 4.2: FIB images of tribofilms of ZDDP and F-ZDDP with and without ADPA. SEM micrographs of the edge of a trench ion-milled by focused ion beam show the cross sections of the substrate and the tribofilm for the formulations (a) ZDDP (0.1 wt.% P) + base oil, (b) F-ZDDP (0.1 wt.% P) + base oil, (c) ZDDP (0.1 wt.% P) + 2 wt.% ADPA + base oil, and (d) F-ZDDP (0.1 wt.% P) + 2 wt.% ADPA + base oil.

The secondary electron image of the cross section of the tribofilm generated from the formulations having ZDDP and F-ZDDP in mineral oil is shown in Figure 4.2 (a) and Figure 4.2 (b) respectively. From Figure 4.2 (a) it can be seen that the observed thickness of the tribofilm for ZDDP in mineral oil was less than 100 nm which is in agreement with several observations

made by other investigators in fully formulated oil [32, 119-122]. The thickness of the tribofilm for fluorinated ZDDP in mineral oil was almost twice of that of ZDDP in mineral oil. It can also be seen that the micrograph 4.2(b), shows the presence of two distinct layers of tribofilm. For the tribofilm generated from ZDDP on the other hand, the distinction between the two layers is not that clear. The thickness of the tribofilm generated from Fluorinated ZDDP is around 180 nm.

Figure 4.2 (c) and (d) shows the scanning electron micrograph of the cross section of the tribofilm generated from the formulation ZDDP (0.1 wt.% P) and F-ZDDP(0.1 wt.% P) with 2wt.% Alkylated DPA in mineral oil. As shown in Figure 4.2 (c) and Figure 4.2 (d), the tribofilm that has covered the surface of the steel substrate has a thickness of around 135nm in the case of formulations having ZDDP (0.1 wt.% P) + 2 wt.% Alkylated DPA and tribofilm generated from formulation having F-ZDDP (0.1 wt.% P) + 2 wt.% Alkylated DPA has a thickness of around 235 nm at the place of observation. This finding of the thickness of tribofilm is confirmed by the Auger spectroscopy analysis described in section 3.2.3. These measurements of thickness were performed at several locations on the tribofilm and the values were found to be consistent. This indicates that for similar test conditions, F-ZDDP always yields tribofilms that are thicker than films formed with ZDDP both when antioxidant are used and when they are not used.

4.2.3 Surface Analysis of Tribofilms by Auger Electron Spectroscopy

Tribofilm was generated by testing the ring for 15,000 cycles at a load of 24Kg for four different formulations. After the wear test, the rings were cut using a low speed saw with pure mineral oil, cut specimens were washed with acetone and hexane to remove any contamination and examined in the Auger electron spectrometer. As antiwear film is believed to be composed of phosphorus, sulphur, zinc, iron, oxygen and carbon, these elements were selected for analysis [68, 115].

A 2mm by 2mm area of uniform tribofilm was sputtered with an argon ion beam for one minute each time and the spectra were always derived in spot mode at identical locations inside the film-covered wear track within the sputtered region. Each scan was run for 5 minutes at the

center of the sputtered area to obtain an overall spectrum as well as the spectra for oxygen, sulphur, iron, phosphorus and carbon peaks. Total time of sputtering time in all formulations is about 4 minutes which corresponds to top layer of the tribofilm of approximately 20 - 25nm. The plot of relative concentration as a function of sputtering time of P, S, Fe, O, and C is shown in Figure 4.3 (a) for ZDDP and Figure 4.3 (b) ZDDP with alkylated DPA in mineral oil and Figure 4.4 (a) for fluorinated ZDDP and Figure 4.4 (b) F- ZDDP with alkylated DPA in mineral oil.

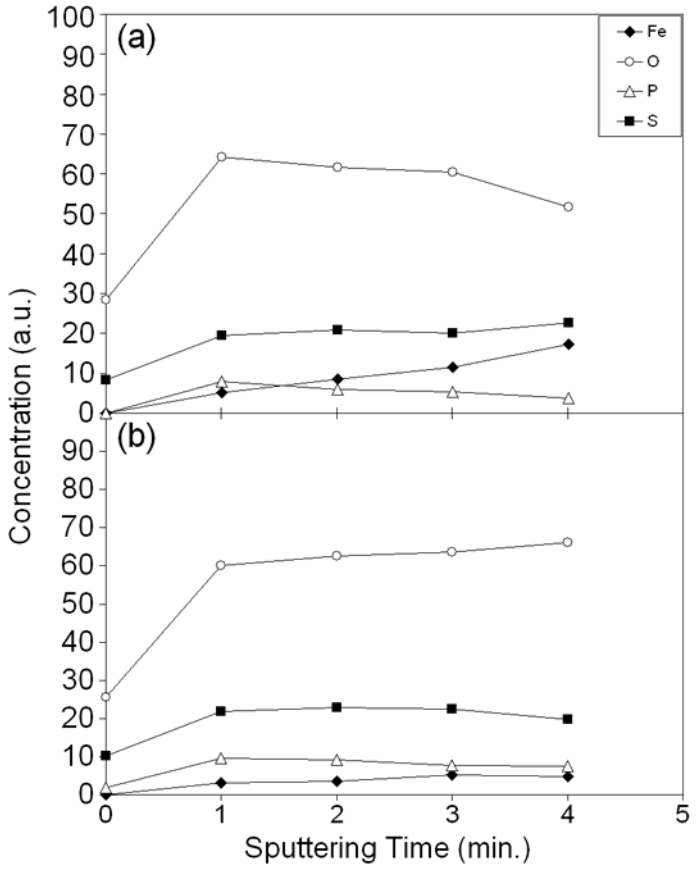

Figure 4.3: Elemental composition of tribofilms of ZDDP with and without ADPA. Graphs show concentration (a.u.) vs. sputtering time (min) of phosphorus, sulphur, iron, oxygen and carbon for (a) ZDDP (0.1 wt.% P) and (b) ZDDP (0.1 wt.% P) + ADPA in mineral oil.

It can be seen in Figure 4.3 (a) and (b) that sulphur level in the case of ZDDP with alkylated DPA is slightly higher than in the case of ZDDP in mineral oil. The phosphorus level is almost the same in both formulations. Oxygen concentration in ZDDP being high at the top

layer and decreases as sputtering time increases and decrease in oxygen concentration is very slow in the case of ZDDP with alkylated DPA. In both cases concentration of iron slowly increases as sputtering time increases.

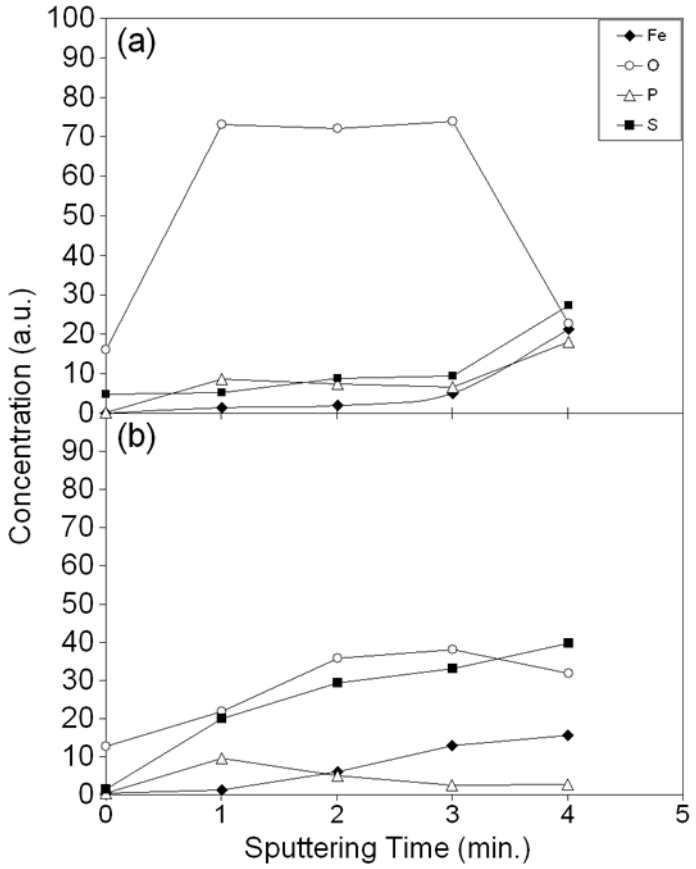

Figure 4.4: Elemental composition of tribofilms of F-ZDDP with and without ADPA. Graphs show concentration (a.u) vs. sputtering time (min) of phosphorus, sulphur, iron, oxygen and carbon for (a) F-ZDDP (0.1 wt.% P) and (b) F-ZDDP (0.1 wt.% P) +2 wt.% ADPA in mineral oil.

Figure 4.4 (a) and (b) indicate that the phosphorus concentration in F-ZDDP and alkylated DPA increases up to sputtering time of one minute beyond which, there is a decrease in phosphorus concentration with increase in sputtering time. F-ZDDP with alkylated DPA shows larger concentrations of sulphur compared to F-ZDDP in mineral oil. Iron concentration increases and oxygen concentration decreases in both formulations as the sputtering time increases. Comparison of the auger spectra for ZDDP and F-ZDDP indicates more phosphorus

in F-ZDDP than ZDDP. F-ZDDP with alkylated DPA has more sulphur when compare to ZDDP with alkylated DPA in mineral oil. In particular the F-ZDDP with alkylated DPA has the lowest levels of oxygen and the highest levels of P, S and Fe indicating the stable formation of a tribofilm on the surface.

4.2.4 Transmission Electron Microscopy Studies of Tribological Debris

Oil samples from wear tests described in section 3.1.2, containing wear debris were collected and prepared according to the procedure described in section 4.1.5 and the wear debris were observed under TEM. The chemical composition as well as the structure of wear debris collected from the wear track are representative of those of the tribofilm and consist of phosphorus, sulphur, oxygen, carbon, iron and zinc as the main constituents similar to those reported by others [74, 115, 123-125]. Figure 4.5 shows the bright field images and the corresponding diffraction patterns for the following four formulations:

a) ZDDP (0.1 wt.% P) in mineral oil

b) ZDDP (0.1 wt.% P) with 2 wt.% ADPA in mineral oil

c) F-ZDDP (0.1 wt.% P) in mineral oil

d) F-ZDDP (0.1 wt.% P) with 2 wt.% ADPA in mineral oil

The first column in Figure 4.5 shows the bright field images at low magnification (20Kx), while the second column shows these images at high magnification (200Kx). The third column represents the respective selected area diffraction patterns of wear debris for formulations. In all cases, the images at low magnification show the wear debris that is representative in size and shape for most of the debris seen for these samples.

Although the tribofilm is believed to be amorphous, the bright field image taken at high magnification shows the presence of particles, the selective area diffraction pattern indicates the crystalline nature of these particles. Earlier study conducted for longer duration of times (100,000 cycles) indicated that the oxides were Fe_2O_3 [115]. Indexing the ring patterns, the interplanar spacings d_{hkl} were calculated in each case and are compared to the same values for

pure iron [123], α-Fe_2O_3 [125] and Fe_3O_4 [126] in Table 4.1. It can be seen that the values of interplanar spacings observed in all four cases closely match those for Fe_3O_4 which indicates that these particles are primarily composed of Fe_3O_4 suggesting that the shorter duration of these tests result in lower oxidation states of iron. Careful observation of selective area diffraction patterns of the above formulations however, indicates subtle differences in the nature of the tribofilm. Tribofilms formed from formulations containing ZDDP are richer in crystalline particles content, containing a larger number of nanocrystalline particles (< 20 nm) of Fe_3O_4 and films containing F-ZDDP are more amorphous in nature which reflects in the better wear performance of formulations containing F-ZDDP [82, 83, 110].

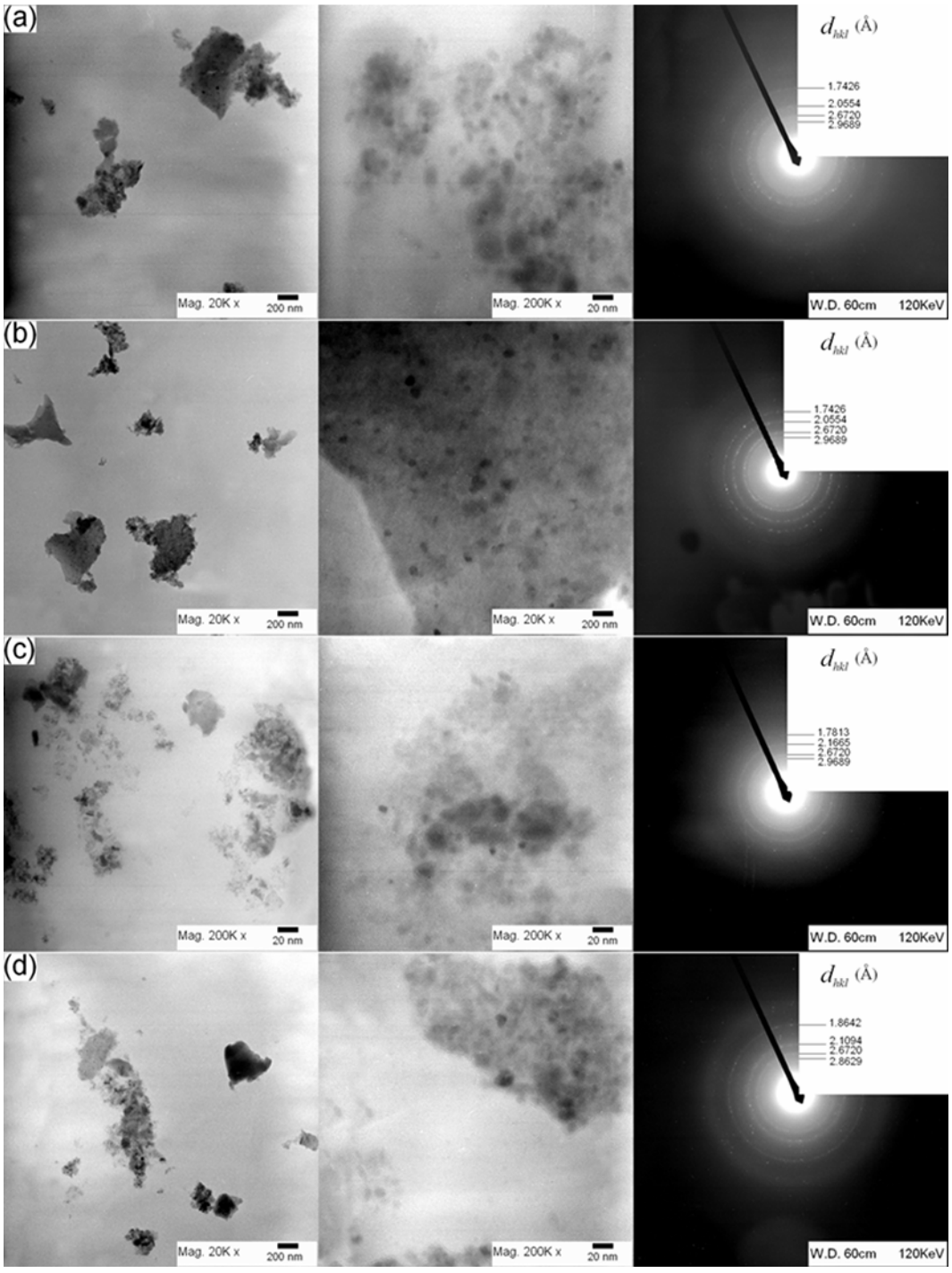

Figure 4.5: TEM of wear debris. Bright-field images at 200KX magnification and selected area diffraction patterns of wear debris from formulations (a) ZDDP (0.1 wt.% P) in mineral oil, (b) ZDDP (0.1 wt.% P) with 2 wt.% ADPA in mineral oil, (c) F-ZDDP (0.1 wt.% P) in mineral oil and (d) F-ZDDP (0.1 wt.% P) with 2 wt.% ADPA in mineral oil The tests were run at 24 Kg loads with ¼" tungsten carbide ball on 50 mm Timken ring for 15,000 cycles at 700 rpm.

The nucleation of Fe_3O_4 particles in the tribofilm and the resulting coherency strains created in the film are believed to be the precursor to the failure of the antiwear film. Hence, films with fewer oxide particles provide improved wear resistance as they are more likely to endure longer times. No significant differences in the extent of crystalline particles of Fe_3O_4 are seen with the addition of alkylated DPA. This indicates that the addition of the antioxidant helps preserve the lubricity and stability of the base oil but does not necessarily influence the oxidation and crystallization of oxides in the tribofilm.

Table 4.1: The calculated d_{hkl} spacings for the ring patterns observed in Figure 4.5 compared to observed values for iron and two types of iron oxide [123, 125, 126].

d Spacing (Å)						
			Observed Values			
Fe_3O_4	**Fe_2O_3**	**Fe**	**ZDDP**	**ZDDP + ADPA**	**F-ZDDP**	**F-ZDDP + ADPA**
2.96	1.69	2.03	2.9689	2.9689	2.9689	2.8629
2.53	1.452	1.43	2.6720	2.6720	2.6720	2.6720
2.096	1.055	1.17	2.0554	2.1095	2.1665	2.1095
1.712	0.931	–	1.7426	1.7426	1.7813	1.8642
1.614	–	–	–	–	–	–
1.483	–	–	–	–	–	–

4.2.5 Nano Indentation of Tribofilms

Tribofilms generated from the four different oil formulations, by running wear tests for 15000 cycles at a 3.56 GPa Hertzian contact load were examined using the nanoindenter. Each indentation consisted of a 5-second loading segment, a 2-second holding segment with the indentation force remaining constant at the peak value, and a 5-second unloading segment. A series of nano indentations with peak loads ranging from 15 μN to 1500 μN were run on an area inside the wear track of each sample where uniform tribofilm existed and an indentation force vs. vertical displacement of the indenter tip was plotted for four different formulations as shown in Figure 4.6 and Figure 4.7. Figure 4.6 (a) and (b) show a force vs. vertical displacement for the formulations with ZDDP and fluorinated ZDDP in mineral oil but no antioxidant, for the peak

indentation loads ranging from 25 to 80 μN. Indentations with peak loads of 100, 200, 500 and 1500 μN were also performed, but were not included in Figure 4.6 and Figure 4.7 for clarity. Each of the force vs. vertical displacement plots shown in Figure 4.6 (b) i.e., fluorinated ZDDP show overlap during the loading segment of each indentation and are observed to have two distinct regions of different slopes, i.e. at penetration depths below 15 nm, the slope of each curve is steeper than the slope of the same curves at penetration depths beyond 15 nm. This is in correlation with the observations made in the FIB/SEM images of Figure 4.2 where the tribofilm generated from Fluorinated ZDDP has two visually distinctive layers while this is not the case for the film generated from ZDDP.

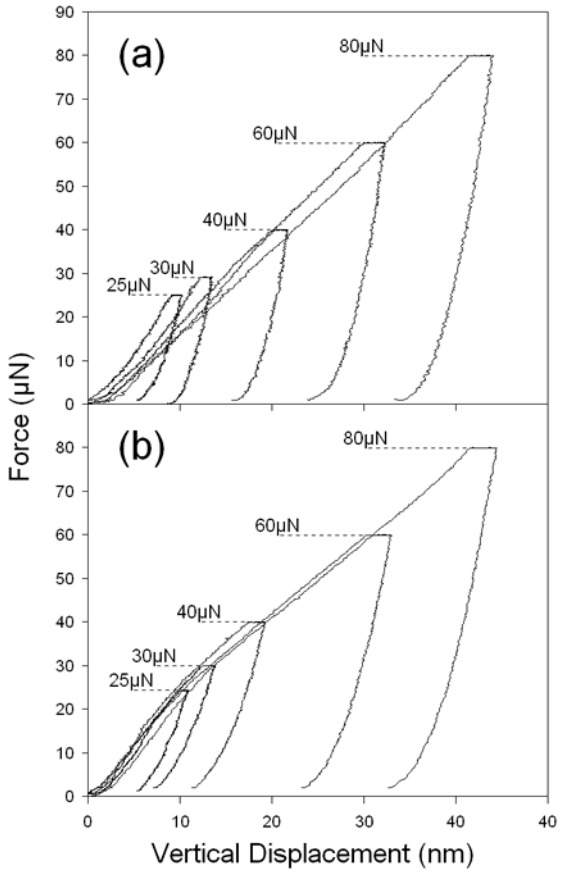

Figure 4.6: Nano indentation graphs of ZDDP and F-ZDDP tribofilms. Plots show force vs. vertical displacement for peak indentation loads ranging from 25 to 75 μN for tribofilms generated from (a) ZDDP + Base oil and (b) F-ZDDP + Base oil.

Figure 4.7 shows force vs. vertical displacement for indentation tests on tribofilms from formulations where 2 wt% alkylated DPA is present together with ZDDP (a) and fluorinated ZDDP (b) in mineral oil for the peak indentation loads ranging from 15 to 75 μN. Figure 4.7 (a) shows that the force vs. vertical displacement curves for ZDDP in presence of alkylated DPA show overlap at low peak indention loads during loading the segment, while no such overlapping is seen in Figure 4.7(b) for the formulation having fluorinated ZDDP and alkylated DPA in mineral oil.

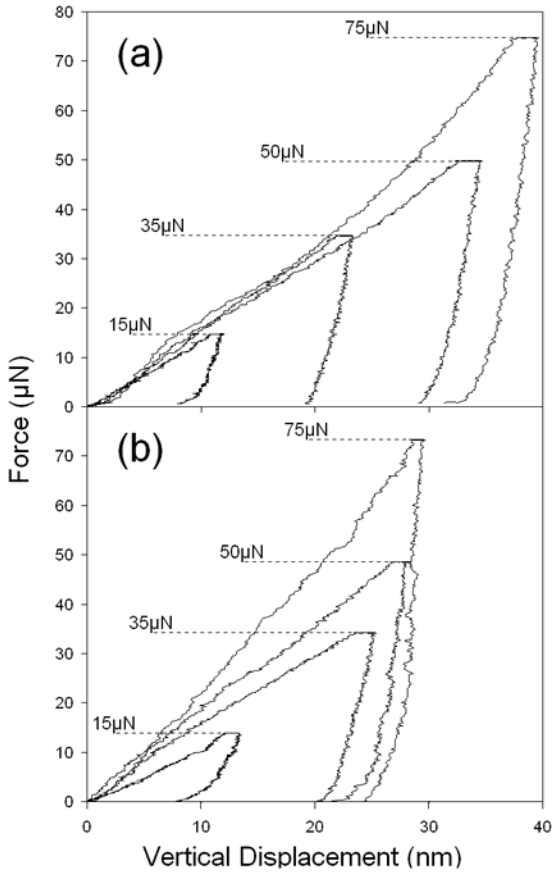

Figure 4.7: Nano indentation graphs of tribofilms of ZDDP and F-ZDDP, with ADPA. Plots show force vs. vertical displacement for peak indentation loads ranging from 25 to 80 μN for tribofilms generated from (a) ZDDP with ADPA in mineral oil and (b) F-ZDDP with ADPA in mineral oil.

The data from nano indentation tests can also be presented in terms of calculated reduced modulus and hardness of the tribofilm. In Figure 4.8 (a), hardness data of the tribofilms

generated from formulations having ZDDP and fluorinated ZDDP in mineral oil for different indentation peak loads are plotted against penetration depths. The hardness data for both the samples follows a decreasing trend until penetration depth of 50 nm; beyond this depth. Observed hardness values remain almost constant in both cases and approach values close or equal to the hardness of the steel substrate. For both samples the hardness of the tribofilm at the surface of the film (depth ≈ 10 nm) is around 20 GPa which decreases rapidly with increasing applied peak force and increasing penetration depths. In a quantum chemical modeling study by Müser et al [116] it was shown that pressure-induced cross linking of zinc polyphosphate near the surface result in tribofilms that are harder near the surface. This result is consistent with our experimental results that indicate a near surface region with hardness as high as 20 GPa compared to substrate of 8 GPa. In addition the cross linked network of zinc polyphosphates result in moduli of tribofilm (100-120 GPa) that are substantially lower than the that of the steel substrate (200 GPa). Thus the tribofilms behave as compliant surfaces absorbing and dissipating energy when they come and go out of contact.

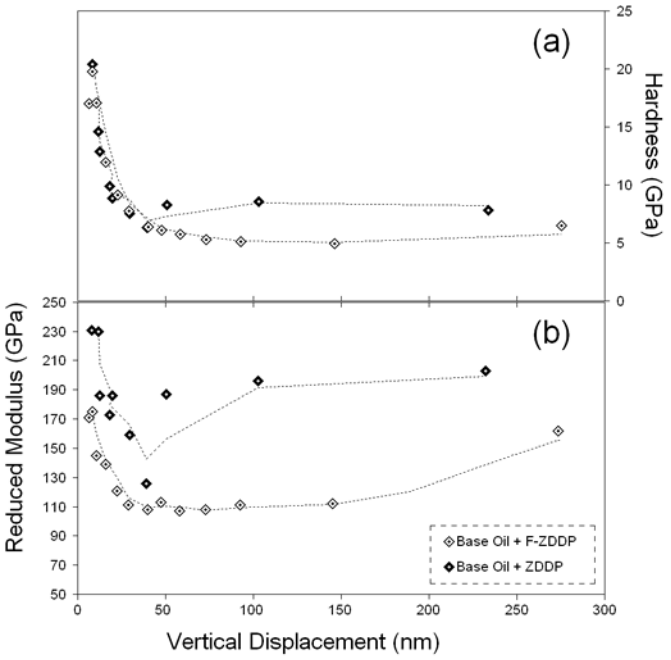

Figure 4.8: Hardness and reduced modulus plots for ZDDP and F-ZDDP tribofilms. Graphs show (a) hardness and (b) reduced modulus vs. contact depths for peak indentation loads

ranging from 25 to 80 μN for tribofilms generated from (a) ZDDP in mineral oil and (b) F-ZDDP in mineral oil.

In the presence of antioxidants this behavior is reversed with the presence of a softer and more compliant layer approximately 20 nm thick near the surface. In Figure 4.9 (a), hardness of the tribofilms generated from formulations having ZDDP and fluorinated ZDDP with alkylated DPA in mineral oil for different indentation peak loads are plotted as a function of penetration depths. For both formulations hardness increases from around 4 GPa in the near surface region (depth > 10 nm) to approximately 7.5 GPa as the penetration depth increases up until 50 nm.

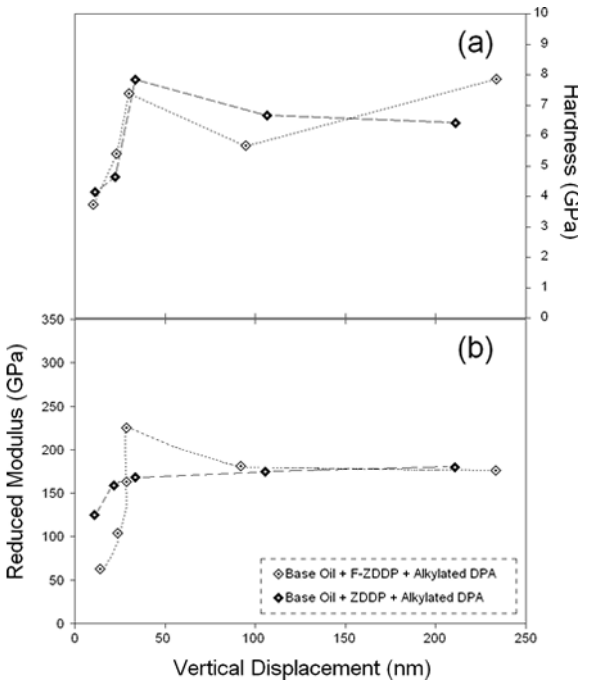

Figure 4.9: Hardness and reduced modulus plots for tribofilms of ZDDP and F-ZDDP, with ADPA. Graphs show (a) hardness and (b) reduced modulus vs. contact depths for peak indentation loads ranging from 15 to 75 μN for tribofilms generated from (a) ZDDP with ADPA in mineral oil and (b) F-ZDDP with ADPA in mineral oil.

This observation is indicative of a much softer layer of the film on top of a harder layer in the case of both ZDDP and fluorinated ZDDP when alkylated DPA is present. Hardness values observed with addition of antioxidants are much lower than those of ZDDP and fluorinated

ZDDP in mineral oil which indicate the formation of softer a film when antioxidant is added to ZDDP as well as Fluorinated ZDDP. A tribofilm with a top layer of lower hardness and reduced modulus than underlying tribofilm has been documented in fully formulated oils by Ye et al [102] and is consistent with the data presented in Figure 4.9. At higher penetrations depths (>200 nm) the values of hardness is almost same for all four different formulations indicting that the penetration is occurring into the steel substrate.

Figure 4.8 (b), shows the calculated reduced moduli against penetrations depths for different peak loads for ZDDP and F-ZDDP in mineral oil. Figure 4.9 (b) shows the same data for ZDDP with alkylated DPA and F-ZDDP with alkylated DPA in mineral oil. In Figure 4.8 (b), the values of reduced modulus decrease rapidly from a maximum value at the surface region of both tribofilm samples, however, for the case where the tribofilm is generated by ZDDP the decreasing trend of value of the modulus with higher penetration depths is abruptly reversed at a penetration depths less than around 60 nm where it increases to a constant value of approximately 200 GPa which is consistent with modulus of the steel substrate. For the tribofilm generated by F-ZDDP, the decreasing trend does not start to reverse until penetration depth of around 150 nm where it slowly starts to increase to values close to that of substrate steel modulus. Thus while the thickness of the tribofilm is well below 100 nm for the tribofilm generated from ZDDP, the film thickness is approximated to be around >150 nm for the film generated from F-ZDDP. This also is in agreement with the values approximated for the thickness of the two tribofilms from the FIB/SEM images of Figure 4.2.

From Figure 4.9 (b), it is evident that the values of reduced modulus increases rapidly for both samples with minimum values at the surface region being around 60 GPa for fluorinated ZDDP with alkylated DPA and 130 GPa for ZDDP with alkylated DPA where as much higher values of modulus were found for ZDDP and fluorinated ZDDP in the absence of the antioxidant alkylated diphenyl amine. The maximum value of modulus observed for tribofilm generated from formulation fluorinated ZDDP with alkylated DPA is 230 GPa and 160 GPa for

ZDDP with alkylated DPA in mineral oil at a penetration depth of around 40nm for both the samples. Beyond the penetration depth of 40nm, the tribofilm from fluorinated ZDDP with alkylated DPA start to show decrease in reduced modulus and slowly reaches a constant value of approximately 170 GPa where as for tribofilm from ZDDP with alkylated diphenyl amine the modulus value slowly increases to a value of 170GPa and remains constant at this value.

4.2.6 Nano-Scratch Behavior of Tribofilms

The breakdown of the tribofilm is usually initiated by a piece of tribofilm that breaks loose and scratches the surface of the film. The outer surface of the film being harder also yields debris that is able to scratch and breakdown the tribofilm. The evidence of scratched tribofilms is evident in Figure 4.1 (a) for the surface of a film formed by ZDDP alone that exhibits several long scratches. In order to investigate the scratch resistance of the tribofilm, scratch tests were performed on the tribofilms formed in tests performed as described earlier for the four different formulations using a 90° cube corner conical probe with 2μm tip radius. The scratch load function consisted of a linearly ramped scratch force to a peak normal load of 5000 μN in 30 seconds while the tip is moved laterally over a distance of 6 μm. The plot of the vertical applied force versus the vertical displacement of the tip of the probe through out the scratch is shown in Figure 4.10 (a) for tribofilms generated from ZDDP and Fluorinated ZDDP in base oil and in Figure 4.11 (a) for ZDDP and Fluorinated ZDDP with alkylated DPA in base oil. In this case the control variable is the load which is increased continuously from 0 to 5000μN over 30 seconds and the depth of penetration is a response. The comparison of Figure 4.10 (a) and Figure 4.11 (a) indicates the presence of thicker and softer film in the case of F-ZDDP with alkylated DPA and ZDDP with alkylated DPA in mineral oil compared to fluorinated ZDDP and ZDDP in mineral oil. In Figure 4.11 (a) it can be seen that plot shows a change in slope at around 129 nm with the slope increasing, indicating that penetration occurring into the steel substrate which is agreement with thickness of film observed by FIB analysis for ZDDP with alkylated diphenyl amine in mineral oil. The observation of curve 12 (a) indicates the presence

of more complaint film up until penetration depth of 40 nm in the case of fluorinated ZDDP with alkylated DPA after this penetration depth, the slope of the curve for fluorinated ZDDP with alkylated DPA becomes similar to that of ZDDP with alkylated DPA in mineral oil.

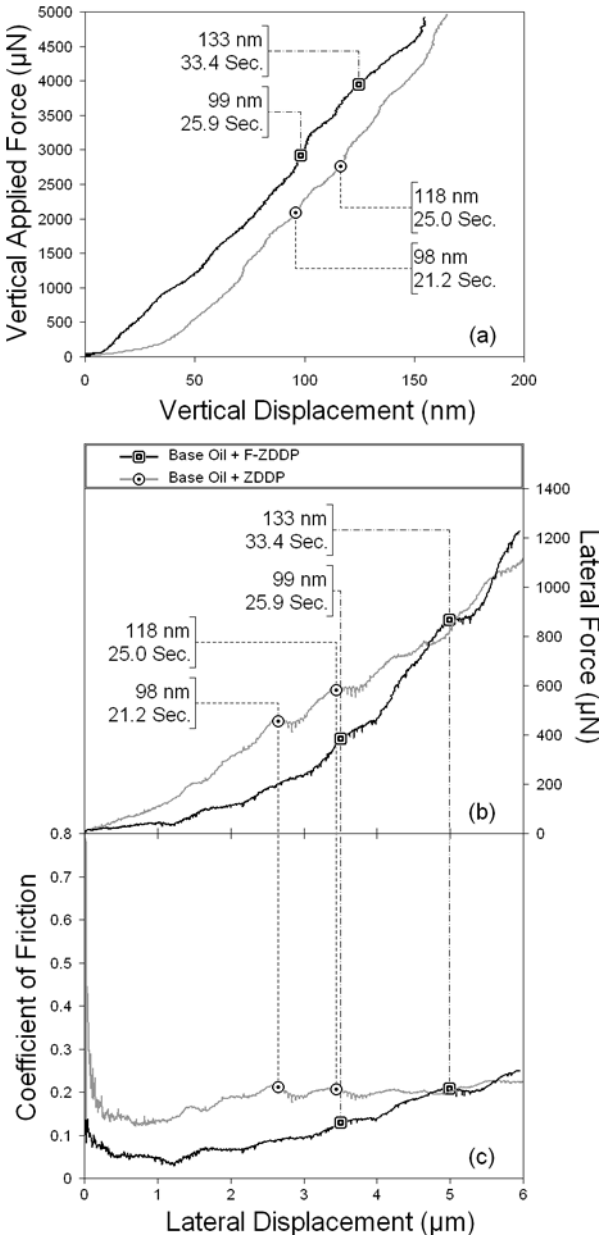

Figure 4.10: Scratch test results of ZDDP and F-ZDDP tribofilms. Scratch tests were conducted with ramp force of 5000 μN on tribofilms from ZDDP and F-ZDDP in mineral oil: (a) vertical applied force vs. vertical displacement, (b) lateral force vs. lateral displacement and (c) coefficient of friction vs. lateral displacement.

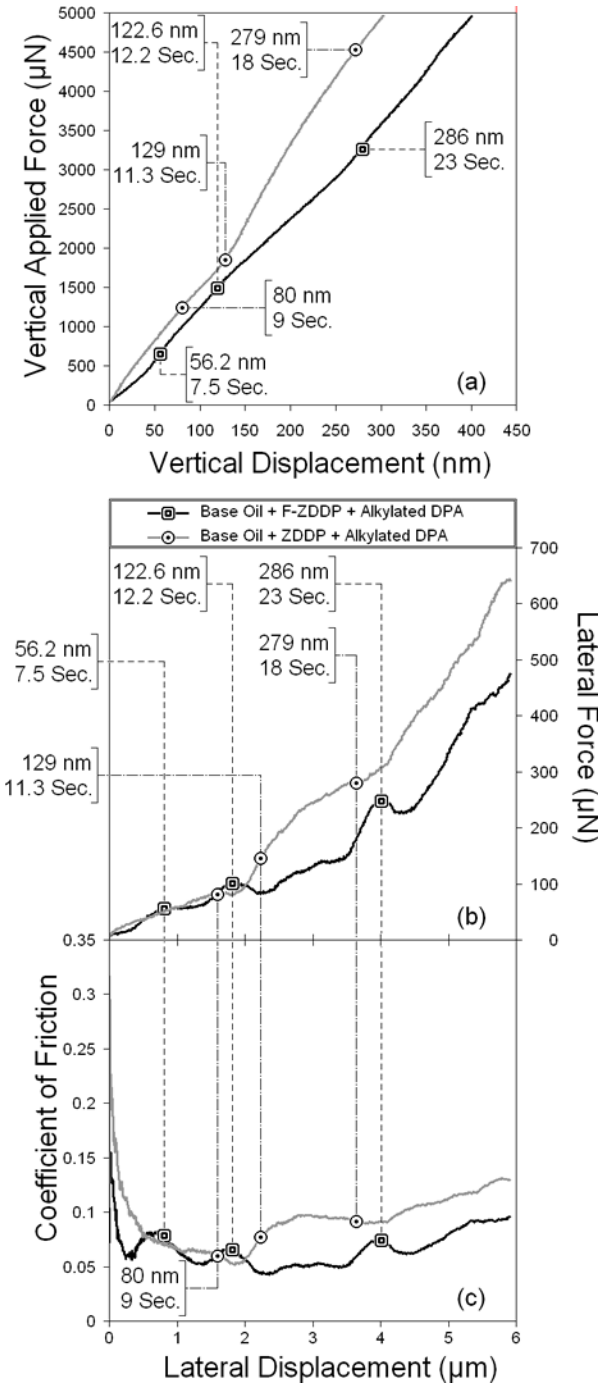

Figure 4.11: Scratch test results of tribofilms of ZDDP and F-ZDDP, with ADPA. Scratch tests were conducted with alkylated DPA in mineral oil: (a) vertical applied force vs. vertical displacement, (b) lateral force vs. lateral displacement and (c) coefficient of friction vs. lateral displacement.

In Figure 4.10 (b) and Figure 4.11 (b), the lateral force through out the scratch is plotted against lateral displacement (displacement along the length of the scratch) for four different formulations. In this case the lateral displacement is increased from 0 to 6 μm continuously over the same period of 30 seconds when the vertical load is increased from 0 to 5000 μN and the lateral force is the response observed. From Figure 4.10 (b) and Figure 4.11 (b), it is evident that the lateral force required to continue through the scratch increases as the probe moves laterally and deeper to create the scratch. As the probe digs deeper into the scratch, the contact area increases resulting in increased resistance to further lateral motion. In addition the pileup of material ahead of the scratch increases the resistance to lateral motion. Figure 4.10 (b) and Figure 4.11 (b) indicate that the formulations having ZDDP and fluorinated ZDDP with alkylated DPA required smaller lateral force for the movement along the length of the scratch compared to formulation having ZDDP and fluorinated ZDDP only in mineral oil. This indicated the generation of softer film with addition of antioxidant which is in agreement with observations made by nano-indentation and hardness. The scratch test for the film formed by ZDDP shows several points of interest at lateral scratch positions of approximately 2.5 μm and 3.4 μm and at 1.75 and 3.75 μm for ZDDP with alkylated DPA in mineral oil where parts of the tribofilm comes free as evidenced by the constant to small drop in lateral force. In the scratch test conducted on the tribofilm formed by Fluorinated ZDDP small drops in load are seen at lateral scratch positions of 3.5 μm and more significant drops in lateral force at 5 μm and in the case of fluorinated ZDDP with alkylated DPA it was 0.75, 1.75 and 4 μm.

The ratio of the lateral resistance to scratch to the applied vertical load is the coefficient of friction. The coefficient of friction is plotted as a function of the lateral displacement in Figure 4.10 (c) and Figure 4.11 (c). The coefficient of friction is much higher at the very beginning of the scratch test for tribofilms formed from all four formulations. This is because the lateral force needed to break into the film which is much harder near the surface is much higher than the lateral force needed to continue though the length of the scratch (in films without alkylated

DPA). The films generated from ZDDP and fluorinated ZDDP shows higher coefficient of friction through out the duration of test than film generated with the presence of antioxidant. However from the comparison of Figure 4.10 (c) and Figure 4.11 (c) is evident that tribofilms generated from ZDDP exhibits much higher coefficient of friction than seen in all other formulations in the scratch test. Once the scratch is initiated, the coefficient of friction stabilizes to a value of around 0.2 for films from ZDDP and 0.1 for Fluorinated ZDDP. This differences in coefficient of friction between the two cases can be attributed to the fact that the ZDDP offers less resistance to abrasion and consequently in a scratch test, as the test proceeds there is a larger amount of debris that the indenter has to plough through as the scratch proceeds. Towards the end of the scratch both the scratches have large pileups ahead of the indenter and have coefficients of friction that are comparable at 0.2. The undulations in the coefficient of friction with local peaks and valleys relate to points where the tribofilm cracks and peels off from the wear track which corresponds to the locations where lateral forces is constant or shows some drop in Figure 4.10 (b) and Figure 4.11 (b). It can be seen from Figure 4.11 (b) that in the case ZDDP with alkylated DPA there is sharp increase in lateral force to move laterally from 2 sec to 3.5 μm this may be due to the penetration occurring in different regions or different grains of the steel substrate. There is also increase in coefficient of friction for this formulation for this duration. After this penetration depth slopes observed for both curves are similar indicting that penetration is occurring into the substrate.

4.2.7 Nanoscale Wear Resistance of Tribofilms by Scanning Wear

Scanning wear tests were performed on the samples using the in-situ Scanning Probe Microscopy (SPM) mode of the TriboIndenter®. In this mode, the instrument can create wear regions by raster scanning the indenter tip across the surface of the tribofilm samples while maintaining a specified normal force. The wear tests were run with a 75 μN normal force and four passes were performed on each sample. A 2 μm by 2 μm area of each sample was selected to run a scanning wear test. Three-dimensional topographical in-situ SPM images of

the tested area of each tribofilm are shown in Figure 4.12 (a), (b), (c) and (d) for tribofilms generated from ZDDP, Fluorinated ZDDP, ZDDP with alkylated DPA and fluorinated ZDDP with alkylated DPA in mineral oil respectively.

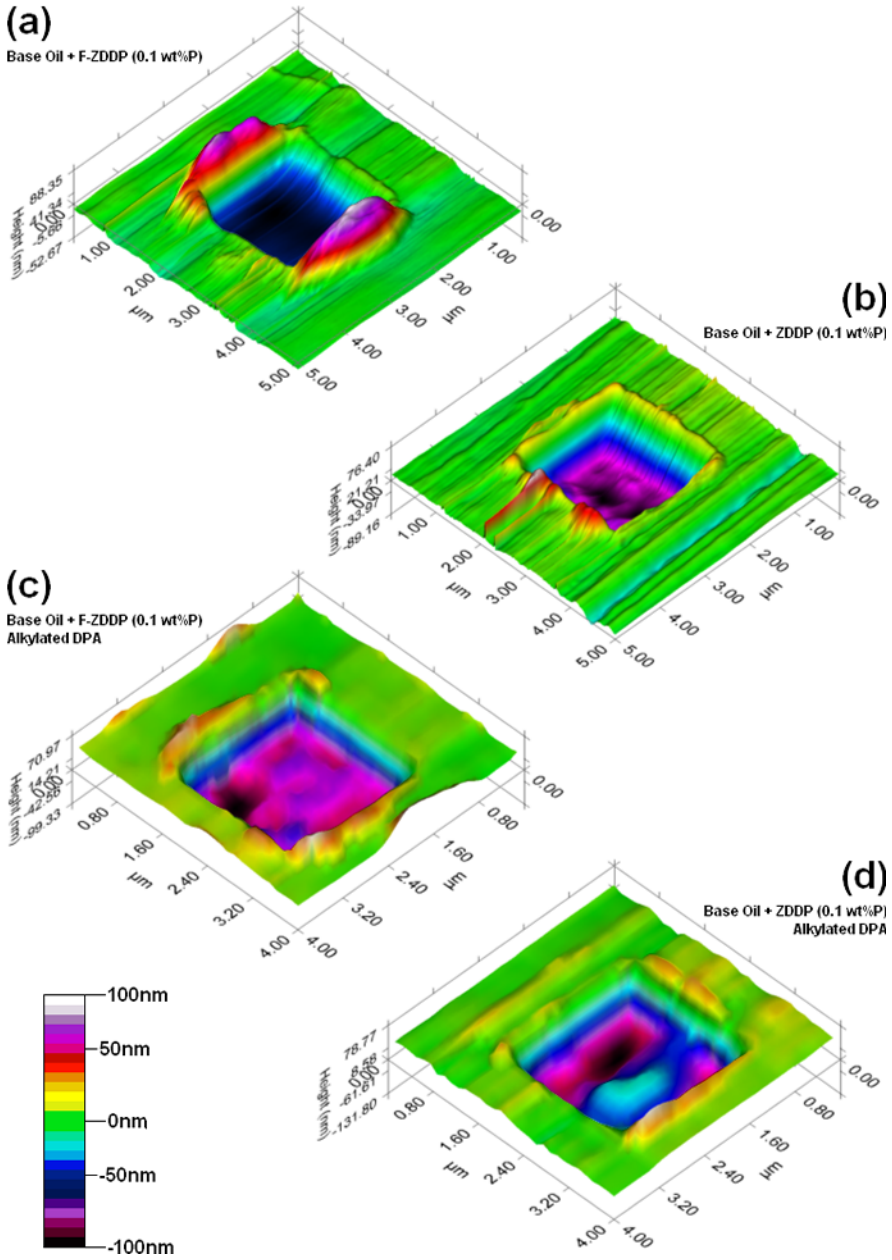

Figure 4.12: Scanning wear SPM images of ZDDP and F-ZDDP tribofilms with and without ADPA. Figure shows three-dimensional images of the post-wear-test surfaces of the sample generated from topographical in-situ SPM imaging of tribofilms: (a) ZDDP, (b) F-ZDDP, (c) ZDDP with ADPA, (d) F-ZDDP with ADPA in mineral oil.

From Figure 4.12 (a) and (b) it is evident that the tribofilm generated using the oil sample containing base oil with Fluorinated ZDDP (0.10 wt.% P) is more resistant to wear as the wear depth in tribofilms is smaller in the case of F-ZDDP compared to ZDDP in mineral oil. This observation is in correlation with scratch test data shown in Figure 4.10 (a) which also indicates deeper probe penetrations for tribofilms generated from ZDDP compared to the case of the Fluorinated ZDDP at equal vertical applied loads. It can be seen from Figure 4.12 (c) and (d), formulation containing ZDDP with alkylated DPA shows wear depth comparable to F-ZDDP with alkylated DPA. From the comparison of all formulations, it can be seen that the tribofilm created by F-ZDDP was more resistance to wear than all other formulation and ZDDP with alkylated DPA has less resistance to wear than all other formulations.

4.3 Summary

Tribofilms with thickness ranging from 100 – 200 nm were developed in-situ during wear tests using a Zinc Dialkyl Dithiophosphates (ZDDP) and fluorinated ZDDP (F-ZDDP). The influence of the antioxidant alkylated diphenyl amine on the formation and properties of these tribofilm was examined. Results indicate that the thickness of the tribofilms formed when F-ZDDP is used is always thicker than the tribofilm formed with ZDDP. In addition, in the presence of antioxidants the tribofilm thickness is increased. The hardness of these tribofilms in the absence of the antioxidants is significantly higher at the near surface region (0-30nm) when compared to the films formed in the presence of antioxidant.

Nanoscratch tests conducted to examine the abrasion resistance of the tribofilms also indicate that the tribofilms formed by F-ZDDP are more resistant to scratch compared to films formed by ZDDP. In the presence of antioxidants, tribofilms formed by F-ZDDP are significantly thicker while both films behave in a similar fashion in nanoscratch tests. Nanowear tests on the tribofilms indicate that films formed using F-ZDDP are more abrasion resistant than films formed by ZDDP. Transmission electron microscopy of the wear debris formed during the tests were examined and results indicate the nucleation and growth of nanoparticles of Fe_3O_4 with an

approximate size of 5–10 nm embedded within an otherwise amorphous tribofilm. The number of these Fe_3O_4 nano particles is lower in the tribofilms formed with F-ZDDP compared with tribofilms formed with ZDDP indicating that the amorphous structure persists in the F-ZDDP films and may be attributed to their stable structure and better wear behavior.

CHAPTER 5

THERMAL AND OXIDATION STABILITY STUDIES

Hydrocarbons lubricants such as base stocks decompose to produce alkyl free radicals as a result of exposure of the lubricants to high temperatures, light and /or metal catalysts [23, 85, 86]. These free radicals react with molecular oxygen dissolved in the lubricant or from the environment to produce oxygen-containing species such as peroxy radicals and hydroperoxides [40]. These oxygen-containing intermediate products are very unstable and hence undergo a series of reaction steps called propagation, branching and termination. These processes lead to the formation of oil-insoluble products such as carboxylic acids, aldehydes and ketones [23, 87]. Formation of these insoluble materials causes changes in the oil that result in a loss in the desired physical properties of the lubricant. These detrimental changes include an increase in viscosity and acidity of the formulation [86, 127-129]. All of these qualities can influence the overall performance, life expectancy and operating costs of the lubricant. As effects of oxidation include changes in viscosity and acidity of the oil, it is very important to monitor the oxidation stability – i.e., the resistance of a lubricant to its molecular decomposition or alteration at raised temperatures in an ordinary air environment [20] – of the lubricant for safe operation of machines.

F-ZDDP has been proven to be a much better antiwear additive than ZDDP in base oil [82]. To address regulatory requirements, the goal is to replace the latter with lower levels of the former additive at a mass-production scale. Meanwhile, it is also extremely important that F-ZDDP has at least the same or better oxidation stability than ZDDP to make this product viable in mainstream applications. This work aims to explore the oxidation stability of formulations with F-ZDDP and compare it to formulations with ZDDP. This study intends to address the following objectives:

1. Investigate the oxidation stability of F-ZDDP and compare it to that of ZDDP.
2. Study the effects of antioxidants on the oxidation stability of oils containing F-ZDDP and compare it with that of oils containing ZDDP.

Oil samples containing F-ZDDP and ZDDP and various types of antioxidants such as alkylated diphenyl amine (ADPA), hindered phenols (HP), methylene bis dibutyl dithiocarbamate (MBDTC) and molybdenum dithiocarbamate (MoDTC) were oxidized in flowing air. Viscosity and total acid number (TAN) were examined using ASTM D-445, and ASTM D-664 standards respectively, and the amount of oxidation products produced were quantified using FT-IR. All these above tests are aimed at helping to assess oil oxidation, understanding the effectiveness of the antioxidant in retarding the oxidation of the oil and aiding in the determination of whether or not F-ZDDP has superior oxidation stability over ZDDP, thereby adding to the knowledge base of properties and characteristics of F-ZDDP as a lubricant additive.

5.1 Experimental Procedure

5.1.1 Formulations used in this Study

The formulations containing antiwear agents such as ZDDP and fluorinated ZDDP alone were prepared in base oil. Base oil used in the study was 100 neutral. Phosphorus amounts in all formulations were kept constant at 0.08 wt.% according to current GF-4 levels. In addition, the formulations containing ZDDP and F-ZDDP with different types of antioxidants were also prepared in base oil. Types of antioxidants chosen for this study represent those commonly used in formulating engine oils. The total amount of antioxidants in all mixtures is maintained at 1.5 wt.%, with the exception of MoDTC. This is because MoDTC contains a metal, which tends to contribute to ash content in the material when they burn. The chemical structures of the some of the antioxidants used in this study are shown in Figure 5.1.

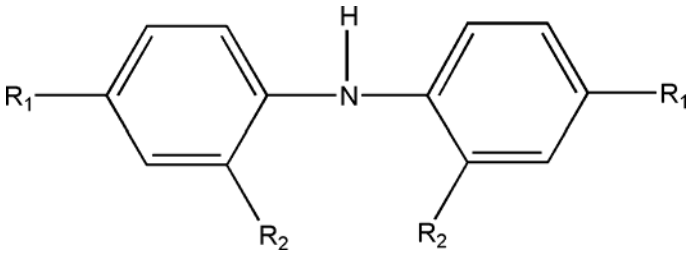

(a)

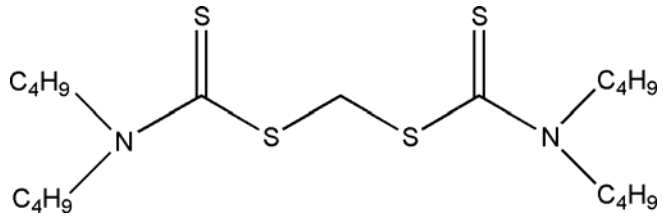

(b)

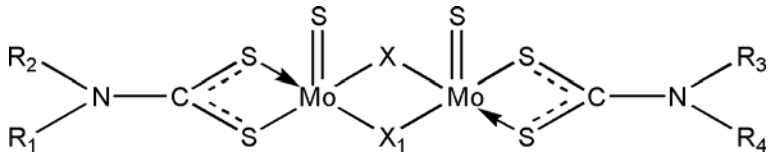

(c)

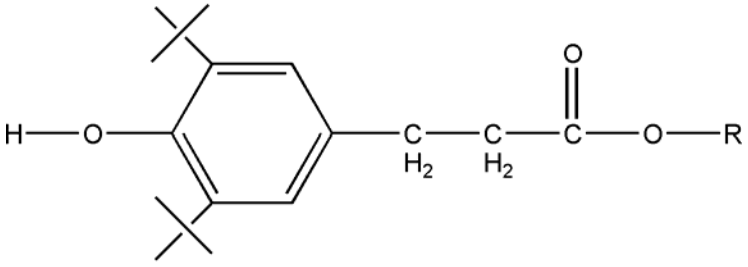

(d)

Figure 5.1: Chemical structures of antioxidants used in oxidation stability studies: (a) Alkylated diphenyl amine (ADPA); (b) Methylene bis dibutyl dithiocarbamate (MBDTC); (c) Molybdenum dithiocarbamate (MoDTC); (d) Hindered phenol (HP).

In order to study the oxidation stability of ZDDP and F-ZDDP with various antioxidants commonly used in engine oils, the oxidation of base oil was first studied using FT-IR. Next, the antioxidants were added to evaluate the effects of these additives on the on the oxidation of base oil. Finally, F-ZDDP was added to the base oil, both with and without antioxidants, and the

performances of these formulations were assessed. A similar sequence was executed for identical compositions but with ZDDP instead of F-ZDDP in order to undertake a comparative study.

Additionally, mixtures of antioxidants are also used to exploit any synergy effect (the condition where the benefit observed from certain combination of antioxidants is better than the sum of the effects from individual constituents) that may arise from such antioxidant combinations. Formulations of the various oil samples in base oil are:

1. Base oil alone
2. Base oil + individual antioxidants
3. Base oil + F-ZDDP
4. Base oil + F-ZDDP + alkylated diphenyl amine (ADPA)
5. Base oil + F-ZDDP + methylene bis dibutyl dithiocarbamate (MBDTC)
6. Base oil + F-ZDDP + hindered phenol (HP)
7. Base oil + F-ZDDP + molybdenum dithiocarbamate (MoDTC)
8. Base oil + F-ZDDP + alkylated diphenyl amine + methylene bis dibutyl dithiocarbamate
9. Base oil + F-ZDDP + alkylated diphenyl amine + hindered phenol
10. Base oil + F-ZDDP + hindered phenol + methylene bis dibutyl dithiocarbamate
11. Base oil + F-ZDDP + alkylated diphenyl amine + molybdenum dithiocarbamate
12. Base oil + F-ZDDP + hindered phenol + molybdenum dithiocarbamate

Similar solutions were also prepared with ZDDP for comparison with F-ZDDP.

5.1.2 Oxidizing Conditions

The parameters used for oxidizing the oil samples are based on the ASTM Standard – ASTM D-4871. Oxidized samples were checked for oxidation products using FT-IR and measured for changes in viscosity and TAN. Based on this standard, the oxidation was initially performed at a temperature of 120°C and an air flow of 70 ml/min. However, the FT-IR spectra and viscosity measurements of the resulting products showed no noticeable oxidation due to

heating under these conditions, even after a period of eight days. The temperature and air flow were therefore raised to 160°C and 90 ml/min (5.4 l/hr) respectively to enable the observation of oxidation within a week for each formulation, while ensuring that these conditions continued to conform to the ASTM D-4871 standards.

5.1.3 Fourier Transform Infrared Spectroscopy

The process of oxidation produces various carbonyl-containing products such as carboxylic acids, aldehydes, ketones and esters. The formation of these carbonyl compounds were examined using FT-IR spectroscopy. All of the above mentioned products can be detected in the same region of the FT-IR spectrum i.e., 1800–1700 cm^{-1}. While the FT-IR spectra do not provide insight into the exact identity of the specific compounds present, they are nonetheless useful in observing changes in the amounts of these carbonyl-containing groups. By observing the intensity changes, the amount of oxidation products thus formed can be studied.

Samples were taken out of the baking chamber every 24 hours and subjected to FT-IR analysis. FT-IR spectra were obtained in absorbance mode by using a KBr cell of known path length (0.5mm thick) with a Thermo Nicolet 6700-FTIR Spectrometer in the range of 4000–400 cm^{-1} with 32 scans in each case. This path length was kept constant so that the thickness of the oil film between the KBr windows was the same for all formulations. Quantitative analysis of the area under the respective carbonyl peaks could then be made to asses the oxidation of the lubricant.

5.1.4 Measurement of Kinematic Viscosity

The progression of oxidation eventually produces myriad of oxidation products, both of low and high molecular weight. All these increase the viscosity of the lubricant under use. Changes in the viscosity of lubricants thus indicate the oxidation degradation of the lubricant. Measurement of changes in viscosity hence signifies the oxidation stability of the oil, with lower change in viscosity over time representing better oxidation stability and vice versa.

Samples were taken out of the baking chamber every 48 hours. Oil samples thus baked are then measured for viscosity using ASTM D-445 testing procedures and standards. Viscosity measurements are conducted at two different temperatures namely 40°C and 100°C.

If the samples are thought or known to contain solid particles, it is necessary to filter these particles using nylon filter of 80μm screen, prior to the measurement. This step is important since one of the most common sources of error in viscosity measurement is caused by particles of dust lodged in the capillary bore of the viscometer. Viscosity was calculated by measuring the time required for a known volume of a liquid to flow under gravity through the capillary of a calibrated viscometer under a reproducible driving head and at a controlled and known temperature. The kinematic viscosity (cSt) is then obtained by the product of the measured flow and the calibration constant of the viscometer used for the experiment. Kinematic viscosity is calculated by taking the average of two such acceptable determined values. $v_{1,2} = C\ t_{1,2}$ where

C is the calibration constant of the viscometer (mm^2/s^2)

$t_{1,2}$ are the measured flow times for t_1 and t_2 (seconds)

$v_{1,2}$ are the calculated kinematic viscosity values for v_1 and v_2 respectively (mm^2/s)

The obtained kinematic viscosity is then the average of v_1 and v_2.

5.1.5 Total Acid Number Determination:

The TAN of these baked samples is measured using the ASTM D-664 standards. The measurement of TAN indicates the amount of oxidation products formed which are acidic in nature. However, formulated lubricants can contain a variety of additives which may be acidic in nature, such as antiwear agents, oxidation inhibitors etc. The relative amounts of acidic constituents before and after oxidation may be determined through titration with bases. This process may be performed by dissolving samples in titration solvent which is a mixture of toluene and propan-2-ol with a small quantity of water and potentiometrically titrating with 0.1N alcoholic potassium hydroxide (KOH) using glass indicating and reference electrodes. Denver

Instruments automatic titrator model 350 was used for titration. This titrator is capable of dispensing 0.05ml of KOH per min. The tests were done in continuous inflection point mode. The meter readings can be plotted automatically against respective volumes of alcoholic KOH and the end points are selected at well defined inflection points. When the inflection points are ill-defined, the end points are selected at a meter reading corresponding to those found for freshly prepared aqueous basic buffer solution (usually the mV value corresponding to that of P^H 10). Total acid number is then calculated using the following formula:

$$\text{Acid Number (mg KOH/g)} = \frac{(A - B) \times M \times 56.1}{W} \qquad (5.1)$$

where A is the volume of KOH solution used to titrate the sample to the end point that occurs at the meter reading of the inflection point closest to the meter reading corresponding to the P^H 10 aqueous buffer. In the case of ill-defined or no inflection point, the volume of KOH, expressed in ml, corresponding to a P^H 10 reading of the aqueous buffer is considered. For additives, A is the volume of KOH used at the last inflection point. B is the volume of KOH required for blank titration, expressed in ml. M is the concentration of alcoholic KOH solution in mol/l, and W is the mass of the sample, in grams. Figure 5.2 shows a typical potentiometric titration curve.

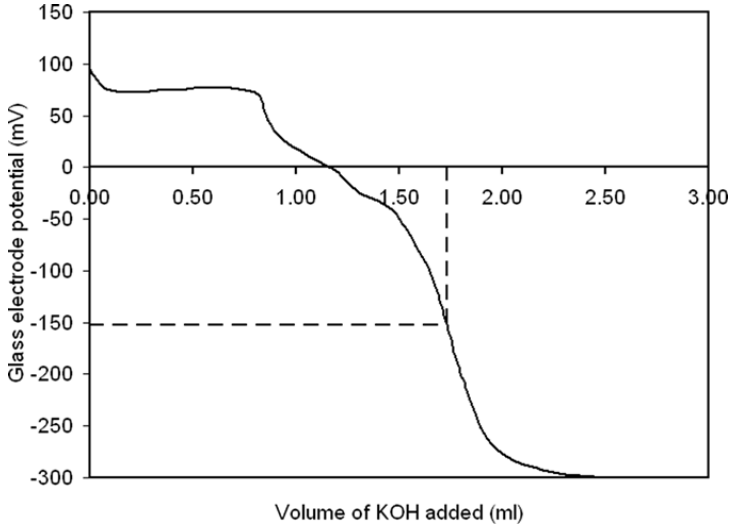

Figure 5.2: A typical potentiometric titration curve.

5.2 Results and Discussion

5.2.1 General Oxidation Mechanism

Automotive lubricants contain hydrocarbon base stock as carrier fluid along with other additives that serve specific purposes. The exposure of these lubricants to high temperatures, light and/or metal catalysts result in their decomposition and subsequent generation of alkyl free radicals [20, 23, 85, 86].

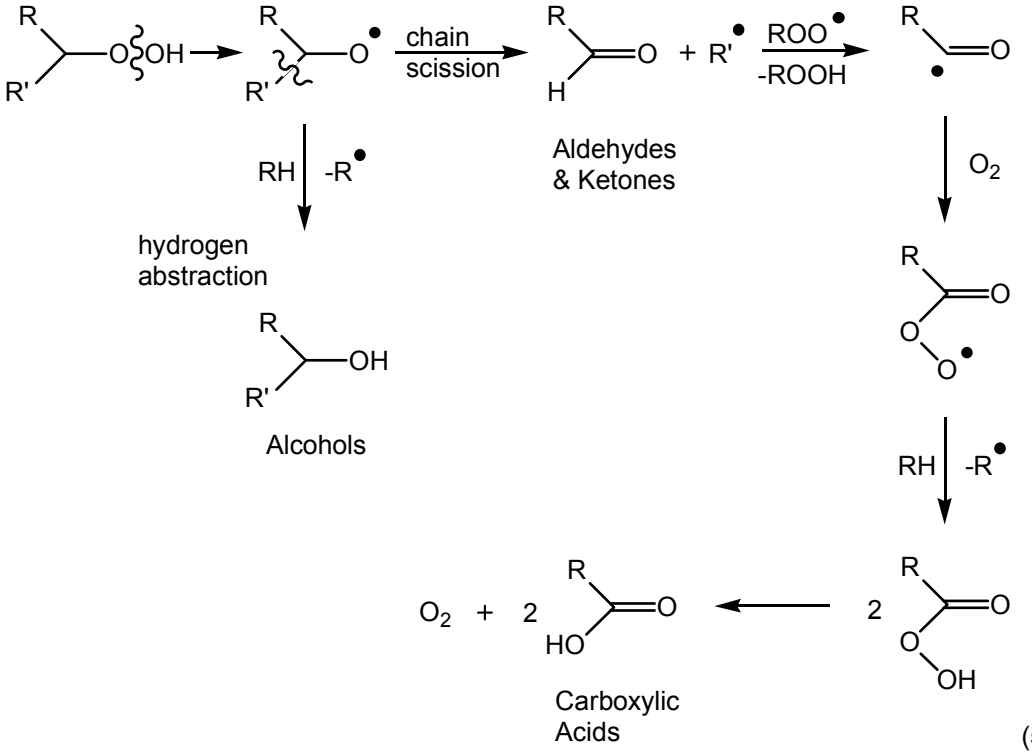

(5.2)

As seen in the processes, the first step in the oxidation process involves the conversion of alkyl radical to hydroperoxide. At high temperatures, hydroperoxide decomposes to form an alkoxy radical and hydroxyl radical. The generated alkoxy radical can degrade by two different pathways. It can either abstract a hydrogen radical from an oil molecule to form an alcohol, or the alkoxy radical can undergo chain scission reaction to produce low molecular weight carbonyl-containing compounds such as aldehydes and ketones and subsequently carboxylic acids. The aldehydes, ketones and carboxylic acids have carbonyl groups which produce a

peak in the same region (1800-1700cm^{-1}) of the FT-IR spectrum and hence changes in the intensity of this peak may be used to monitor the oxidation. Many authors have extensively employed FT-IR to study such oxidation products [55, 87, 127, 128, 130].

Figure 5.3 and Figure 5.4 show the FT-IR spectrum of base oil before and after it is subjected to oxidation at elevated temperatures respectively. The FT-IR spectrum of base oil at 0hr (prior to baking) contains mainly CH peaks from base oil. On the other hand, the FT-IR spectrum of base oil subjected to oxidation for 192hrs contains a new peak in the region 1800–1700 cm^{-1}, which is formed due to the oxidation of base oil and belongs to carbonyl-containing groups. The peaks in these spectra corresponding to specific wavenumbers are assigned to the respective functional groups (bonds) as described in Table 5.1.

Table 5.1: Assignment of peaks to wave number.

Wave Number (cm^{-1})	**Assignment of Peaks**
3000–2800	Saturated CH stretching
1400–1200	CH bending
3480–3380	N–H of aminic antioxidant
3650–3640	–OH of phenolic antioxidant
1275–1030	–C=S of MBDTC
1360–1180	–C–N– of MODTC
1770–1710	Carbonyl of carboxylic acids, aldehydes, ketones, esters

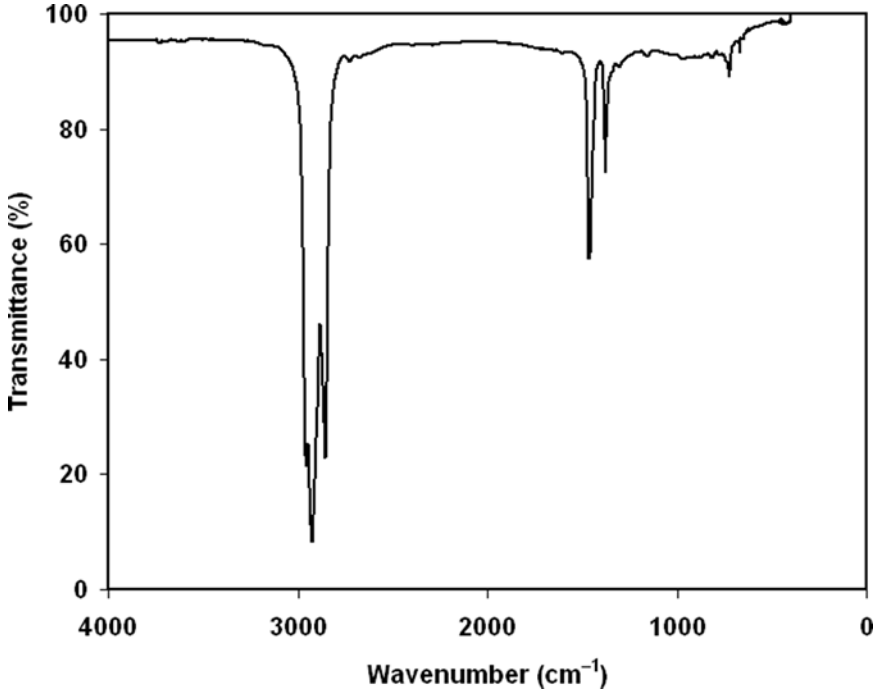

Figure 5.3: FT-IR spectrum of base oil at 0hr.

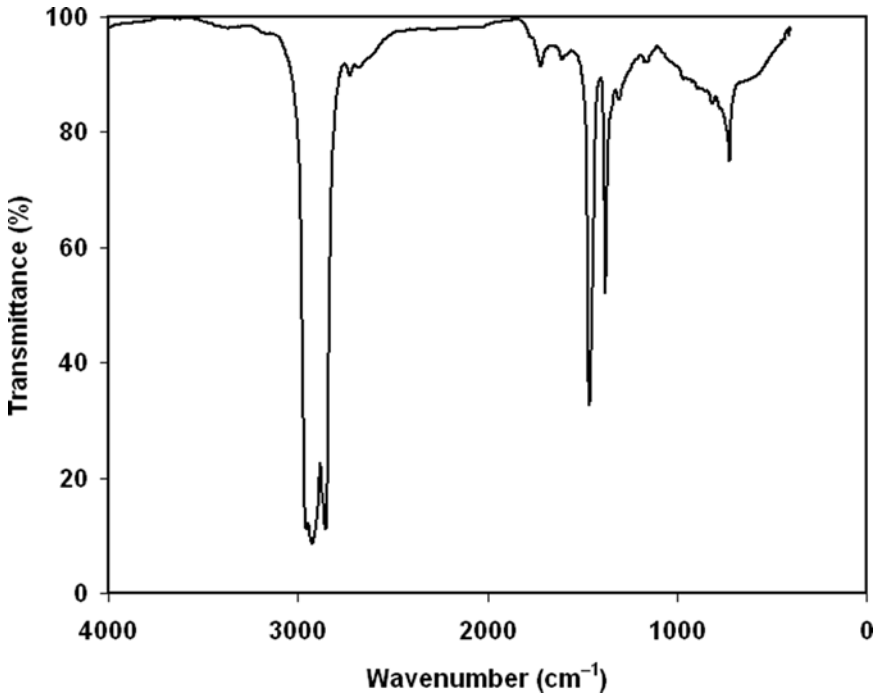

Figure 5.4: FT-IR spectrum of base oil at 192hrs of oxidizing time at 160°C. A new peak corresponding to the presence of carbonyl groups (1700–1800cm^{-1}) is observed.

Since oxidation produces acids, aldehydes, ketones and esters which exhibit a signature peak corresponding to carbonyl compounds, this FT-IR study focuses on the area under these peaks. Measuring the area under the carbonyl peaks helps to quantify the amount of oxidation. Increasing values of the area under peak as a function of time signifies increasing amounts of carbonyl-containing groups formed in these formulations as a result of oxidation.

5.2.2 General Antioxidant Mechanisms

The main role of antioxidants is to retard the oxidation of lubricating oil. Antioxidants may be classified either as primary or secondary, based on the nature of their role in the various oxidation stages. Primary antioxidants break the propagation step of oxidation by reacting with peroxy radicals, whereas secondary antioxidants inhibit the branching step by reacting with hydroperoxide (ROOH) molecules, preventing the formation of peroxy radicals. Antioxidant mechanisms have been described in detail in section 2.6.1

The primary antioxidants such as hindered phenols [86, 131] and aromatic amines function by donating a hydrogen atom to a peroxy radical [86]. The reaction steps of primary antioxidants for the specific cases of alkylated diphenyl amine (Eq. 5.3) and hindered phenol (Eq. 5.4) are described below. It has been shown that the mechanism action of alkylated diphenyl amine depends upon the operating temperature that the formulation encounters [85].

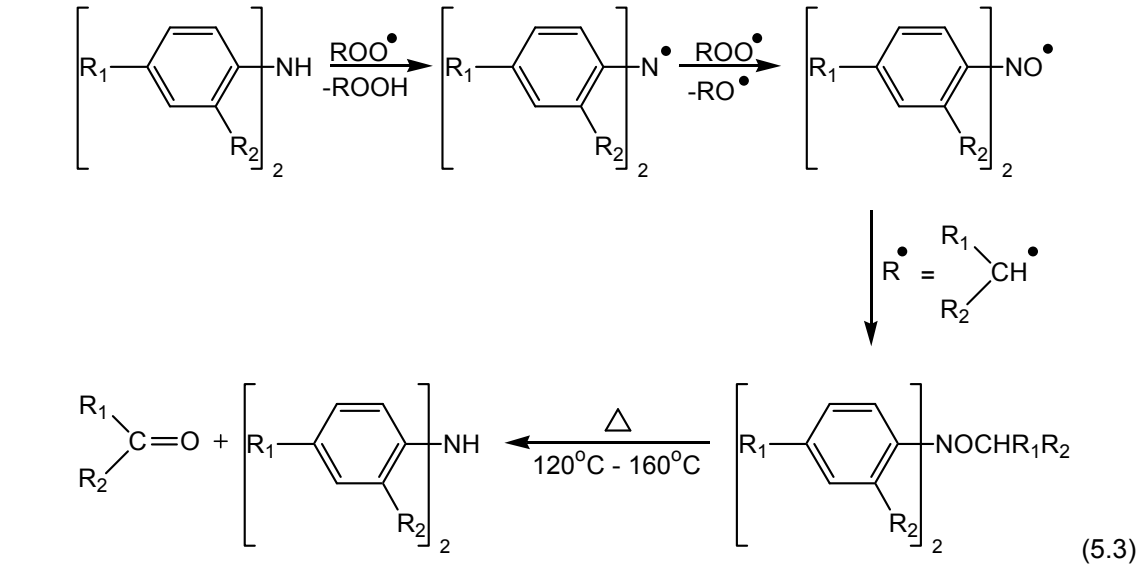

(5.3)

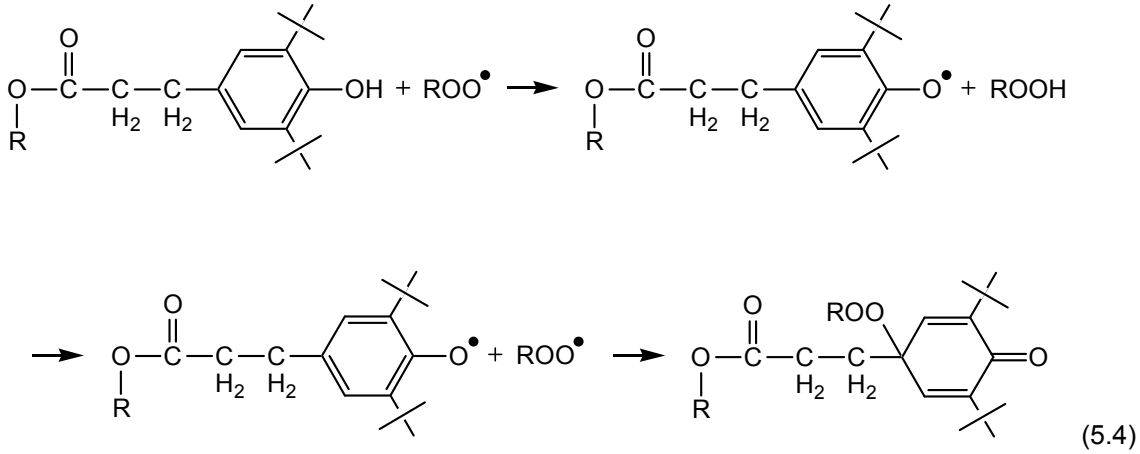

(5.4)

Secondary antioxidants include Zinc dithiocarbamate, Molybdenum dithiocarbamate and Methylene bis dibutyl dithiocarbamate, each of which inhibit the branching step by operating as hydroperoxide decomposers. An example of such a reaction process in the case of zinc dithiocarbamate is described herein [85, 132].

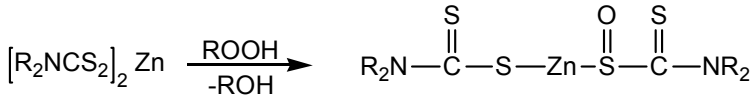

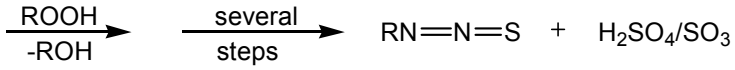

(5.5)

5.2.3 FT-IR of base oil and base oil with antioxidants

From Figure 5.5, it is observed that for formulations containing hindered phenol, some amount of carbonyl group was already present in the original material. The observed carbonyl group in this formulation is therefore a combination of the quantities of the carbonyl group present before and after oxidation. Calculations of the area under the peak are hence performed by correcting for any pre-oxidation quantities present in mixtures containing hindered phenol.

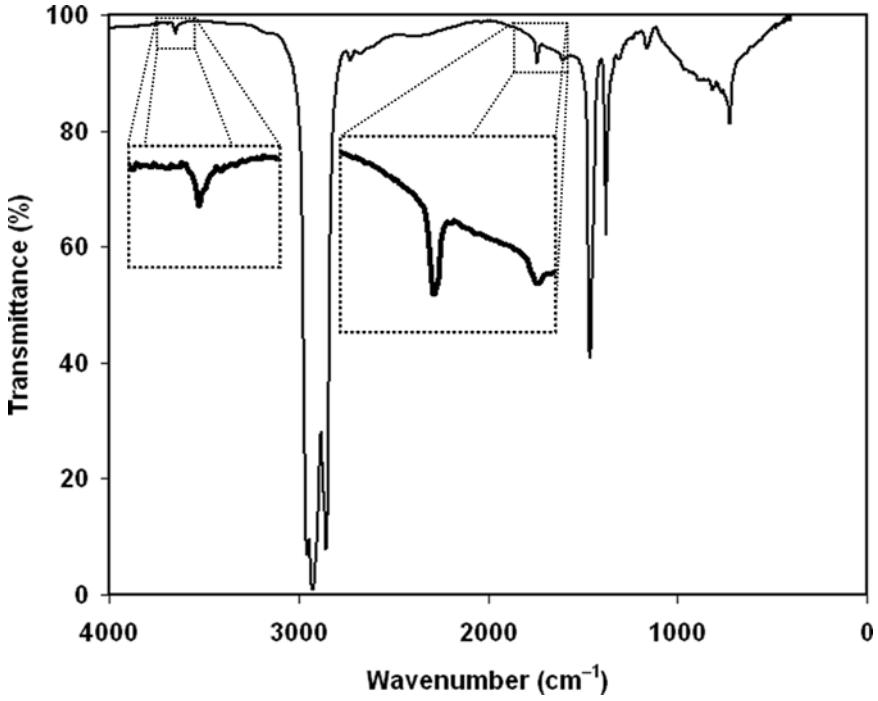

Figure 5.5: FT-IR spectrum of hindered phenol at 0 hrs of baking time.

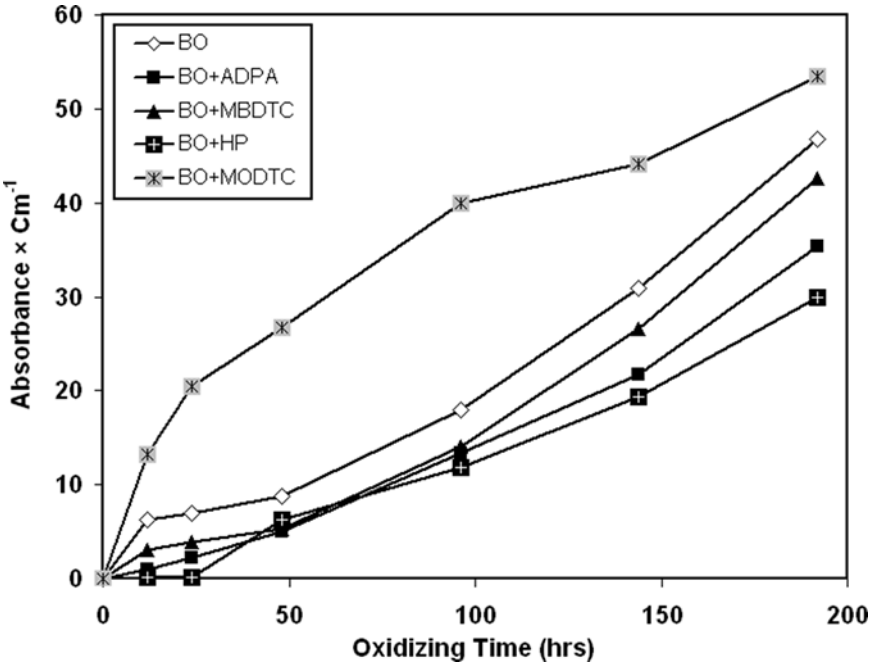

Figure 5.6: Area under the FT-IR carbonyl peak for base oil with and without antioxidants. Plot shows the area under the peak (Absorbance × cm^{-1}) vs. aging time for the formulations containing base oil and base oil + various antioxidants.

In Figure 5.6, the observed area under the carbonyl peak was less for base oil with ADPA, MBDTC and HP when compared to that of base oil only, indicating the effectiveness of these antioxidants. Alkylated diphenyl amine and hindered phenol being primary antioxidants work to retard the propagation step of the oxidation mechanism as proposed by various sources. Methylene bis dibutyl dithiocarbamate is a sulphur-containing antioxidant and act as hydroperoxide decomposer. As described in section 2.6.1, primary antioxidants tend to be more effective than their secondary counterparts. However under the test conditions employed in this study, all the antioxidants except MoDTC were nearly identical to one another. It can be seen from Figure 5.6 that the base oil with MoDTC showed an increase in the area under the peaks after 12 hours of oxidation and continued to remain high, indicating the poorer inhibition ability of this antioxidant under these conditions. This observation of the performance of MoDTC does not support claims by other researchers [133, 134] that MoDTC is a good antioxidant. It is a well-known fact that metals such as iron, chromium, copper and nickel have

known catalytic activities with hydrocarbons [23, 87]. Since molybdenum exists in the same group as chromium in the periodic table, it has similar characteristic properties. It can therefore be reasoned that Mo acts as a catalyst during the oxidation reaction, resulting in antagonistic effects in the base oil formulation containing MoDTC.

5.2.4 FT-IR of ZDDP and F-ZDDP with and without Antioxidants

Figure 5.7 shows the area under the carbonyl peak for the formulations with ZDDP and F-ZDDP alone in base oil.

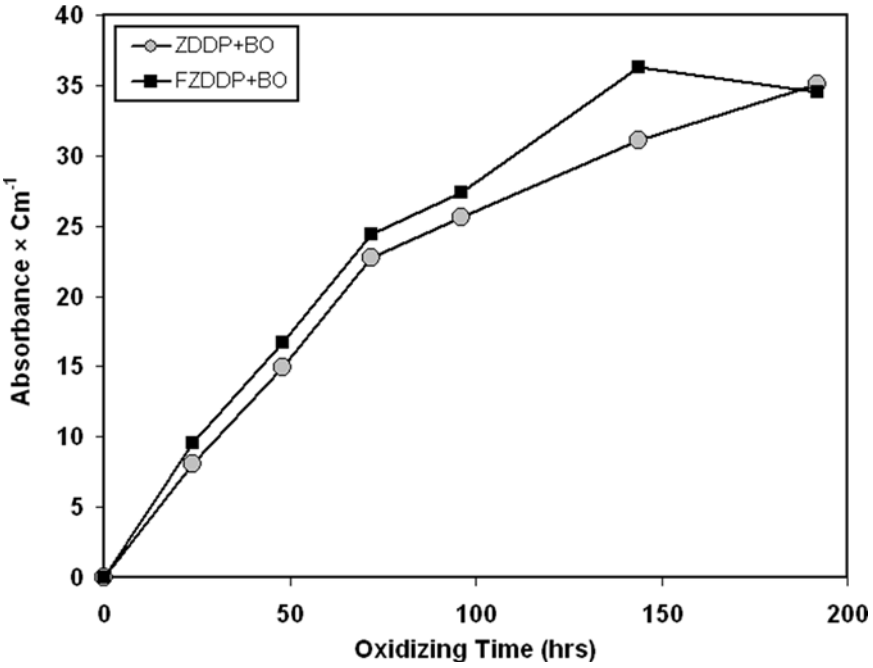

Figure 5.7: Area under the carbonyl peak for ZDDP and F-ZDDP in base oil. Plot shows the area under the peak (Absorbance × cm^{-1}) vs. oxidizing time (hrs) for the formulations with ZDDP and F-ZDDP alone in base oil.

The value of the area under the carbonyl peak for F-ZDDP in base oil was similar to that of ZDDP, indicating similar levels of oxidation in F-ZDDP when compared to ZDDP. This similarity may be attributed to the fact that the structure of F-ZDDP differs little from ZDDP, with the minor exception that F-ZDDP contains a few hundred ppm of fluorine in the form of P–F bonds in its structure.

The antioxidant process of ZDDP involves a complex sequence of steps, whose proposed mechanism is explained in detail in section 2.6.2. A brief recap of this proposed process is given below.

$$(RO)_2P(S)SH + 4R'OOH \rightarrow (RO)_2P(S)OH + H_2SO_4 + R'OH + R''CHO \quad (5.6)$$

$$[(RO)_2P(S)S]_2Zn + 4R'OOH \rightarrow (RO)_2P(S)OH + (RO)_2P(S)SZn^{+}OH + H_2SO_4 + 3R'OH + R''CHO \quad (5.7)$$

However, closer examination of the area under the peak vs. oxidizing time of base alone and ZDDP or F-ZDDP in base oil as seen in Figure 5.6 and Figure 5.7 shows that the area under the carbonyl peak observed in all these cases are almost similar, i.e., there is not much change in the observed area under the peak when either ZDDP or F-ZDDP is added. This similarity could be due to the fact that in the case of base oil (BO) alone, the base oil oxidation completely contributes to the carbonyl peaks observed. However, with BO+ZDDP & BO+F-ZDDP (or BO + any antioxidant), carbonyl comes not only from BO oxidation, but also from the decomposition products of ZDDP after prolonged oxidation. The oxidation conditions in this study are rather extreme, which could lead to a significant decomposition of ZDDP/F-ZDDP very quickly past its usefulness as an antioxidant, thereby yielding the end products of oxidation prematurely. This outcome results in more carbonyl groups than expected during normal operation. ZDDP has sulphur which is easy to oxidize, leading to CO-containing groups in subsequent steps.

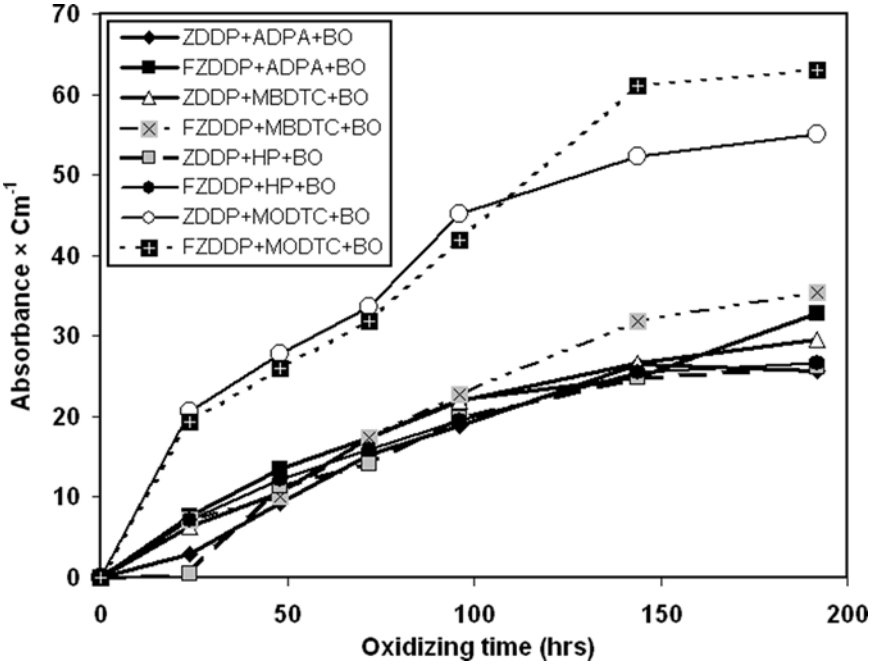

Figure 5.8: Area under the carbonyl peak for ZDDP and F-ZDDP with individual antioxidants. Plot shows the area under the peak (Absorbance × cm^{-1}) vs. oxidizing time (hrs) for formulations containing ZDDP and F-ZDDP with various individual antioxidants in base oil.

From Figure 5.8, it may be seen that the observed area under the peak was similar for the formulations containing ZDDP and F-ZDDP with the antioxidants ADPA, MBDTC and HP (after base line correction for HP). It can be seen that for formulations containing MoDTC, the observed area under the peak was larger than for the other antioxidant formulations regardless of whether either ZDDP or F-ZDDP antiwear agent was used. In this case, both F-ZDDP and ZDDP appeared to have similar performance characteristics for most of the oxidation period.

5.2.5 FT-IR of Mixture of Antioxidants with ZDDP and F-ZDDP

This section deals with formulations containing mixtures of antioxidants with ZDDP or F-ZDDP. An effort has been made to understand any beneficial (synergystic) or antagonistic effects that may arise due to concurrent utilization of multiple antioxidants in these mixtures. More information on synergism in lubricant formulations may be found in section 2.6.3.

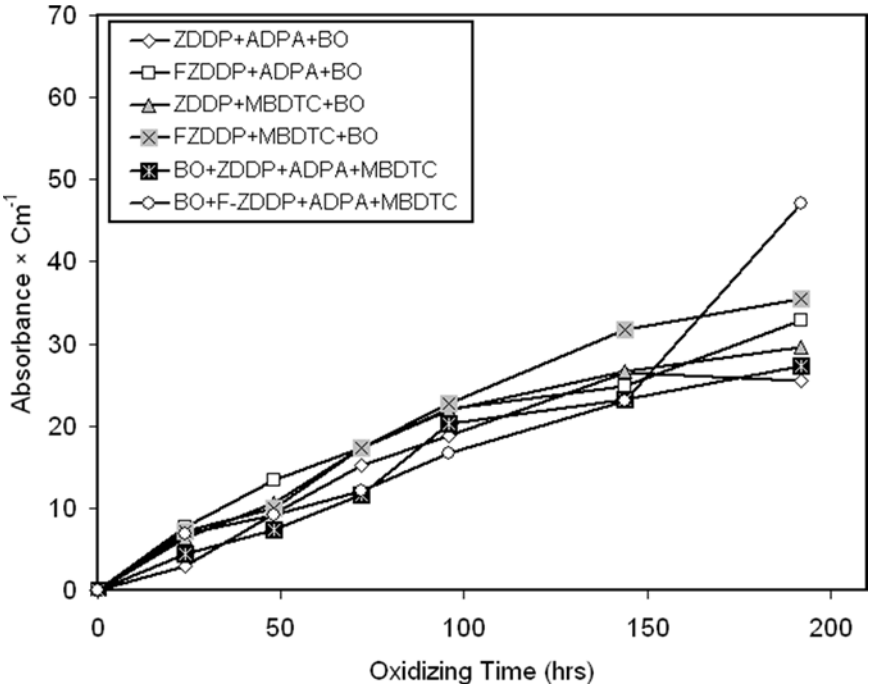

Figure 5.9: Area under the peak for ZDDP/F-ZDDP formulations with individual antioxidants and ADPA+MBDTC. Plot shows the area under the carbonyl peaks (Absorbance × cm^{-1}) vs. oxidizing time (hrs) for formulations containing ZDDP and F-ZDDP with ADPA+MBDTC mixture in base oil, being compared to the corresponding formulations with individual antioxidants.

Figure 5.9 shows a slight decrease in the carbonyl peak area for mixtures of antioxidants such as ADPA+MBDTC when compared to individual antioxidants with ZDDP and F-ZDDP. This difference does not represent a significant change in antioxidant behavior. In the case of mixtures of antioxidants such as ADPA and HP with ZDDP or FZDDP (Figure 5.10) there was no noticeable benefit due to the presence of a mixture of antioxidants. Under similar conditions, ZDDP with a mixture of antioxidants is slightly better than F-ZDDP with the same mixture of antioxidants.

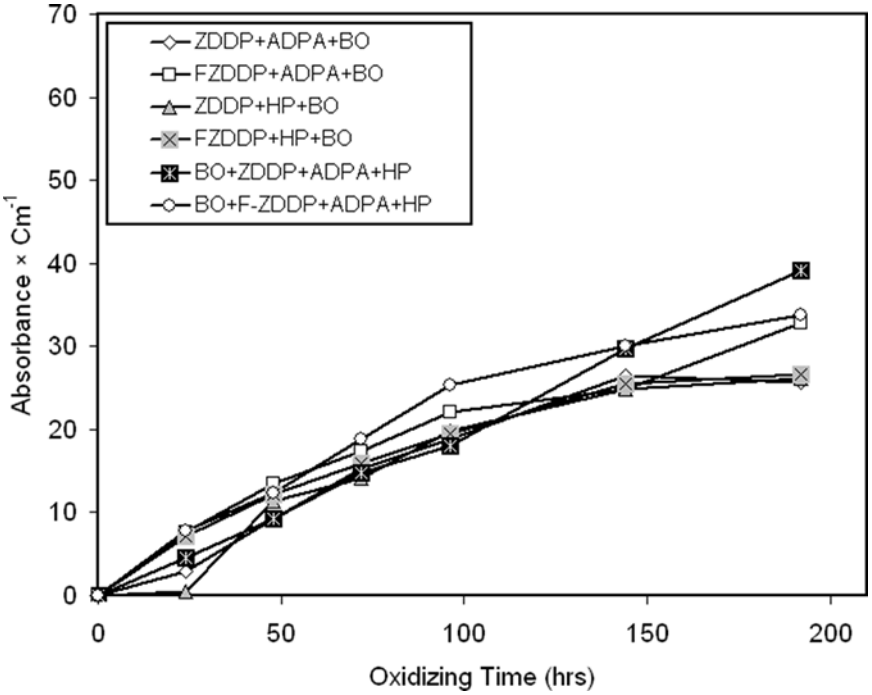

Figure 5.10: Area under the peak for ZDDP/F-ZDDP formulations with individual antioxidants and ADPA+HP. Plot shows the area under the carbonyl peaks (Absorbance × cm^{-1}) vs. oxidizing time (hrs) for formulations containing ZDDP and F-ZDDP with ADPA+HP mixture in base oil, being compared to the corresponding formulations with individual antioxidants.

In Figure 5.11, the area under the carbonyl peak was less for the mixtures of antioxidants (HP+MBDTC) than when they are used individually, thereby showing the beneficial effect of mixtures of antioxidants in retarding oxidation. In this case, it appears that synergism is achieved when MBDTC functions by inhibiting the branching step by decomposing hydroperoxides while HP operates during the propagation steps.

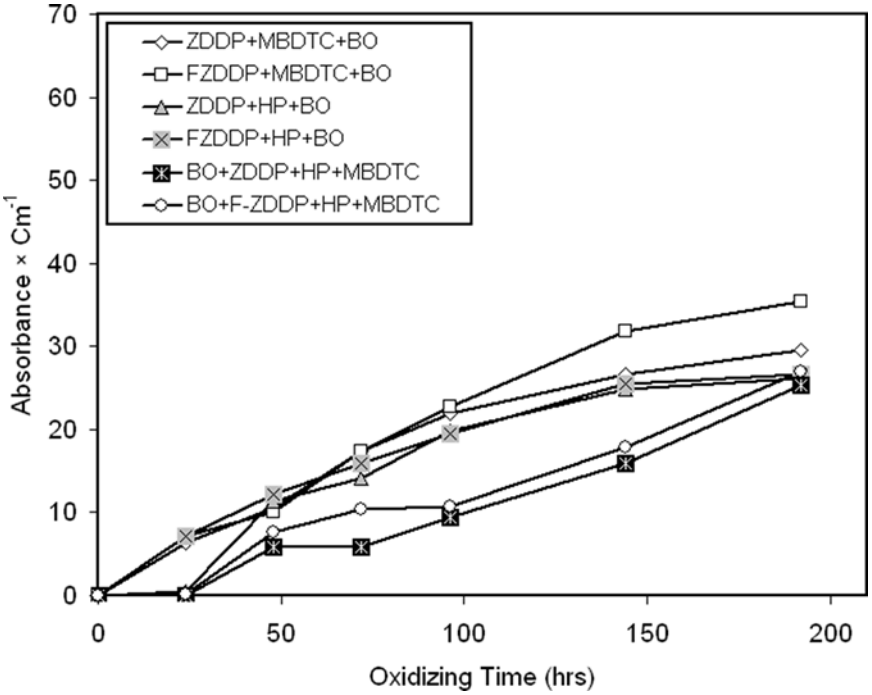

Figure 5.11: Area under the peak for ZDDP/F-ZDDP formulations with individual antioxidants and HP+MBDTC. Plot shows the area under the carbonyl peaks (Absorbance × cm^{-1}) vs. oxidizing time (hrs) for formulations containing ZDDP and F-ZDDP with HP+MBDTC mixture in base oil, being compared to the corresponding formulations with individual antioxidants.

Figure 5.12 and Figure 5.13 show the carbonyl peaks for ADPA+MODTC and HP+MODTC combinations, as well as individual antioxidants with ZDDP or F-ZDDP. From these figures, it may be observed that in general when MODTC is used with other antioxidants such as ADPA or HP, the amount of carbonyl-containing products are less than that formed with formulations containing MoDTC alone. From Figure 5.12, it can be inferred that under similar conditions, ZDDP with a mixture of antioxidants is slightly better than F-ZDDP with the same mixture of antioxidants. This indicates that the relatively poor performance of MoDTC is offset by the presence of the other antioxidants present in the mixture. Under similar conditions F-ZDDP with a mixture of antioxidants performs slightly better than ZDDP for HP+MoDTC combinations.

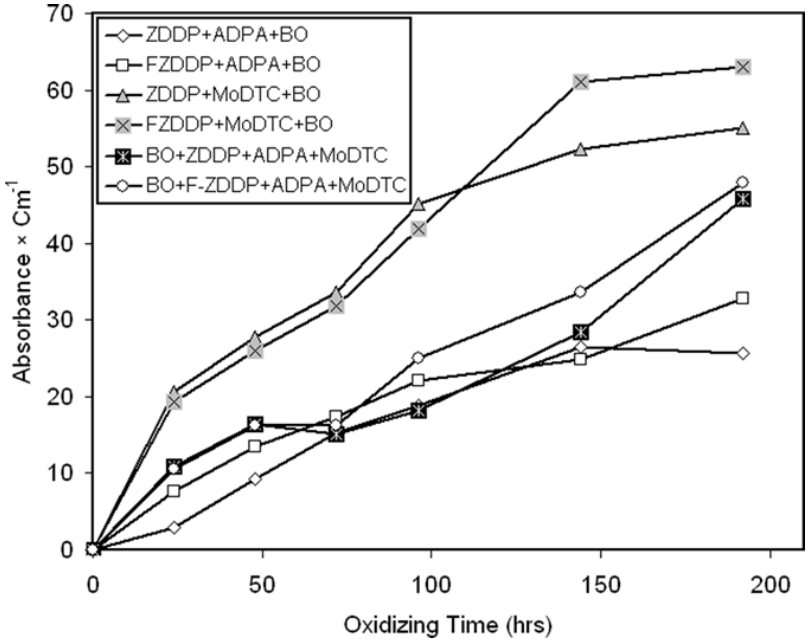

Figure 5.12: Area under the peak for ZDDP/F-ZDDP formulations with individual antioxidants and ADPA+MoDTC. Plot shows the area under the carbonyl peaks (Absorbance × cm^{-1}) vs. oxidizing time (hrs) for formulations containing ZDDP and F-ZDDP with ADPA+MoDTC mixture in base oil, being compared to the corresponding formulations with individual antioxidants.

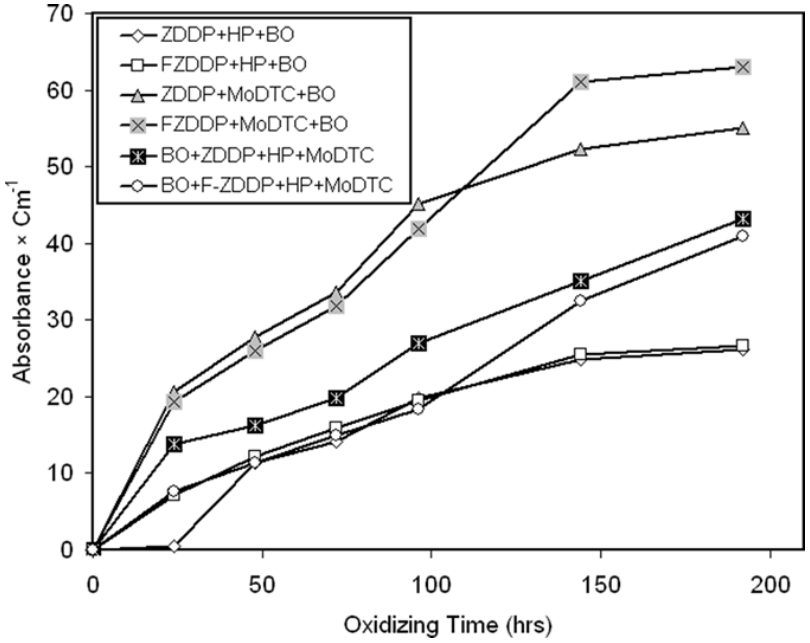

Figure 5.13: Area under the peak for ZDDP/F-ZDDP formulations with individual antioxidants and HP+MoDTC. Plot shows the area under the carbonyl peaks (Absorbance × cm^{-1}) vs. oxidizing time (hrs) for formulations containing ZDDP and F-ZDDP with HP+MoDTC mixture in base oil, being compared to the corresponding formulations with individual antioxidants.

5.2.6 Viscosity Measurements with Individual Antioxidants

Since viscosity and acidity are important indicators of oxidation levels of lubricating oils, safe and reliable functioning of machinery during its operating lifecycle is greatly aided by continued monitoring of these informative properties [49, 128, 133]. In this research, the initial viscosity of all the formulations prior to the commencement of oxidation (0 hrs of heating time) was measured and was found to be very close to that of base oil, due to the fact that base oil constitutes the major amount of total formulations.

Table 5.2 shows the increase in viscosity for formulations containing ZDDP and F-ZDDP with and without antioxidants at 40°C and 100°C.

Table 5.2: Viscosity values for formulations containing ZDDP or F-ZDDP, with and without antioxidants at 40°C and 100°C.

	Viscosity @ 40°C			Viscosity @ 100°C		
Baking Time (hours) / Formulation	0 hr	48 hrs	96 hrs	0 hr	48 hrs	96 hrs
BO+ZDDP	21.11	24.380	28.55	4.14	4.58	5.18
BO+FZDDP	20.98	24.38	29.07	4.11	4.55	4.89
BO+ZDDP+ADPA	21.02	24.19	28.29	4.28	4.47	4.74
BO+FZDDP+ADPA	21.17	24.43	26.57	4.25	4.57	5.42
BO+ZDDP+MBDTC	21.17	24.41	28.35	4.15	4.61	5.00
BO+FZDDP+MBDTC	20.97	24.35	25.25	4.18	4.55	4.68
BO+ZDDP+HP	20.95	22.53	26.39	4.15	4.36	4.83
BO+FZDDP+HP	21.32	23.79	26.33	4.23	4.54	4.84
BO+ZDDP+MODTC	20.80	29.44	33.55	4.19	6.08	6.65
BO+FZDDP+MODTC	20.99	27.24	29.64	4.21	5.36	5.91

From

Table 5.2, it is evident that all the formulations show an increase in viscosity as the oxidizing time is increased, indicating the progress of oxidation as the samples are heated at high temperatures in the presence of flowing air.

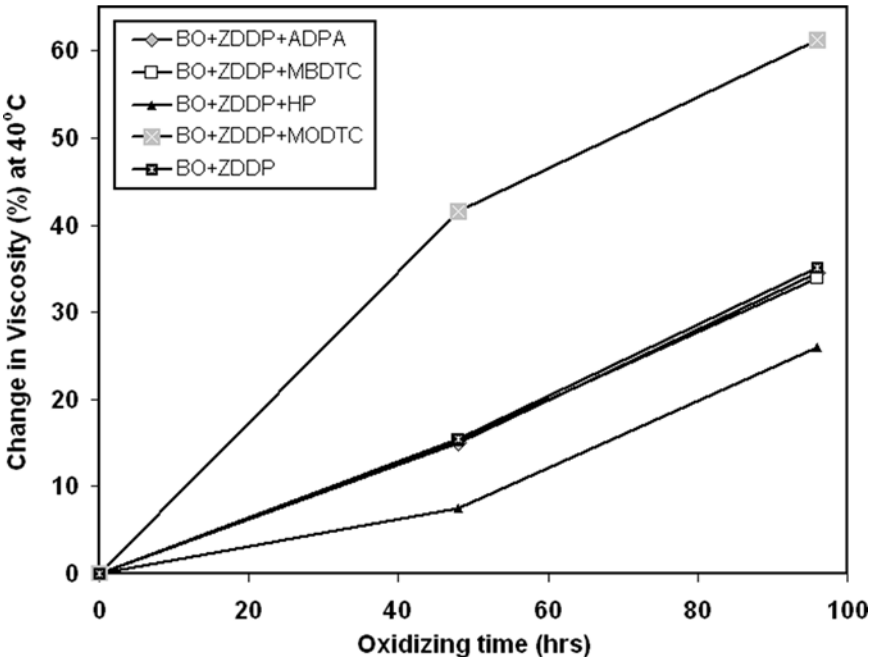

Figure 5.14: Change in viscosity (%) vs. oxidizing time (hrs) for the formulations containing ZDDP and ZDDP with antioxidants at 40°C.

Figure 5.14 shows the percent change in viscosity measured at 40°C for the formulations containing ZDDP alone in base oil and formulations having ZDDP with different antioxidants after oxidizing at 160°C. The sample containing molybdenum dithiocarbamate and ZDDP showed a large change in viscosity compared to all other formulations – a result that is corroborated by the corresponding FT-IR measurements. As described previously, this outcome is believed to be due to the metal catalytic nature of molybdenum which expedites the oxidation process, leading to quicker accumulation of carbonyl compounds.

The formulation containing hindered phenol showed the best viscosity performance indicating lower amounts of oxidation products. The observed viscosity change for formulations having HP as antioxidant was lower, indicating the presence of lower amount of oxidation products. The viscosity changes observed in the formulation containing ZDDP alone in base oil was comparable to those with formulations having alkylated diphenylamine and methylene bis dibutyl dithiocarbamate with ZDDP. This result implies that the presence of these antioxidants

in formulations did not have a significant effect on the oxidation stability of the formulations without these antioxidants. Observation of Figure 5.7 and Figure 5.8 indicates that there is no decrease in the area under the carbonyl peak with the addition to ZDDP or F-ZDDP of ADPA, MBDTC.

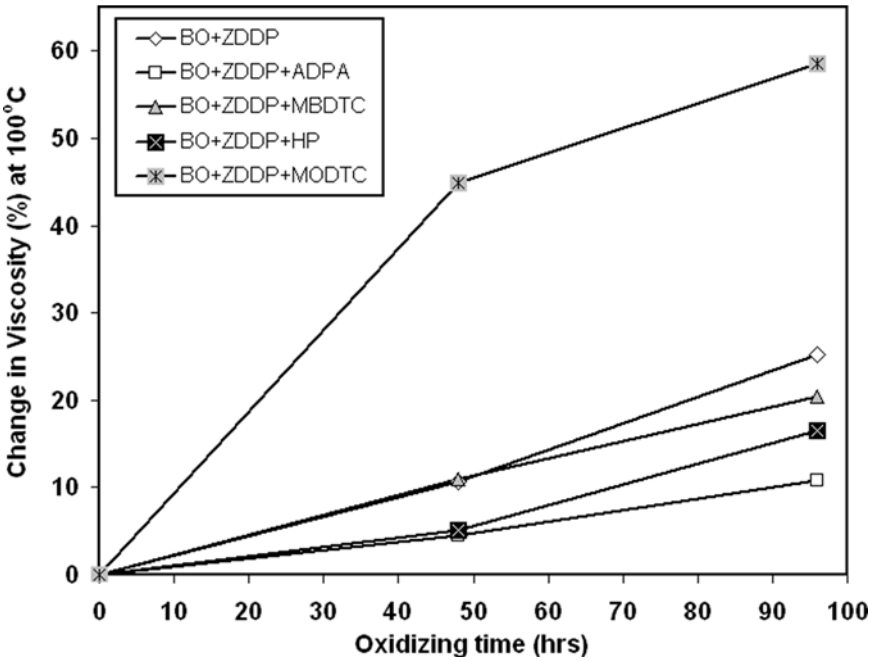

Figure 5.15: Change in viscosity (%) vs. oxidizing time (hrs) for the formulations measured at 100°C containing ZDDP and ZDDP with antioxidants oxidized at 160°C.

Figure 5.15 shows the changes in kinematic viscosity of the above oxidized sample measured at 100^{O}C. As may be seen from Figure 5.15, there is a slight difference in the observed changes in viscosity for some of these formulations. As before, the increase in viscosity was higher in the formulations containing MoDTC compared to all the other formulations. Increase in viscosity was approximately 6% in ZDDP when compared to ZDDP with MBDTC and HP. The percentage change in viscosity with ZDDP alone in base oil was approximately 10% when compared with ZDDP+ADPA in base oil.

Even though samples were baked for a period of 192hrs, viscosity measurement for samples baked for 144hrs and 192hrs were not conducted due to the formation of large

amounts of precipitate material which rendered viscosity measurements challenging. Since formulations were prepared in base oil alone, oxidation produces large amounts of solid particles which tend to precipitate from the solution due to the absence of dispersants in the formulation. Addition of dispersants such as those found in fully formulated oils would help to hold these insoluble particles in suspension. In this work, these particles were filtered using sieves of 80μm pore size before measuring the viscosity to avoid clogging the capillary of viscometer. Particles smaller than 80μm passed through the filter, which resulted in a fair extent of inconsistency of measured viscosity values between two subsequent readings. Viscosity measurements for the samples at these heating periods are therefore not included in this study.

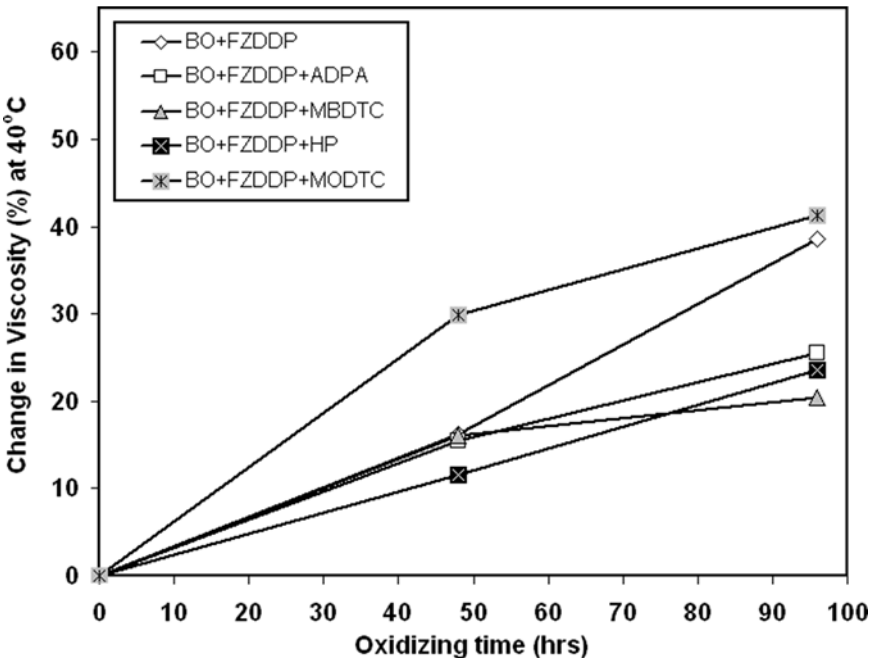

Figure 5.16: Change in viscosity (%) vs. oxidizing time (hrs) the formulations oxidized at 160°C containing F-ZDDP and F-ZDDP with antioxidants measured at 40°C.

Figure 5.16 shows the change in viscosity formulations containing F-ZDDP alone and F-ZDDP with different antioxidants in base oil. In the absence of antioxidant, the viscosity of F-

ZDDP increased and became very close to that of F-ZDDP with MoDTC at 96hrs. In the presence of antioxidants such as ADPA, MBDTC, HP, the observed change in viscosity was smaller compared to F-ZDDP or F-ZDDP with MoDTC, indicating a stabilizing effect of these antioxidant over F-ZDDP. Under these test conditions, F-ZDDP responded to individual antioxidants better than ZDDP.

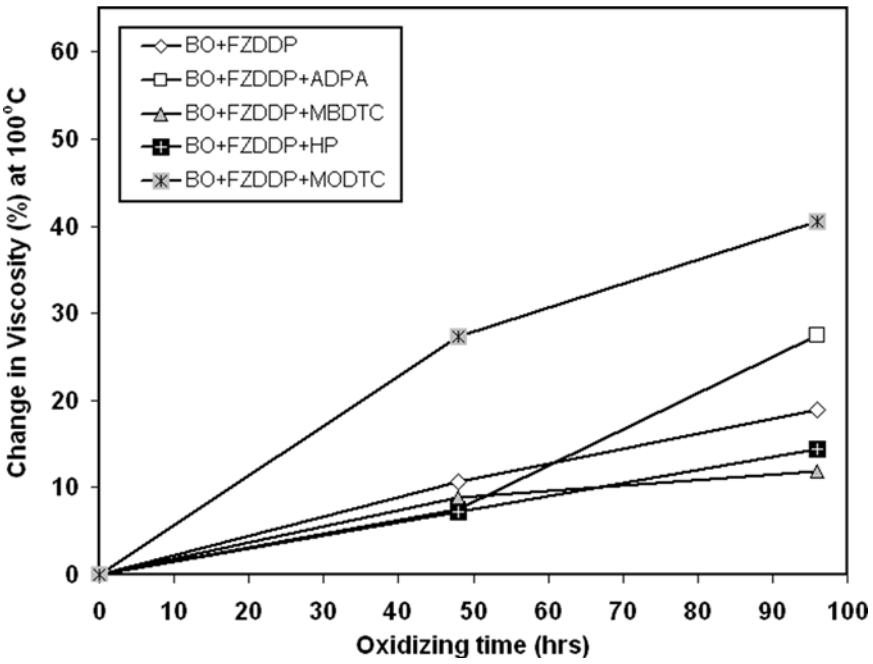

Figure 5.17: Change in viscosity (%) vs. oxidizing time (hrs) for the formulations containing F-ZDDP and F-ZDDP with antioxidants at 100°C.

Figure 5.17 represents the change in viscosity vs. heating time in hours for formulations having F-ZDDP and F-ZDDP with different antioxidants measured at 100^{O}C. As expected, the viscosity changes observed in F-ZDDP with MoDTC was higher than in all other cases. At 48hrs, the change in viscosity for these formulations were similar, but significant variations in viscosity among these formulations began to emerge as the time of oxidation was increased (i.e., at 96hrs).

5.2.7 Viscosity Measurements with Mixtures of Antioxidants

Similar to the case of formulations with individual antioxidants, the initial viscosity of all the formulations prior to the commencement of oxidation (0 hrs of heating time) was measured and was found to be very close to that of base oil, due to the fact that base oil constitutes the major amount of total formulations.

Table 5.3 shows the increase in viscosity for formulations containing ZDDP and F-ZDDP with a mixture of antioxidants at 40°C and 100°C.

Table 5.3: Viscosity values for formulations containing ZDDP or F-ZDDP, with various mixtures of antioxidants at 40°C and 100°C.

	Viscosity @ 40°C			Viscosity @ 100°C		
Baking Time (hours) / Formulation	0 hr	48 hrs	96 hrs	0 hr	48 hrs	96 hrs
BO+ZDDP+ADPA+MBDTC	21.55	25.21	25.45	4.21	4.68	4.94
BO+F-ZDDP+ADPA+MBDTC	20.92	24.99	29.79	4.23	4.76	5.15
BO+ZDDP+ADPA+HP	20.79	24.37	24.36	4.20	4.58	4.72
BO+F-ZDDP+ADPA+HP	20.79	24.71	29.54	4.15	4.60	5.46
BO+ZDDP+ADPA+MoDTC	21.20	25.36	25.90	4.24	4.82	5.14
BO+F-ZDDP+ADPA+MoDTC	20.94	24.79	28.19	4.19	4.89	5.53
BO+ZDDP+HP+MBDTC	21.04	22.63	25.37	4.15	4.41	4.71
BO+F-ZDDP+HP+MBDTC	21.43	21.90	23.33	4.16	4.38	4.58
BO+ZDDP+HP+MoDTC	20.96	26.43	33.23	4.23	5.39	6.78
BO+F-ZDDP+HP+MoDTC	21.33	24.21	33.44	4.18	4.60	6.14

Figure 5.18 shows the changes in the viscosity (%) vs. oxidation time (hrs) measured at 40°C for the formulations containing mixtures of antioxidants with ZDDP.

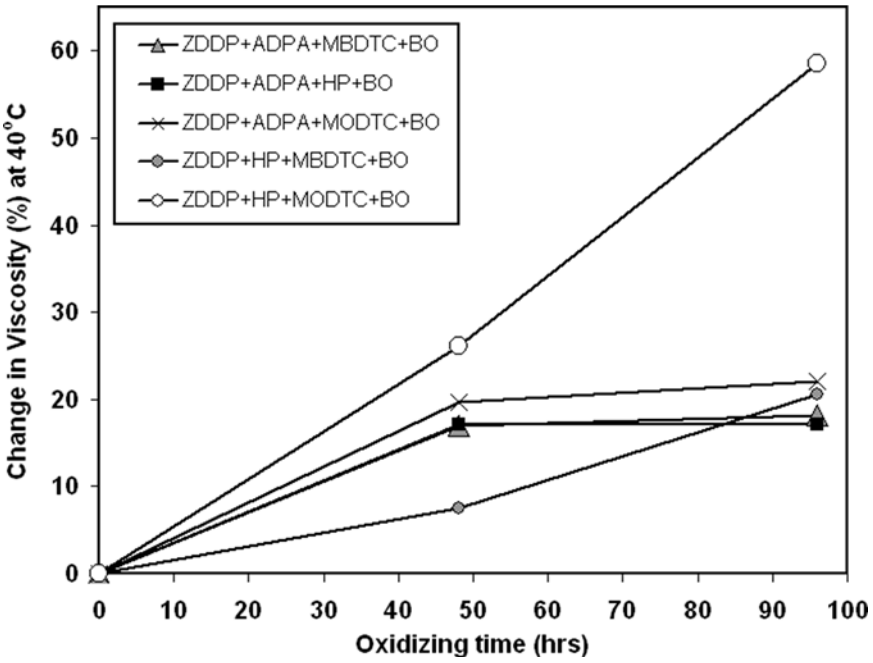

Figure 5.18: Change in viscosity (%) vs. oxidizing time (hrs) for the formulations containing ZDDP with mixtures of antioxidants measured at 40°C.

It can be seen from Figure 5.18 that the change in viscosity for the formulations such as ZDDP+ADPA+MBDTC, ZDDP+ADPA+HP and ZDDP+ADPA+MODTC are almost identical. Effect of MODTC +ADPA with ZDDP was comparatively better than all other formulations having MoDTC. This effect was also independently reported in reference [135]. For the formulation containing ZDDP+HP+MBDTC, the observed change in viscosity at 48 hours (and measured at 40°C) is lower than that of all other combination of antioxidants with ZDDP. The viscosity for this formulation becomes comparable to the other formulations (except ZDDP+HP+MoDTC) only at 96 hrs of baking. The formulation containing HP+MODTC with ZDDP showed the worst change in viscosity (almost 60% over a 96-hour period) compared to other formulations. These results are verified by the corresponding FT-IR analysis.

Changes in viscosity for ZDDP with mixtures of antioxidants at 100°C are shown in Figure 5.19. Trends of viscosity changes observed were nearly identical to that at 40°C.

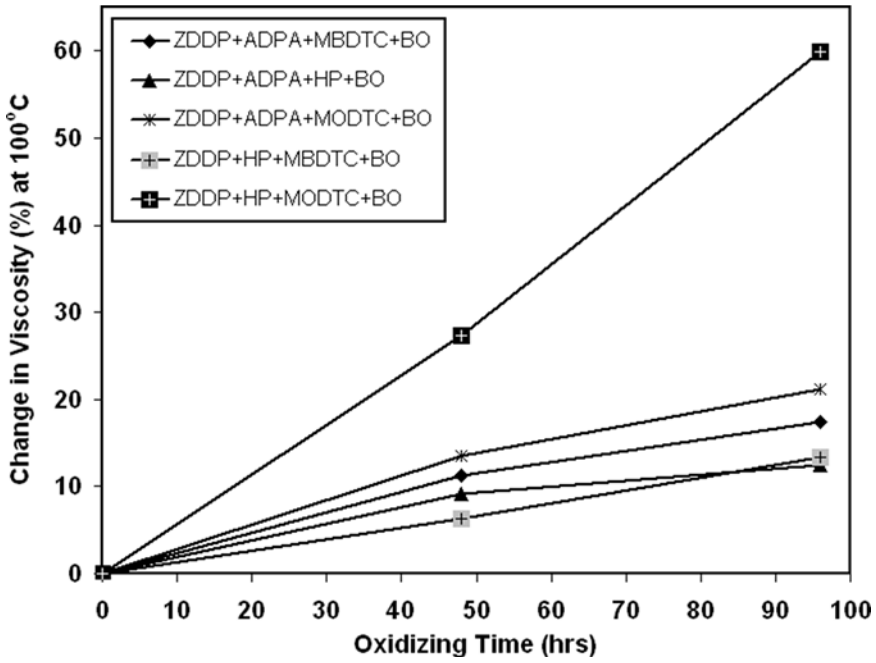

Figure 5.19: Change in viscosity (%) vs. oxidizing time (hrs) for the formulations containing ZDDP with mixtures of antioxidants measured at 100°C.

From the comparison of viscosity at 40°C from Figure 5.14 and Figure 5.19, it may be seen that nearly a ten-percent change (decrease) in viscosity was observed with certain mixtures of antioxidants with ZDDP when compared to ZDDP with same individual antioxidants. This result indicates that a combination of antioxidants proves to be much more effective than individual antioxidants due to the fact that different antioxidants inhibiting different stages of oxidation.

Figure 5.20 shows the measured viscosity at 40°C for the formulations containing mixtures of antioxidants with F-ZDDP. Large increase in viscosity is observed for the formulation F-ZDDP+HP+MoDTC after a small increase at 48hrs (compared to the one at 96hrs). The smallest increase in viscosity at 40°C was observed in this case for F-ZDDP+HP+MBDTC. The viscosity effects observed for F-ZDDP with mixtures of antioxidants at 100°C is similar to those observed at 40°C for the same formulations.

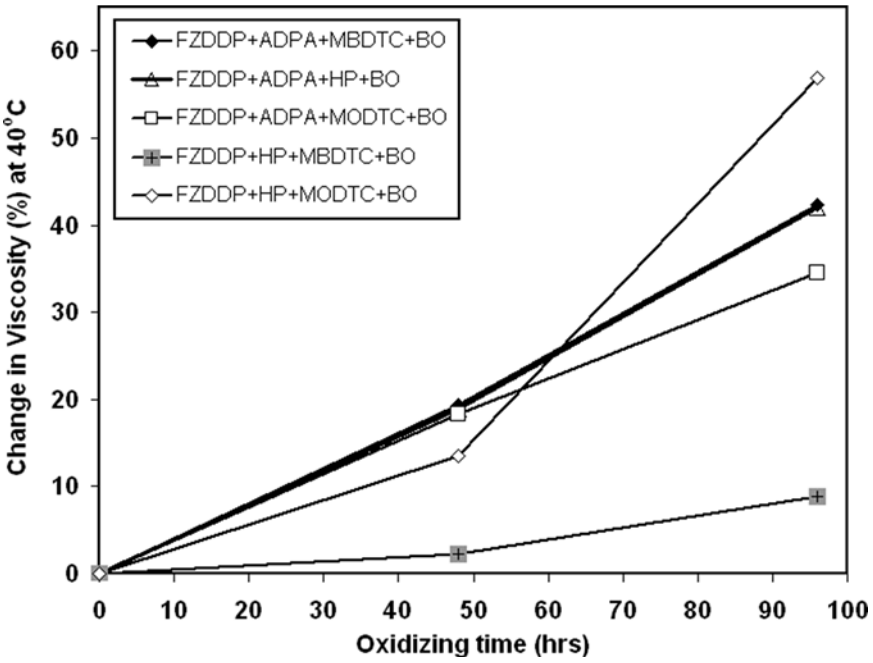

Figure 5.20: Change in viscosity (%) vs. oxidizing time (hrs) for the formulations containing F-ZDDP with mixtures of antioxidants measured at 40°C.

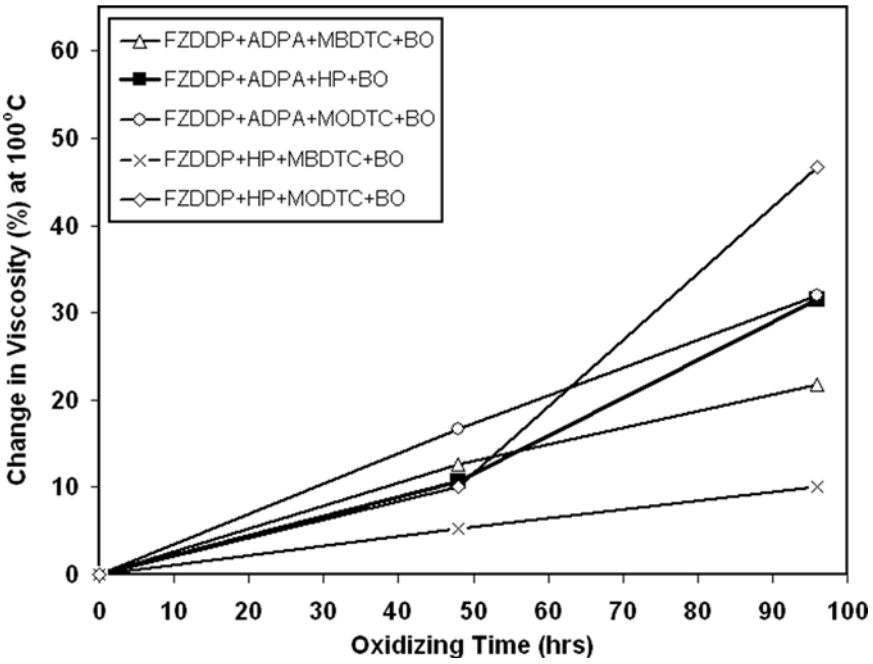

Figure 5.21: Change in viscosity (%) vs. oxidizing time (hrs) for the formulations containing F-ZDDP with mixtures of antioxidants measured at 100°C.

From Figure 5.7, it is observed that the behavior of ZDDP and F-ZDDP in base oil without antioxidants differ little from each other. On the other hand, from the comparison of Figure 5.16 and Figure 5.21, i.e. viscosity of individual antioxidants and mixtures of antioxidants, it can be seen that in the case of F-ZDDP, individual antioxidants rather than mixtures showed better oxidation resistance – a trend that is opposite to that seen in ZDDP (which works better with mixtures of antioxidants). It therefore appears that the differences in the chemical structures between ZDDP and F-ZDDP (such as the presence of P–F bonds in the latter) while insignificant enough to affect the relative stability in base oil alone begin to play a much larger role when antioxidants are introduced into the equation.

5.2.8 TAN of ZDDP and F-ZDDP with and without Antioxidants

Figure 5.22 shows the TAN vs. oxidation time for the formulations containing ZDDP alone in base oil and ZDDP with different antioxidants in base oil. The initial values of observed TAN in all formulations are almost similar and are due to the presence of ZDDP or F-ZDDP. The measured value of TAN of base oil alone without any additives was found to be 0.02 mg/g of KOH, while that of base oil + ADPA was found to be 0.019 mg/g of KOH. The major contribution to TAN at 0 hours for these formulations hence comes from either ZDDP or F-ZDDP.

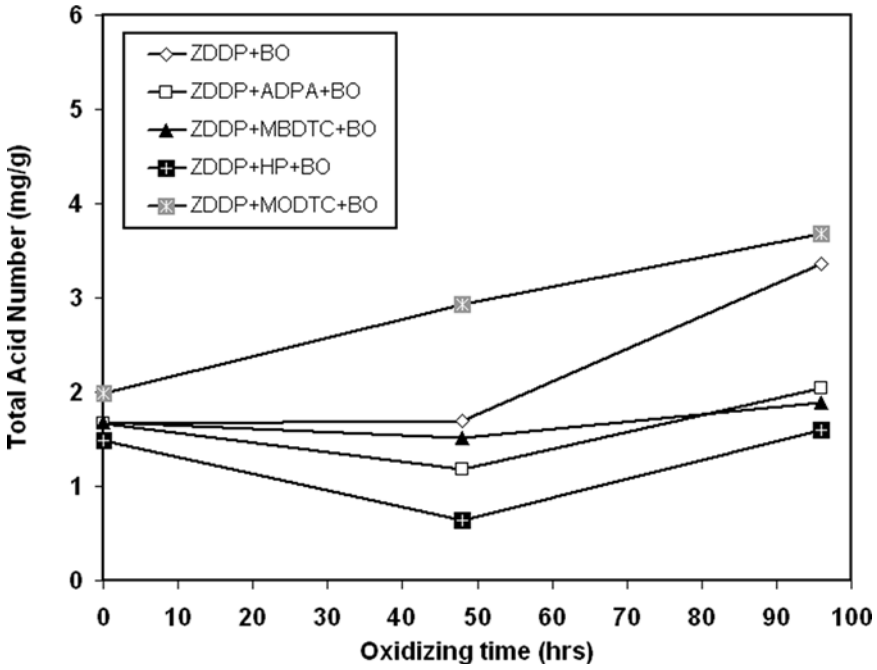

Figure 5.22: Total acid number (mg/g) vs. oxidizing time (hrs) for the formulations containing ZDDP and ZDDP with antioxidants in base oil.

In the case of formulations with ADPA, MBDTC and HP as shown in Figure 5.22, there is first a decrease in the value of TAN after 48 hrs of heating, which then increases as time increases. The magnitude of this increase is different for different antioxidants. The observed TAN for almost all the formulations decreased at 48hrs. This is contradictory to the generally observed trend where TAN should increase with time due to an increase in oil acidity as the oxidation progresses. However, the measurement of TAN at 0 hr (prior to commencement of heating) does not take into account the influences of elevated temperatures and continuous bubbling of air. At 48 hrs, the oil is oxidized at 160°C, and air is bubbled through continuously, which works to drive out some of the insoluble acids, thereby reducing the quantity of acid in the samples. In addition, some oil is also lost due to evaporation. This effect is more pronounced in base oil as it is quite susceptible to evaporation compared to fully formulated oil. These effects could combine to lower the measured TAN values at 48 hrs. Once the system stabilizes

past this point, the baseline would not change much, resulting in increasing measurements of acidity as heating time increases.

As expected, the TAN observed for ZDDP in base oil was high compared to that for ZDDP with antioxidants (except ZDDP+MoDTC combination). ADPA, MBDTC and HP all showed similar TAN numbers upon oxidation when used as antioxidants with ZDDP in base oil. For the formulation ZDDP+MoDTC, the initial TAN at 0 hr was higher than that of all other formulations and remained high for all heating durations. However, accurate TAN measurements of all formulations containing MoDTC were made difficult by the formation of a yellow sticky material that coated the potentiometer electrodes as titration progressed.

Figure 5.23 below shows the total acid number (mg/g) vs. oxidizing time (hrs) for the formulations containing F-ZDDP with and without antioxidants in base oil.

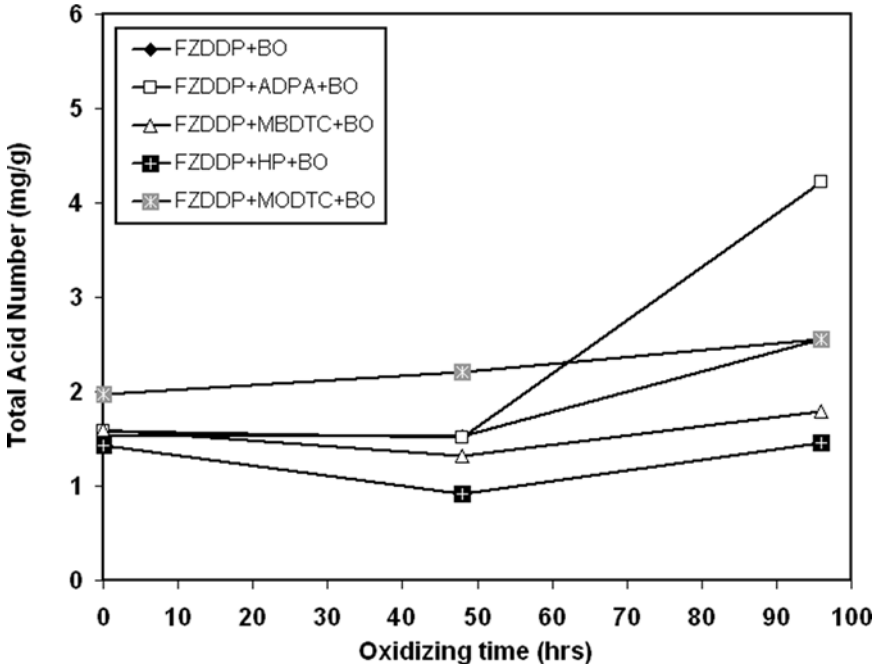

Figure 5.23: Total acid number (mg/g) vs. oxidizing time (hrs) for the formulations containing F-ZDDP with and without antioxidants in base oil.

From Figure 5.23, among the formulations containing F-ZDDP alone in base oil and F-ZDDP with individual antioxidants, the lowest TAN values were observed for F-ZDDP+HP and

F-ZDDP+MBDTC. For the formulation F-ZDDP+ADPA, increase in TAN after 48 hrs is higher than F-ZDDP with HP and MBDTC combinations. Earlier NMR studies described in section 3.2.1 also showed the milder antagonistic effect of F-ZDDP in the presence of ADPA. The acidity trends for formulations containing MoDTC were similar to that seen in identical formulations with ZDDP.

5.2.9 TAN of ZDDP and F-ZDDP with Mixtures of Antioxidants

In the case of ZDDP with mixtures of antioxidants, the observed TAN was less for ZDDP+MBDTC+HP. The observed TAN was higher for ZDDP+HP+MoDTC. This increased oxidation was also seen through viscosity and FT-IR measurements. The observed TAN was similar for other combinations of antioxidants with ZDDP. Trends for ZDDP are shown in Figure 5.24.

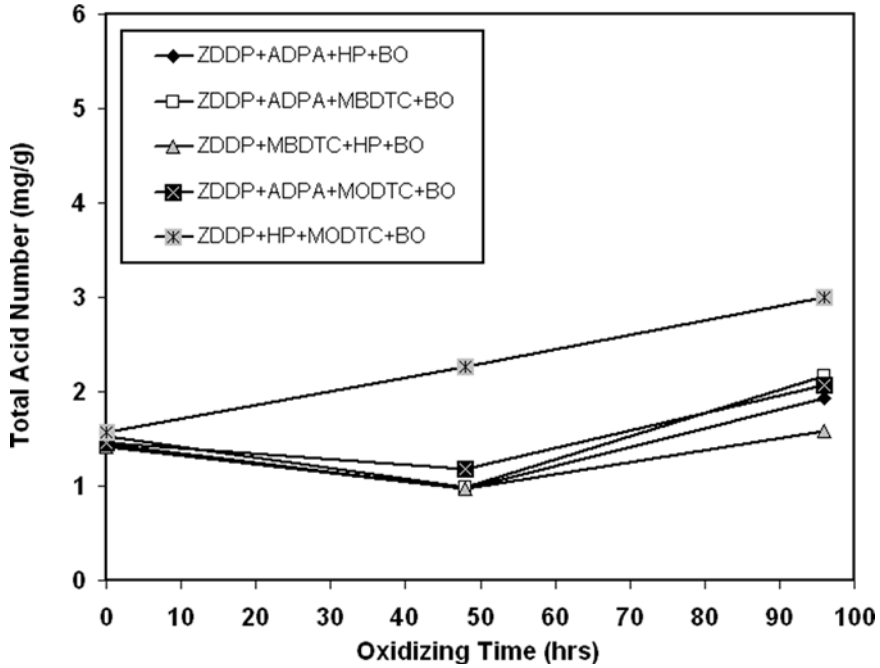

Figure 5.24: Total acid number (mg/g) vs. oxidizing time (hrs) for the formulations containing ZDDP with mixtures of antioxidants in base oil.

In the case of F-ZDDP with mixtures of antioxidants, the observed TAN was the least for ZDDP+MBDTC+HP. The observed TAN was higher for ZDDP+HP+MoDTC and F-

ZDDP+ADPA+HP. This higher level of oxidation was confirmed by viscosity and FT-IR measurements. For other combination of antioxidants with F- ZDDP, the observed TAN was similar to one another.

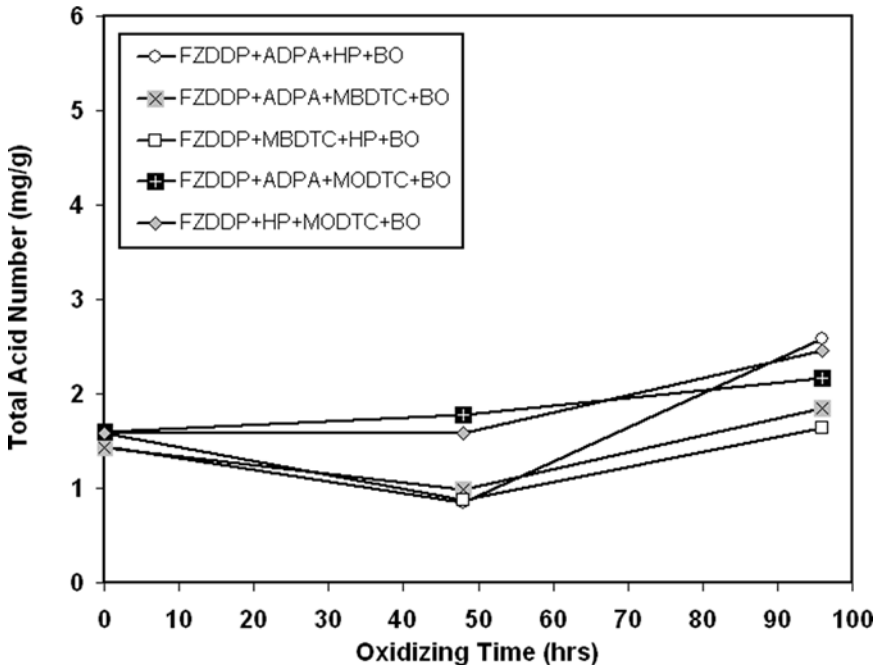

Figure 5.25: Total acid number (mg/g) vs. oxidizing time (hrs) for the formulations containing F-ZDDP with mixtures of antioxidants in base oil.

5.3 Summary

This study investigated the oxidation stability of F-ZDDP and compared it to that of ZDDP in varying formulations in base oil with a range of individual and mixtures of antioxidants. The effects of antioxidants on the oxidation stability of oils containing F-ZDDP were examined and compared with that of oils containing ZDDP. Absorption and transmittance spectra of oxidized samples were evaluated using Fourier transform infrared spectroscopy. Changes in oxidation were quantified through measurements of viscosity and total acid number, to assess the stability of various formulations.

- The oxidation stability of F-ZDDP was similar to ZDDP when used alone in base oil. This similarity may be attributed to the fact that the structure of F-ZDDP differs little from ZDDP,

with the minor exception that F-ZDDP contains a few hundred ppm of fluorine in the form of P–F bonds in its structure.

- FT-IR showed similar oxidation results for both ZDDP and F-ZDDP, when used in formulations containing individual antioxidants such as alkylated diphenyl amine, hindered phenol, methylene bis dibutyl dithiocarbamate and molybdenum dithiocarbamate.
- In almost all cases, molybdenum dithiocarbamate exhibited poor antioxidant properties, regardless of whether it was used individually or in mixtures. This is because molybdenum is a metal and exists in the same group as chromium in the periodic table, with similar characteristic properties as chromium. It can therefore be reasoned that Mo acts as a catalyst during the oxidation reaction. These catalytic activities with hydrocarbons result in antagonistic effects in the base oil formulation containing MoDTC.
- Oxidation stability of formulations containing ZDDP benefit more from mixtures of antioxidants, than from the presence of individual antioxidants, as seen from viscosity measurements. On the other hand, the stability of F-ZDDP is greater in the presence of individual antioxidants, as opposed to mixtures. It appears that the differences in the chemical structures between ZDDP and F-ZDDP (such as the presence of P–F bonds in the latter) while insignificant enough to affect the relative stability in base oil alone begin to play a much larger role when antioxidants are introduced.

CHAPTER 6

XANES ANALYSIS OF ANTIWEAR FILMS

The experimental techniques thus far used such as AES, TEM and SEM have provided valuable information on the nature and morphology of tribofilms that form on surfaces. However, these methods are unable to provide detailed information on the chemical bonding of tribofilms as a function of thickness. Investigating the chemical composition of tribofilms that form during tribological conditions is crucial to understanding the factors affecting a tribofilm's antiwear performance. A technique called X-Ray absorption near-edge spectroscopy (XANES) has been extensively used by various authors to study the nature of ZDDP tribofilms [7, 8, 32, 106, 136]. This is a powerful technique that is very useful to characterize chemical polyphosphate chain lengths.

This section deals with the XANES analysis of the some of the tribofilms generated from ZDDP and F-ZDDP in the presence and absence of antioxidants. The XANES facility at the Canadian Light Source Center at Saskatoon [137] was used to conduct the near-edge spectroscopy experiments for phosphorus L-edge and sulphur L-edge. The Canadian Synchrotron Radiation Facility at Wisconsin, Madison was used to study phosphorus K-edge and sulphur K-edge spectra of the tribofilms. Information on the role of antioxidants on the film formation capability can be extracted from these XANES tests by comparing the composition of films formed with and without antioxidants.

6.1 Experimental Procedure

6.1.1 Formulations used to Generate Antiwear Films:

The formulations containing ZDDP and F-ZDDP were prepared in base oil, separately with and without antioxidants. Antioxidants in these formulations were used individually as well as in mixtures in the same compositions as described in section 5.1.1. Base oil used in the study was 100 neutral. The amount of phosphorus in all formulations was kept constant at 0.08 wt.%. The total amount of all antioxidants in the formulations is maintained at 1.5 wt.%, with the sole exception of MoDTC which was maintained at 0.75 wt.%. Additionally, mixtures of antioxidants are also used to exploit any beneficial effects that may arise from such antioxidant combinations. Formulations of the various oil samples in base oil are:

1. ZDDP + base oil
2. ZDDP + alkylated diphenyl amine (ADPA) + base oil
3. ZDDP + methylene bis dibutyl dithiocarbamate (MBDTC} + base oil
4. ZDDP + hindered phenol (HP) + base oil
5. ZDDP + molybdenum dithiocarbamate (MoDTC) + base oil
6. ZDDP + alkylated diphenyl amine + methylene bis dibutyl dithiocarbamate + base oil
7. ZDDP + alkylated diphenyl amine + hindered phenol + base oil

Similar formulations as above were also prepared with F-ZDDP.

Wear tests were conducted on all the above formulated oil samples for 15K cycles at 24Kg load using BOCLE. All the tests were done under boundary lubrication conditions [138, 139]. After the wear tests, rings containing the generated wear tracks were cut using a diamond blade. Care was taken to preserve the antiwear film during this process. The rings were then cleaned using hexane and acetone and mounted on a small piece of flat steel to subject the sample to XANES analysis.

Phosphorus L-edge and sulphur L-edge were recorded at the Canadian Light Source (CLS) Center at Saskatoon, Canada, by using collimated plane grating monochromator (PGM),

which covers the photon energy range of 5–250 eV with photon resolution of 0.1 eV and 0.1eV at P L-edge and S L-edge respectively. Phosphorus K-edge and sulphur K-edge absorption near edge spectra (XANES) were obtained at the 1GeV Aladdin storage ring at the University of Wisconsin, Madison. The P and S K-edge spectra were obtained on the double crystal monochromator (DCM) beam line covering the region of 1500–4000eV. The photon resolution at the P K-edge and S K-edge was 0.3eV and 0.5eV respectively. XANES spectra were recorded both in fluorescence yield (FLY) and total electron yield (TEY) modes.

6.2 Results and Discussion

6.2.1 P L-Edge of ZDDP and F-ZDDP with Model Compounds

XANES has been extensively used to study the nature of antiwear films by many researchers [8, 68, 76, 77, 106, 123]. Recently, XANES has found increasing utility in tribofilm analysis since it is capable of probing the local structural environment around selected atoms. XANES is used to understand the chemical environment around phosphorus and sulphur atoms in tribofilms. In order to identify the chemical nature of phosphorus and sulphur in complex matrices such as antiwear films, it is essential to compare the XANES spectra of films with those of different model compounds in which the local chemical environment of S and P are known. Yin et al [140] showed from XANES study of the tribofilm that chemical state of the phosphorus in antiwear films generated from ZDDP correspond closely to polyphosphates and depend on the alkyl group in ZDDP. It is been known that antiwear film is made of phosphates and sulphates [5] and polyphosphates found in the antiwear film could be either long-chain or short-chain polyphosphates. In this study, $FePO_4$, $Zn_3(PO_4)_2$, ZnS, $ZnSO_4$ are used as some of the phosphates, sulphates and sulfides model compounds to understand the chemical nature of the tribofilms formed under this study. Figure 6.1 shows the comparison of XANES P L-edge spectra of tribofilms derived from ZDDP and F-ZDDP in base oil to the XANES P L-edge spectra of $Zn_3(PO_4)_3$, $FePO_4$, $Fe_4(P_2O_7)_3$ recorded in the FLY mode. TEY mode for phosphorus or sulphur L-edge was not included due to technical difficulties associated with the detector.

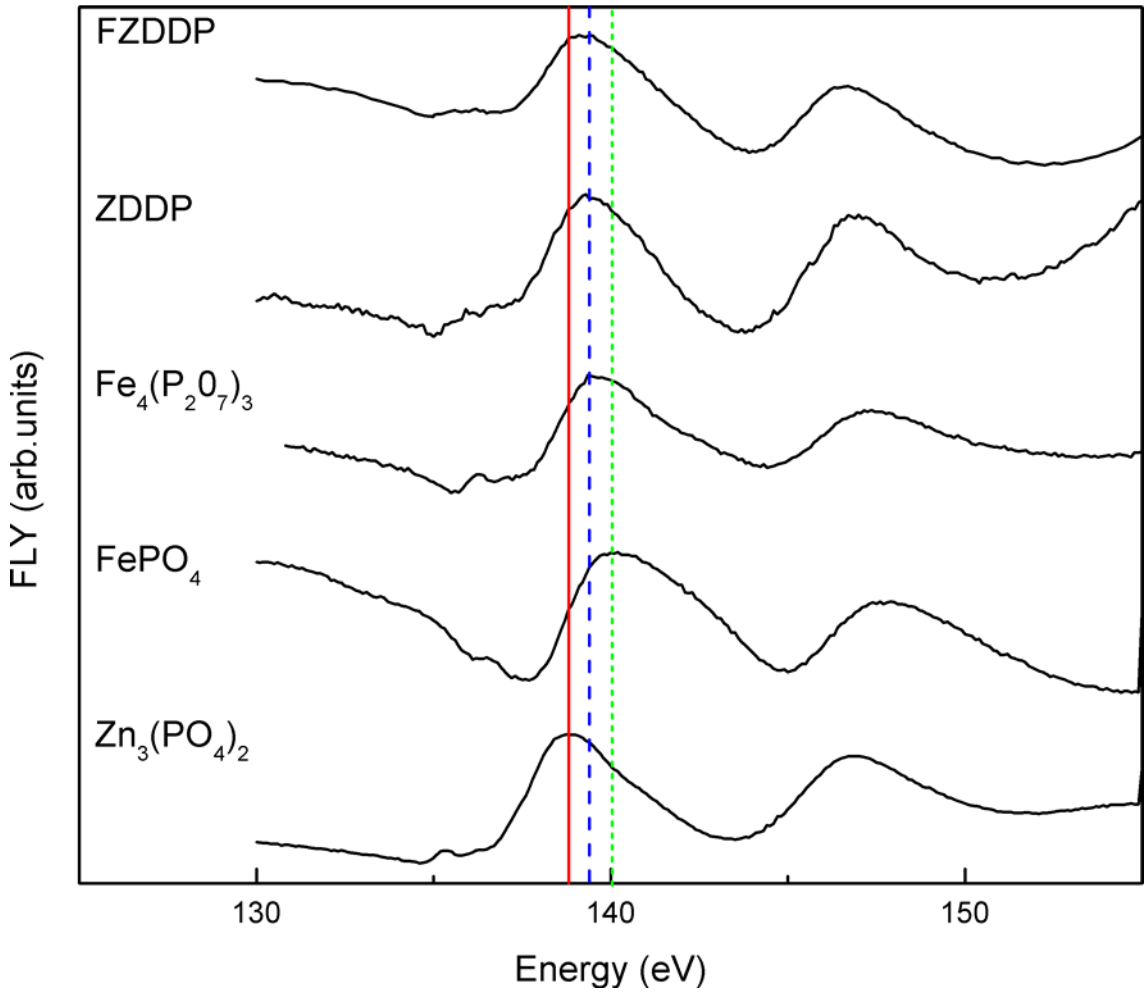

Figure 6.1: P L-edge XANES spectra in FLY form of ZDDP and F-ZDDP antiwear films with model compounds.

The solid red line, dashed blue line and the dotted green line in Figure 6.1 indicate the positions of the peaks for $Zn_3(PO_4)_2$, $Fe_4(P_2O_7)_3$ and $FePO_4$ respectively. It can be seen from Figure 6.1 that P L-edge spectra of both ZDDP and F-ZDDP derived antiwear films contain both short-chain iron and zinc pyrophosphates. The position of ZDDP and F-ZDDP tribofilms matches with that of some of the model phosphate compounds, indicating that ZDDP or F-ZDDP has undergone tribochemical transformations in the process of forming antiwear films. It can be seen from Figure 6.1 that the position of the ZDDP tribofilm matches closely with $Fe_4(P_2O_7)_3$ (dashed blue line), indicating the presence of $Fe_4(P_2O_7)_3$ as the primary form of

polyphosphate in this tribofilm. The spectra of ZDDP tribofilm also shows a shoulder (which aligns with the solid red line) indicating the possibility of some amounts of $Zn_3(PO_4)_2$ in the tribofilm. However, the presence of this shoulder is not very obvious. The spectra of F-ZDDP tribofilm has a wider peak which matches with both $Zn_3(PO_4)_3$ (solid red line) and $Fe_4(P_2O_7)_3$ (dashed blue line). This match is a clear indication that both these compounds are present in the tribofilm of F-ZDDP. The presence of polyphosphates such as $Fe_4(P_2O_7)_3$ and/or $Zn_3(PO_4)_2$ (i.e., iron pyrophosphate and/or zinc pyrophosphate) is only in the top 50 nm depth of the tribofilm since the information obtained in the FLY L-edge of P and S is emanating from this depth. The observation made by Yin et al [67] showed that tribofilms formed from aryl ZDDP contained long-chain polyphosphates throughout the film and films generated from alkyl ZDDP consisted of long-chain polyphosphates on the topmost surface and short-chain polyphosphates in the bulk of the film. However in this case, only short-chain polyphosphates were observed at depths of 50 nm in the tribofilm.

6.2.2 S L-Edge of ZDDP and F-ZDDP with Model Compounds

Figure 6.2 shows the comparison of S L-edge XANES spectra in the FLY mode of tribofilms derived from ZDDP and F-ZDDP in base oil, to that of model compounds such as ZnS and FeS.

Antiwear films from ZDDP and F-ZDDP were low in sulphur, with sulphur (in the top 50nm depth of the tribofilm) being present mostly as a sulphide. This is verified by the fact that the peaks in ZDDP align with that of FeS (blue dashed and green dotted lines). However, sulphur was present in appreciable amounts in ZDDP tribofilms when compared to that of F-ZDDP, where the sulphur signal was very weak.

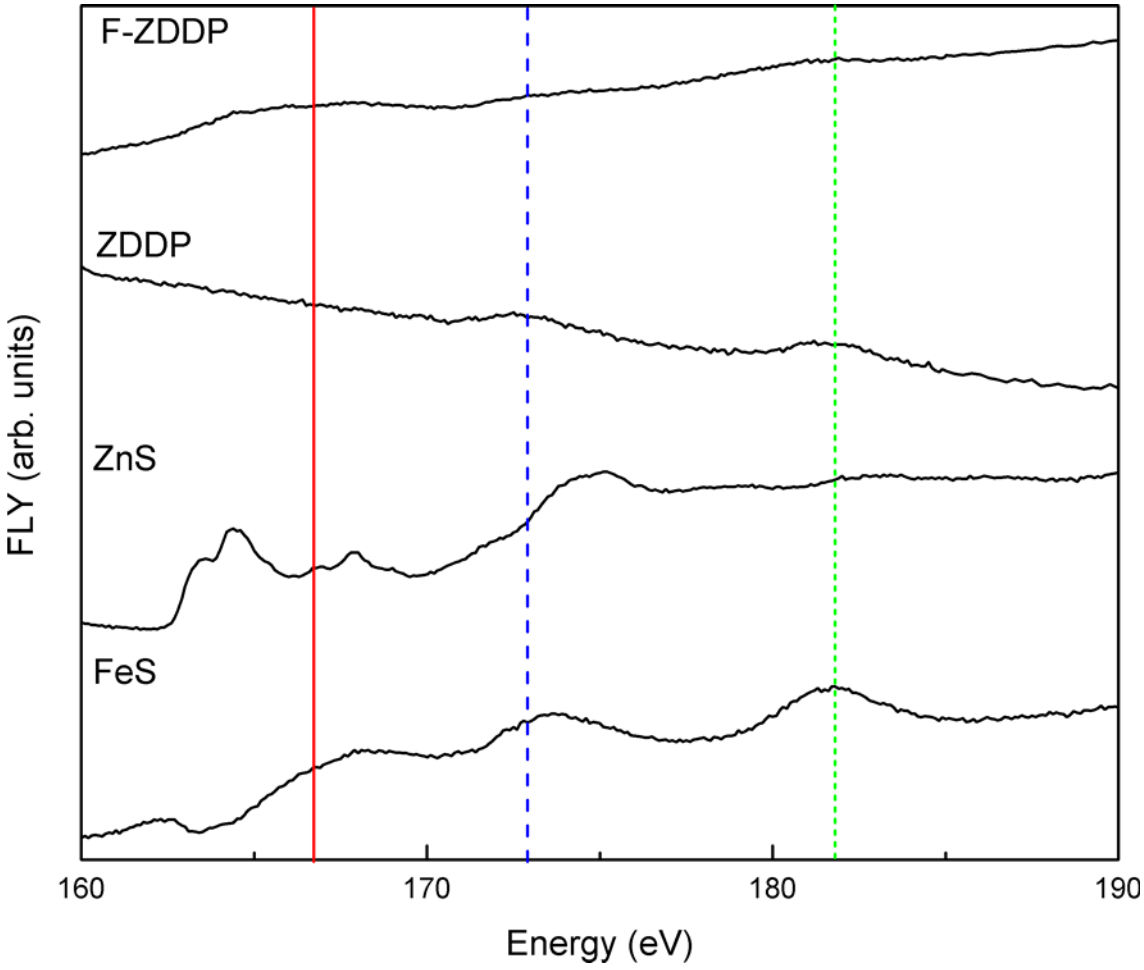

Figure 6.2: S L-edge XANES spectra in FLY form of ZDDP and F-ZDDP antiwear films with model compounds.

6.2.3 P L-Edge of ZDDP and F-ZDDP with and without Antioxidants

FLY spectra of P L-edge from ZDDP and F-ZDDP with different individual as well as mixtures of antioxidants were compared with that of ZDDP and F-ZDDP as shown in Figure 6.3 and Figure 6.4.

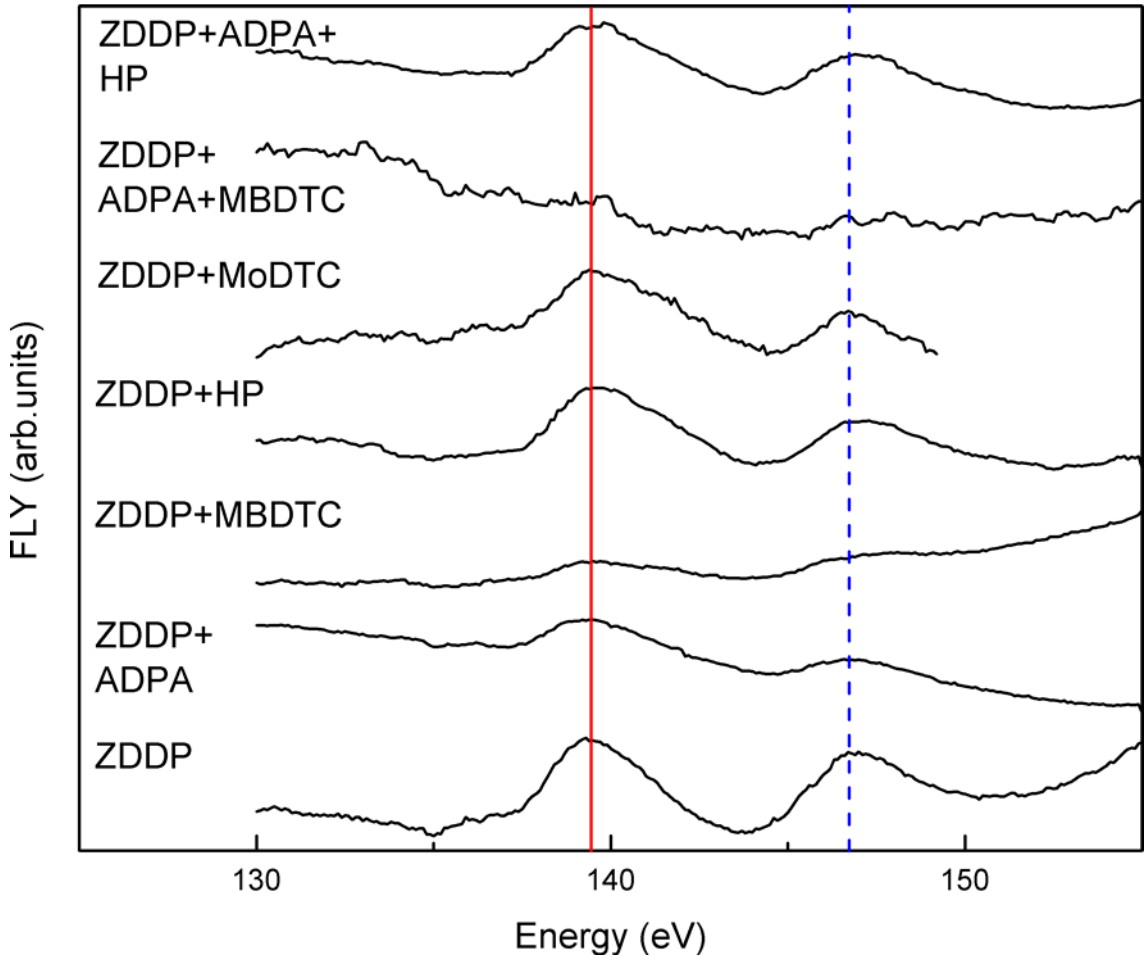

Figure 6.3: P L-edge XANES spectra in FLY form of antiwear films generated from ZDDP and ZDDP with antioxidants with model compounds.

P L-edge peaks obtained with ZDDP and F-ZDDP with different antioxidants are quite similar to that of ZDDP and F-ZDDP (alone in base oil), indicating that phosphorus is in the form of mixtures of short-chain polyphosphates such as zinc and iron polyphosphates. As there were no shifting of peaks observed in the ZDDP or F-ZDDP tribofilms with antioxidants, this represents that the presence of antioxidants in the formulation does not influence film formation chemistry at least on the top 50 nm of the tribofilm. In the case of both ZDDP and F-ZDDP with antioxidants, very strong phosphorus signal was observed for HP, ADPA+ HP and also for ZDDP with MoDTC. Data for F-ZDDP with MoDTC could not be obtained and therefore this

spectrum is not shown in Figure 6.4. However, the spectra of ADPA+MBDTC with both ZDDP and F-ZDDP did not show a presence of phosphorus peaks which points to an absence of tribofilm (or a very thin film) in this case.

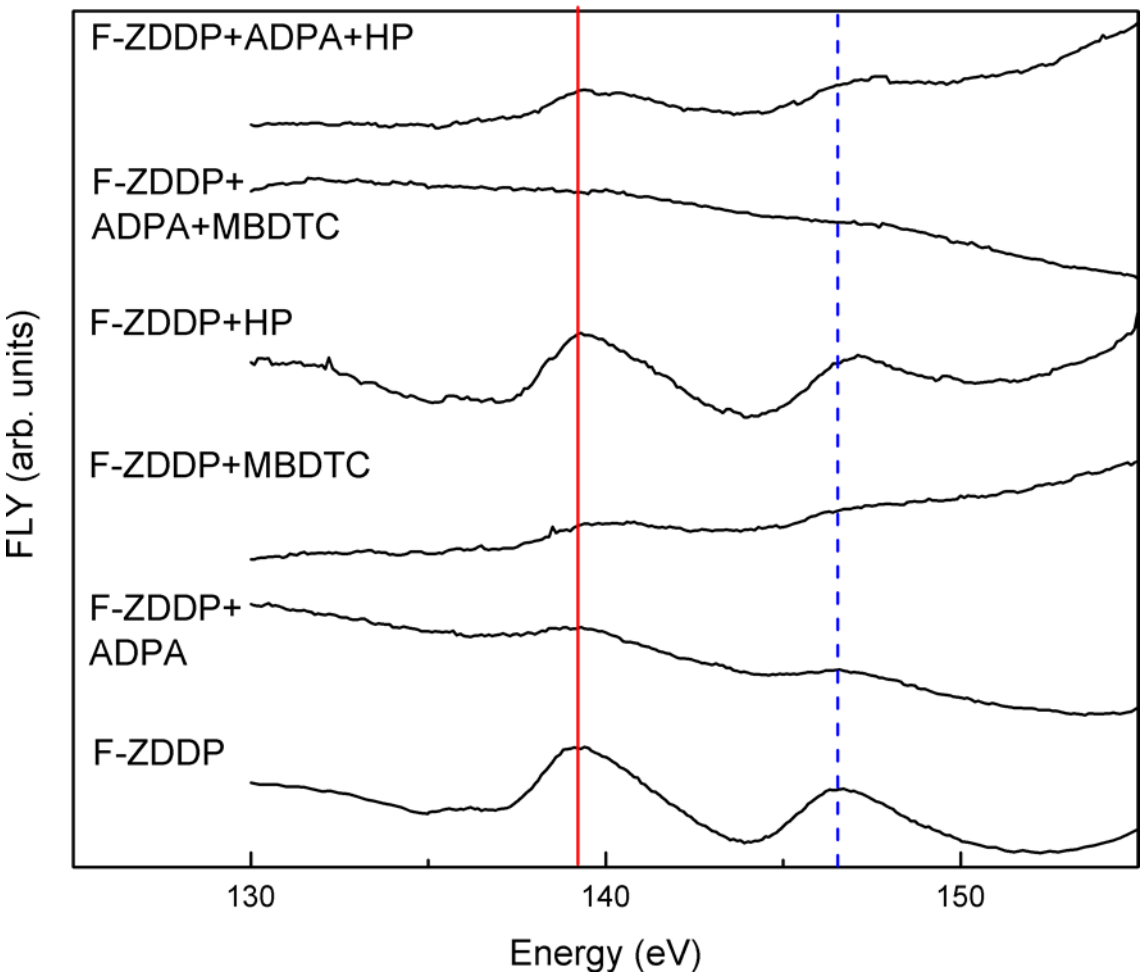

Figure 6.4: P L-edge XANES spectra in FLY form of antiwear films generated from F-ZDDP and F-ZDDP with antioxidants with model compounds.

6.2.4 S L-Edge of ZDDP and F-ZDDP with and without Antioxidants

S L-edge spectra (FLY or TEY) of ZDDP with antioxidants and F-ZDDP with antioxidants did not show the presence of sulphur in any form, indicating that the presence of antioxidant in the formulation has no direct influence on the chemistry of the tribofilm.

6.2.5 P K-Edge of ZDDP with and without Antioxidants

In Figure 6.5, the XANES P K-edge spectra of tribofilms derived from ZDDP and ZDDP with different antioxidants in base oil are compared to the XANES P K-edge spectra of model compounds such as $Zn_3(PO_4)_2$, $FePO_4$ in the FLY mode.

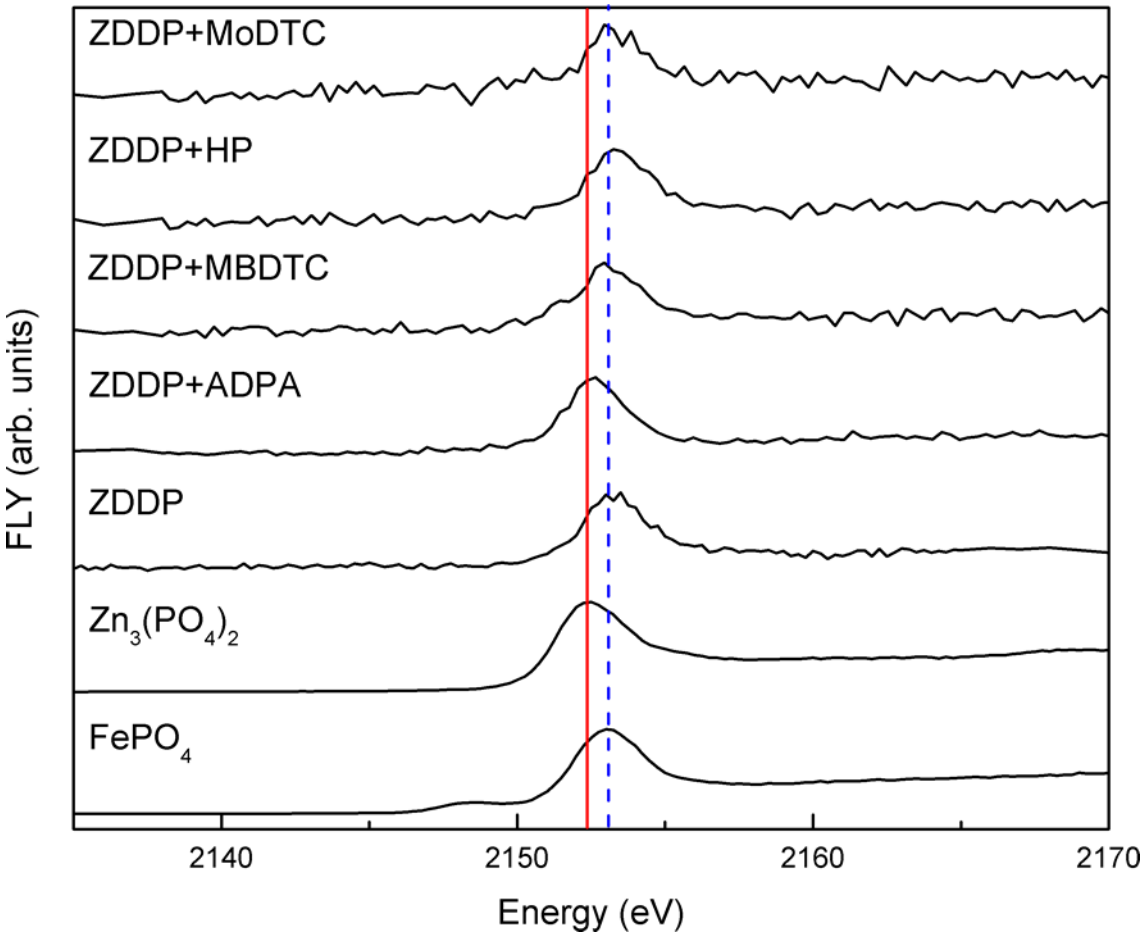

Figure 6.5: P K- edge XANES spectra of antiwear films generated from ZDDP and ZDDP with antioxidants with model compounds in FLY mode.

It can be seen from Figure 6.5 that tribofilms from all of the formulations contain phosphates such as $FePO_4$ (blue dashed line) and $Zn_3(PO_4)_2$ (red solid line), as the major peak in the spectra of these compounds matches those of tribofilms generated from ZDDP or ZDDP with antioxidants but in different proportions. FLY P K-edge spectrum of ZDDP with alkylated diphenyl amine showed a shift to lower energy with the major peak of phosphate aligning with

that of $Zn_3(PO_4)_2$ (solid red line). This could suggest that the primary phosphate in this case could be $Zn_3(PO_4)_2$, with $FePO_4$ present in small amounts. The type of the phosphate observed is a mixture of short-chain phosphates. FLY P K-edge of ZDDP and ZDDP with antioxidants such as HP, MBDTC and MODTC matches exactly with the major peak of $FePO_4$ with the shoulders of these peaks matching that of $Zn_3(PO_4)_2$. This indicates that the major form of phosphates in these cases is $FePO_4$, with some amount of $Zn_3(PO_4)_2$. The spectra obtained for these tribofilms in the TEY mode with the previously explained model compounds are shown in Figure 6.6.

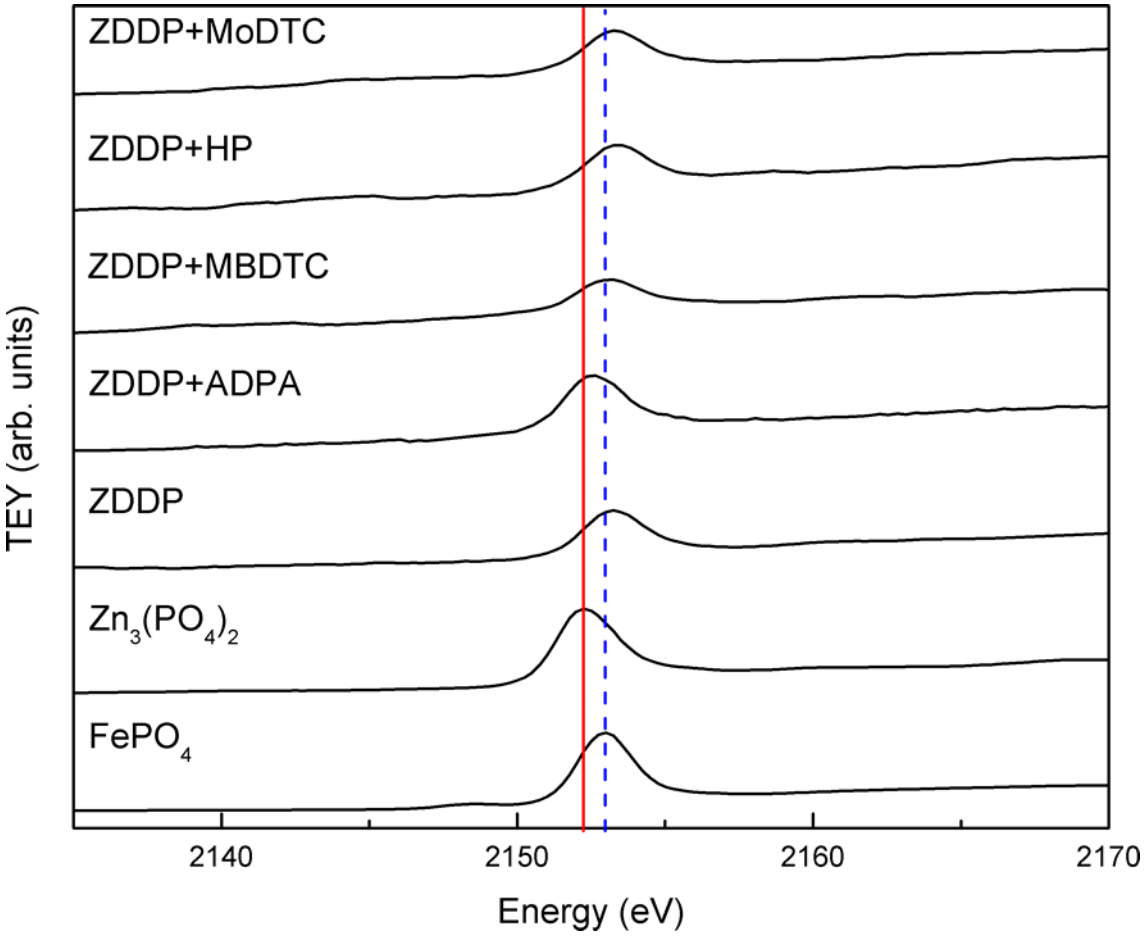

Figure 6.6: P K- edge XANES spectra in TEY form of antiwear films generated from ZDDP and ZDDP with antioxidants with model compounds.

The results show that the information obtained this case is not very different from that of FLY mode, except that the information is obtained from the deeper region of the tribofilm in FLY (~300nm) than that obtained for TEY. The presence of shoulders corresponding to $Zn_3(PO_4)_2$ was very clear in FLY mode.

6.2.6 P K-Edge of F-ZDDP with and without Antioxidants

FLY P K-edge of F-ZDDP and F-ZDDP with antioxidants with model compounds are shown in Figure 6.7.

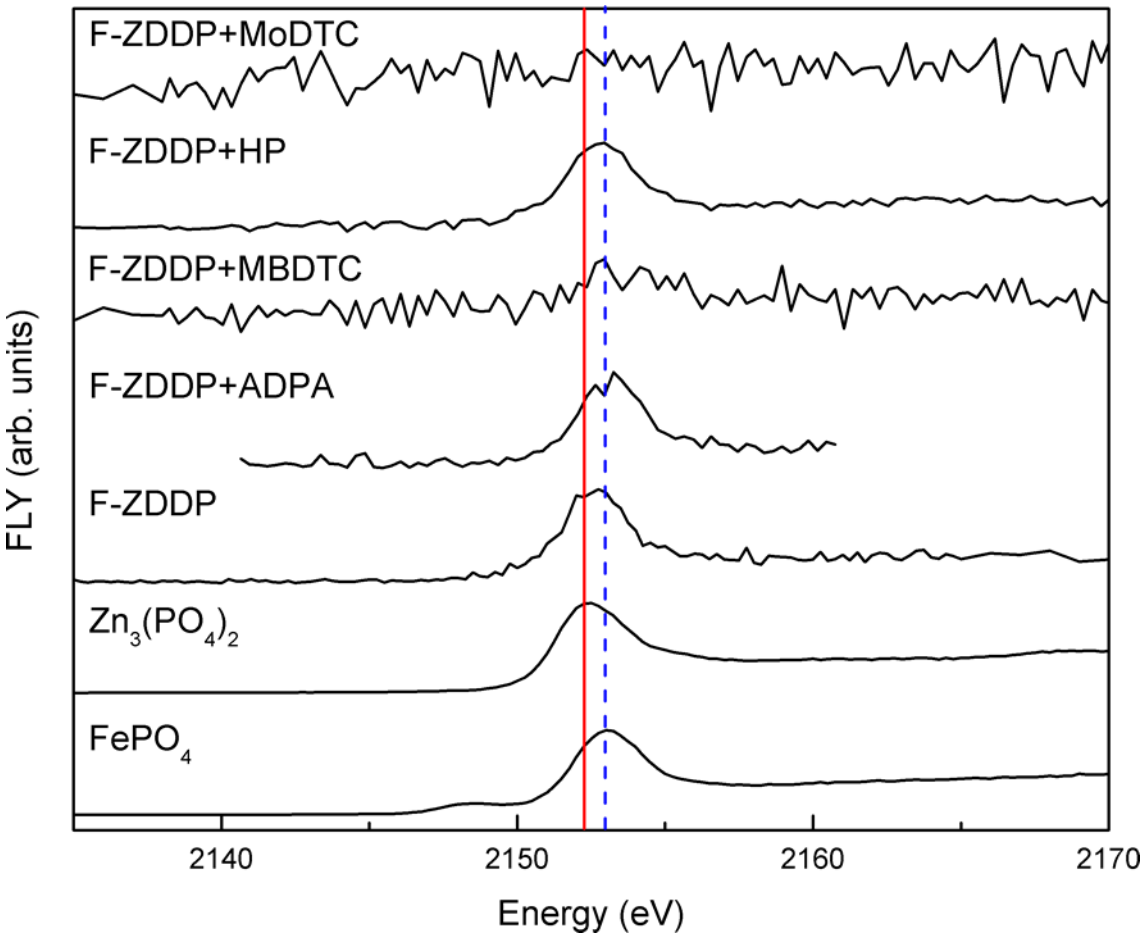

Figure 6.7: P K- edge XANES spectra in FLY form of antiwear films generated from F-ZDDP and F-ZDDP with antioxidants with model compounds.

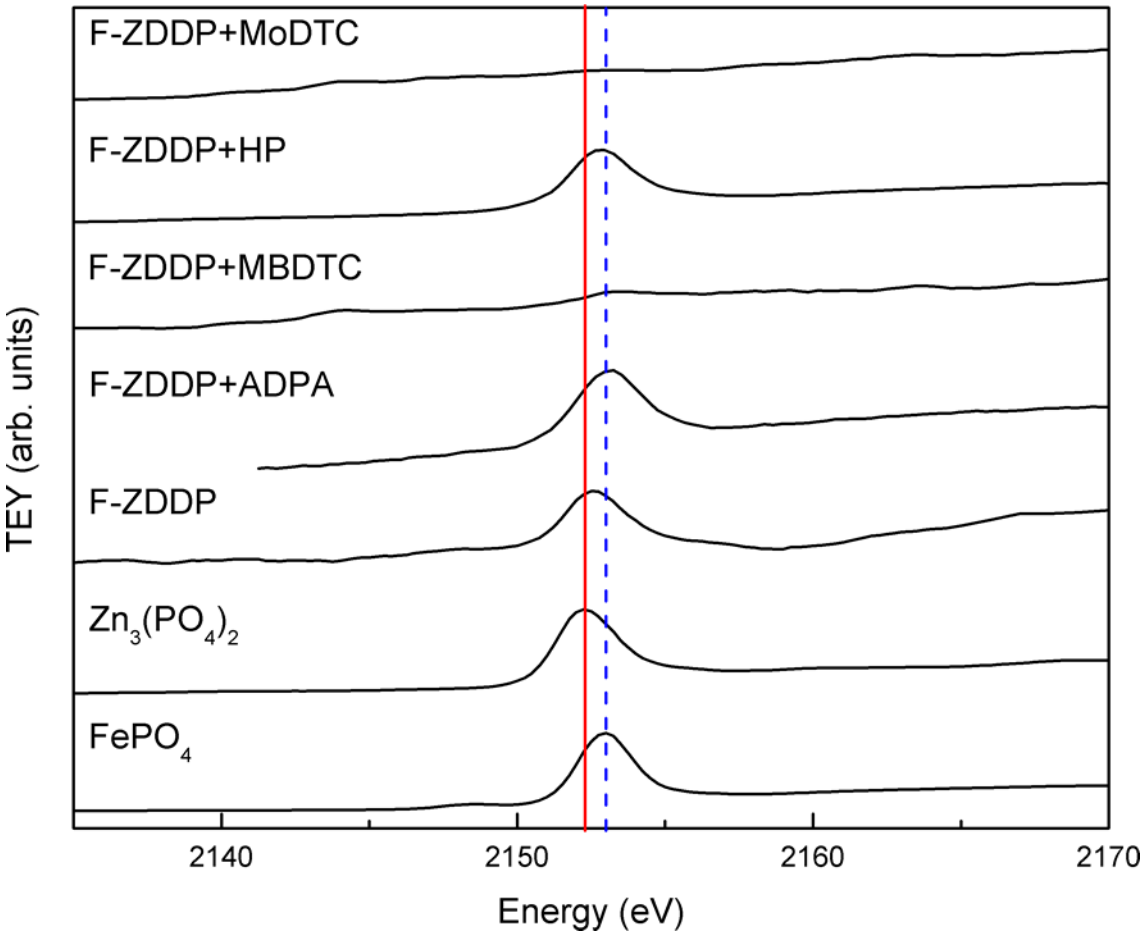

Figure 6.8: P K- edge XANES spectra in TEY form of antiwear films generated from F-ZDDP and F-ZDDP with antioxidants with model compounds.

All of the formulations contain mixtures of $FePO_4$ (blue dashed line) and $Zn_3(PO_4)_2$ (red solid line) in different proportions. In this case major peak of $FePO_4$ (blue dashed line) matched those of the major peak of F-ZDDP+ADPA and F-ZDDP+HP. F-ZDDP showed more $Zn_3(PO_4)_2$. It can be seen from Figure 6.8 that there is no phosphorous signal obtained for F-ZDDP with MBDTC and F-ZDDP with MODTC, implying that the focused region could be outside the wear track.

TEY modes of F-ZDDP and F-ZDDP (Figure 6.8) with antioxidants are not much different from that of FLY with FLY spectra showing the presence of a very clear shoulder corresponding to Zinc phosphate.

6.2.7 S K-Edge of ZDDP and F-ZDDP with and without Antioxidants

TEY (Figure 6.9 and Figure 6.10) and FLY (Figure 6.11 and Figure 6.12) S K-edge of ZDDP and F-ZDDP with antioxidants were also recorded and compared with model compounds such a ZnS and $ZnSO_4$.

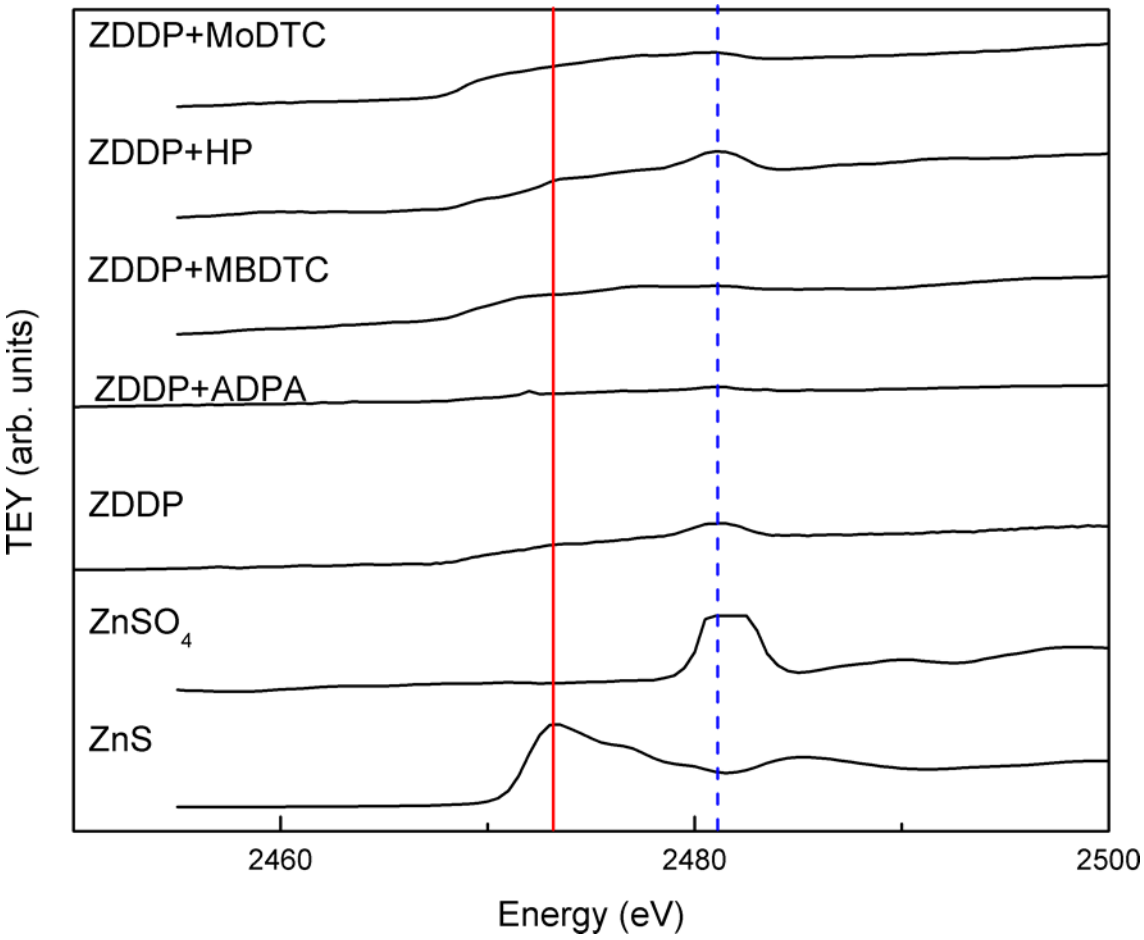

Figure 6.9: S K- edge XANES spectra in TEY form of antiwear films generated from ZDDP and ZDDP with antioxidants with model compounds.

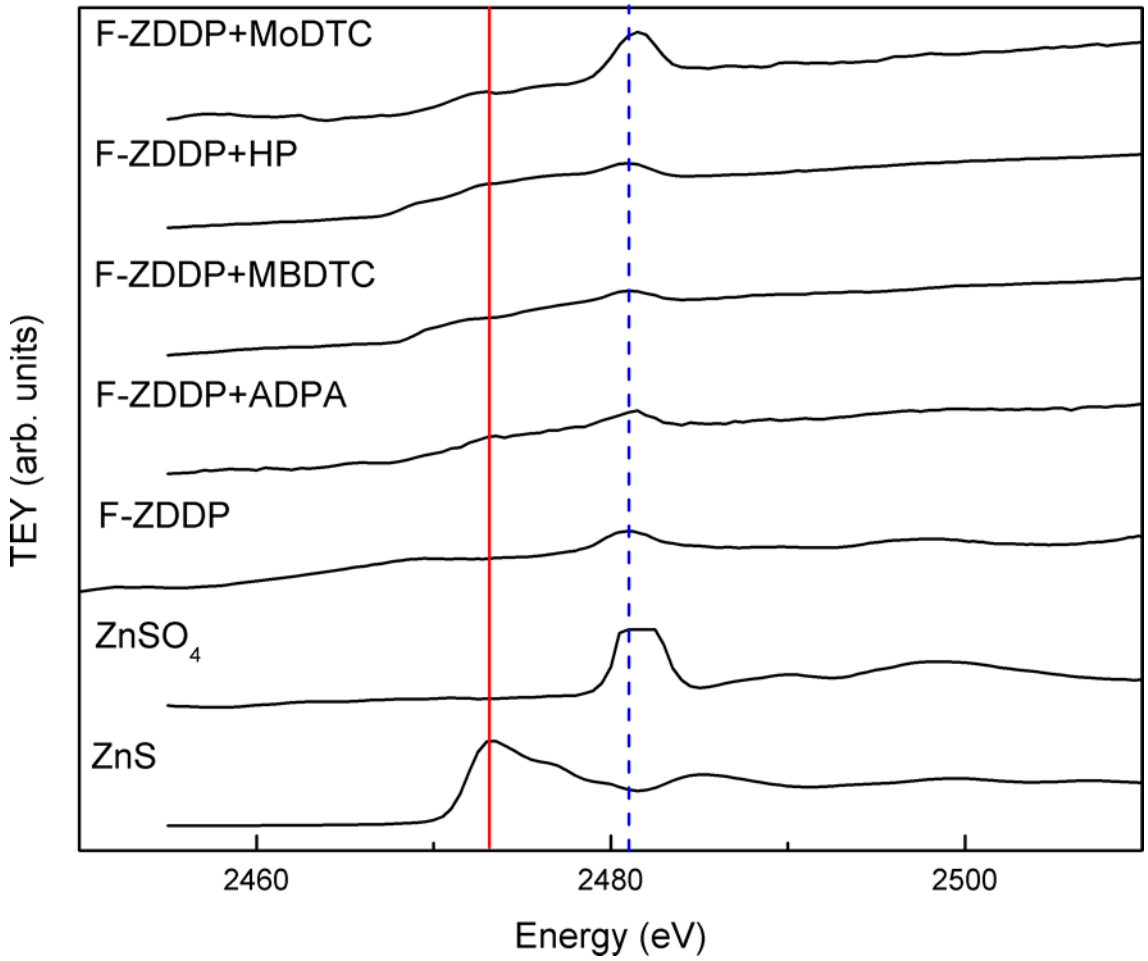

Figure 6.10: S K- edge XANES spectra in TEY form of antiwear films generated from F-ZDDP and F-ZDDP with antioxidants with model compounds.

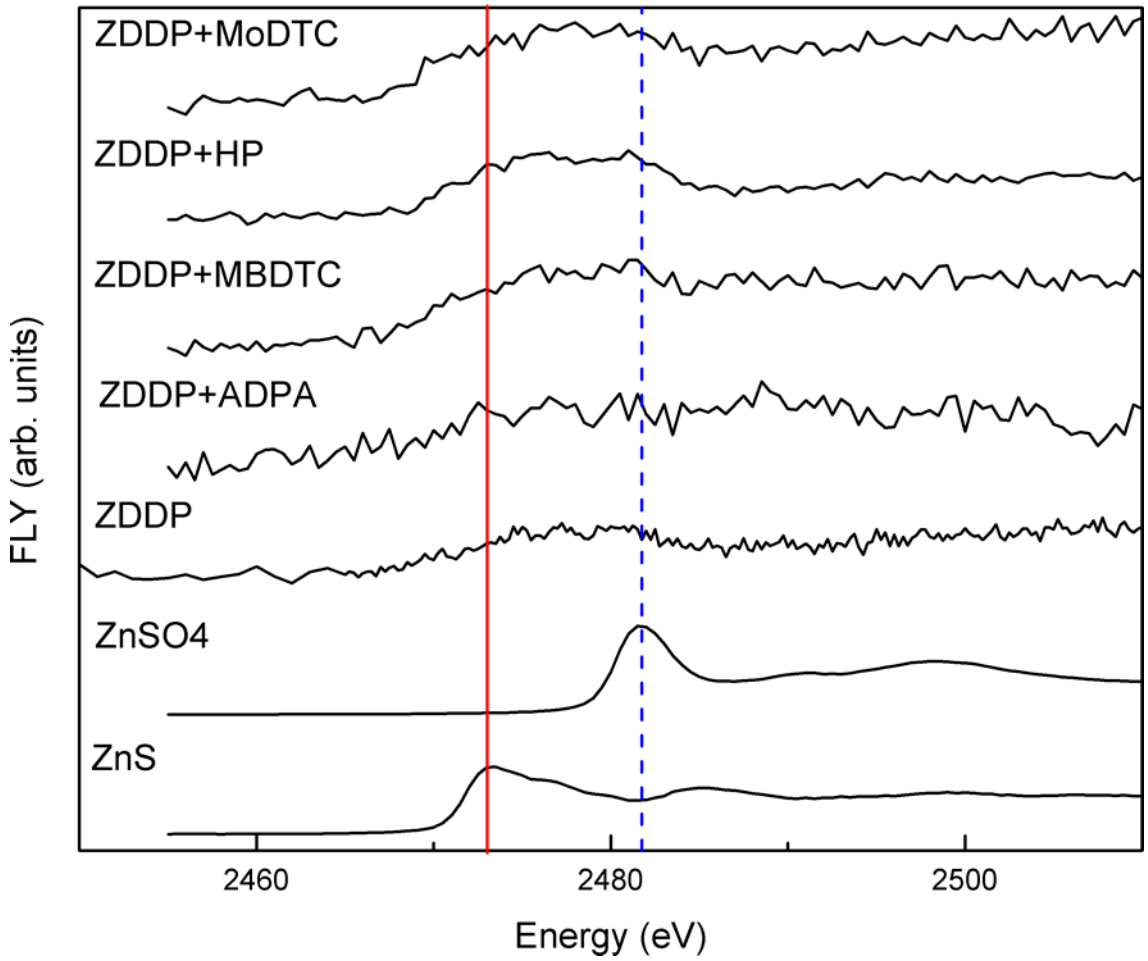

Figure 6.11: S K- edge XANES spectra of antiwear films generated from ZDDP and ZDDP with antioxidants with model compounds in FLY form.

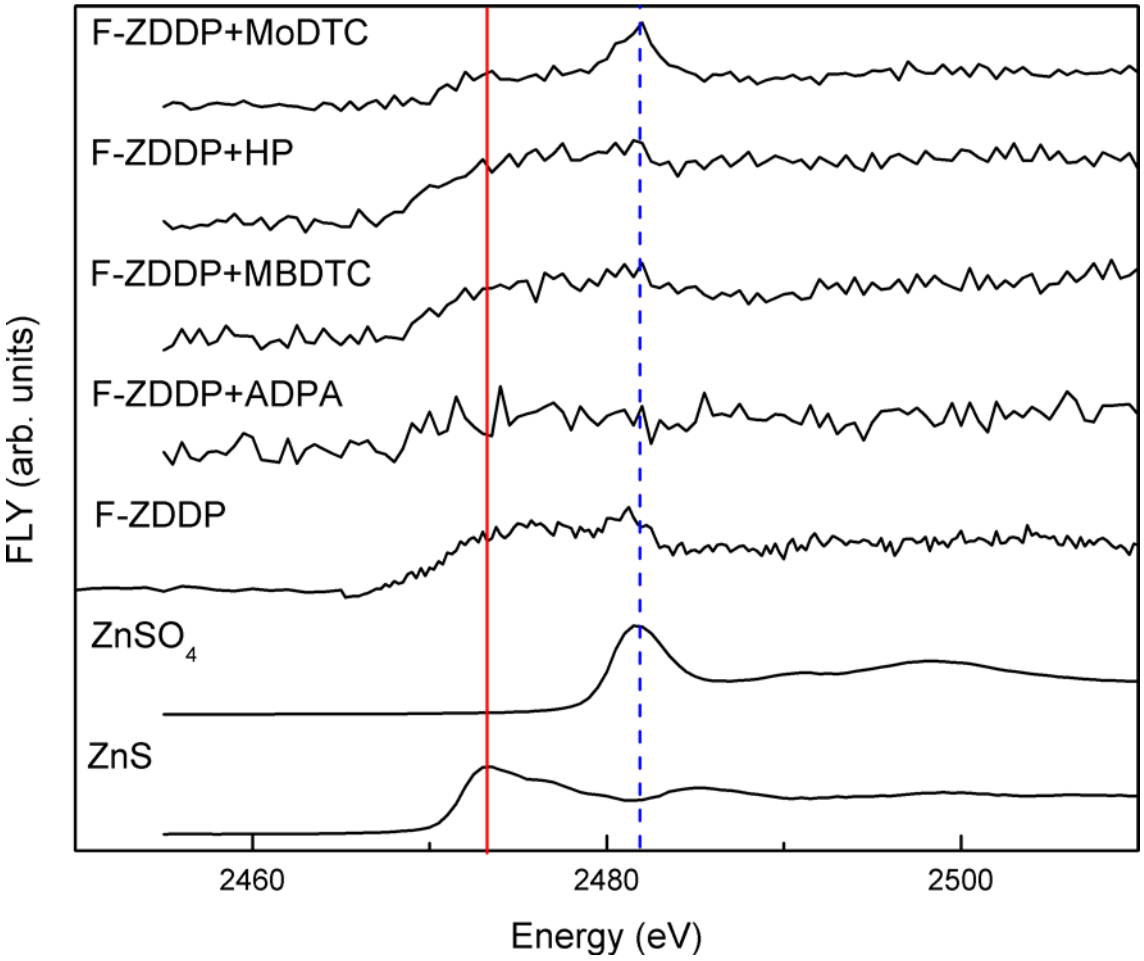

Figure 6.12: S K- edge XANES spectra of antiwear films generated from F-ZDDP and F-ZDDP with antioxidants with model compounds in FLY form.

Sulphur observed at this level i.e., both in FLY and TEY (50nm for TEY and ~300nm FLY) was on average very low. In general, FLY signals recorded were noisier than TEY spectra. This indicated the presence of more sulphur on the surface layer than in the bulk. The spectra of ZDDP and F-ZDDP showed very little difference if any. Sulphur observed in ZDDP and ZDDP and antioxidants were in the form of sulfides (red solid line) and sulphates (blue dashed line) – both in minute amounts. ZDDP with ADPA did not show the presence of any kind of sulphur (Both in FLY and TEY) and ZDDP with antioxidants such as MBDTC, HP and MODTC showed significantly stronger signal of sulphur when compared to ZDDP. In F-ZDDP,

sulphur was present as a sulphate, since the peak from F-ZDDP matched the major peak of $ZnSO_4$. F-ZDDP with ADPA did not show any form of sulphur (both in TEY and FLY). In other combinations of F-ZDDP with antioxidants such as MBDTC, HP and MoDTC, sulphur was present in both sulfide and sulfate forms, with F-ZDDP+MoDTC showing a strong sulphate signal compared to the others. Because of the technical problems encountered while obtaining the TEY and FLY K-edge, P and S signals for the tribofilms obtained from ZDDP and F-ZDDP with mixture of antioxidants such as ADPA+MBDTC and ADPA+HP are not included here.

6.3 Summary

Antiwear films were generated from various formulations containing ZDDP and F-ZDDP with antioxidants, using the ball-on-cylinder lubricity evaluator. The tribofilms thus formed were subjected to XANES analysis at the phosphorus and sulphur K and L edges in the FLY and TEY modes in order to explore the chemical nature of the tribofilms. The following conclusions were drawn from the above analysis of XANES.

- The tribofilms generated from ZDDP and F-ZDDP with antioxidants showed the presence of short-chain polyphosphates such as $Zn_3(PO_4)_2$, $Fe_4(P_2O_7)_3$ and $FePO_4$ in different proportions throughout the thickness of the tribofilms.
- There was no difference in the types of the polyphosphate with the introduction of antioxidants to ZDDP or F-ZDDP, indicating that there are no changes in the structure of glasses present in the tribofilm. The presence of antioxidant therefore does not influence the tribofilm chemistry. The only difference observed could be in the amounts of different types of polyphosphates observed.
- Sulphur was present in minute quantities and was in the form of sulfide in the top 50nm region of the tribofilm (FLY-Ledge). Small amounts of sulphur were present in the form of sulphates in the deeper part of the tribofilm (~300nm – FLY-K edge).

CHAPTER 7

PHENOMENOLOGICAL MODEL FOR OXIDATION OF BASE OILS IN THE PRESENCE OF ANTIWEAR AGENTS AND ANTIOXIDANTS

ZDDP is a very effective antiwear agent and an antioxidant. However, it is well-known that the antiwear potency of ZDDP is diminished upon its oxidation. In addition, studies have shown that when ZDDP acts as an antioxidant, the ensuing products formed serve to reduce its effectiveness in producing an antiwear film, thereby reducing its antiwear properties [5, 40].

When additional antioxidants such as ADPA are introduced into the formulation, they would then function as the main vehicle of oxidation mitigation, thereby allowing ZDDP to maintain its effectiveness as an antiwear agent for prolonged intervals. The amount of wear in the presence of ADPA was reduced in formulations with ZDDP. On the other hand, the addition of ADPA to formulations containing F-ZDDP showed a marginal increase in wear when compared to F-ZDDP alone in base oil. Given that ADPA is basic in nature, it could scavenge some of the fluorine present in the form of P-F bonds in F-ZDDP. This was reflected in the fact that the ^{31}P NMR spectra of F-ZDDP with ADPA showed a decrease in the observed intensity of P-F bonds compared to that of F-ZDDP. Since P-F bonds are responsible for the improved wear performance in the case of F-ZDDP over ZDDP, it is evident that depletion of these bonds would result in the observed marginal increase in wear. However, the overall antiwear performance of F-ZDDP with ADPA was still better than the formulation of ZDDP with ADPA, and this can be attributed to the fact that P-F bonds, though reduced in number, were still present in sufficient quantities to provide enhanced antiwear action.

A second reason for the observed weak antagonistic effect of F-ZDDP with ADPA when compared to F-ZDDP alone could be due to the fact that ADPA being basic, it complexes with some of the fluorine (which is electronegative) present in F-ZDDP to form a weak hydrogen-like bonding. This proposed complex formation mechanism is illustrated below.

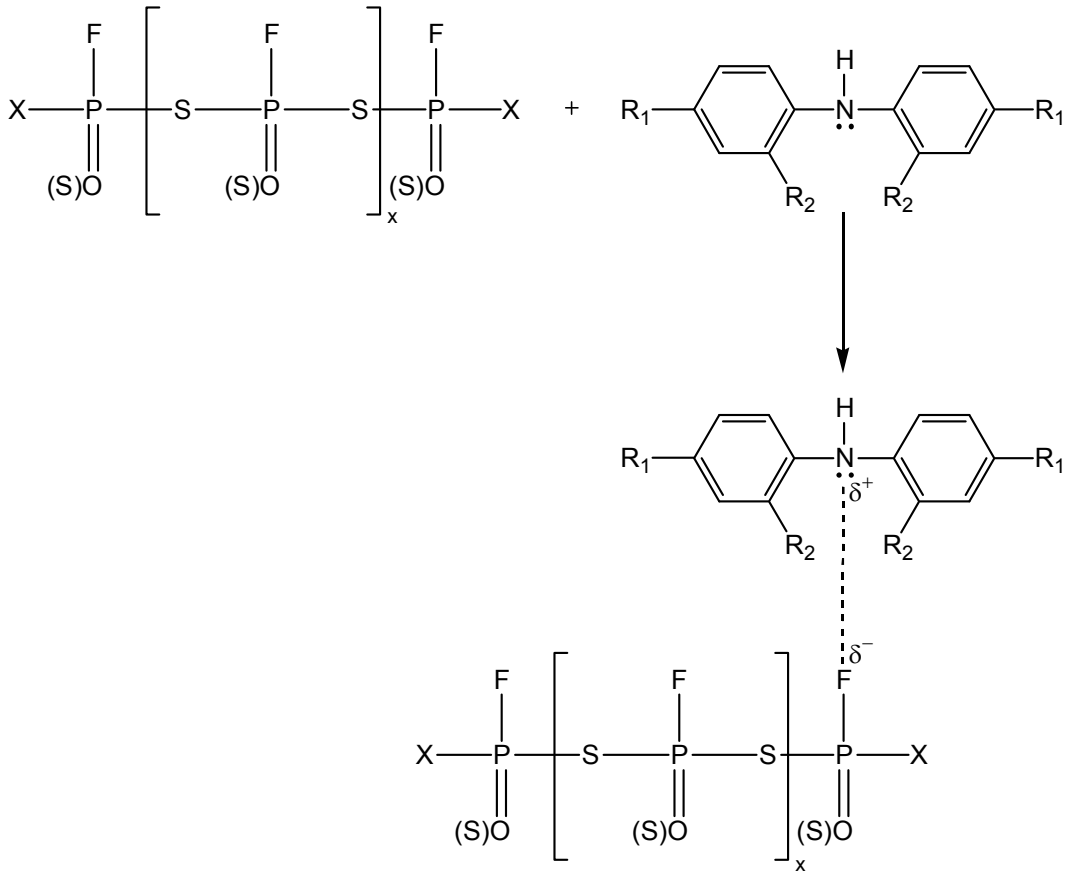

(7.1)

This complex formation inhibits the ability of F-ZDDP to quickly reach the surface and form a protective film. Since this complex formation is weak, significant quantities of F-ZDDP could remain free of complex formation and be available for wear protection.

In fully formulated oils, it is known that additives compete for the surface and are responsible for observed changes in the expected wear behavior of ZDDP [16, 19]. A similar phenomenon could occur in the case of F-ZDDP. This complex formation in the liquid phase could reduce the chemical activity of F-ZDDP, which could lower its adsorption capabilities and also increase it decomposition temperature, thereby resulting in the observed increase in wear. The observations and reasoning indicate that even though the presence of ADPA in the formulation with ZDDP had a beneficial effect, it may not be a good companion antioxidant in formulations containing F-ZDDP, when wear performance is evaluated.

7.1 Oxidation Stability

The primary antioxidants such as hindered phenols [86, 131] and aromatic amines operate by donating a hydrogen atom to a peroxy radical and retard the propagation step of oxidation [86]. The reaction steps of primary antioxidants for the specific cases of alkylated diphenyl amine (Eq. 7.2) and hindered phenol (Eq. 7.3) are given below. It has been shown that the mechanism of alkylated diphenyl amines depends upon the operating temperature [85].

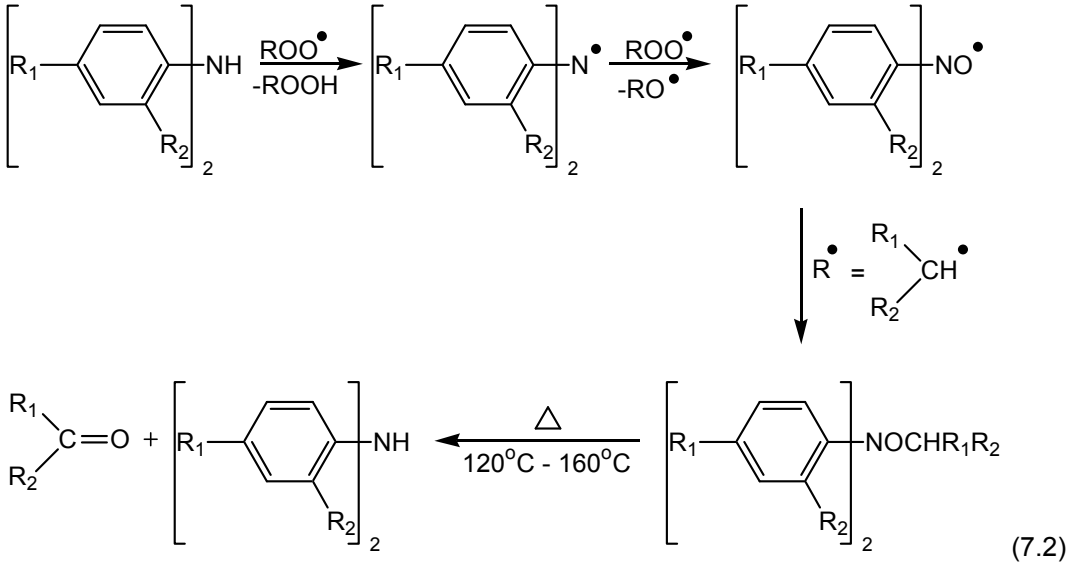

(7.2)

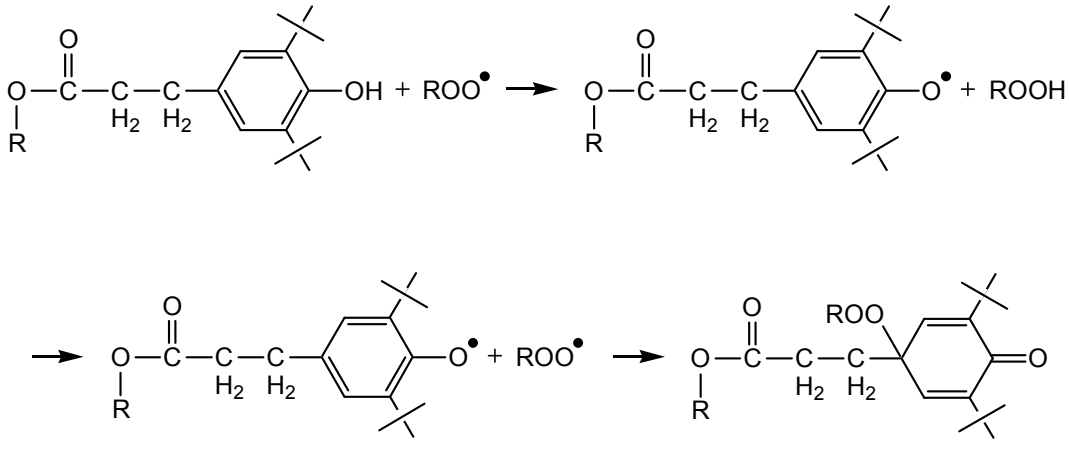

(7.3)

Secondary antioxidants such as Methylene bis dibutyl dithiocarbamate inhibit the branching step by functioning as hydroperoxide decomposers and reacting with hydroperoxide (ROOH) molecules, thereby retarding the creation of peroxy radicals. The reactions are terminated by the formation of sulphur-containing end products and alcohols as described below.

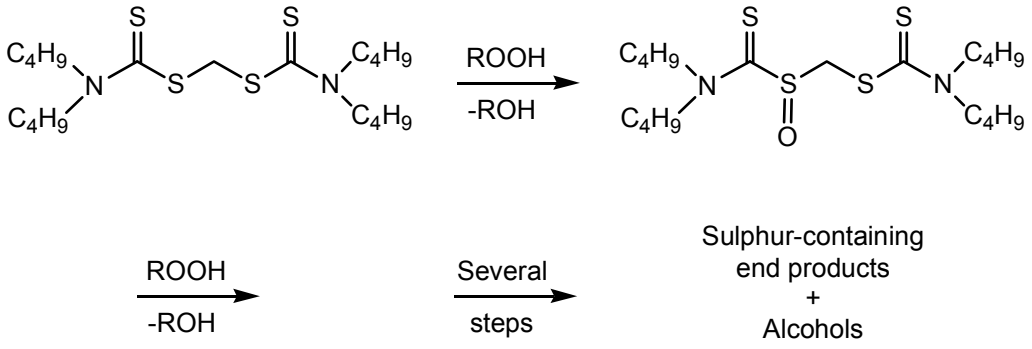

(7.4)

It can be seen from this research that base oil with MoDTC showed poorer inhibition ability under the conditions employed in this work, an outcome which does not follow observations of good antioxidant behavior by other researchers [133, 134]. Oxidation process in engines is generally catalytic in nature. In engines, the interaction of bearing surfaces and acidic oxidation products of the engine oil cause an accumulation of oil-soluble copper [87]. These conditions are simulated in laboratory environments by adding iron or copper naphthenate into the formulation, which produce soluble cations such as iron and copper respectively. It is known that hydroperoxides can be decomposed by the catalytic action of metal ions that can exist in two oxidation states. Examples of such metal cations include iron, copper, nickel and chromium [23, 87]. Given that molybdenum falls below chromium (and therefore in the same group) in the periodic table of the elements, its characteristic properties are similar to that of the latter. Molybdenum may therefore be inferred to behave as a catalyst during oxidation, and therefore possesses limited effectiveness in retarding oxidation. In this study, Mo existed in +5 oxidation state. The proposed mechanism is shown below.

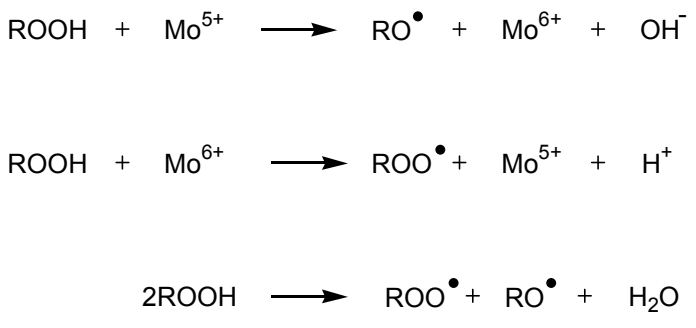

(7.5)

The above reaction was observed when MoDTC was used as the sole antioxidant in the formulation. However, when MoDTC was used in conjunction with other antioxidants such as ADPA, there was improvement in performance in oxidation inhibition. It may be reasoned that when MoDTC (with oxidation state of +5) was used with ADPA, the reaction was stabilized by the formation of quinone stabilized alkylated DPA. This indicates that the antagonistic effect of MoDTC is countered by the other antioxidants present in the mixture. An example of such a reaction is shown below [135].

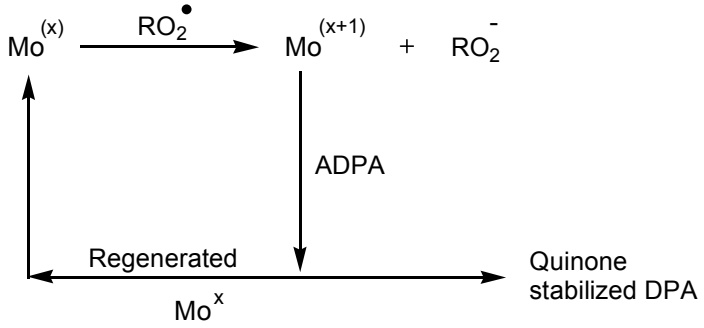

(7.6)

Synergy (the phenomenon wherein the combined benefit of two or more entities is greater than the sum of the individual enhancements) was observed for the formulation containing a mixture of HP and MBDTC. These two antioxidants complement each other – HP functions to retard the propagation step while MBDTC slows down the branching process. The reaction processes are previously described for individual antioxidants in Eqs. (7.3) and (7.4).

7.2 Summary

Results of this study show that while the addition of ADPA to the formulation containing ZDDP results in improved antiwear performance, it may not be a preferred antioxidant in formulations containing F-ZDDP from a wear performance perspective.

Combination of HP and MBDTC proved to have a synergistic effect on the oxidation stability due to the complementary nature of their oxidation inhibition at various stages of the oxidation process.

MoDTC when used as a primary antioxidant in base oil formulations had a catalytic effect on the oxidation of hydrocarbons. However, the inclusion of ADPA counteracted this antagonistic effect of MoDTC.

CHAPTER 8

CONCLUSIONS

8.1 Summary of Work

Global efforts to reduce phosphorus levels in engine oils have resulted in widespread research programs aimed at exploring alternatives to current antiwear solutions available in the mainstream market. One such program at the University of Texas at Arlington has led to the invention of F-ZDDP, which has shown to exhibit superior antiwear performance with lower levels of phosphorus over its original counterpart, namely ZDDP. However, the promising antiwear performance characteristics of F-ZDDP can only be exploited on large commercial scales if its utilization in conventional power plants offers the same or better maintenance overheads as seen with ZDDP. Key indicators of its reliability include its performance in the presence of antioxidant additives as well as the oxidation stability of formulations containing this new antiwear agent. This research has examined the antiwear performance of F-ZDDP in the presence of various antioxidants and evaluated the oxidation stability of several different types of oil formulations containing F-ZDDP in order to better understand the usefulness of this new compound as a lubricant additive. A brief summary of studies conducted and results obtained is provided herein.

The interactions between F-ZDDP and ZDDP with alkylated diphenylamine were studied using NMR, and their impact on wear performance was examined using ball-on-cylinder tribometer. The surface of the tribofilm was examined using SEM, TEM and Auger spectroscopy. Thermal degradation studies of ZDDP and F-ZDDP with alkylated diphenyl amine conducted using ^{31}P NMR showed that

- There were no new peaks formed due the interaction of ZDDP with alkylated diphenyl amine

- F-ZDDP with alkylated diphenyl amine showed drastic decrease in basic ZDDP and there was considerable decrease in the intensity of P–F bonds when compared to F-ZDDP alone, showing the weak antagonistic effect of alkylated diphenyl amine on F-ZDDP.

Ball-on-cylinder wear tests conducted on ZDDP and F-ZDDP with alkylated diphenyl amines in base oil indicated that the addition of the antioxidant alkylated diphenyl amine to ZDDP showed an improved wear performance over ZDDP alone, while the addition of alkylated diphenyl amine to F-ZDDP showed marginal increase in wear when compared to F-ZDDP. However, the overall wear performance of the formulation containing F-ZDDP and antioxidant was still superior to that of ZDDP with antioxidant.

FIB analysis of the tribofilms from ZDDP and F-ZDDP with and without alkylated diphenyl amine revealed that thickness of the tribofilm formed with F-ZDDP was always higher than that formed with ZDDP. This trend persisted in the presence of antioxidants, with the thickness of the tribofilm increasing when antioxidant was present.

SEM analysis of the tribofilm indicated that wear track generated from F-ZDDP with and without antioxidants was smoother than that ZDDP with and without alkylated diphenyl amine, signifying the superior wear performance of F-ZDDP.

The Auger electron spectroscopy of ZDDP and F-ZDDP with alkylated diphenylamines, indicated that films from F-ZDDP with alkylated diphenylamine were thicker than that of ZDDP with alkylated diphenylamine.

Nano mechanical properties of the tribofilm such as hardness, nanoscratch and scanning wear analysis of the tribofilms with ZDDP and F-ZDDP with and without alkylated diphenyl amines indicated that

- The hardness of the tribofilms in the absence of the antioxidants was significantly higher at the surface region when compared to the films formed in the presence of antioxidants.

- Nano scratch tests of the tribofilms indicated that tribofilms from F-ZDDP were more resistant scratch than the films from ZDDP. However in the presence of antioxidants nano scratch behavior of both the films were similar.
- Nano wear tests on the tribofilms indicate that films from F-ZDDP were more resistance to abrasion than films from ZDDP.

Investigations on the oxidation stability of F-ZDDP and ZDDP with various antioxidants showed that

- The oxidation stability of F-ZDDP was similar to ZDDP when used alone in base oil, implying that the largely similar structures of F-ZDDP and ZDDP yield comparable performance in the absence of the influence of antioxidants.
- Formulations containing ZDDP exhibited better oxidation stability in the presence of a mixture of antioxidants, as opposed to F-ZDDP, which displayed improved performance with individual antioxidants. It therefore appears that the differences in the chemical structures between F-ZDDP and ZDDP (such as the presence of P–F bonds in the former) while of little consequence to affect the relative stability in base oil alone begin to manifest themselves in greater magnitude when antioxidants are introduced.

Tribofilms generated from formulations containing ZDDP and F-ZDDP with different antioxidants were subjected to the XANES analysis in order to investigate the composition and nature of the polyphosphates formed in these tribofilms. The XANES analysis revealed that

- The major type of the polyphosphates observed in the case of ZDDP and F-ZDDP with antioxidants was of the short-chain type.
- Tribofilms contained short-chain polyphosphates such as $Zn_3(PO_4)_2$, $Fe_4(P_2O_7)_3$ and $FePO_4$ in different proportions throughout the thickness of the tribofilms.
- Introduction of antioxidants to ZDDP or F-ZDDP did not change the type of the polyphosphates in the tribofilms, but altered the amount of these polyphosphates.

- Sulphur was present in minute quantities in the form of sulfide in the top 50nm region of the tribofilm. However deeper parts of the films contained small amount of sulphur in the form of sulphates.

8.2 Directions for Further Study

Contemporary automotive lubricants are seldom a simple mixture of base oil and a few additives such as antiwear agents and antioxidants. Rather, they encompass a sophisticated blend of a multitude of additives, each with a specific function in the lubrication process. Introducing a new additive into the equation is often hardly a simple matter of investigating an oil's performance in the presence of the new additive alone. The research presented herein is therefore only the tip of the proverbial iceberg. This work has so far examined the antiwear behavior and oxidation stability of F-ZDDP in the presence of a number of individual and combined anti-oxidants. However, the introduction of F-ZDDP into the mix opens up a completely new realm of research possibilities wherein the behavior of this new additive could be studied in the presence of several of the other additives, both individually and in mixtures, that make up a commercial lubricant. Conducting further research into these new avenues would thus be a logical progression of the work presented in this dissertation.

One of the many directions that could be pursued would involve expanding the scope of the oxidation stability studies conducted thus far to include more of the resultant products formed during a lubricant's oxidation process. Specifically, the heated samples studied in this body of work contained both soluble and insoluble products of oxidation. However, this analysis focused mainly on the soluble products during the oxidation stability studies. A more comprehensive understanding of the performance of F-ZDDP may therefore be obtained by expanding the experimental model to also incorporate these insoluble products into the analysis.

This study was conducted largely on specific formulations of ZDDP and F-ZDDP in the presence of antioxidants in base oil. While this is an important starting point for this research,

real-life conditions are more accurately reflected by studying the behavior of these additives in fully-formulated oils.

Another course of investigation could be to study oxidation stability in the presence of certain catalysts. It is well-known that several metals such as iron, copper, nickel and chromium have catalytic effects on hydrocarbon reactions [23]. It would therefore be a useful exercise to introduce soluble metal ions such as copper or iron napthenates into the formulations being studied.

This research studied the viability of FZDDP almost from an oxidation stability point of view. However, these studies should be complemented by research into the wear performance and tribofilm characterization involving the various antioxidants used in the former study. Exploring the wear performance of formulations containing antioxidants with ZDDP and FZDDP, together with analyses on the durability of the resulting films formed would therefore be an interesting direction of investigation.

Lubricant additives being active chemicals, they can interact with each other synergistically or antagonistically. As synergistic interactions augment the performance, they are obviously preferred over antagonistic interactions. It would hence be beneficial to study the additive interaction effects of ZDDP and FZDDP with different detergents and dispersants. Evaluation of their performance interaction with ZDDP alone in base oil and in fully formulated oil would help yield a clearer picture of additive interactions. It has been known that dispersants present in fully formulated oils form a complex with ZDDP, resulting in antagonistic effects on the wear performance of formulations containing these additives. F-ZDDP being new, it is important to evaluate any synergistic or antagonistic effects that may arise due to the presence of other additives.

In conclusion, a comprehensive analysis of the behavior of F-ZDDP as an automotive lubricant would not only impart a greater understanding of its characteristics, but also help to critically evaluate the advantages and shortcomings of various additive combinations from the

perspectives of wear prevention, oxidation stability and other important performance metrics. Such analyses would greatly serve to add to existing scientific knowledge on automotive lubrication and push the frontiers of research in this important, yet relatively nascent field.

REFERENCES

[1] Vrana, G., 2001, "Analytic Technology: Diagnose what Ails Your Auto," Electronics Design, Strategy, News, pp. 37-42.

[2] Quinn, T. F. J., 1977, "Tribology," Physics Education, pp. 140-143.

[3] Kramer, D. C., Lok, B. K., and Krug, R. R., "The Evolution of Base Oil Technology," Turbine Lubrication in the 21st Century, ASTM STP #1407, pp. 25-38.

[4] Khorramian, B. A., Iyer, G. R., Kodali, S., 1993, "Review of Antiwear Additives for Crankcase Oils," Wear, **169**(1) pp. 87-95.

[5] Spikes, H. A., 2004, "The History and Mechanisms of ZDDP," Tribology Letters, **17**(3) pp. 469-489.

[6] Minfray, C., Martin, J. M., Esnouf, C., 2004, "A multi-technique approach of tribofilm characterisation," Proceedings of the 30th International Conference on Metallurgie, Apr 28-May 2 2002, Elsevier, San Diego, CA, United States, **447-448,** pp. 272-277.

[7] Barcroft, F. T., Bird, R. J., Hutton, J. F., 1982, "The Mechanism of Action of Zinc Thiophosphates as Extreme Pressure Agents," Wear, **77**(3) pp. 355-384.

[8] Ferrari, E. S., Roberts, K. J., Sansone, M., 1999, "A Multi-Edge X-Ray Absorption Spectroscopy Study of the Reactivity of Zinc Di-Alkyl-Di-Thiophosphates Anti-Wear Additives: 2. in Situ Studies of steel/oil Interfaces," Wear, **236**(1-2) pp. 259-275.

[9] Ferrari, E. S., Roberts, K. J., and Adams, D., 2002, "An X-Ray Absorption Spectroscopy Examination of Structural Changes to Zinc Di-Alkyl-Di-Thiophosphate (ZDDP) Following Milling in the Presence of Iron Oxides and Subsequent Thermal Processing," Wear, **253**(7-8) pp. 759-767.

[10] Ramakumar, S. S. V., Aggarwal, N., Madhusudhana Rao, A., 1994, "Studies on Additive-Additive Interactions: Effects of Dispersant and Antioxidant Additives on the Synergistic Combination of Overbased Sulphonate and ZDDP," Lubrication Science, **7**(1) pp. 25-38.

[11] Canter, N., 2006, "Special Report: Additive Challenges in Meeting New Automotive Engine Specifications," Tribology & Lubrication Technology, pp. 10-19.

[12] Rokosz, M. J., Chen, A. E., Lowe-Ma, C. K., 2001, "Characterization of Phosphorus-Poisoned Automotive Exhaust Catalysts," Applied Catalysis B: Environmental, **33**(3) pp. 205-205-215.

[13] Kroger, V., Lassi, U., Kynkaanniemi, K., 2006, "Methodology Development for Laboratory-Scale Exhaust Gas Catalyst Studies on Phosphorus Poisoning," Chemical Engineering Journal, **120**(1-2) pp. 113-113-118.

[14] Angelidis, T. N., and Sklavounos, S. A., 1995, "SEM-EDS Study of New and used Automotive Catalysts," Applied Catalysis A:General, **133**(1) pp. 121-121.

[15] Angove, D. E., and Cant, N. W., 2000, "Position Dependent Phenomena during Deactivation of Three-Way Catalytic Converters on Vehicles," Catalysis Today, **63**(2-4) pp. 371-371-378.

[16] Rounds, F. G., 1978, "Additive Interactions and their Effect on the Performance of a Zinc Dialkyl Dithiophosphate," Tribology Transactions, **21**(2) pp. 91-101.

[17] Parekh, K., and Aswath, P. B., 2006, "Synthesis of Fluorinated ZDDP Compounds," STLE/ASME International Joint Tribology Conference, IJTC 2006.

[18] Clough, A. E., 1997, "The Relative Strengths of Oxidation Inhibitors used in Lubricants and the Monitoring of their Consumption – an Electroanalytical Approach," Recent Developments in Oil Chemistry, .

[19] Spikes, H. A., 1989, "Additive-Additive Interaction and Additive-Surface Interaction in Lubrication," Lubrication Science, **2**(1) pp. 3-23.

[20] Stachowiak, G., and Batchelor, A.W., 2005, "Engineering Tribology," Elsvier, BUTTERWORTH HEINEMANN, pp. 832.

[21] Taylor, C. M., 1998, "Automobile Engine tribology—design Considerations for Efficiency and Durability," Wear, **221**(1) pp. 1-8.

[22] Tung, S. C., and McMillan, M. L., 2004, "Automotive Tribology Overview of Current Advances and Challenges for the Future," Tribology International, **37**(7) pp. 517-536.

[23] Bhushan, B., 2000, "Modern Tribology Handbook, Volume 1," C R C Press LLC, United States of America, pp. 1760.

[24] Bayer, R.G., 1994, "Mechanical Wear Prediction and Prevention," Marcel Dekker, New York, .

[25] Burwell, J. T., 1957/58, "Survey of Possible Wear Mechanisms," Wear, **1**pp. 119-141.

[26] Hamrock, B.J., and Dowson, D., 1981, "Ball Bearing Lubrication, The Elastohydrodynamics of Elliptical Contacts," John Willey & Sons, .

[27] Hertz, H., 1881, "Uber Die Beruhrung Fester Elastischer Korper, (on the Contact of Elastic Solids)," J. Reine Und Angewandte Mathematik, **92**pp. 156-171.

[28] Hsu, S. M., and Gates, R. S., 2005, "Boundary Lubricating Films: Formation and Lubrication Mechanism," Tribology International, **38**(3) pp. 305-312.

[29] Buschow, K.H.J., Cahn, R., Flemings, M.C., 2001, "The Encyclopedia of Materials: Science and Technology," pp. 10000.

[30] Tonck, A., Martin, J. M., Kapsa, P., 1979, "Boundary Lubrication with Anti-Wear Additives: Study of Interface Film Formation by Electrical Contact Resistance," Tribology International, **12**(5) pp. 209-213.

[31] Parekh, K., 2006, "Interactions between Antiwear Agent and Novel Additive in Engine Oils"

[32] Nicholls, M. A., Do, T., Norton, P. R., 2005, "Review of the Lubrication of Metallic Surfaces by Zinc Dialkyl-Dithiophosphates," Tribology International, **38**pp. 15-39.

[33] Harrison, P. G., and Kikabhai, T., 1987, "Proton and Phosphorous 31 NMR Study of ZDDP in Solution," Journal of the Chemical Society, Dalton Transactions: Inorganic Chemistry, **16**(4) pp. 807-807-813.

[34] Harrison, J. J., Chan, C. Y., Onopchenko, A., 2007, "Neutral Zinc(II) *O*,*O*-Di-Alkyldithiopho- Sphates - Variable Temperature ^{31}P NMR and Quantum Chemical Study of the ZDDP Monomer-Dimer Equilibrium," Magnetic Resonance in Chemistry, **46**(2) pp. 115-115 - 124.

[35] Yamaguchi, E. S., Primer, R. L., Aragón, S. R., 1997, "Dynamic Light Scattering Studies of Neutral Diisobutyl Zinc Dithiophosphate," Tribology Transactions, **40**pp. 330-330-338.

[36] Yamaguchi, E. S., Primer, R. L., Aragón, S. R., 1998, "Dynamic Light Scattering Studies of Basic Diisobutyl Zinc Dithiophosphate," Tribology Transactions, **41**pp. 233-233-240.

[37] Fuller, M., Yin, Z., Kasrai, M., 1997, "Chemical Characterization of Tribochemical and Thermal Films Generated from Neutral and Basic ZDDPs using X-Ray Absorption Spectroscopy," Tribology International, **30**(4) pp. 305-315.

[38] Yamaguchi, E. S., Ryason, P. R., Labrador, E. Q., 1996, "Comparison of the Relative Wear Performance of Neutral and Basic ZnDTP Salts," Tribology Transactions, **39**(1) pp. 220-224.

[39] Varlot, K., Kasrai, M., Martin, J. M., 2000, "Antiwear Film Formation of Neutral and Basic ZDDP: Influence of the Reaction Temperature and of the Concentration," Tribology Letters, **8**(1) pp. 9-16.

[40] Willermet, P. A., Dailey, D. P., Carter, R. O.,III, 1995, "Mechanism of Formation of Antiwear Films from Zinc Dialkyldithiophosphates," Tribology International, **28**(3) pp. 177-187.

[41] Habeeb, J. J., and Stover, W. H., 1987, "The Role of Hydroperoxides in Engine Wear and the Effect of Zinc Dialkyldithiophosphate," ASLE Transactions, **30**(4) pp. 419-426.

[42] Martin, J. M., Belin, M., Mansot, J. L., 1985, "Friction-Induced Amorphization with Zddp - an Exafs Study." ASLE Preprints Presented at the ASLE/ASME Tribology Conference. ASLE, Park Ridge, IL, USA, Atlanta, GA, USA, pp. 9.

[43] Wu, Y. L., and Dacre, B., 1997, "Effects of Lubricant-Additives on the Kinetics and Mechanisms of ZDDP Adsorption on Steel Surfaces," Tribology International, **30**(6) pp. 445-453.

[44] Bovington, C. H., and Dacre, B., 1984, "The Adsorption and Reaction of Decomposition Products of Zinc Di-Isopropyldithiophosphate on Steel," ASLE Transactions, **27**(3) pp. 252-258.

[45] Plaza, S., 1987, "The Adsorption of Zinc Dibutyldithiophosphates on Iron and Iron Oxide Powders," ASLE Transactions, **30**(2) pp. 233-240.

[46] Bridgewater, A. J., Dever, R. J., and Sexton, M. D., 1980, "Mechanism of Antioxidant Action. Part 2. Reaction of Zinc Bis[OO-Dialkyl(Aryl)Phosphorodithioates] and Realted Compounds with Hydroperoxides," Journal of Chemical Society Perkin II, pp. 1006-1006-1016.

[47] Spedding, H., and Watkins, R. C., 1982, "Antiwear Mechanism of ZDDP's - 1," Tribology International, **15**(1) pp. 9-12.

[48] Willermet, P. A., Kandah, S. K., Siegel, W. O., 1983, "The Influence of Molecular Oxygen on Wear Protection by Surface Active Compounds," ASLE Transactions, **26**(4) pp. 523-531.

[49] ColClough, T., 1987, "Role of Additives and Transition Metals in Lubricating Oil Oxidation," Industrial Engineering Chemistry, **26**(9) pp. 1888-1895.

[50] Elliot, A. D., and Brazier, J. S., 1967, "Thermal Stability of Zinc Dithiophosphate," J.of Institute of Petroleum, **53**(518) pp. 63-76.

[51] Coy, R. C., and Jones, R. B., 1981, "The Thermal Degradation and EP Performance of Zinc Dialkyldithiophosphate Additives in White Oil," Tribology Transactions, **24**(1) pp. 77-90.

[52] Jones, R. B., and Coy, R. C., 1981, "The Chemistry of the Thermal Degradation of Zinc Dialkyldithiophosphate Additives," Tribology Transactions, **24**(1) pp. 91-97.

[53] Watkins, R. C., 1982, "The Antiwear Mechanism of Zddp's. Part II," Tribology International, **15**(1) pp. 13-15.

[54] Willermet, P. A., and Kandah, S. K., 1993, "Some Observations on the Role of Oxygen in Lubricated Wear," Lubrication Science, **5**(2) pp. 129-147.

[55] Willermet, P. A., Carter, R. O.,III, and Boulos, E. N., 1992, "Lubricant-Derived Tribochemical Films-an Infra-Red Spectroscopic Study," Tribology International, **25**(6) pp. 371-371-380.

[56] Dacre, B., and Bovington, C. H., 1982, "EFFECT OF METAL COMPOSITION ON THE ADSORPTION OF ZINC DI-ISOPROPYLDITHIOPHOSPHATE." ASLE Preprints presented at the ASME/ASLE Lubrication Conference. ASLE, Park Ridge, IL, USA, Washington, DC, USA, **26,** pp. 333-343.

[57] Yamaguchi, E. S., and Ryason, P. R., 1993, "Inelastic Electron Tunneling Spectra of Lubricant Oil Additives on Native Aluminum Oxide Surfaces," Tribology Transactions, **36**(3) pp. 367-374.

[58] Mosey, N. J., Woo, T. K., Kasrai, M., 2006, "Interpretation of Experiments on ZDDP Anti-Wear Films through Pressure-Induced Cross-Linking," Tribology Letters, **24**(No. 2) pp. 105-105-114.

[59] Mosey, N. J., Woo, T. K., and Müser, M. H., 2005, "Mechanism of Wear Inhibition by ZDDP Lubricant Additives - Insights from Molecular Scale Simulations," American Chemical Society, Division of Petroleum Chemistry, Preprints, **50**(3) pp. 332-335.

[60] Li, Y., Pereira, G., Lachenwitzer, A., 2007, "X-Ray Absorption Spectroscopy and Morphology Study on Antiwear Films Derived from ZDDP Under Different Sliding Frequencies," Tribology Letters, **27**(3) pp. 245-253.

[61] Bancroft, G. M., Kasrai, M., Fuller, M., 1997, "Mechanisms of Tribochemical Film Formation: Stability of Tribo- and Thermally-Generated ZDDP Films," Tribology Letters, **3**(1) pp. 47-47-51.

[62] Aktary, M., McDermott, M. T., and McAlpine, G. A., 2002, "Morphology and Nanomechanical Properties of ZDDP Antiwear Films as a Function of Tribological Contact," Tribology Letters, **12**(3) pp. 155-155-162.

[63] Suominen Fuller, M. L., Rodriguez Fernandez, L., Massoumi, G. R., 2000, "The use of X□ray Absorption Spectroscopy for Monitoring the Thickness of Antiwear Films from ZDDP," Tribology Letters, **8**(4) pp. 187-187-192.

[64] Aktary, M., McDermott, M. T., and Torkelson, J., 2001, "Morphological Evolution of Films Formed from Thermooxidative Decomposition of ZDDP," Wear, **247**(2) pp. 172-179.

[65] Suominen Fuller, M. L., Kasrai, M., Bancroft, G. M., 1998, "Solution Decomposition of Zinc Dialkyl Dithiophosphate and its Effect on Antiwear and Thermal Film Formation Studied by X-Ray Absorption Spectroscopy," Tribology International, **31**(10) pp. 627-644.

[66] Fujita, H., and Spikes, H. A., 2004, "The Formation of Zinc Dithiophosphate Antiwear Films," Proceedings of the Institution of Mechanical Engineers, Part J: Journal of Engineering Tribology, **218**(4) pp. 265-277.

[67] Yin, Z., Kasrai, M., Bancroft, G. M., 1997, "Application of Soft x-Ray Absorption Spectroscopy in Chemical Characterization of Antiwear Films Generated by ZDDP Part II: The Effect of Detergents and Dispersants," Wear, **202**(2) pp. 192-201.

[68] Martin, J. M., Grossiord, C., Le Mogne, T., 2001, "The Two-Layer Structure of Zndtp Tribofilms: Part I: AES, XPS and XANES Analyses," Tribology International, **34**(8) pp. 523-530.

[69] Kasrai, M., Bancroft, G. M., Brunner, R. W., 1994, "Sulphur Speciation in Bitumens and Asphaltenes by X-Ray Absorption Fine Structure Spectroscopy," Geochimica Et Cosmochimica Acta, **58**(13) pp. 2865-2872.

[70] Bec, S., Tonck, A., Georges, J. M., 1999, "Relationship between mechanical properties and structures of zinc dithiophosphate anti-wear films," London, UK, **Volume 455,** pp. 4181-4181 - 4203.

[71] Barnes, A. M., Bartle, K. D., and Thibon, V. R. A., 2001, "A Review of Zinc Dialkyldithiophosphates (ZDDPS): Characterisation and Role in the Lubricating Oil," Tribology International, **34**(6) pp. 389-395.

[72] Willermet, P. A., 1998, "Some Engine Oil Additves and their Effects on Antiwear Film Formation," Tribology Letters, **5**pp. 41-41-47.

[73] Unnikrishnan, R., Jain, M. C., Harinarayan, A. K., 2002, "Additive-Additive Interaction: An XPS Study of the Effect of ZDDP on the AW/EP Characteristic of Molybdenum Based Additives," Wear, **252**(3-4) pp. 240-249.

[74] Varlot, K., Martin, J. M., Grossiord, C., 1999, "A Dual-Analysis Approach in Tribochemistry: Application to ZDDP/calcium Borate Additive Interactions," Tribology Letters, **6**(Nos. 3-4) pp. 181-181-189.

[75] Varlot, K., Kasrai, M., Bancroft, G. M., 2001, "X-Ray Absorption Study of Antiwear Films Generated from ZDDP and Borate Micelles," Wear, **249**(12) pp. 1029-1035.

[76] Kasrai, M., Fuller, M. S., Bancroft, G. M., 2003, "X-Ray Absorption Study of the Effect of Calcium Sulfonate on Antiwear Film Formation Generated from Neutral and Basic ZDDPs: Part 1 - Phosphorus Species," Tribology Transactions, **46**(4) pp. 534-542.

[77] Kasrai, M., Fuller, M. S., Bancroft, G. M., 2003, "X-Ray Absorption Study of the Effect of Calcium Sulfonate on Antiwear Film Formation Generated from Neutral and Basic ZDDPs: Part 2 - Sulfur Species," Tribology Transactions, **46**(4) pp. 543-549.

[78] Rounds, F. G., 1980, "Some Effects of Amines on Zinc Dialyldithiophosphate Antiwear Performance as Measured in 4-Ball Wear Tests," ASLE Transactions, **24**(4) pp. 431-431-440.

[79] Li, Y., Pereira, G., Kasrai, M., 2007, "Studies on ZDDP Anti-Wear Films Formed Under Different Conditions by XANES Spectroscopy, Atomic Force Microscopy and 31P NMR," Tribology Letters, **28**(3) pp. 319-328.

[80] Huq, M. Z., Chen, X., Aswath, P. B., 2005, "Thermal Degradation Behaviour of Zinc Dialkyl Dithiophosphate in Presence of Catalyst and Detergents in Neutral Oil," Trib.Lett., **19**(2) pp. 127-134.

[81] Patel, K., Aswath, P. B., and Elsenbaumer, R. L., 2005, "Development of Low Phosphorous Engine Oils," American Society of Mechanical Engineers, New York, NY 10016-5990, United States, pp. 557-558.

[82] Parekh, K., Mourhatch, R., and Aswath, P. B., 2005, "ZDDP-additive-catalyst interactions in engine oil," American Society of Mechanical Engineers, New York, NY 10016-5990, United States, pp. 661-662.

[83] Parekh, K., and Aswath, P. B., 2006, "Synthesis of Fluorinated ZDDP," American Society of Mechanical Engineers, pp. IJTC-12053.

[84] Parekh, K., Aswath, P. B., Shaub, H., 2006, "Low-Phosphorous Lubricant Additive," **11/182,023**(US 2006/0014652) .

[85] Reyes-Gavilan, J. L., and Odorisio, P., 2001, "A Review of the Mechanisms of Action of Antioxidants, Metal Deactivators, and Corrosion Inhibitors," NLGI Spokesman, **64**(11) pp. 22-33.

[86] Mahoney, L. R., 1969, "Antioxidants," Chemistry International, **8**(8) pp. 547-547-555.

[87] Vipper, A. B., Zadko, I. I., Ermolaev, M. V., 2002, "Engine Oil Ageing Under Laboratory Conditions," Lubrication Science, **14**(3) pp. 363-375.

[88] Korcek, S., Mahoney, L. R., Johnson, M. D., 1981, "Mechanisms of Antioxidant Decay in Gasoline Engines: Investigations of Zinc Dialkyldithiophosphate Additives," SAE Preprints, (810014) pp. 14.

[89] Willermet, P. A., and Kandah, S. K., 1984, "Lubricant Degradation and Wear v. Reaction Products of Zinc Dialkyldithiophosphate and Peroxy Radicals," ASLE Transactions, **27**(1) pp. 67-67-72.

[90] Marshall, G. L., 1984, "Characterization of Lubricants using ^{31}P Fourier Transform Nuclear Magnetic Resonance Spectroscopy," Appl.Spec., **38**(4) pp. 522-526.

[91] Paddy, J. L., Lee, N. C., Waters, J., 1990, "Zinc Dialkyl Dithiophosphate Oxidation by Cumene Hydroperoxide: Kinetic Studies by Raman and ^{31}P NMR Spectroscopy," Trib.Trans., **33**(1) pp. 15-20.

[92] Ohkatsu, Y., Kikkawa, K., and Osa, T., 1978, "Study on Zinc O,O- Diisobutyl Dithiophosphate as Antioxidant." Bulletin of the Chemical Society of Japan., **51**(12) pp. 3606-3606-3609.

[93] Howard, J. A., Ohkatsu, Y., Chenier, J. H. B., 1973, "Metal Complexes as Antioxidants. I. the Reaction of Zinc Dialkyldithiophosphates and Related Compounds with Peroxy Radicals," Canadian Journal of Chemistry, **51**pp. 1543-1543-1553.

[94] Bartha, L., Kis, G., Auer, J., 2001, "Thickening Effects of Interactions between Engine Oil Additives," Lubrication Science, **13**(3) pp. 231-231-249.

[95] Herguth, W. R., and Phillips, S., 1998, "Comparison of common analytical techniques to voltammetric analysis of antioxidants in industrial lubricating oils," pp. 499-509.

[96] Briggs, D., and Grant, J.T., 2003, "Surface Analysis by Auger and X-ray Photoelectron spectroscopy," IM Publications and Surface Spectra Limited, Manchester, UK, pp. 1-885.

[97] Skoog, D.A., and Leary, J.J., 1992, "Principles of Instrumental Analysis," Saunders College Publishing, USA, pp. 700.

[98] Zhang, Z., Yamaguchi, E. S., Kasrai, M., 2005, "Tribofilms generated from ZDDP and DDP on steel surfaces: Part 1. Growth, wear and morphology," 2005 World Tribology Congress III, American Society of Mechanical Engineers, New York, NY 10016-5990, United States, Washington, D.C., United States, pp. 617-618.

[99] Bec, S., Demmou, K., Loubet, J., 2005, "Mechanical properties of ZnDTP tribofilms measured by nanoindentation at controlled temperature," 2005 World Tribology Congress III, Sep 12-16 2005, American Society of Mechanical Engineers, New York, NY 10016-5990, United States, Washington, D.C., United States, pp. 823-824.

[100] Komvopoulos, K., Yamaguchi, E. S., Do, V., 2004, "Nanomechanical and nanotribological properties of an antiwear tribofilm produced from phosphorus-containing additives on boundary-lubricated steel surfaces," 2004 ASME/STLE International Joint Tribology Conference, American Society of Mechanical Engineers, New York, NY 10016-5990, United States, Long Beach, CA, United States, pp. 1631-1636.

[101] Ye, J., Kano, M., and Yasuda, Y., 2002, "Evaluation of Local Mechanical Properties in Depth in MoDTC/ZDDP and ZDDP Tribochemical Reacted Films using Nanoindentation," Tribology Letters, **13**(1) pp. 41-41-47.

[102] Ye, J., Araki, S., Kano, M., 2005, "Nanometer-Scale Mechanical/Structure Properties of Molybdenum Dithiocarbomate and Zinc Dialkylsithiophosphate Tribofilms and Friction Reduction Mechanism," Japanese Journal of Applied Physics, Part 1: Regular Papers and Short Notes and Review Papers, **44**(No. 7B) pp. 5358-5361.

[103] Nicholls, M. A., Norton, P. R., Bancroft, G. M., 2004, "Nanometer Scale Chemomechanical Characterization of Antiwear Films," Tribology Letters, **17**(No. 2) pp. 205-205-216.

[104] Lin-Vien, D., Colthup, N.B., Fateley, W.G., 1991, "THE HANDBOOK OF *Infrared and Raman Characteristic Frequencies of Organic Molecules*," Academic Press, Inc., USA, pp. 1-499.

[105] Pretsch, E., Buhlmann, P., and Affolter, C., 2000, "Structure Determination of Organic Compounds," Springer, Germany, pp. 1-421.

[106] Ferrari, E. S., Roberts, K. J., and Adams, D., 1999, "A Multi-Edge X-Ray Absorption Spectroscopy Study of the Reactivity of Zinc Di-Alkyl-Di-Thiophosphates (ZDDPS) Anti-Wear Additives: 1. an Examination of Representative Model Compounds," Wear, **236**(1-2) pp. 246-258.

[107] Yin, Z., Kasrai, M., Fuller, M., 1997, "Application of Soft x-Ray Absorption Spectroscopy in Chemical Characterization of Antiwear Films Generated by ZDDP Part I: The Effects of Physical Parameters," Wear, **202**(2) pp. 172-191.

[108] Kasrai, M., Yin, Z., Fuller, M., 1997, "Application of XAFS in Tribology: P and S L-Edge XANES Spectroscopy of Antiwear Films," Journal De Physique.IV : JP, **7**(2) pp. 2-847.

[109] Belin, M., Martin, J. M., Tourillon, G., 1995, "Local Order in Surface ZDDP Reaction Films Generated on Engine Parts, using EXAFS and Related Techniques," Lubrication Science, **8**(1) pp. 3-14.

[110] Mourhatch, R., Parekh, K., and Aswath, P. B., 2006, "A multi technique study of the tribological behavior and the tribofilms generated from fluorinated thiophosphate compounds in comparison to normal ZDDP," STLE/ASME International Joint Tribology Conference, IJTC 2006, American Society of Mechanical Engineers, New York, NY 10016-5990, United States, San Antonio, TX, United States, **2006,** pp. 12.

[111] Peng, P., Hong, S., and Lu, W., 1994, "The Degradation of Zinc Dialkyl Dithiophosphate Additives in Fully Formulated Engine Oil as Studied by 31P NMR Spectroscopy," Lub.Engg., **50**(3) pp. 230-235.

[112] Kapur, G. S., Chopra, A., Sarpal, A. S., 1999, "Studies on Competitive Interactions and Blending Order of Engine Oil Additives by Variable Temperature 31P NMR and IR Spectroscopy." Trib.Trans., **42**(4) pp. 807-812.

[113] Bansal, V., Sastry, M. I. S., Sarpal, A. S., 1997, "Characterization of Nitrogen and Phosphorous Components in a Multifunctional Lubricant Additive by NMR and IR Techniques," Lubrication Engineering, **53**(4) pp. 17-23.

[114] Zhang, Z., Su, C., Liu, W., 1996, "Study on Tribological Properties of the Complex of Rare Earth Dialkyldithiocarbamate and Phenanthroline in Lubricating Grease," Wear, **192**(1-2) pp. 6-10.

[115] Huq, M. Z., Aswath, P. B., and Elsenbaumer, R. L., 2007, "TEM Studies of Anti-Wear films/wear Particles Generated under Boundary Conditions Lubrication," Tribology International, **39**(1) pp. 111-111-116.

[116] Mosey, N. J., Müser, M. H., and Woo, T. K., 2005, "Molecular Mechanisms of Anti-Wear Pad Formation and Functionality of Lubricant Additives," Science, **307**(No. 5715) pp. 1612-1612-1615.

[117] Kasrai, M., Vasiga, M., Fuller, M. S., 1999, "Study of the Effects of Ca Sulfonate on Antiwear Film Formation by X-Ray Absorption Spectroscopy using Synchrotron Radiation," Journal of Synchrotron Radiation, **6**(3) pp. 719-721.

[118] Lin, Y. C., and So, H., 2004, "Limitations on use of ZDDP as an Antiwear Additive in Boundary Lubrication," Tribology International, **37**(1) pp. 25-33.

[119] Ji, H., Nicholls, M. A., Norton, P. R., 2005, "Zinc-Dialkyl-Dithiophosphate Antiwear Films: Dependence on Contact Pressure and Sliding Speed," Wear, **258**(5-6) pp. 789-799.

[120] Pidduck, A. J., and Smith, G. C., 1997, "Scanning Probe Microscopy of Automotive Anti-Wear Films," Wear, **212**(2) pp. 254-264.

[121] Shakhvorostov, D., Pohlmann, K., and Scherge, M., 2006, "Structure and Mechanical Properties of Tribologically Induced Nanolayers," Wear, **260**(4) pp. 433-437.

[122] Scherge, M., Martin, J. M., and Pohlmann, K., 2006, "Characterization of Wear Debris of Systems Operated Under Low Wear-Rate Conditions," Wear, **260**(4) pp. 458-461.

[123] Martin, J. M., Mansot, J. L., Berbezier, I., 1984, "The Nature and Origin of Wear Particles from Boundary Lubrication with a Zinc Dialkyl Dithiophosphate," Wear, **93**(2) pp. 117-126.

[124] Martin, J. M., 1999, "Antiwear Mechanisms of Zinc Dithiophosphate: A Chemical Hardness Approach," Tribology Letters, **6**(No. 1) pp. 1-1-8.

[125] Kundu, T. K., Mukherjee, M., Chakravorty, D., 1998, "Growth of Nano-α-Fe2O3 in a Titania Matrix by the sol–gel Route," Journal of Materials Science, **33**(No. 7) pp. 1759-1759-1763.

[126] Li, J., Zeng, H., Sun, S., 2004, "Analyzing the Structure of CoFe-Fe3O4 Core-Shell Nanoparticles by Electron Imaging and Diffraction," Journal of Physical Chemistry B, **108**(37) pp. 14005-14005-14008.

[127] Kumar, S., Mishra, N. M., and Mukherjee, P. S., 2005, "Additives Depletion and Engine Oil Condition – a Case Study," Industrial Lubrication and Tribology, **57**(2) pp. 69-72.

[128] Jefferies, A., and Ameye, J., 1998, "RULERTM and used Engine Oil Analysis Programs(c)," Lubrication Engineering, **54**(5) pp. 29-34.

[129] Levermore, D. M., Josowicz, M., Rees, Jr., William S., 2001, "Headspace Analysis of Engine Oil by Gas Chromatography/Mass Spectrometry," Analytical Chemistry, **73**(6) pp. 1361-1365.

[130] Stipanovic, A. J., Schoonmaker, J. P., de PaZ, E. F., 1996, "Base Oil and Additive Effects in the Thermo-oxidation Engine Oil Simulation Test (TEOST)," pp. 111-120.

[131] Gatto, V. J., Moehle, W. A., Cobb, T. W., 2007, "The Relationship between Oxidation Stability and Antioxidant Depletion in Turbine Oils Formulated with Groups II, III and IV Base Stocks," Journal of Synthetic Lubrication, **24**pp. 111-111-124.

[132] Al-Malaika, S., Marvgi, A., and Scott, G., 1987, "Mechanism of Antioxidant Action; Transformations Involved in the Antioxidant Function of Metal Dialkyl Dithiocarbamates III." Journal of Applied Polymer Science, **33**pp. 1455-1455-1471.

[133] Gao, H., Bjornen, K. K., Gangopadhyay, A. K., 2005, "Oxidation and Antiwear Retention Capability of Low-Phosphorus Engine Oils," SAE Technical Paper, **2005-01-3822**.

[134] Hu, J., Wei, X., Dai, G., 2007, "Synergistic Antioxidation of Organic Molybdenum Complex with Dithicarbamate Antioxidant Evaluated by Differential Scanning Calorimetry and Thin Film Microoxidation Test," Thermochimica Acta, **453**pp. 21-21-26.

[135] Shaub, H., 1997, "Mixed Antioxidant Composition," **PCT/EP94/03064**(EP0719313B1) pp. 1-1-17.

[136] De Barros, M. I., Bouchet, J., Raoult, I., 2003, "Friction Reduction by Metal Sulfides in Boundary Lubrication Studied by XPS and XANES Analyses," Wear, **254**(9) pp. 863-870.

[137] The Canadian Light Source; www.lightsource.ca.

[138] Somayaji, A., and Aswath, P. B., Accepted (2008), "Antiwear Perforce of ZDDP and Fluorinated ZDDP in the Presence of Antioxidants," Tribology Transactions, .

[139] Mourhatch, R., and Aswath, P. B., 2006, "Mechanism of Boundary Lubrication with Zinc Dialkyl Dithiophosphate," American Society of Mechanical Engineers, **Under Review,** pp. IJTC-12054.

[140] Yin, Z., Kasrai, M., Bancroft, G. M., 1993, "Chemical Characterization of Antiwear Films Generated on Steel by Zinc Dialkyl Dithiophosphate using X-Ray Absorption Spectroscopy," Tribology International, **26**(6) pp. 383-388.

BIOGRAPHICAL INFORMATION

Anuradha Somayaji received her Bachelor of Science, Master of Science and Master of Technology degrees in Materials Science and Engineering from Mangalore University (India) in 1994, 1996 and 1998 respectively. From 1999 to 2000, she worked at the Structure Properties Correlation Lab at the Indian Institute of Science, Bangalore, India on failure analysis of high-performance alloys for aircraft engines. During her doctoral program at the University of Texas at Arlington, she spearheaded several departmental programs and community outreach efforts in engineering education as the vice president of the student chapter of ASM international. She is also the recipient of the Carl D. Wiseman award for outstanding service to her department at UTA. Her research interests include finding new ways to improve the performance of low phosphorus engine oils with emphasis on antioxidants.